# APPLICATION OF GEOPHYSICAL AND GEOCHEMICAL METHODS FOR SOIL CHARACTERISATION IN SUSTAINABLE PRECISION AGRICULTURE IN SELECTED FARMS

**BY**

**KAYODE, OLUSOLA TITILOPE**
**(MATRIC NO: 13PCE00497)**
**B.Sc Geology, University of Ado Ekiti, Ado – Ekiti**
**M.Sc Industrial Physics (Applied Geophysics), Covenant University, Ota**

**A THESIS SUBMITTED TO THE SCHOOL OF POSTGRADUATE STUDIES IN PARTIAL FULFILMENT OF THE REQUIREMENTS FOR THE AWARD OF THE DEGREE OF DOCTOR OF PHILOSOPHY (Ph.D) IN INDUSTRIAL PHYSICS (APPLIED GEOPHYSICS) IN THE DEPARTMENT OF PHYSICS, COLLEGE OF SCIENCE AND TECHNOLOGY, COVENANT UNIVERSITY, OTA.**

**APRIL, 2021**

## ACCEPTANCE

This is to attest that this thesis is accepted in partial fulfilment of the requirements for the award of the degree of Doctor of Philosophy (Ph.D) in Industrial Physics (Applied Geophysics) in the Department of Physics, College of Science and Technology, Covenant University, Ota, Nigeria.

Mr. John A. Philip ……

**(Secretary, School of Postgraduate Studies)** Signature and Date

Prof. Akan B. Williams ..…….....

**(Dean, School of Postgraduate Studies)** Signature and Date

## DECLARATION

I, **KAYODE OLUSOLA TITILOPE (13PCE00497)**, declare that this research was carried out by me under the supervision of Prof. Ahzegbobor P. Aizebeokhai of the Department of Physics, College of Science and Technology, Covenant University, Ota, and Dr. Abiodun M. Odukoya of the Department of Geosciences, Faculty of Science, University of Lagos, Akoka. I attest that the thesis has not been presented either wholly or partially for the award of any degree elsewhere. All sources of data and scholarly information are duly acknowledged.

**KAYODE, OLUSOLA TITILOPE** **……**

Signature and Date

## CERTIFICATION

We certify that the thesis titled **Application of Geophysical and Geochemical Methods for Soil Characterisation in Sustainable Precision Agriculture in Selected Farms** is an original research work carried out by **KAYODE, OLUSOLA TITILOPE (13PCE00497)** in the Department of Physics, College of Science and Technology, Covenant University, Ota, Nigeria, under the supervision of Prof. Ahzegbobor P. Aizebeokhai and Dr. Abiodun M. Odukoya. We have examined and found the research work acceptable as part of the requirements for the award of the degree of Doctor of Philosophy (Ph.D) in Industrial Physics (Applied Geophysics).

Prof. Ahzegbobor P. Aizebeokhai ……
**(Supervisor)** Signature and Date

Dr. (Mrs) Abiodun M. Odukoya …...……..
**(Co-supervisor)** Signature and Date

Prof. Mojisola R. Usikalu ….……..
**(Head of Department)** Signature and Date

Dr. Michael A. Oladunjoye ..……
**(External Examiner**) Signature and Date

Prof. Akan B.Williams ……..
**(Dean, School of Postgraduate Studies)** Signature and Date

## DEDICATION

I dedicate this thesis to God the Father, Omnipotent, Omniscient and Omnipresent God, who sustained me from the beginning to the end of this work.

## ACKNOWLEDGEMENTS

My heartfelt gratitude goes to the Almighty God, the Alpha and Omega, for His unending grace, and sound health and mind He granted me to complete this work. My expression goes thus “if it had not been the LORD who was on my side”. To Him alone be all the glory!

I immensely appreciate the Chancellor, Covenant University, Dr. David O. Oyedepo, for his visionary leadership, and all members of the Board of Regent for establishing the CUCRID platform. I equally acknowledge the immediate past Vice Chancellor, Covenant University, Prof. Aderemi A. Atayero, the Acting Vice Chancellor, Prof. A. B. Williams, the current Vice Chancellor, Prof. Abiodun H. Adebayo, the Registrar, Dr. Oluwasegun P. Omidiora and members of the management team for their support and several training platforms made available during the course of this work. I also acknowledge Dr. Oluwasegun P. Omidiora, the present Registrar of Covenant University, for his assistance during my field work exercise at Omu-Aran through Dr. Ezenwoke A. Azubuike, the former Registrar of Landmark University. I am thankful to the immediate Acting Dean, School of Postgraduate Studies, Prof. Obinna C. Nwinyi, the Dean, School of Postgraduate Studies, Prof. Akan B. Williams and the Dean, College of Science and Technology, Prof. Temidayo V. Omotosho, for their commitment to ensuring a speedy completion of the Ph.D programme.

Special thanks go to my supervisor, Prof. Ahzegbobor P. Aizebeokhai for sacrificing his time to help improve the quality of this thesis with constructive criticism of each chapter despite his tight schedule as the immediate past Head, Department of Physics. Also, to my co-supervisor, Dr. Abiodun M. Odukoya, for her motherly support and advice.

I appreciate the Head, Department of Physics, Prof. Mojisola R. Usikalu, for her useful contribution to the thesis. I also wish to appreciate all the senior colleagues in the Department of Physics, Prof. Marvel L. Akinyemi, Prof. Temidayo V. Omotosho, Dr. Moses E. Emetere and Dr. Maxwell Omeje for their role in ensuring a quality thesis is presented from the Department. I also appreciate all the Faculty and Staff members of the Department.

I deeply acknowledge the assistance of Dr. Moses E. Emetere, Mr. Gideon Adeyemi and Mr. Ezekiel Ogunyemi with the satellite imagery aspect of the work. Also, to Jean de Chavez of Bureau de Veritas, ACME Laboratory, Canada for the timely analysis of the soil samples, I say thank you. My thanks and appreciation also go to friends and colleagues in persons of Dr. Kehinde D. Oyeyemi, Mr. Nathaniel Obafemi, Mr. Emmanuel Ogunwale, Mr. Oladapo Oyetade, Mr. Segun Ayanbisi and Mr. Alaka Omotayo for the assistance rendered during my field work exercise at both Covenant University farm and Landmark University farm.

I appreciate the kind gestures of Mr. Richard Nwadimuya, the human resource manager of Landmark University farm for helping to recruit workers from Omu-Aran that assisted me on the field. I acknowledge Dr. Hilary Okagbue for helping with the statistical analysis aspect of the work. I also acknowledge the moral support and encouragement of Dr. Olusegun O. Adewoyin, Dr. Anuoluwa A. Akinsiku, Dr. Justina A. Achuka and Dr. Imhade Okokpujie.

I deeply appreciate the unflinching support of Dr. Molu Olumolade referred to as “Big Daddy” for sponsoring my soil analysis at the Acme Laboratory in Canada. My deepest appreciation goes to my mom, Pastor Mrs. C. M. Ogunleye, for her unrelenting prayers and words of encouragement that upheld me throughout the research work. To my late dad, Pastor, Engr. Kayode Ogunleye, for the confidence and godly virtues he imputed in me to overcome every life challenge. My siblings, Pastor Mrs. A. Ojeifo, Mrs. Okanmiyin Ogundele, Funmilayo and Deacon Barrister Moyoninuoluwa, thank you for being there for me. Also, my appreciation goes to supportive extended family members such as Pastor Chuks Ojeifo, Pastor Gideon Oladokun and Mrs. Alice Oladokun, Deacon Gbenga Oladokun and Mrs. Opeyemi Oladokun.

Finally, I submit that it has been God’s love and your prayers that I am alive to complete this research study.

# TABLE OF CONTENTS

# LIST OF TABLES

## LIST OF FIGURES

## LIST OF ABBREVIATIONS

| | |
|---|---|
| CU: | Covenant University |
| EU: | European Union |
| FAO: | Food and Agricultural Organisation |
| GIS: | Geographic Information System |
| GPS: | Ground Positioning System |
| ICPMS: | Inductively Coupled Plasma Mass Spectrometry |
| LU: | Landmark University |
| MERRA: | Modern-Era Retrospective Analysis for Research and Application |
| NASA: | National Aeronautics and Space Administration |
| PA: | Precision Agriculture |
| SMC: | Soil Moisture Content |
| SOC: | Soil Organic Carbon |
| SOM: | Soil Organic Matter |
| UV: | Ultra Violet |
| UNESCO: | United Nations Educational Scientific and Cultural Organisation |
| USEPA: | United State Environmental Protection Agency |
| USGS: | United State Geological Survey |
| VES: | Vertical Electrical Sounding |
| WHO: | World Health Organisation |

## ABSTRACT

All soils have potential for high yield for specific crops. Nigerian soils have potential for medium to high yield, but poor farming practices including the misuse of chemical fertilizers result in a number of constraints such as soil salinity, degradation and declining fertility, which militate against high crop yields. Nigeria, currently battling with food insecurity because population growth is not commensurate with agricultural production. Thus, there is need for urgent intervention in the agricultural sector. The aim of this study was to integrate geophysical and geochemical methods for sustainable precision agriculture in two farm sites of Covenant University and Landmark University, Nigeria. In this study, electrical resistivity, geochemical and satellite imagery methods were used for soil characterisation in farm sites at Covenant University, Ota, Southwest and Landmark University, Omu-Aran, North-central Nigeria between June, 2018 and January, 2019. The electrical resistivity data were processed using RES2DINV and Win-Resist software. Geochemical analysis of soil samples from the sites was conducted using ICP-MS in ACME laboratory, Canada. Monthly MERRA satellite data was used to determine the soil temperature and soil moisture content while soil salinity was estimated from Landsat-8 satellite imagery. The study showed that electrical resistivity of the topsoil in Covenant University farm ranged from 120 -500 Ωm, while that of Landmark University farm ranged from 345-527 Ωm. The soil types delineated at the Covenant University farm were clayey sand and lateritic clay; sand/lateritic gravelly sand was delineated at Landmark University farm. Potentially toxic elements were detected in the soil samples of both sites; arsenic (As), chromium (Cr), lead (Pb) and copper (Cu) exceeded FAO/WHO recommended standard limits in Covenant University farm. The pollution indices of Co, Cr, Ni, Pb and Mn in the Covenant University farm were within low to high contamination, while As was within medium to high contamination. In Landmark University farm, the pollution indices of Pb, Cu, Zn, Co and Cd ranged from low to medium, while As has pollution index within low to high contamination. Results showed elevated concentrations of As in all samples. Ca-Mg, P-Mg, Fe-Al, Ca-K, Mg-K and Na-K paired nutrients were positively correlated at 5% level of significance in both farmlands, indicating similar increase in both farmlands. Also, the geospatial maps revealed zones of high and low accumulation of essential macro nutrients within the farmlands. Landmark University farmland indicated higher soil salinity than Covenant University farm land. Soil temperature (ST) data at Covenant University farm ranged from 296 - 314 K, while ST at Landmark University farm ranged from 289 - 317 K. Soil moisture content data for both farms ranged from 23 – 113 $m^3/m^3$ and 10 - 110 $m^3/m^3$ in Covenant and Landmark University farms, respectively. The sandy gravelly soil of Landmark University farm is suitable for the planting of root and tuber crops such as carrot, yam, potatoes, turmeric and beets. Cabbage, leafy vegetables and lemon grass can be grown successfully in Covenant University farm. The ecological risk assessment of toxic metals, showed that arsenic may present a moderate to very high biological risk to both plants and animals that feed on the soil of both farm lands. The site-specific information of the farm sites has been provided. This study provides database that can serve as useful guide in soil management decision making for better yield.



**Keywords**: Electrical resistivity, Food security, Geochemical analysis, Precision agriculture, Soil characterisation, Nigeria

# APPLICATION OF GEOPHYSICAL AND GEOCHEMICAL METHODS FOR SOIL CHARACTERISATION IN SUSTAINABLE PRECISION AGRICULTURE IN SELECTED FARMS

**BY**

**KAYODE, OLUSOLA TITILOPE**
**(MATRIC NO: 13PCE00497)**
**B.Sc Geology, University of Ado Ekiti, Ado – Ekiti**
**M.Sc Industrial Physics (Applied Geophysics), Covenant University, Ota**

**A THESIS SUBMITTED TO THE SCHOOL OF POSTGRADUATE STUDIES IN PARTIAL FULFILMENT OF THE REQUIREMENTS FOR THE AWARD OF THE DEGREE OF DOCTOR OF PHILOSOPHY (Ph.D) IN INDUSTRIAL PHYSICS (APPLIED GEOPHYSICS) IN THE DEPARTMENT OF PHYSICS, COLLEGE OF SCIENCE AND TECHNOLOGY, COVENANT UNIVERSITY, OTA.**

**APRIL, 2021**

## ACCEPTANCE

This is to attest that this thesis is accepted in partial fulfilment of the requirements for the award of the degree of Doctor of Philosophy (Ph.D) in Industrial Physics (Applied Geophysics) in the Department of Physics, College of Science and Technology, Covenant University, Ota, Nigeria.

Mr. John A. Philip ……

**(Secretary, School of Postgraduate Studies)** Signature and Date

Prof. Akan B. Williams ..…….....

**(Dean, School of Postgraduate Studies)** Signature and Date

## DECLARATION

I, **KAYODE OLUSOLA TITILOPE (13PCE00497)**, declare that this research was carried out by me under the supervision of Prof. Ahzegbobor P. Aizebeokhai of the Department of Physics, College of Science and Technology, Covenant University, Ota, and Dr. Abiodun M. Odukoya of the Department of Geosciences, Faculty of Science, University of Lagos, Akoka. I attest that the thesis has not been presented either wholly or partially for the award of any degree elsewhere. All sources of data and scholarly information are duly acknowledged.

**KAYODE, OLUSOLA TITILOPE** **……**

Signature and Date

## CERTIFICATION

We certify that the thesis titled **Application of Geophysical and Geochemical Methods for Soil Characterisation in Sustainable Precision Agriculture in Selected Farms** is an original research work carried out by **KAYODE, OLUSOLA TITILOPE (13PCE00497)** in the Department of Physics, College of Science and Technology, Covenant University, Ota, Nigeria, under the supervision of Prof. Ahzegbobor P. Aizebeokhai and Dr. Abiodun M. Odukoya. We have examined and found the research work acceptable as part of the requirements for the award of the degree of Doctor of Philosophy (Ph.D) in Industrial Physics (Applied Geophysics).

Prof. Ahzegbobor P. Aizebeokhai ……
**(Supervisor)** Signature and Date

Dr. (Mrs) Abiodun M. Odukoya …...……..
**(Co-supervisor)** Signature and Date

Prof. Mojisola R. Usikalu ….……..
**(Head of Department)** Signature and Date

Dr. Michael A. Oladunjoye ..……
**(External Examiner**) Signature and Date

Prof. Akan B.Williams ……..
**(Dean, School of Postgraduate Studies)** Signature and Date

## DEDICATION

I dedicate this thesis to God the Father, Omnipotent, Omniscient and Omnipresent God, who sustained me from the beginning to the end of this work.

## ACKNOWLEDGEMENTS

My heartfelt gratitude goes to the Almighty God, the Alpha and Omega, for His unending grace, and sound health and mind He granted me to complete this work. My expression goes thus “if it had not been the LORD who was on my side”. To Him alone be all the glory!

I immensely appreciate the Chancellor, Covenant University, Dr. David O. Oyedepo, for his visionary leadership, and all members of the Board of Regent for establishing the CUCRID platform. I equally acknowledge the immediate past Vice Chancellor, Covenant University, Prof. Aderemi A. Atayero, the Acting Vice Chancellor, Prof. A. B. Williams, the current Vice Chancellor, Prof. Abiodun H. Adebayo, the Registrar, Dr. Oluwasegun P. Omidiora and members of the management team for their support and several training platforms made available during the course of this work. I also acknowledge Dr. Oluwasegun P. Omidiora, the present Registrar of Covenant University, for his assistance during my field work exercise at Omu-Aran through Dr. Ezenwoke A. Azubuike, the former Registrar of Landmark University. I am thankful to the immediate Acting Dean, School of Postgraduate Studies, Prof. Obinna C. Nwinyi, the Dean, School of Postgraduate Studies, Prof. Akan B. Williams and the Dean, College of Science and Technology, Prof. Temidayo V. Omotosho, for their commitment to ensuring a speedy completion of the Ph.D programme.

Special thanks go to my supervisor, Prof. Ahzegbobor P. Aizebeokhai for sacrificing his time to help improve the quality of this thesis with constructive criticism of each chapter despite his tight schedule as the immediate past Head, Department of Physics. Also, to my co-supervisor, Dr. Abiodun M. Odukoya, for her motherly support and advice.

I appreciate the Head, Department of Physics, Prof. Mojisola R. Usikalu, for her useful contribution to the thesis. I also wish to appreciate all the senior colleagues in the Department of Physics, Prof. Marvel L. Akinyemi, Prof. Temidayo V. Omotosho, Dr. Moses E. Emetere and Dr. Maxwell Omeje for their role in ensuring a quality thesis is presented from the Department. I also appreciate all the Faculty and Staff members of the Department.

I deeply acknowledge the assistance of Dr. Moses E. Emetere, Mr. Gideon Adeyemi and Mr. Ezekiel Ogunyemi with the satellite imagery aspect of the work. Also, to Jean de Chavez of Bureau de Veritas, ACME Laboratory, Canada for the timely analysis of the soil samples, I say thank you. My thanks and appreciation also go to friends and colleagues in persons of Dr. Kehinde D. Oyeyemi, Mr. Nathaniel Obafemi, Mr. Emmanuel Ogunwale, Mr. Oladapo Oyetade, Mr. Segun Ayanbisi and Mr. Alaka Omotayo for the assistance rendered during my field work exercise at both Covenant University farm and Landmark University farm.

I appreciate the kind gestures of Mr. Richard Nwadimuya, the human resource manager of Landmark University farm for helping to recruit workers from Omu-Aran that assisted me on the field. I acknowledge Dr. Hilary Okagbue for helping with the statistical analysis aspect of the work. I also acknowledge the moral support and encouragement of Dr. Olusegun O. Adewoyin, Dr. Anuoluwa A. Akinsiku, Dr. Justina A. Achuka and Dr. Imhade Okokpujie.

I deeply appreciate the unflinching support of Dr. Molu Olumolade referred to as “Big Daddy” for sponsoring my soil analysis at the Acme Laboratory in Canada. My deepest appreciation goes to my mom, Pastor Mrs. C. M. Ogunleye, for her unrelenting prayers and words of encouragement that upheld me throughout the research work. To my late dad, Pastor, Engr. Kayode Ogunleye, for the confidence and godly virtues he imputed in me to overcome every life challenge. My siblings, Pastor Mrs. A. Ojeifo, Mrs. Okanmiyin Ogundele, Funmilayo and Deacon Barrister Moyoninuoluwa, thank you for being there for me. Also, my appreciation goes to supportive extended family members such as Pastor Chuks Ojeifo, Pastor Gideon Oladokun and Mrs. Alice Oladokun, Deacon Gbenga Oladokun and Mrs. Opeyemi Oladokun.

Finally, I submit that it has been God’s love and your prayers that I am alive to complete this research study.

# TABLE OF CONTENTS

# LIST OF TABLES

## LIST OF FIGURES

## LIST OF ABBREVIATIONS

| | |
|---|---|
| CU: | Covenant University |
| EU: | European Union |
| FAO: | Food and Agricultural Organisation |
| GIS: | Geographic Information System |
| GPS: | Ground Positioning System |
| ICPMS: | Inductively Coupled Plasma Mass Spectrometry |
| LU: | Landmark University |
| MERRA: | Modern-Era Retrospective Analysis for Research and Application |
| NASA: | National Aeronautics and Space Administration |
| PA: | Precision Agriculture |
| SMC: | Soil Moisture Content |
| SOC: | Soil Organic Carbon |
| SOM: | Soil Organic Matter |
| UV: | Ultra Violet |
| UNESCO: | United Nations Educational Scientific and Cultural Organisation |
| USEPA: | United State Environmental Protection Agency |
| USGS: | United State Geological Survey |
| VES: | Vertical Electrical Sounding |
| WHO: | World Health Organisation |

## ABSTRACT

All soils have potential for high yield for specific crops. Nigerian soils have potential for medium to high yield, but poor farming practices including the misuse of chemical fertilizers result in a number of constraints such as soil salinity, degradation and declining fertility, which militate against high crop yields. Nigeria, currently battling with food insecurity because population growth is not commensurate with agricultural production. Thus, there is need for urgent intervention in the agricultural sector. The aim of this study was to integrate geophysical and geochemical methods for sustainable precision agriculture in two farm sites of Covenant University and Landmark University, Nigeria. In this study, electrical resistivity, geochemical and satellite imagery methods were used for soil characterisation in farm sites at Covenant University, Ota, Southwest and Landmark University, Omu-Aran, North-central Nigeria between June, 2018 and January, 2019. The electrical resistivity data were processed using RES2DINV and Win-Resist software. Geochemical analysis of soil samples from the sites was conducted using ICP-MS in ACME laboratory, Canada. Monthly MERRA satellite data was used to determine the soil temperature and soil moisture content while soil salinity was estimated from Landsat-8 satellite imagery. The study showed that electrical resistivity of the topsoil in Covenant University farm ranged from 120 -500 Ωm, while that of Landmark University farm ranged from 345-527 Ωm. The soil types delineated at the Covenant University farm were clayey sand and lateritic clay; sand/lateritic gravelly sand was delineated at Landmark University farm. Potentially toxic elements were detected in the soil samples of both sites; arsenic (As), chromium (Cr), lead (Pb) and copper (Cu) exceeded FAO/WHO recommended standard limits in Covenant University farm. The pollution indices of Co, Cr, Ni, Pb and Mn in the Covenant University farm were within low to high contamination, while As was within medium to high contamination. In Landmark University farm, the pollution indices of Pb, Cu, Zn, Co and Cd ranged from low to medium, while As has pollution index within low to high contamination. Results showed elevated concentrations of As in all samples. Ca-Mg, P-Mg, Fe-Al, Ca-K, Mg-K and Na-K paired nutrients were positively correlated at 5% level of significance in both farmlands, indicating similar increase in both farmlands. Also, the geospatial maps revealed zones of high and low accumulation of essential macro nutrients within the farmlands. Landmark University farmland indicated higher soil salinity than Covenant University farm land. Soil temperature (ST) data at Covenant University farm ranged from 296 - 314 K, while ST at Landmark University farm ranged from 289 - 317 K. Soil moisture content data for both farms ranged from 23 – 113 $m^3/m^3$ and 10 - 110 $m^3/m^3$ in Covenant and Landmark University farms, respectively. The sandy gravelly soil of Landmark University farm is suitable for the planting of root and tuber crops such as carrot, yam, potatoes, turmeric and beets. Cabbage, leafy vegetables and lemon grass can be grown successfully in Covenant University farm. The ecological risk assessment of toxic metals, showed that arsenic may present a moderate to very high biological risk to both plants and animals that feed on the soil of both farm lands. The site-specific information of the farm sites has been provided. This study provides database that can serve as useful guide in soil management decision making for better yield.



**Keywords**: Electrical resistivity, Food security, Geochemical analysis, Precision agriculture, Soil characterisation, Nigeria

# CHAPTER ONE
# INTRODUCTION

## 1.1 Background to the Study

Precision agriculture is a modern farming practice that makes food production more efficient and large fields well managed. It is a whole-farm management approach based on information technology, remote sensing and various data gathering techniques (Allred et al., 2004). The product of technological developments that promote spatial understanding of soil-water-plant relationships using soil electrical conductivity measurements is termed precision agiculture (Corwin & Lesch, 2003). Precision agriculture is also a new management technology based on georeferenced information for controlling agricultural systems (Varella, Gleriani & Santos, 2015). This agricultural practice works on the integration of soil, plant and climate characteristics, and the application of monitoring processes (Vieria, Fernandez, Vega & Keizer, 2015). When properly utilized, precision agriculture helps farmers to manage and conserve soil for sustainable food production. In countries like USA, France and Germany, various geophysical techniques such as electromagnetic induction, electrical resistivity, ground penetrating radar (GPR) and remote sensing have been used to determine soil parameters and their spatial and/or temporal variability (Tokekar, Hook, Mulla & Isler, 2016). Precision farming helps to minimize the environmental impacts of agricultural activities and allows for optimum crops yield with little or no use of chemical fertilizers and pesticides thereby; exploiting the farm soils more efficiently and sustainably (Balafoutis et al., 2017).

Accurate knowledge of soil characteristics is very useful in agricultural and environmental impact analyses. Agriculture is an integral part of any buoyant economy; thus, the implementation of new methods for boosting crop production must be imbibed by any country that aspires to achieve food security. Population growth, decline in global oil price and its impacts on the economy have further necessitated the need for precision farming. However, information on the spatial and temporal variability of soil properties is needed for agricultural, engineering and forestry applications, as well as for erosion and run-off simulations (King et al., 2005).

Nigeria is endowed with vast population and a range of ecological belts that can enable the production of a wide variety of agricultural produce such as cereals, legumes, roots, fruits, vegetables, cash crops, forestry and shrubs, livestock and fishery; however, the nation is still bedeviled with poverty and hunger. In fact, Nigeria has been recently tagged the poverty capital of the world (Adebayo, 2018). One of the reasons for this is that the Nigeria agricultural production system has not kept pace with the trends in drastic population increase and technological development. The sector has largely been left to peasant farmers that use little or no technology. Over time, scarce foreign exchange is used for importing food produce such as rice, fruits and agro raw materials to balance the demand and supply chain. However, currently Nigerian government has ordered the closure of its border with the Benin and Niger Republic as a result of the massive smuggling activities; especially, of rice, taking place on that corridor. Consequently, this has necessitated the need for governmental agricultural policies, which has sent more people back to the farms and the country has saved huge sum of money. Hence, there is a need to adopt precision agriculture (PA) as an approach to farm management in other to boost crop yield and attain food security.

Over time, farm management decision making and improved economy efficiency operations have been enjoyed by the agricultural managers as a result of information communication technology. The rate of development in technology is opening new ways for meaningful changes in agricultural and crop management decision making. Therefore, interdisciplinary approaches are required to boost the understanding of the complex interactions between several factors affecting the growth of crops and agricultural decision making (Yemefack, Njomgang & Rossiter, 2019). The principles of geophysical exploration have been utilized in soil science non-intrusively for a substantial period (Allred, Ehsani & Daniels, 2008). The geophysical methods are non-destructive and very sensitive to variations in the subsurface physical properties thereby; offering a very desirable tool for characterising the subsurface properties without pitting. Geophysical soil investigation tends to be heavily concentrated on the interval from the ground surface to a depth of about two meters (2 m) depending on the geological environment as well as the plant/crop to be cultivated. At this depth of investigation, all or most of the whole soil profile and the crop root zone is usually covered (Allred et al., 2008).

Precision/modern farming practices are less labour intensive and give specific attention to crop development than the traditional farming practices because there is greater reliance on machinery and technology (Table 1.1). Also, soil quality improvement and precise management of all production factors in time and space for consistent high-level production without causing environmental damages require precision agricultural practices (Cassman, 1999). Brady & Weil (1999) defined soil quality as the capacity of a specific soil to function, within managed or natural ecosystem boundaries, sustaining plant and animal productivity, maintaining air and water quality and supporting human health. Thus, soil quality assessment speculates the interactions within the biological, chemical and physical properties, processes, and each resource unit (Karlen, Andrews & Doran, 2001; Parent, 2017). Geophysical methods such as electrical resistivity, electromagnetic induction and ground penetrating radar have been used to address a number of environmental and agricultural practices (Jayawickreme, Jobbagy & Jackson, 2014; Bitella et al., 2015). Particularly for near-surface investigations, geophysics provides information that can be used to estimate the physical properties of the shallow layers of soil and subsoil (Bitella et al., 2015). Improvements in soil management and monitoring for its effective utilisation have been achieved by tools such as remote sensing, global positioning system (GPS) and geographic information systems (GIS). These tools become necessary as achieving sustainable agricultural and environmental management require better understanding of the soil properties at increasingly higher resolutions.

Furthermore, geophysical methods have been applied to various aspects of agriculture such as mapping the depth of flood deposited sand on farmlands (Corwin & Lesch, 2005), monitoring soil nutrient from manure applications (Toushmalani, 2010; Heil & Schmidhalter, 2017), soil quality improvement surveys (Puckett, Collins & Schellentrager, 1990), measurement of micro-variability in soil profile horizon depths (Collins & Doolittle, 1987), site-specific management units (Nawar, Constanje, Halcro, Mullar & Mouazin, 2017), spatial variability of soil quality (Doolittle and Brevik, 2014), bedrock determination in glaciated landscape with thin soil cover (Nishiyama et al., 2019) and plant root biomass surveying (Amato et al., 2009; Binley et al., 2015). Also, in soil salinity assessment (Jadoon et al., 2015) and golf course drainage pipe detection and farm field (Corwin and Lesch, 2005; Douaoui, Nicholas & Walter, 2006; Allred et al., 2018). Therefore, the future of precision agriculture rests on the understanding, reproducibility and reliability of these technologies.

Precision agriculture ensures that the soil and crops receive exactly what they need for optimum growth and productivity. Therefore, this research is concerned with the evaluation of soil characteristics for sustainable precision farming using remote sensing, electrical resistivity and geochemical methods in two sites locations namely: Ota in Southwest and Omu-Aran in North-central Nigeria, respectively.

**Table 1.1**: Traditional farming and precision farming practices

| S/N | Traditional Farming | Precision Farming |
|---|---|---|
| 1 | Unit of treatment and organization: field is assumed as a homogeneous arable site Sowing same plant and variety | Arable site is considered distinct from point to point and at field scale as heterogeneous. |
| 2 | | Plant-variety specific sowing |
| 3 | Averaged plant protection damage assessment and intervention. | Plant protection treatment based on ground penetrating sensors (GPS) and point-like plant survey |
| 4 | Nutrient management based on average sample taking | GPS is used for nutrient management and taking point-like sampling. |
| 5 | Same machine operation practice | Machine operation adjusted to arable site |
| 6 | Unified plant stock in space and time | At arable sites, unified plant stock are organized into homogeneous blocks |
| 7 | Few data influencing decision preparation | Lot of data influencing decision preparation |
| 8 | Information and communication tool part task supported | Information technology is present in all spheres of production |

Source: Katalin (2011).

## 1.2 Statement of the Problem

Globally, the demand for energy, food and raw materials has multiplied due to population growth and has resulted to a decline in the availability of cultivable land and freshwater resources (Sadeghi, Noorhosseini & Damalas, 2018). In 2018, 821 million of world population was estimated to have suffered hunger and if nothing changes, the target of achieving food security by 2030 may be short-lived (FAO, 2019a). Overcoming the challenge of inadequate crop production over the years, the use of fertilizers and pesticides have been dependent on; improper use of fertilizers and pesticides is economically wasteful and can potentially contaminate both surface water and groundwater resources which could pose serious environmental and health threat. Karlen and Rice (2015) noted that the extent of inappropriate agricultural management practices with adverse effects on soil quality; especially, as it relates to crop production and sustainability, has become a global concern.

Nigerian farmers had limited capacity to feeding its teeming population and used techniques that adversely affect soil fertility, groundwater and biodiversity. Unless farmers are supported with adequate soil information, the problem might remain with us for a long time. It is, therefore, paramount to study soil characteristics and its effects on crop production in selected locations in southern and north-central Nigeria using geophysical and geochemical methods coupled with satellite imagery and GIS to ascertain the soil status, boost crop yield and reduce environmental degradation.

### 1.2.1 Research Questions

This study seeks to address the following research questions:

i. How do geophysical and geochemical tools assist in precision agricultural researches to delineate soil profiles and address the effect of soil health?
ii. How does satellite imagery and geographic information system help in determination of soil health parametres such as soil temperature, moisture, and reveal areas with salinity issues on farmlands?
iii. How can geospatial maps help detect zones of interests on the farmlands?

## 1.3 Aim and Specific Objectives

The aim of this study is to integrate geophysical and geochemical methods for soil characterisation in sustainable precision agriculture in Covenant University farm and Landmark University farm, which are located in the Southwest and North-central Nigeria, respectively. The specific objectives of the study are to:

i. delineate the soil profile and assess soil health parameters using geoelectrical resistivity technique and satellite remote sensing imagery;
ii. characterise soil geochemical compositions through laboratory analyses of soil samples from the study locations using Inductively Coupled Plasma Mass Spectrometry (ICP-MS); and
iii. determine the level of concentration and geospatial distribution of essential/ macro-elements in the study area.
iv. evaluate the degree of elemental contamination and potential ecological risks using pollution indicators.

## 1.4 Justification of the Study

Feeding the ever-increasing world population will require a sustainable agricultural system that can keep pace with population growth and conserve the natural environment. Previous studies have identified some soil properties in the agricuitural soils but there is limited studies on the fertility status and geospatial distribution of contaminants in the agricultural soils. Thus, near-surface geophysics, remote sensing and geochemical methods with the advantages of rapid surveys over large areas and spatial continuity can help generate information on soil parameters that will be useful in preserving the environment as well as aiding sustainable precision agriculture.

## 1.5 Scope of the Study

The study focused predominantly on the determination of soil properties in selected locations in Southwest and the North-central Nigeria. This study adopts the use of electrical resistivity method, geochemical analysis and satellite imagery to assess the farmlands at Covenant University, Ota and Landmark University, Omu-Aran, both in Nigeria.

# CHAPTER TWO
# LITERATURE REVIEW

## 2.1 Soil and Agricultural Practices in Nigeria

### 2.1.1 Soil Classification

Soil is the loose material of the earth surface that comprised humus and disintegrated rock which provides the medium for plant growth. It consists of inorganic particles and organic matter that provides the source of water and nutrients for plants and structural support used in agriculture. Basically, soil comprises of organic matter, minerals, water and air in varying proportions (McCauley, Jones & Jacobsen, 2005). Soil condition and water availability, if effectively managed, will help boost food production and address food crisis in the nation (Food and Agricultural Organisation (FAO), 2005). The soils in southern Nigeria as identified by Smyth and Montgomery (1962) consist mainly of the Egbeda, Ondo and the Iwo Classifications. They are further divided into hill-creep, sedentary and hill-wash soils. The Iwo Classification soils are derived from coarse gneisses and coarse-grained granitic rocks; the Ondo Classification soils are derived from gneisses and medium-grained granitic rocks; and the Egbeda Classification soils are from schists and fine-grained biotite gneisses. Soil classifications such as the Akure, Ondo, Odigbo, Ife, Egbeda, Makun, Olorunda, Ibadan, Apomu and Owo also emanate from each of the previous classifications. The identified soils are suitable for tree crops such as kola, oil palm, rubber, cocoa, and coffee and also support the development of the lowland rainforest (Ekanade, 2007).

Nigeria has a wide diversity of soil with different levels of fertility (Raimi, Adeleke & Roopnarain, 2017). Salako (2003) gave a characteristic feature of soils in Nigeria according to Food and Agricultural Organization (FAO) classifications as stated in Table 2.1. The major soil types according to FAO soil taxonomy legends are Acrisols, Alisols, Fluvisols, Regisols, Gleysols, Ferrasols, Lixisols, Cambisols, Luvisols, Nitosols, Arenosols and Vertisols. These soils vary in their potential for agricultural use. Iloeje (2001) generally classified Nigerian soils into four (climatic) zones of soil classifications. The groups include the interior zone of laterite soils, northern zone of sandy soils, alluvial soils zones and the southern belt of forest soils.

**Table 2.1**: Some characteristics of agro-ecological zones of Nigeria

| Agro-ecological zones | Major soil types (FAO Classification) |
|---|---|
| 1. Humid forest | Ferrasols, Nitosols and Gleysols |
| 2. Derived/Coastal savanna (Moist savanna) | Ferrasols, Luvisols, Nitosols, Arenosols, Acrisols and Lithosols |
| 3. Southern Guinea savanna (Moist savanna) | Luvisols, Acrisols, Ferrasols and Lithosols |
| 4. Northern Guinea savanna (Moist savanna) | Luvisols |
| 5. Mild altitude savanna | Ferrasols and Nitosols |

Source: Salako (2003).

Northern zone of sandy soils is found in the extreme north with proximity to the Sahara desert characterised by soils formed by deposition of sand and wind (Iloeje, 2001). These northern sandy soils are very good in the production of cowpea, groundnut, millet and sorghum. This zone is made up of a mixture of clay and sand. They are seasonally flooded and poorly grey to black clay soils, sticky and impervious to water and have low fertility (Iloeje, 2001). Apart from the lateritic soils discovered in this zone, prospects for cotton production expansion can be offered by the productive and rich soil of the Biu Plateau (Iloeje, 2001).

Rice is the most staple food in Nigeria that can be grown on a wide range of soils with appropriate fertilisation (Aondoakaa & Agbakwuru, 2012). Rice can be grown on the alluvium soils such as in China and the impermeable heavy clay of central Thailand. Although, fertile riverine alluvium soils and the monsoon clay loam soil are the best for rice cultivation because of their high-water retention capacities (Dou, Soriano, Tabien & Chen, 2016). Intense and continuous fertilization is also required for sustainable rice cultivations (Bado, Djaman & Mei, 2018).

### 2.1.2 Soil Characteristics

The characteristics or properties of soil allows for the determination of the type of soil that is in an area. More about regional history and any shift within the region can be learnt by the scientists using the characteristics of soil. The category of soil characteristics are three (3) namely physical, chemical and biological (Figure 2.1). Physical properties of soil are vital for determining the suitability of soil for any agricultural, engineering and environmental uses (Phogat, Tomar & Dahiya, 2015).

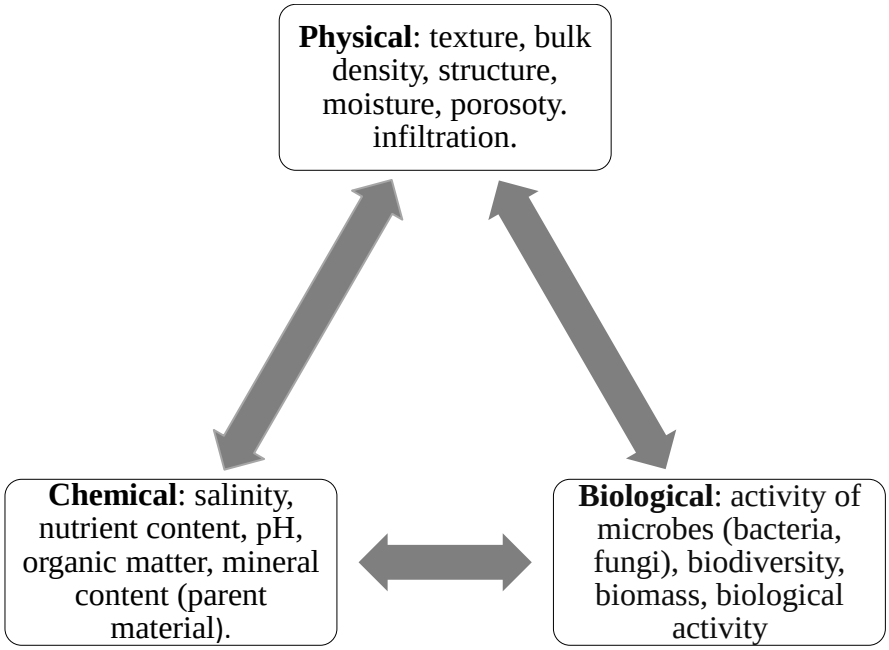


**Figure 2.1**: Classification of soil characteristics by its basic properties.
Source: McCauley et al. (2005)

The physical properties influence both the chemical and biological properties (Phogat et al., 2015). The ease of penetration of roots, movement and retention of water, flow of air and heat, and availability of water and nutrients to plants are directly linked to the physical properties of soil (Phogat et al., 2015; Husson & Reiley, 2018). Nutrients such as phosphorus, potassium, and nitrogen, pH and water are some of the chemical components of soil (Sassenrath, Davis, Sassenrath-Cole & Riding, 2018). This soil chemical properties are vital in the planning of fertigation (Kant & Kafkafi, 2013), and affect soil biological activities (Melo, Delarica & Guede, 2018).

Soil chemical properties have significant effect on the biogeochemical activity of microbial communities (Melo et al., 2018). Sassenrath et al. (2018) also noted that soil chemical components are largely dependent on the soil physical properties. The water holding capacity of the soil partially depends on the size of the mineral particles. Smaller mineral particles significantly have smaller pore size, stronger force to hold water and greater surface area while larger soil pores drain out water quickly (Sassenrath et al., 2018). Therefore, clay soils with small pores and very small soil particles have higher water holding capacity than the sandy soils (Sassenrath et al., 2018). Soil characterisation requires either the extensive field measurements or calibration of several parameters such as texture,

moisture content and organic carbon from reflectance spectra, multivariate statistics and machine learning algorithms (Rossel et al., 2016; Munnaf, Mouazen & Nawar, 2019).

### 2.1.3 Climate

The North-central Nigeria's climate is tropical and of dry grassland Savanna type. Monthly rainfall distribution extends from April to October, with a unimodal peak in August (274.23 mm) (Olayemi et al., 2014). The months of January, February and March are completely rainless while very little rainfall is recorded in April and November; this is regarded as pre- and post-rainy season transition periods. The mean annual humidity in North-central Nigeria is barely above 50% (Olayemi et al., 2014).

Ota in Ogun State, Southwestern Nigeria possesses climate of tropical rain-forest with two distinct climatic conditions; the dry season running through December to March and the rainy season which is from April to October with an interruption in August (Ufoegbune, Atanley, Eruola, Makinde & Ojekunle, 2016). The climate of Ota is humid with a variability of very hot to wet and average monthly temperature of about 28˚C (Ufoegbune et al., 2016). Agricultural produce in Nigeria is mainly rain fed; therefore, unprecedented rainfall variation makes planning difficult for farmers (Anabaraonye, Chukwuma & Okafor, 2019).

### 2.1.4 Relief and Drainage

Southern Nigeria is dominated by the plains which rise gently from the coast northwards to the area of crystalline rocks where isolated rock hills rise abruptly above the surrounding plains (Oyinloye & Oloukoi, 2012). The Idanre hill rises to about 981 meters above the sea level, poses as the highest of these inselbergs. The plains extend into the western side of the Niger Delta, a swampy area of about 3,885 km, composed of the coastal plain sands and lignite series of Cenozoic age in its northern part and of alluvial mud in its southern part (Oyinloye & Oloukoi, 2012). Rivers and north-south coastal rivers which follow regular courses dominate the region. The rivers drain into the sea. In the basement complex of this region, rivers are generally controlled by joints on the more impervious rocks and the trend of the foliated rocks. This structural control is well displayed by the rivers; the major rivers, for example, Ogunpa, Ogbese, Oluwa, Ogun, Osun, Oni, Owena, Shasha and Ominla, are generally parallel but with a dendritic drainage pattern. The gradient of the river valley is extremely low, in the coastal plain where the rivers deposit their load;

thereby, giving rise to the formation of braided channels (Ekanade & Egbe, 1990). Soil formation is particularly rapid in sedimentary terrains with low reliefs and high infiltration rates than in steeply regions where erosion thins out soil profiles, thereby resulting in the formation of less pedogenetically developed soil (Silva, Siqueira, Coastal, Guedes-Filho & Silva, 2018; Dortzbach, Pereira, Cunhados Anjos, Fontana & Silva Neto, 2016).

The North-central has three (3) broad physiographic units especially the Jos plateau landscape and has been divided into; dissected terrain, undulating terrain, and the hills and mountains (Odunuga & Badru, 2015). The relief in nature is intently related to the underlying rock types where older and impenetrable younger granites have formed an impervious core forming hill masses of the recent landscapes of ≥ 1500 metres above the sea level that have been formed through a long erosional history. The joint pattern has generally controlled the morphology of these hills (Odunuga and Badru, 2015). The north central has a radila drainage system which is the major source of several rivers such as the Ngell, Karami and Kaduna, which feed the Mada River; the Niger, Dep, Ankwe, Wase and Shamanker flowing into the Benue; Maijuju, Lere and Bagei, suppling the Kano; and the Gongola, Delimi, Jamaari, Misau and Bunga, which nourch Lake Chad occasionally. The Gurara falls is one of the notable waterfalls the irregular southern slopes of the plateau's steep have produced (Odunuga & Badru, 2015).

## 2.2 Determination of Soil Parameters

Soil parameters such as soil organic matter (SOM), soil moisture content (SMC), temperature, soil drainage, porosity or pore spaces, macro- and micro-nutrients, trace elements and many others when in the right quantity and state are what makes for a healthy crop (Tale & Ingole, 2015). Proper implementation of farm management practices is crucial to the understanding of the soil chemical and physical conditions (Tale & Ingole, 2015).

### 2.2.1 Determination of Soil Moisture Content

Soil moisture content is one of the vital properties of soil. It is the ratio of the weight of water to the weight of solids in a given mass of soil. It is the quantity of water that the soil contains. Water content is widely used to determine material's porosity value and even saturation (Van der Wal et al., 2015). Rainfall or irrigation of plants are the major ways in which water is added to soil in the tropics. As more pores become filled with water as a

result of air exchange, soil moisture increases (Margenot, Parikh & Caldron, 2019). Excess water in soil will infiltrate downwards when all pores become filled with water until irrigation or rain ceases (Rajana, Dass & Venkatesh, 2019). In agriculture, industrial irrigation is a major challenge as under-watered crops may wither or die, putting all investment into a ruin. On the other hand, excess water in soil can lead to soil erosion resulting in significant loss of top-soil and decline in agricultural productivity (Holz, Williard, Edwards & Schoonover, 2015; Tarpanelli, Massari, Giabatta, Filippucci, Amarnath & Brocca, 2017). However, soil water holding capacity varies for different soil types. Peters, Huntington and Hoke (2013) gave the available range of soil water for different soil textures and clearly stated that peat has the highest available holding capacity of 1.9 - 2.9 in/ft (0.05 – 0.24 m) whereas coarse sand has least available water capacity of 0.2 - 0.8 in/ft (0.01 to 0.02 m).

A good understanding of the hydrological cycle will assist in the management of rainwater and soil water. Hydrologic cycle, that is the spatial structure of water storage and subsurface flow paths, affects crop yield pattern for the agricultural soils (Yourek, Brooks, Brown, Poggio & Gasch, 2019). Solar and planetary forces circulate water on the earth and there is a complicated relationship between precipitation and run-offs (Hao, Su & Singh, 2018). Soil moisture content is a vital measurement for weather forecasting, drought and flood predictions, agriculture and more. The amount of water in a soil will determine how much microwave energy such soil emits, as all soil types emit microwave energy. The drier the soil, the more the microwave energy and the wetter the soil, the less the microwave energy the soil emits (Sharma, Kumar & Srivastava, 2018).

### 2.2.2 Soil Organic Matter

Soil organic matter (SOM) is also referred to as soil organic carbon in some contexts. SOM is termed as all organic materials found in soil irrespective of the origin or state of decomposition (Baldock & Skjemstad, 1999). SOM consists of six elements namely carbon, hydrogen, oxygen, nitrogen, phosphorus and sulphur; it is usually estimated through a conversion factor as it is difficult to measure its content in soil directly (Delgado et al., 2015). Maintenance as well as improvement of soil properties is the vital role plays by soil organic matter in soil management practices. Bartsev and Pochekutov (2016) proposed a new modification of the simple continuous model of soil organic matter

transformation. The modification permits the conversion of SOM distribution over humification rate to SOM distribution over depth and vice versa. Also, Ojanen, Makiranta, Penttila and Minkkinen (2017) added the popular belief that logging residue piles have notably increased the decomposition of the underlying peat soil leading to large carbon dioxide emissions, with straightforward decomposition measurements. Their result indicates that logging residue piles can significantly lowered soil temperature and subdued its diurnal variations.

Priming, a chemical and biological effect, has been suggested to increase decomposition. It is a combined effect of carbon (C) and nutrient inputs used to either accelerate or reduce the microbial decomposition of soil organic matter (SOM). The important steering factor of priming effect have been indicated as the physicochemical similarity between added organic compounds and soil organic matter fractions (Di Lonardo et al., 2018; Hicks et al., 2019). The addition of nitrogen has been observed to reduce SOM mineralization suggesting reduced microbial N-mining in higher elevation soils and no influence on SOM mineralization in lowland soils with the addition of nitrogen or phosphorus (Hicks et al., 2019). In general terms, the suitability of soil for sustaining plant growth and other biological activities is a function of chemical and physical properties of soil, many of which are a function of soil organic matter (SOM) content (Doran & Safley, 1997; Murphy, 2015).

### 2.2.3 Soil Temperature

Soil serves as storage for heat and soil temperature depends on the ratio of the solar energy absorbed to that lost from the soil. Soil temperature is affected daily by variations in air temperature and solar radiation, it also fluctuates annually (Marshall & Holmes, 1988; Wu & Nofziger, 1999; Hillel, 2003). Soil properties are majorly influenced by soil temperature. The availability of nutrients, seedling emergence and the amount of radiation received by soil gas exchange processes between the atmosphere and the soil are all influenced by soil temperature (Probert, 2000; Buchan, 2001; Lehnert, 2013; Onwuka, Ozurumba & Nkwwocha, 2016). The soil temperature also alters the mineralisation and the decomposition of soil organic matter (Davidson & Janseen, 2006). Soil water retention, availability and transmissivity to plants are also some of the effects of soil temperature (Ni, Cheng, Wang, Wai Ng & Garg, 2019).

Soil temperature has great impact for shallow geothermal applications and on agricultural production (Xing, Li, Gong, Ren, Liu & Chen, 2018). Data driven models have been developed to accurately measure daily and monthly soil temperature predictions. In United States, the new data model used for daily soil temperature predictions at 16 sites gave lower mean absolute error values compared with the traditional models used (Xing et al., 2018). Araghi, Baygi, Admouski, Martinez and Ploeg (2017) carried out a research to forecast soil temperature with hourly soil temperature data at 0300, 0900 and 1500 GMT. The data were collected from Razari Province of Iran. Artificial neural network and wavelet transform artificial neural network were used and the result indicated that wavelet transform used for the preprocessing improved the accuracy of the forecast and there was no noticeable error at a change in temporal increment using the wavelet transform artificial neural network.

Araghi, Adamouski, Martinez and Olesen (2019) also stated that increased soil temperature can enhance crop development at crop emergence and during the vegetative period. Also, soil processes such as the release of gases and the rate of nutrients from soil organic matter and evaporation rate can be impacted by soil temperature. The knowledge of soil temperature helps agronomists and engineers in decision making as regards the proper planting date, optimizing the application of pesticides and fertilizers, and in the design of drainage and irrigation systems to reduce the effects of chemical pollution on soil and groundwater (Sattari, Dodangeh & Abraham, 2017).

The finding of Gahoonia and Neilsen (2003) corroborated that of Yilvainio and Pettoviori (2012); hence, an increase in soil temperature from 278 K - 298 K caused a significant increase in water-soluble phosphorus. Also, low temperature hinders the release of phosphorus from organic matter and therefore, soils with low temperature have low availability of phosphorus. Pepper, Gerba and Brusseau (2019) also showed evidence of soil temperature influencing the physical, microbiological and chemical processes that occur in soil, but did not attribute this to depths in the subsurface as soil-zone temperature fluctuates all through the year with respect to the above ground temperature.

### 2.2.4 Soil Drainage

A good soil is often termed a well-drained soil. Fausey (2005) stated that soil drainage is a natural process that occurs due to the force of gravity, whereby water moves through, across

and out of the soil. A well-drained soil has about half its volume in actual soil solids, and the other half as air space. This air space is further made up of large spaces and half of small spaces (Smiley, 1990). Water is essential for plant growth, but too much or too little water in the soil can result in stunted growth or death of plants. There must be a balance of air spaces and water capacity in the soil for it to sustain normal plant growth (Haroun, Idris & Syed-Omar, 2007). In periods of irrigation or rainfall, the small pore spaces hold water while the larger ones release water and refill with air to the pull of gravity (Smiley, 1990). Soil drainage has effect on the physical and chemical properties of soil that influence erodibility and stability in soil (Rhoton & Dulker, 2008). Soil drainage is an important factor to be considered when determining the type of plants that grow best in an area. Different classes of soil drainages identified include well-drained, good drainage, poor drainage and very poorly drained soils (Pereira, Brevik, Munoz-Rojas & Miller, 2017).

### 2.2.5 Soil Structure

Soil structure is the arrangement and organisation of primary and secondary particles in a soil mass. Soil particles basically control the amount of water and air present in soil. Germinating seeds and plant roots need sufficient air and oxygen for respiration; also, bacterial activities need the supply of water and air in the soil. Studies have shown that there is a positive correlation between soil organic matter (SOM) and soil structure (Simansky, Juriga, Jonczak, Uzarowicz & Stephen, 2019). However, soil structure is dynamic as a result of the bioturbation and mechanical disturbance by tillage. This dynamism is solely dependent on the soil organic matter (SOM), bulk density and clay content; making soil with higher SOM content have a higher density of cracks with smaller aperture (Diel, Vogel & Schluter, 2019).

Dexter, Horn and Kemper (1988) defined soil structure as the spatial heterogeneity of the different properties or components of the soil (Pagliai & Vignozzi, 2007). Soil particles such as sand, silt and clay, and organic matter combine together to form aggregates or clusters, that is larger particles of various shapes and sizes (Figure 2.2). These aggregates are also referred to as soil peds (occurring naturally in the soil) or clods (clusters of soil caused by tillage). The categories of this soil structure are crumb, columnar, granular, platy, prismatic, massive, blocky and single grain.

### 2.2.6 Soil Texture

Soil texture is the proportion of the three sizes of soil particles, their fineness or coarseness. Mineral matter is the general name for the inorganic material in soil and it originates from the weathering of rocks. Most soils have mineral particles in different sizes namely sand, silt and clay. Sand is the largest of the mineral particles. Sandy soil has a gritty feel touch.

Aeration is improved by the large pores of sand particles. Soils with a high percentage of sand are generally well drained as a result of the easy flow of water through it. The disadvantage of sandy soil is inability to hold nutrient and that makes it not fertile. Silt on the other hand is mid-size soil particles which has good capacity to hold water and are very fertile soils. Clay, the smallest size of the soil particles, can hold water and nutrients that plants use.

Clay has very small pore spaces, poor aeration and poor water drainage. These soil textural fractions 'sand-silt-clay' are commonly used to estimate soil properties (Martin, Reyes & Taguas, 2017).

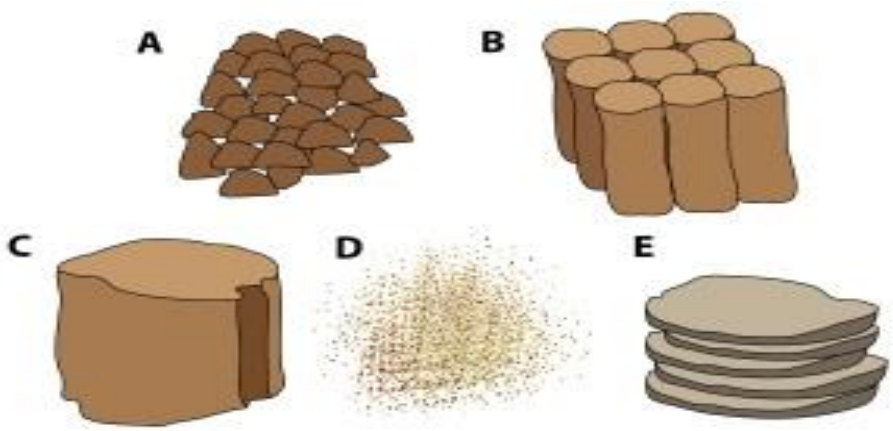


**Figure 2.2**: Types of soil aggregates: (A) blocky, (B) columnar, (C) massive, (D) single grain, and (E) platy
Source: Victorian Resources (2014)

### 2.2.7 Macronutrients and Micronutrients

Macronutrients and micronutrients are known as mineral nutrients. These nutrients in right proportion are essential for plant growth and reproduction. Both are essential nutrients needed for plant growth; macronutrients are required in high quantity while micronutrients

are needed by plants in very small quantities (Akenga, Salim, Oniditi, Yusuf & Waudo, 2014). Macronutrients are further divided into primary and secondary macronutrients. The primary and secondary macronutrients are needed in larger quantities by plants but the secondary macronutrients are less commonly yield limiting than the primary macronutrients (Korb, Jones & Jacobsen, 2002). Nitrogen, phosphorus and potassium are the primary macronutrients needed in large quantities by plants. The secondary macronutrients include calcium, magnesium and sulphur. Micronutrients include copper, manganese, boron, iron and zinc (Akenga et al., 2014).

Fertilizers are normally added in large amounts on vegetable crops; thereby, making soils around the area concentrated in soil nutrients and in higher quantities than those in grain plantation (Zhao, Li, Wang, Li & Yue, 2007). A balance of macronutrients and micronutrients is needed on the farm for a healthy and strong plant. Macronutrients create new plant cells that organize into plant tissue for the growth and survival of crops. Macronutrients are prevalent in many fertilizers to enhance green and flourishing crops (Emerald, 2015). Low concentration of micronutrients in soil has resulted in food and farm crops failing to meet the nutritional requirements in Northern Europe (Watson et al., 2012). Geochemical maps were used to identify areas that need micronutrients in order to boost crop production. Micronutrient fertilization was also used to improve the growth of sorghum in Sudan; the fertilization improved the grain quality, protein and amino acids (Ahmed, Abdalla, Inoue, Ping & Babiker, 2014).

However, soil nutrient status of a swampy area proposed for farming in Delta State, Nigeria was investigated and the result indicates a low level of phosphorus, nitrogen and all exchangeable bases status when compared with the critical levels in soils. Soil organic matter (SOM) and soil's physical properties are recommended to improve the nutrient content of the soil (Osayande, Oviasogie, Orhue, Maidoh & Osaghe, 2015). Extremely poor in fertility soil was evaluated in selected soils of Mbaise area of Imo state, Nigeria (Onwudike et al., 2016). A combination of biochar and inorganic fertilizer were used to enhance a rain-fed rice production (Oladele, Odeigah, Taiwo & Yahaya, 2018). There was an increase in soil nutrients as a result of the interaction between the biochar and the inorganic fertilizer. Soil nitrate leaching was also reduced as a result of this biochar amendment. Kristensen, Roberts, Jones, Jones, Montanarella, Panagos et al. (2019) studied the combined effect of termite bioturbation and water erosion on soil nutrients stocks along

a tropical forest in Ghana. Result revealed that upslope gravelly layer decreases soil nutrient while there was no significant effect on nutrient stock at the movement of soil material down-slope. Also, spatial modelling was used to map selected soil fertility properties in a yam plantation in northcentral and southeast Nigeria (Jemo, Souleymanou, Frossard & Jansa, 2014). Nitrogen (N) and potassium (K) showed moderate spatial dependence while phosphorus (P) showed weak spatial dependence. Jones and Olson-Rutz (2016) noted that nutrients are taken up by soil in their ionic or charged form and not in the elemental or uncharged state. Also, nutrient uptake generally in plants occur regardless of the micro-macro nutrients classification, as plants can take up large number of micronutrients as against the essential macronutrients (Jones & Olson-Rutz, 2016).

### 2.2.8 Trace Elements

Trace elements are in low abundance in natural uncontaminated earth material or plant. They are referred to as minor elements or micro-nutrients in some literature (Thornton & Webb, 1980). Essential and non-essential trace elements move through agricultural ecosystems and food chain. Some trace elements are present in soil in low concentrations but may be elevated as a result of natural processes and human activities such as mining, smelting, fossil fuel combustion, fertilizer application and agricultural practices causing serious health challenge (Banuelo & Ajwa, 1999; Senesil, Baldassarre, Senesi & Radina, 1999). However, all trace elements become toxic at elevated levels causing harm to both plants and human health (Hooda, 2010).

The trace elements found in soil in low concentration include arsenic, boron, cadmium, copper, mercury, nickel, lead, selenium, uranium, vanadium and zinc. Some trace elements are required by plants and they include boron, manganese, silicon, molybdenum, vanadium, zinc and copper; also, trace elements such as copper, cobalt, iron, iodine, zinc, manganese, molybdenum and selenium are required by animals (Thornton & Webb, 1980; Banuelo & Ajwa, 1999). In general, soil fertility and soil stability are some of the soil properties needed for plants growth. Soil fertility deals with the availability of nutrients, while soil stability is the ability of the soil to withstand erosion and this is mostly determined by soil structure and soil texture (Halim, Majumder & Zaman, 2015).

Iron (Fe) is another essential trace element in agricultural soils that plays fundamental roles in biological processes such as photosynthesis, nitrogen fixation, assimilation and respiration (Briat, 2005). Iron is typically present in insoluble oxidized form and thereby making calcareous soils with low iron content constitute about 30% of global cultivated lands (Guerinot & Yi, 1994; Mori, Mariyama, Mitsuno, 1999; Rout & Sahoo, 2015). However, flooded acidic soils containing excess soluble iron can lead to ferrous iron toxicity as a result of iron reactivity with reduced form of oxygen (Briat, 2005). Iron deficiency, which is a common agricultural problem in developing countries, does not only reduce grain yield but also affect the quality of grains (Rout & Sahoo, 2015; Irmak, Surucu & Aydin, 2008).

Potassium (K), as one of the most essential soil nutrients, is widely distributed in the earth crust as silicate minerals constituents (Manning, 2018). Inspite of this abundant potassium in the earth crust, large quantity of soluble potassium compounds accumulation suitable for soil fertility are found in few places (Manning, 2018). As abundant as potassium seems to be in the earth crust, it can be easily loss by leaching process especially, sandy soils in high rainfall zones (Mendes, Alves, da Cunha, da Silva, Evangelista & Casaroli, 2016). Soluble potassium (K), that is those dissolved in soil water and those on clay particles (exchangeable K), are the only available potassium needed for plant growth (Prajapati and Modi, 2012). Potassium (K) as a crop booster improves crop quality, increases yield and plays vital role in photosynthesis processes in plant (Prajapati & Modi, 2012).

Every plant needs calcium as it plays an important role in plant nutrition and growth. Calcium maintains chemical balance in soil, improves water penetration, and reduces soil salinity (Brown, 2018). Rare earth elements (REEs) are other elements present in many earth materials and the effect are recently being studied (Rodrigues et al., 2020). However, Jinxia, Hong, Yin and Liu (2010) have noted the toxic effects of REEs accumulation on the soil macrofauna community and have stated that the application of rare earth fertilizers in agricultural soils should be strictly controlled. REEs such as eurodium (Eu), gadolinium (Gd), lanthanum (La), samarium (Sm), terbium (Tb), selenium (Sr), cerium (Ce) and praseodymium (Pr) have been recently used in agriculture as well as in modern industries (Ramos et al., 2016). Although, few countries such as China, Germany, France and Germany have published related issues on REEs in soils in recent times, limited publications exist on the effects of REE on plants and environment (Ramos et al., 2016).

Rare earth element contents in soils depend on the parent material and the content decreases in this order: granite > basalt > sandstone (Zhu & Liu, 1988; Ramos et al., 2016).

### 2.2.9 Soil Salinity

Soil salinity is a term used to identify a condition whereby soluble salts in the soil reach a harmful level for crops. Salinity is a soil and water quality concern; thus, have profound effects on the water movement, soil structure and the microbial diversity of soils (Artiola, Walworth, Musil & Crimmins, 2019). Soil with electrical conductivity that exceeds $4\,Sm^{-1}$ (approximately 40 mM NaCl) at $25°\,C$ with an exchangeable sodium of 15% is termed saline (Shrivastava & Kumar, 2015). Soil salinity affects plants growth severely and when not quickly checked, it can change fertile land to an unproductive land resulting in economic loss (Imadi, Shah, Kazi, Azooz & Ahmad, 2016). Arid and semi-arid regions with insufficient rain and high demands for irrigation and agriculture water are peculiar to salinity. The natural causes of salinity vary from place to place and this include shallow water table due to excessive evaporation and salts concentrations, poor water quality and irrigation practices, low rainfall in hot arid and semi-arid (Artiola et al., 2019). Soil salinity is a global issue and as such, chemical treatments have been applied for years to get rid of this soil pollution (Lu & Xu, 2014). Qadir, Quresh and Ahmad (2002) noted that some of these chemical treatments such as gypsum treatment are very costly and harmful to the environment but reduces soil salinity and sodicity. The amount of arable land infected by salinity is on the increase across the world and 50% of arable land is estimated to be infected by soil salinity by 2050 (Butcher, Wick, Desutter, Chatterjee & Harmon, 2016; Machado & Serralheiro, 2017).

### 2.2.10 Nigeria Soil Fertility Maps

Nigerian soil fertility maps for calcium (Ca), potassium (K), phosphorus (P), zinc (Zn) and organic carbon content are presented in Figures 2.3 and 2.4 (Chude, Malgwi, Amapu & Ano, 2011). The available fertility maps covering the entire Nigerian states showed areas with high and low soil fertility as presented in Figures 2.3 and 2.4. The farm management practices a farmer adopts influence the level of output at the end of production year (Ogwu, Omotesho & Muhammed-Lawal, 2018). Excessive use of agrochemicals, soil nutrient mining, tillage system used, removal or loss of vegetation cover, soil fertility materials and continuous cropping can be referred to as unsustainable farming practices (Mtambanengwe & Kosina, 2007; FAO, 2017; Ogwu et al., 2018). The capacity of soil to supply essential

nutrients to crops is termed soil fertility (Bleam, 2016). Soil fertility is therefore crucial to sustainable food production and maintenance of the environment (Shah & Wu, 2019). Ayeni and Akinbani (2015) reported that the low fertility exhibited by some of the arable lands used for farming without the application of fertilizers in southwestern Nigeria might be as a result of continuous cropping or gross mismanagement of the land.

a)

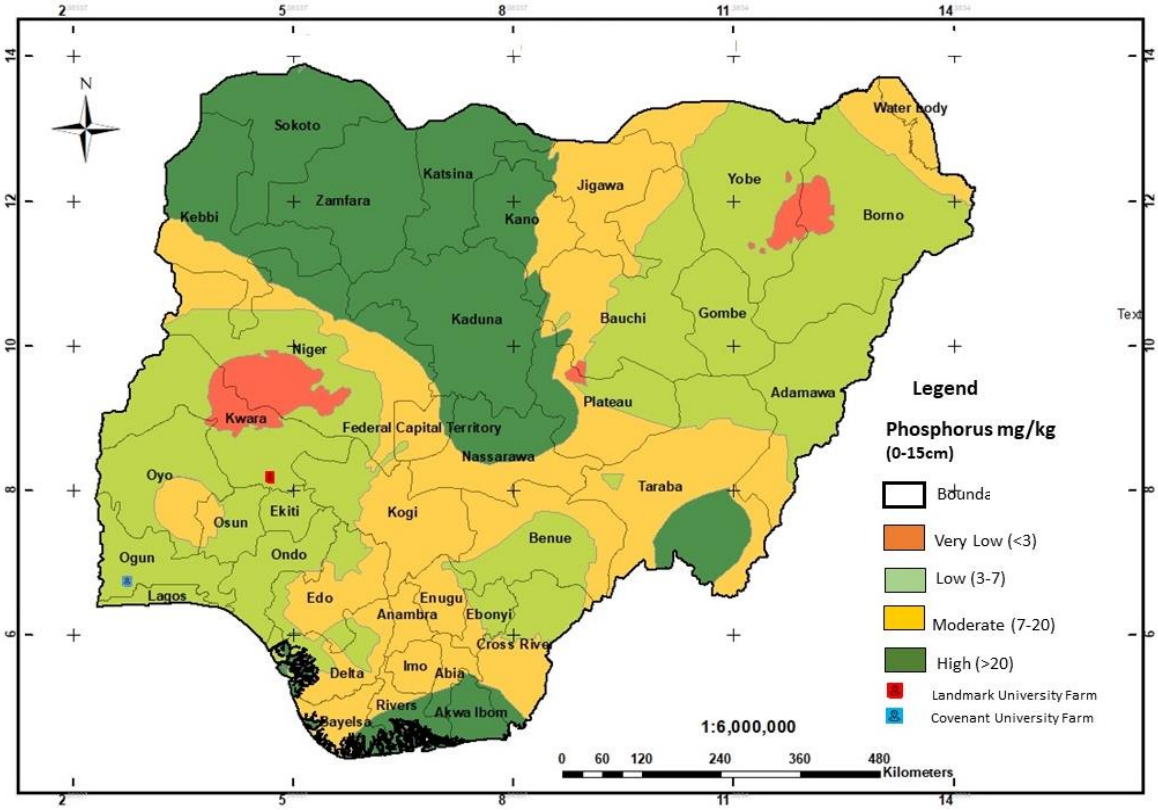


b)

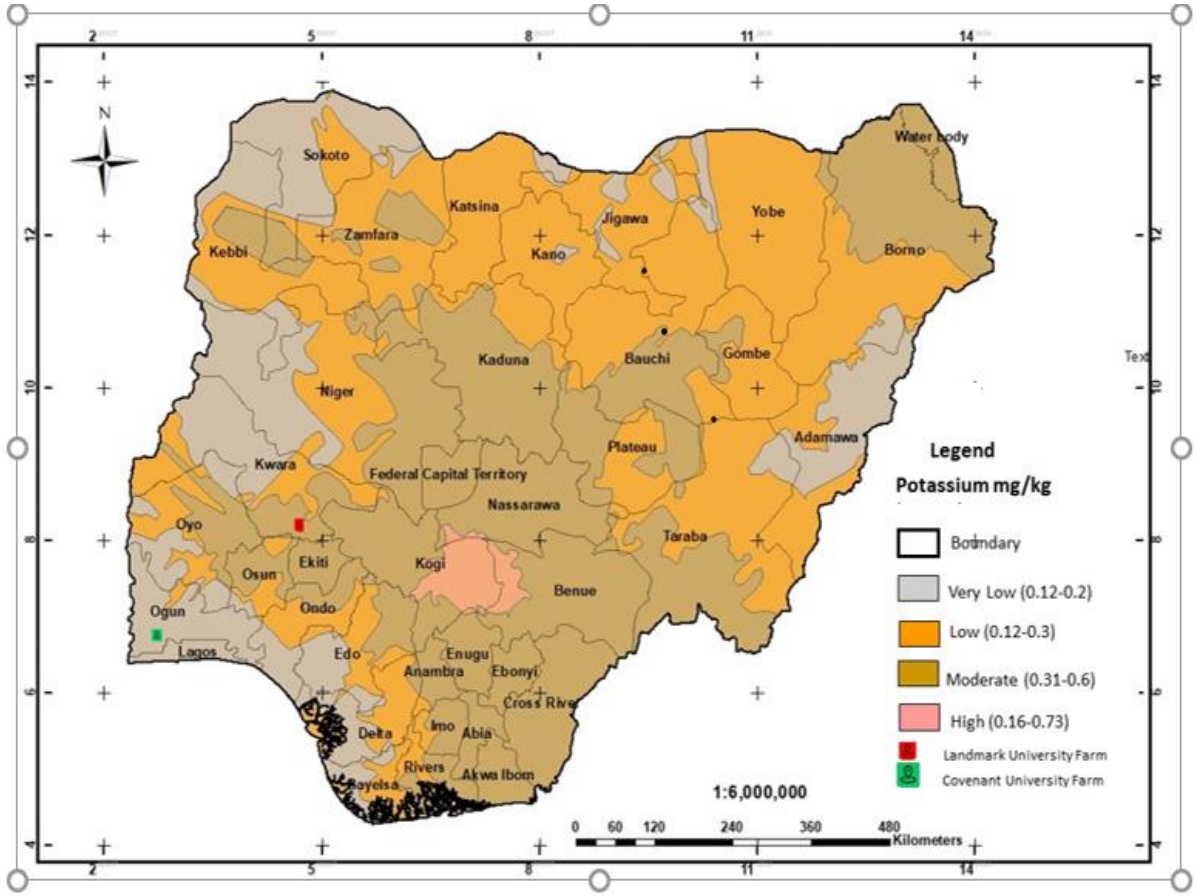


**Figure 2.3**: Nigerian geospatial maps for: (a) phosphorus, and (b) potassium
Source: Chude et al. (2011)

a)

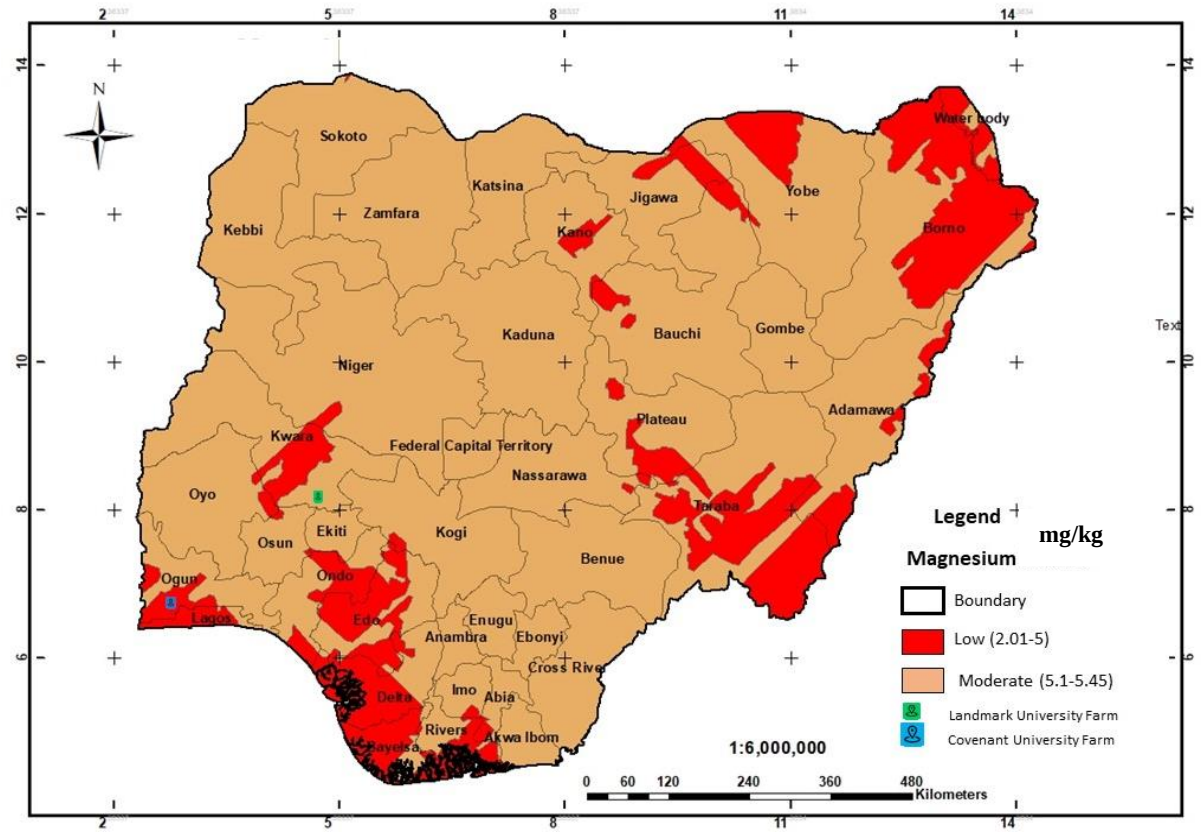


b)

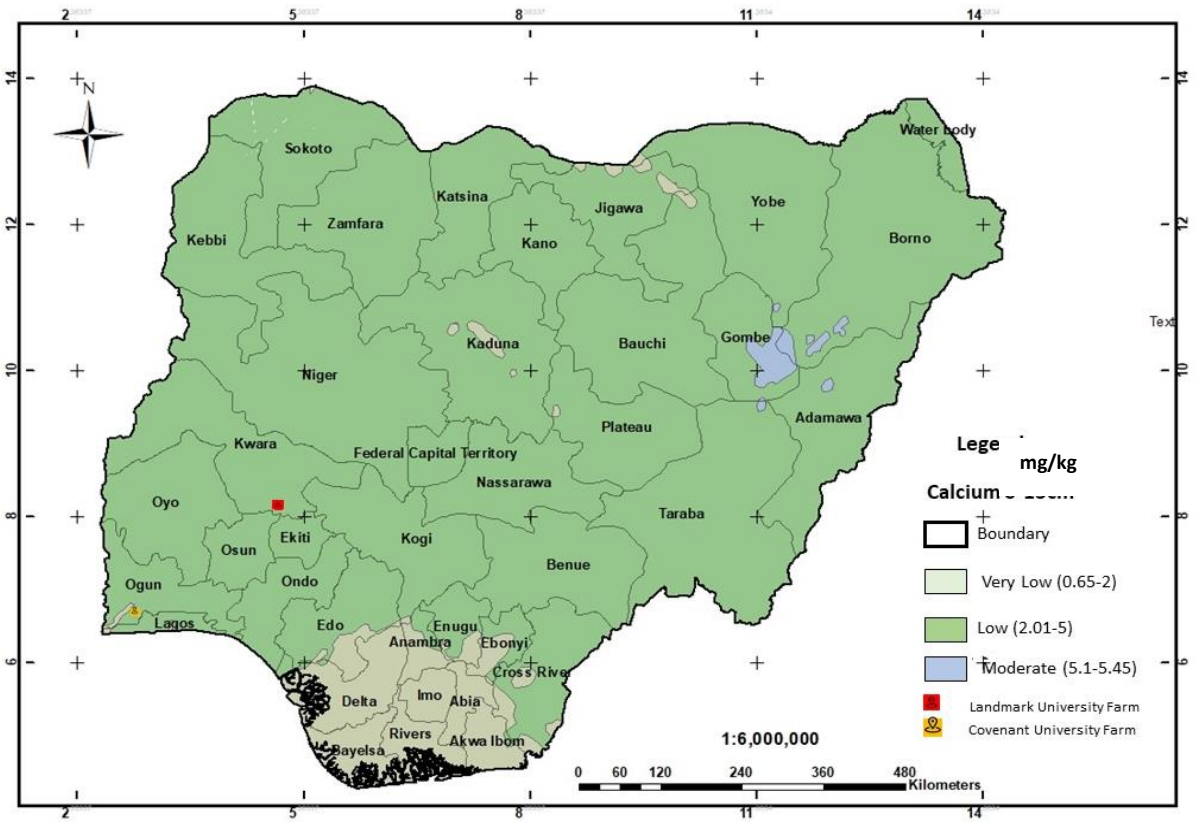


**Figure 2.4**: Nigerian geospatial maps for: (a) magnesium (Mg), and (b) calcium (Ca)

Source: Chude et al. (2011)

Nigerian soils are reported to be naturally low in fertility and get little replenishment of soil nutrients (Ojuola, 2015; Adiaha, 2016). Sub-Saharan countries of which Nigeria is one, consume low mineral fertilizer of 10 kg/hectare per year as compared with the world averages of greater than 60 kg in East Africa and greater than 120 kg/hectare per year in Asia (Ojuola, 2015).

Soil fertility entails the physical, chemical and biological components of soil properties and the interactions between these components (Smith & Powlson, 2003). However, fertile soil is the abundance of all essential nutrients such as potassium, phosphorus, nitrogen and calcium in right proportion (Chakraborty & Mistri, 2015). Proper management of the farmland, bush fallow, organic fertilizers, right chemical fertilizer application and proper crop rotation practices are some of the methods that can be used to manage declining soil fertility (FAO, 2001; Ojuola, 2015; McRoberts et al., 2016).). For soil erosion challenge faced in steeply topography such as that of Ethiopia, Omu-Aran farm and other similar topography in Nigeria, soil conservation practices such as tied ridging, minimum tillage and residue management should be encouraged (Yebo, 2015).

Soil salinity is a major threat to agricultural productivity across the world. Effects of salt infected soils include nutritional disorder, poor soil physical conditions, osmotic stress, reduced crop yield and toxicity (Etesami & Noori, 2019). Tully, Sullivan, Weil and Sanchez (2015) have reported that 19 million hectares of sub-Saharan African are already affected by soil salinity. Therefore, agricultural technologies are needed to better manage soil salinisation on Nigerian agricultural soils to achieve sustainable agricultural systems.

Rare earth elements (REEs) such as terbium, lanthanum and cerium found in contaminated soils have been recently used in modern technology, hence its abundance in the environment (Carpenter, Boutin, Allison, Parson & Ellis, 2015; Meryem, Ji, Gao, Ding & Li, 2016). Though, China has used REE in agricultural fertilizers to boost crop yield and quality for decades, there is still little research on the overall importance of REE to agriculture (Pang, Li & Peng, 2001).

Challenges faced with agriculture in major countries of the world such as Italy, China, Russia, Israel, USA, Germany, Ireland and United Kingdom (Higgins, Schellberg & Bailey, 2019) range from climate change, excessive drought, weather anomaly, erosion and

the likes have been subdued by precision agricultural practices. Calicioglu, Flammini, Braccos, Bellu and Sims (2019) have noted that the future challenge of agriculture is feeding the growing population despite the falling global soil fertility rate.

## 2.3 Precision Agricultural Practices

For decades, African governments have attempted to use various policy instruments to improve farm productivity. However, majority of the farmers have only marginally improved yields while others still practice traditional methods based on the use of tools such as hoes and cutlasses (Adama, Esena, Mensah-Fosu & Yirenya-Tawiah, 2016; Ndubuisi, 2017). The Nation (2019) has highlighted the need for Nigeria to embrace the modern high technology farming approach which will help to manage soil, crops and ensure the most efficient use of resources. According to international standards, a farm that is less than 10 hectares of land is termed small scale farming, making about 80% of Nigerian farmers small scale farmers (Mgbenka & Mbah, 2016) with enormous constraints which include economic, political and financial constraints. This is as a result of lack of proper education for the farmers (The Nation, 2019) and lack of governmental support. Othman and Leskovar (2018) related precision agriculture to smart farming and stated that the easy pathway for the world to achieving food sufficiency is through massive adoption of this improved technologies. The advent of technology has improved field measurement techniques in advanced nations; field measurement techniques can now be conducted rapidly at relatively low cost. The use and application of precision agriculture in advanced nations such as Israel, USA, Australia, Iran, China, India and the United Kingdom have been widely reported in literature, but limited scholarly attention has been given to precision of agriculture in Africa.

The success of precision agriculture (PA) depends strongly upon the use of efficient and accurate methods for soil properties determination, and remote sensing imagery techniques are becoming one of the most established methods for soil properties determination (Ge et al., 2011). Geophysical methods have been used extensively for various agricultural purposes (Barry, McQuinn, Chung, Besuden & Giovannoni, 2008; Brevik, Homburg, Miller, Fenton & Doolittle, 2016); the three predominantly used geophysical methods include electromagnetics induction, electrical resistivity and ground penetrating radar (Allred & Smith, 2010). Other geophysical methods such as seismic, self-potential, remote

sensing and magnetometry are being employed sparingly but have great potential for future agricultural studies (Allred & Smith, 2010; Allred et al., 2016). Consequently, the potential of remote sensing data in improving knowledge of local scale soil information have not been fully explored in West Africa (Forkuor, Hounkpatin, Welp & Thiel, 2017).

### 2.3.1 Remote Sensing Techniques

Remote sensing is the science of detecting and measuring electromagnetic radiations of different wavelengths reflected or emitted from a target without being in physical contact. It works on the distribution of electromagnetic radiation according to energy, wavelength or frequency as in the electromagnetic spectrum. Electromagnetic radiation propagates as wave motion at a velocity of $c = 3 \times 10^8\, ms^{-1}$ as a dynamic form of energy. The parameters that characterise a wave motion are velocity (c), wavelength (λ) and frequency (ν). The relationship between the parameters is given by:

$$c = \nu\lambda \tag{2.1}$$

The electromagnetic spectrum ranges from the shorter wavelengths (gamma rays and X-rays) to the longer wavelengths of microwaves and radio waves (Figure 2.5). The ultraviolet (or UV) portion of the spectrum, having the shortest wavelength, is the most useful for remote sensing. Primarily, some earth materials such as rocks and minerals, emit visible lights when illuminated by UV radiation. Irrespective of the chemical properties and physical features of the different objects of the earth's surface, they reflect, emit, and reradiate additional amounts of electromagnetic energy in various wavelength bands. The basis for understanding the characteristics of the earth's surface features is the measurement of the reflected, re-emitted, or the re-radiated electromagnetic radiation (Pepe, Fregonese & Scaioni, 2018).

However, electromagnetic spectrum region with relatively little attenuation when passing through the earth's atmosphere is usually used for remote sensing purpose. This region includes the infrared band of 0.4 to 0.7 μm to the infrared band of 0.7 to 3.0 μm. Also, the thermal infrared band of 3 to 5 μm and 8 to 14 μm and the microwave band of 0.1 to 30 cm are included (Ge, Thomasson & Sui, 2011). The progress made in remote sensing for mapping soil properties using optical, thermal infra-red, visual imaging, microwave, multispectral and hyperspectral are discussed in the following sections.

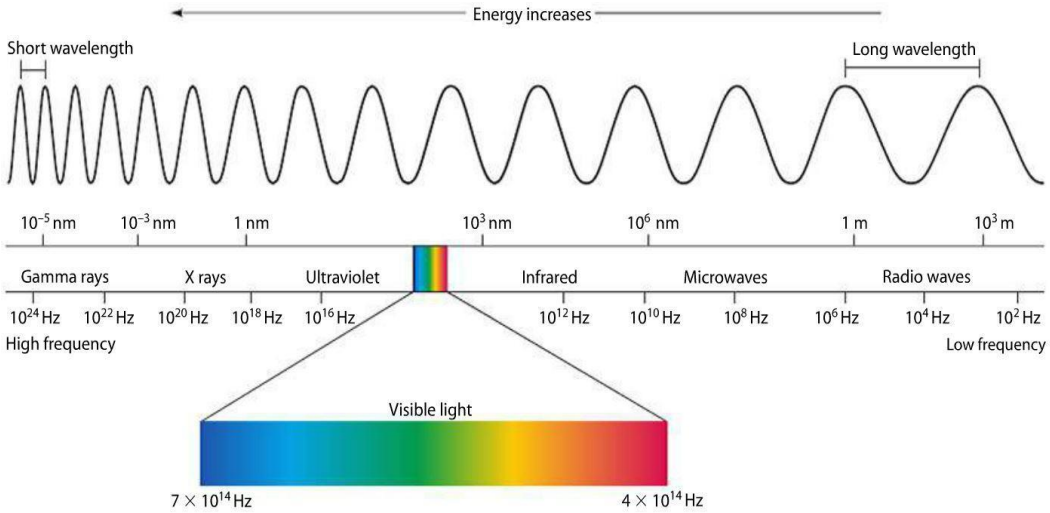


**Figure 2.5**: Electromagnetic spectrum

Source: Born and Wolf (1999)

Remote sensing method for soil property characterisation includes both the satellite aerial imagery as well as proximal, that is, spectrometry reflectance (Ge et al., 2011). The earliest attempt to using remote sensing for soil studies was in 1930s, when US base maps for soil surveys were prepared in aerial photographs of black and white (Baumgardner, Silva, Biehl & Stoner, 1986). Soil scientists in the 1960s and early 1970s then started using multispectral-sensor (MSS) data to distinguish differences in surface soils. Digital analysis of aerial MSS data discovered partial success (Hubacek, Almasiova, Dejmal & Mertova, 2017). Condit (1970, 1972) also attempted to quantify soil reflectance using proximal sensing from 160 soil samples from 36 states in the US. However, there was no attempt made to quantitatively relate these spectral properties to the chemical and physical properties of soil. In recent times, remote sensing has witnessed significant advancement in sensing technology and data analysis techniques. Useful soil property information is being extracted from the soil spectra data recorded in hundredths and thousands of connected narrow bands of extensive large data sets (Ge et al., 2011).

### 2.3.1.1 Multispectral and Hyperspectral Imagery

A multispectral image contains bands or several channels with each one containing measured radiation in specific wavelength ranges for each pixel; examples are red or near infra-red and green (Ose, Corpetti & Demagistri, 2016). Multispectral satellites began in the 1970's by the use of optical satellite images for civilian purposes and this has improved over time from high resolution to very high resolution imaging (Ose et al., 2016). The new

generation multispectral sensors with improved spectral and spatial resolutions are the hyperspectral remote sensors (Royimani, Mutanga, Odindi, Dube & Matongera, 2018). The hyperspectral dataset promotes precise characterisation of the earth's surface and optimal resource monitoring for a long term and large scale mapping (Royimani et al., 2018). Hyperspectral imaging technique is an extension of multispectral imaging which applies radiometry, conventional imaging, and spectrometric principles in large data set (Mahesh, Jayas, Palwal & White, 2015). It has been termed an emerging technology for improving and monitoring grading of agricultural materials such as field crops (e.g., oilseeds and cereals) and horticultural crops (e.g., strawberries and apples).

Hyperspectral imaging facilitates thorough non-destructive analyses by simultaneous acquisition of both spectral and spatial information on agricultural samples (Mahesh et al., 2015), and has become a popular research tool. The main difference between multispectral imaging and hyperspectral imagery is in the number of bands and how narrow the bands are (Figure 2.6). Multispectral, for example, Landsat-8, has 3 to 10 wider bands while the hyperspectral imagery has narrower bands (10 – 20 nm) and could have hundreds and thousands of bands (Rimjhim, Sushmiya & Malata, 2013). The nine spectral bands with pan band of Landsat-8 include: the visible band 1 (0.43 - 0.45 μm) 30 m; visible band 2 (0.450 – 0.51 μm) 30 m; visible band 3 (0.53 – 0.59 μm) 30 m; band 4 Red (0.64 – 0.67 μm) 30 m; Band 5 near-infrared (0.85 – 0.88 μm) 30 m; band 6 SWIR 1 (1.57 – 1.65 μm) 30 m; band 7 SWIR (2.11 – 2.29 μm) 30 m; band 8 panchromatic (PAN) (0.50 - 0.68 μm) 15 m and cirrus band 9 (1.36 - 1.38 μm) 30 m (Markham, Storey & Morfitt, 2015).

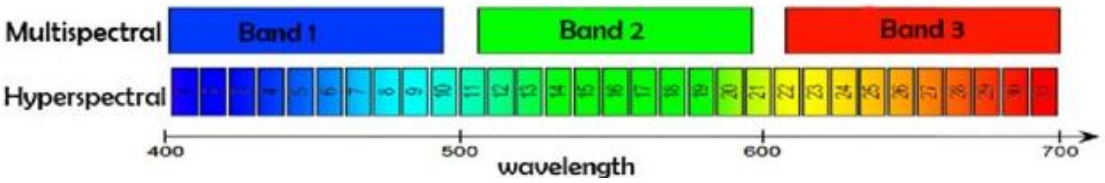


**Figure 2.6**: Multispectral imaging with wide bands and hyperspectral imagery with multiple narrow bands (Jasinski, Pietrek, Walczykowski & Orych, 2010)

### 2.3.1.2 Optical Remote Sensing

Optical remote sensing have been used to monitor various soil properties such as vegetation, land cover and soil moisture content. Optical remote sensing works by measuring the surface reflectance of reflected radiation of the sun from the Earth's surface (Rimjhim et al., 2013). These reflected radiations are related to soil properties such as moisture content, organic matter, and soil particle size. These soil properties influence soil reflectance by producing broad-spectrum expression through average surface reflectance (Irons, Weismiller & Petersen, 1989; Rimjhim et al., 2013; Zeeshan, Deshmulch & Syed, 2017). Five characteristic soil spectral reflectance curves, which were considered representative of the soil reflectance diversity found in ranges of naturally occurring surface soils, were identified (Lacerda, Dematte, Sato, Fongaro, Gallo & Sauza, 2016). Curve shapes and the presence or absence of absorption features representing specific iron content, organic matter, and soil texture were used to identify the curve forms (Mulder, Bruina, Schaepmana & Mayre, 2011). Lobell and Asner (2002) explained the soil reflectance variations due to the change in moisture based on the analysis of the reflectance of four (4) different soils at various moisture contents. He developed a physical model for the study. Liu and Bando (2003) also investigated the potential of estimating soil moisture from reflectance measurement using 18 soil samples representing a large area.

### 2.3.1.3 Thermal Infra-Red Remote Sensing

Soil moisture content and salinity are the commonest soil properties thermal infra-red is used to estimate. The thermal emission of the earth having electromagnetic wavelength of between 8 and 14-micrometer range is being measured by the thermal infra-red (Curran, 1985). The moisture content is measured by thermal inertia and the vegetation/temperature index methods (Wang & Qu, 2009). Also, Boulet, Mougenot and Abdelouahab (2009) selected the appropriate soil hydraulic properties using thermal infra-red remote sensing. Thermal infra-red (longwave infra-red) was used to detect and measure small ranges of soil properties such as sand, clay and soil organic carbon (SOC) content in a semi-arid agricultural landscape of Western Australia (Eisele et al., 2015). The results indicated that the longwave infra-red wavelength region has higher accuracy and precision than the visible near infra-red and shortwave infra-red wavelength region especially for quantitative farm area monitoring for erosion related soil properties (Eisele et al., 2015). Khanal, Fulton and Shearer (2017) noted that thermal remote sensing is a promising tool for precision

agriculture because of its viability in estimating surface temperature. Also, thermal remote sensing for precision agriculture has been limited in use compared to the optical remote sensing.

#### 2.3.1.4 Visual Image Interpretation

Visual interpretation is relatively simple and inexpensive. Soils are surveyed and mapped using the remote sensing imagery or aerial photographs, field survey and cartography (Mulder, Van Grinsven & Van Breemen, 1987; Sehgal, Challo, Gajja & Yadav, 1989). Visual interpretation is based on size, shapes, tone, shadow and pattern of the features. The technique of visual interpretation has been used to identify and map soil elements such as land use, vegetation, land type, slope and relief (Rimjhim et al., 2013). Colour infra-red photograph from aerial photographs interpretation has been used to map salinity on farmlands (Wiegand, Rhoades, Escobar & Everitt, 1994).

#### 2.3.1.5 Microwave

Microwave remote sensing is used specially for mapping soil moisture content and for detecting salt affected areas (Crites & Lucey, 2015; Dong et al., 2020), sandy coastal and waterlogged areas (Metternicht, Zinck, Bianco & del Valle, 2010). Two types of microwave remote sensing are used for soil property mapping; these are active and passive microwave sensing. Active microwave sensing has been successfully used for regional soil moisture mapping, while the surface soil moisture over land surfaces can be monitored by the passive systems (Wang & Qu, 2009). The active sensors yield poor imagery when repeated over time inspite of its high spatial resolution of the order of tens of meters at initial take off. Both active and passive sensors measure the intensity of microwave emission from the soil which is the brightness of temperature (Mohanty, Cosh, Lakshmi & Montzka, 2017). In Canada, Champagne, McNaima and Bergb (2011) used passive microwave remote sensing to monitor agricultural soil moisture extremes and the result provided useful information on the soil moisture anomalies for the area investigated. Very recently, Fang, Lakshmi, Jackson, Bindlish and Colliande (2019) used active and passive microwave remote sensing to determine the accuracy of the disaggregated change in soil moisture content at a southern province of Manitoba, Canada. The result indicated that disaggregated soil moisture was better characterised by soil moisture spatial variability and it has good resolution which was in agreement with *in situ* measurements and disaggregated

estimates. Fang et al. (2019) suggested that a simultaneous passive soil moisture retrieval and high-resolution active microwave should be applied to estimating soil moisture for both agricultural and hydrology studies.

#### 2.3.1.6 Remote Sensing Data Characteristics

The quality of remote sensing imagery is presented in various resolutions while resolution is the amount of details that can be observed from an image. Images that show finer details are said to be of finer resolution than those of coarser details. Platform specifications and the type of sensor used determine the characteristics of the remotely sensed data (Liang, Li & Wang, 2012). Types of resolution in remote sensing systems are the spatial, spectral, temporal and radiometric resolutions (Gupta & Follette-Cook, 2017).

i. **Spatial Resolution:** This is the measure of the smallest object that can be resolved on the sensor. It is the image produced of an area for instantaneous field of view.

ii. **Spectral Resolution:** This resolution indicates the number and width of spectral bands in a sensor system. Multispectral bands in the visible near infra-red or Thermal infra-red, and single wide band in the visible spectrum have a panchromatic band in many sensor systems. For example, multispectral systems have wider bands while the hyperspectral systems usually have hundreds of spectral narrow bands.

iii. **Temporal Resolution:** Temporal resolution measures the frequency or the repeat cycle with which sensors revisit the same part of the Earth's surface. The design of the satellite sensor and its orbit pattern is of importance here.

iv. **Radiometric Resolution:** This resolution pertains to the number of different output numbers in each band of data and it is determined by the number of bits into which the recorded radiation is divided. It reflects the ability of sensors to identify or ignore very slight difference in reflected or emitted energy (Khanal, Uddin, Matin & Tenneson, 2019). Data in remote sensing is digitized and recorded as positive digital number (DN) which varies from zero to a selected power of 2. More

bits give higher radiometric accuracy of the sensor. The digital numbers can range from 0 – 255 for each pixel ($2^8$ = 256 total possible numbers), in a 8-bit data.

### 2.3.1.7 Application of Remote Sensing in Agriculture

The advancement in technology has introduced new group of tools, methods and systems. Technologies such as remote sensing, global positioning system (GPS) and geographic information systems (GIS) have provided new approaches to resource planning and the study of various aspects of soils in spatial and temporal domains (Yeung & Lo, 2002; Shreatha, 2006), making soil survey more efficient. Remote sensing and GIS have been applied to aid precision agriculture in advanced nations (Figure 2.7).

Sahoo, Ray and Manjunath (2015) reviewed the status of the applications of GPS and GIS, and high-resolution remote sensing data (IRS-P6, LISS IV, PAN, Cartosat-I), in characterisation at large scale level agricultural planning and soil resource inventory. They noted that the integrated use of these advanced computer technologies can assist in decision making and in future plans. These advanced tools can assist in studies on regional or larger map scales as previous studies have been on small scales. Patra, Shekher, Solanki, Ramachandran and Krishnan (2011) noted that the field of remote sensing and GIS have become exciting and glamorous with rapidly expanding opportunities.

**Figure 2.7**: Remote sensing and GIS applications to monitor crops and weather conditions
Source: FAO (2019b)

Remote sensing applications in agriculture are, basically, the interaction of electromagnetic radiation with soil or plant materials. Remote sensing primarily measures reflected radiation and not absorbed or transmitted radiation. Several platforms such as aircraft, satellites, tractors, and hand-held sensors mainly make remote sensing measurements. Proximal sensing is the type of measurement that does not involve measurements of reflected radiations, that is, those measurements made with hand-held sensors or tractors. Plant leaves also emit energy known as fluorescence or thermal emission (Apostol & Zwiazek, 2003; Cohen, Alchanatis, Meron, Saranga & Tsipris, 2005). However, the most useful wavelengths in remote sensing are the visible light (VIS), near infra-red (NIR), shortwave infrared (SWIR), thermal infrared and microwave bands (Wiesmeier et al., 2015).

Various techniques of remote sensing for soil characterisation are prevalent, but the major soil parameters studied include moisture, roughness, temperature and texture (Zribi et al., 2011); others include mineralogy, soil iron, carbonate content and soil salinity (Mulder et al., 2011). Incomplete spatial and thematic coverage of global soil databases is expected to be improved by remote sensing (Mulder et al., 2011). Satellite remotely sensed data were used to predict soil parameters such as organic matter and calcium carbonate content in the Apennine Mountain of southern Italy (Leone, Wright & Coves, 1995). The result illustrates that useful reconnaissance soil mapping information can be obtained from satellite data. The factors that influence quality remote sensing imagery are highlighted in Figure 2.8. Land and water use have been profitably determined, that is environmentally and economically, as a result of precision farming. Remote sensing and geographic information system (GIS) have been used to manage required zones for variable application of fertilizers on farm lands. Tonnes of fertilizers have been saved as a result of variable rate application of fertilizers (e.g., El Nahry, Ali & El Barouudy, 2011).

Precision agriculture (PA) practices also include soil sampling, field scouting and variable rate application and its technology (El Nahry et al., 2011). The application of PA on a pilot maize cultivation in Ismaila Province in Egypt caused a dramatic change on the field by identifying management zones (zones with high accumulation or decreasing essential nutrients) within the cultivation (El Nahry et al., 2011). Also, Ghazali, Wikantika, Harto and Kondoh (2019) used remote sensing technology to estimate the changing soil moisture content and soil salinity in an agricultural field in Indonesia. Soil moisture index and soil

salinity index were estimated from the analysis of the Landsat-8 satellite images, soil data of field surveys, statistical computation and laboratory analyses (Ghazali et al., 2019). The soil data from the Landsat-8, survey and laboratory analyses were combined and integrated to build multiple regression equations based on bare soil and paddy leaf models to explain the changes in the soil moisture and the soil salinity. The results revealed an increase in soil moisture after 30 days, but a trace amount of salt content.

In Egypt, soil salinisation is a major threat to crop production and sustainable agricultural development (Hamman & Mohammed, 2018) hence, the adoption of geographic information system (GIS) to evaluate the degree of soil salinization at the East of Nile area of the country (Hamman & Mohammed, 2018). Agronomic classification and Russian classification of salt-affected soils were used for the soil analysis. The obtained data and soil maps generated presented salinity levels of the agronomic classification area to be 40% and that of the Russian classification was found to be 29%. Adoption of precision agricultural technology (PAT) has reduced inputs, optimize yield and quality of crops and also minimize environmental impacts (Robertson et al., 2007; Silva, Dias de Moraes & Molin, 2011; Aubert, Schroeder & Grimaudo, 2012; Smith, Dhuyvetter, Kastens, Kastens & Smith, 2013; Eory et al., 2015; Schimmelpfennig and Ebel, 2016; Van der Wal & De Boer, 2017). The gateway for the future of commercial and sustainable agricultural systems have been tagged with these PAT technologies (Gebbers & Adamchuck, 2010; Telabpour, Turker & Yegul, 2015).

### 2.3.2 Electrical Resistivity Technique

For decades, electrical resistivity methods have aided in the mapping of subsurface features by making electrical measurements on the ground surface. Technological advancement in electrical resistivity instrumentation, field survey, data processing and interpretation has made electrical resistivity a widely employed method for environmental, hydrogeological and engineering investigations (Dahlin, 2001; Loke, Chambers & Kuras, 2011; Chambers, Guevara, Boyer, Troxter & Davis, 2016; Obiora, Alhassan, Ibuot & Okeke, 2016; Ibuot, Obiora, Ekpa & Okoroh, 2017; Tang et al., 2018; An, Tang, Cheng, Wang & Shi, 2020; Ezema, Ibuot & Obiora, 2020).

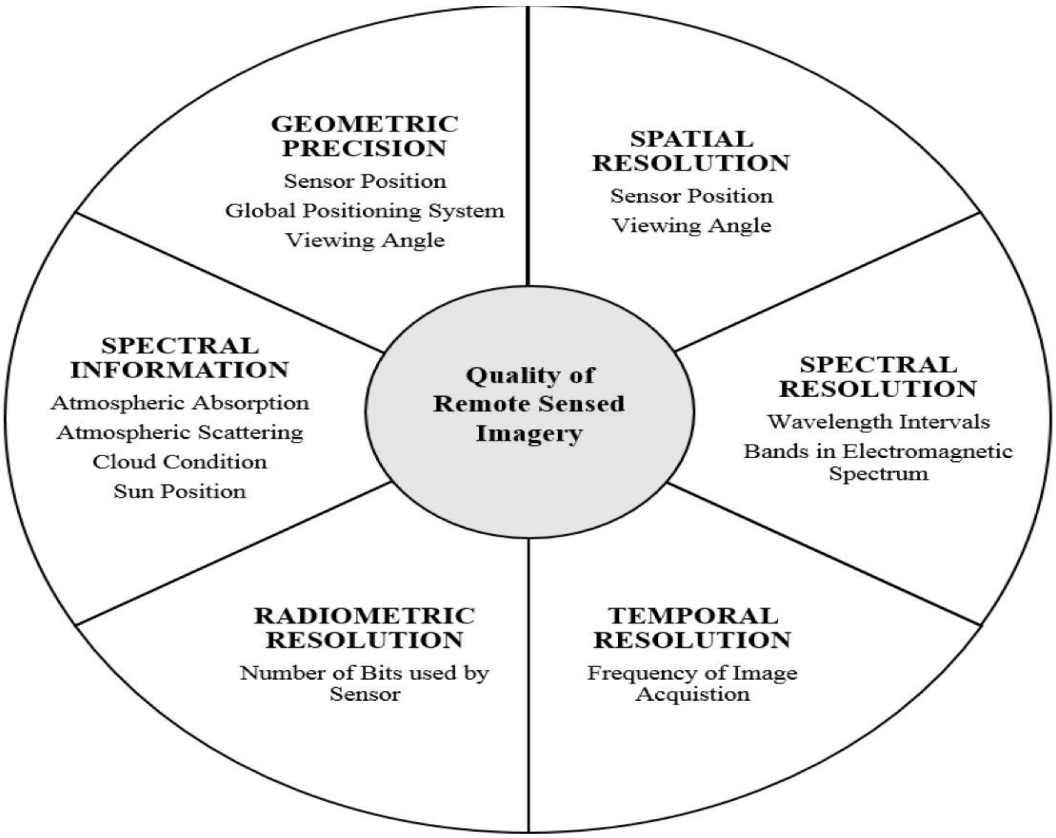


**Figure 2.8**: Factors influencing the quality of remotely sensed images
Source: Khanal et al. (2019)

Electrical resistivity (ER) method has been applied to soil science over time and the technique is very promising because soil materials exhibit significant electrical properties depending on their physical and chemical properties such as texture, salinity and water or moisture content (Samouelian, Cousin, Tabbagh, Bruand & Richard, 2005; Dick, Tetzlaff, Bradford & Soulsby, 2018; Chen, Garre, Liu, Yan, Liu, Gong & Mei, 2019; Hovhannissian, Podwojewski, Troquer, Mttimkhulu & Antwerpen, 2019; Won, Park, Choo & Burns, 2019). The electrical resistivity of the subsurface is a function of various soil properties including the solid constituents, that is mineralogy and particle size distribution, degree of water saturation, arrangement of voids (pore size distribution and connectivity), solute concentrates, and temperature (Samouelian et al., 2005).

For soils overlying crystalline rocks, electrical resistivity exhibits large range of values (1 Ωm to several $10^3$ Ωm) from the saline sand to dry non-saline soil (Figure 2.9). Giao, Chung, Kim & Tanaka (2003) recorded a range of electrical resistivity of 1 to 12 Ωm for 25 clay soils they collected worldwide. Lamotte, Bruand & Pedro (1997) investigated two

cultivated sandy soils of similar composition but different electrical resistivity. The result revealed that clay aggregates attached to the sand grains of one of the sandy soils gave a lower resistivity than the other with a discontinuity of the clay phase thereby leading to higher resistivity. Fukue, Minatoa, Horibe & Taya (1999) noted, in their study, that electrical charges at the surface of clay particles resulted to greater electrical conductivity than the coarse textured soils because of the magnitude of the specific surface charge.

### 2.3.2.1 Basic Theory and Principles of Electrical Resistivity Method

The electrical resistivity method is an active geophysical method. The principle of electrical resistivity survey involves the injection of low-frequency alternating current into the ground through two electrodes and the voltage difference is measured between two other electrodes. Apparent resistivity is calculated by measuring the potential difference at different positions of the current and potential electrodes. The current electrodes are used to inject current into the ground, while the potential electrodes are used to measure the potential difference (Figure 2.10).

The measured apparent resistivity data are based on the current $(I)$ injected into the ground and the resulting voltage difference $(\Delta V)$ between the potential electrodes. The current and voltage measurements are converted to apparent resistivity $(\rho_a)$ using the relation:

$$\rho_a = k\frac{\Delta V}{I} \qquad (2.2)$$

where the geometric factor $k$ depends on the configuration of the current and potential electrodes. Apparent resistivity is usually measured by four electrodes; $A$ and $B$ are used as the current electrodes, while $M$ and $N$ serve as the potential electrodes.

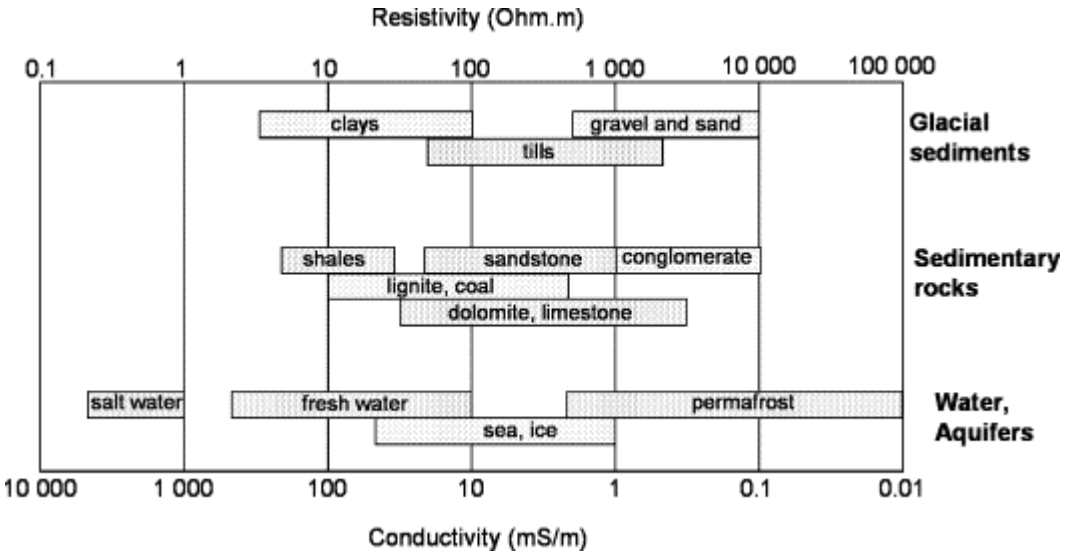


**Figure 2.9**: Range of typical resistivity of earth materials

Source: Samouelian et al. *(*2005)

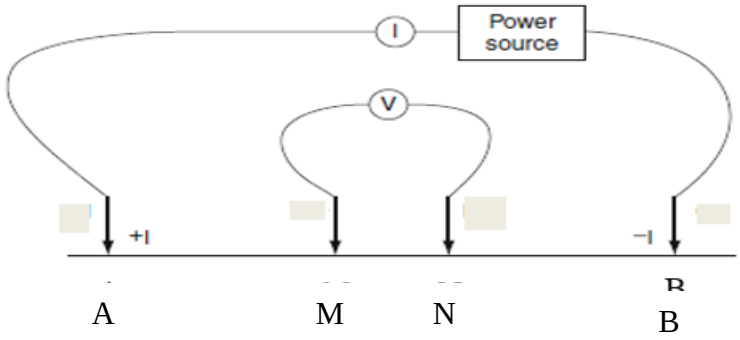


**Figure 2.10**: Basic set-up for electrical resistivity survey

Source: Loke et al. (2011)

The potential difference $(\Delta V)$ measured between the two potential electrodes is given as

$$\Delta V = \frac{\rho_a}{2\pi}\left(\frac{1}{AM} - \frac{1}{BM} - \frac{1}{AN} + \frac{1}{BN}\right) \tag{2.3}$$

where the geometric distance between the electrodes $A, \mathrm{B}, \mathrm{M}$ and $N$ is represented by $AM, BM, AN$ and $BN$.

$$\rho_a = \left(\frac{2\pi}{\frac{1}{AM} - \frac{1}{BM} - \frac{1}{AN} + \frac{1}{BN}}\right)\frac{\Delta V}{I} = k\frac{\Delta V}{I} \tag{2.4}$$

The apparent electrical resistivity is then calculated using $K$ as the geometric coefficient which depends on the arrangement of the four electrodes. Apparent resistivity is the measured resistivity which is not equal to the true resistivity of the inhomogeneous

subsurface (Meheni, Guerin, Benderitter & Tabbagh, 1996; Reynolds, 1997). The true resistivity is determined by the inversion of the measured apparent resistivity.

Electrical resistivity surveys are used to determine the resistivity distribution in the soil volume. The potential difference obtained from the measurements provides information on the electrical properties of the subsurface heterogeneities (Keary, Brooks & Hill, 2002; Samouelian et al., 2005). The survey can be performed in one-, two- or three-dimensions at different scale resolutions (centimeters to the regional scales) depending on the area's heterogeneities (Samouelian et al., 2005).

### 2.3.2.2 Arrays for Electrical Resistivity Survey

The conventional arrays for electrical resistivity surveys are Wenner, Schlumberger, pole-pole and dipole-dipole arrays.

**(a) Wenner Array:** The Wenner array consists of four collinear, equally spaced electrodes, where $A$ and $B$ represent the current electrodes, and $M$ and $N$ are the potential electrodes (Figure 2.11a). The current electrodes are the outer ones and the potential electrodes are the two inner electrodes. The advantage of this array is that the apparent resistivity can easily be calculated on the field and small current magnitudes are needed to produce measurable potential difference. The movement of electrodes after each measurement and its sensitivity to near-surface inhomogeneities thereby skewing deeper electrical responses are some of the disadvantages of this array. However, longer current cables are also necessary but handling these cables in difficult terrains can be cumbersome. Apparent resistivity ($\rho_a$) for Wenner configuration is given as:

$$\rho_a = 2\pi a \frac{V}{I} \tag{2.5}$$

where a is the spacing of the probe.

**(b) Schlumberger Array:** The four collinear electrodes in the Schlumberger array have the outer two electrodes as the current electrodes and the inner electrodes as the potential electrodes Figure $2.11a$. The potential electrodes, placed at the centre of the electrode array, have a small separation relative to the outer current electrodes separation. The potential electrodes remain fixed until the voltage is too small to be detected, but the current

electrodes separation is progressively increased during the survey. The main advantage of this array is that only the current electrodes need to be moved for each measurement. The potential electrodes have shorter cables, and the operations allows for greater probing depth because of the spacing between $A$ and $B$ Also, lesser time for field operation than that of Wenner array is required (Aizebeokhai, 2010). The demerits of the Schlumberger array type are that long current cables are needed and the recording instrument must be highly sensitive to small changes in resistivity.

Lack of proper coordination of the field crew, especially in a large field, can make field measurements with the array relatively difficult. The apparent resistivity $(\rho_a)$ for Schlumberger array is given as:

$$\rho_a = \frac{V}{I}\pi\frac{b^2}{a} \qquad \text{if } a \ll b \tag{2.6}$$

where $V$ is the voltage and $I$ is the current.

**(c) Dipole-Dipole Array:** The dipole-dipole array consists of two sets of dipoles, the current and the potential dipoles (Figure 2.11c). Here, equal distance is maintained for both the current and the potential dipoles. Integer multiple of $'a'$ is the distance between the current and potential dipoles. Electrodes can be located outside the conventional survey line.

The major advantage of this array is that the current electrode dipole is separated from the potential electrode dipole and this minimise electromagnetic coupling between the measuring cables (Aizebeokhai, 2010). However, for deep soundings, external power source such as the generating set may be needed to transmit a greater current magnitude. The apparent resistivity is given as:

$$\rho_a = \frac{V}{I}\pi an(n+1)(n-1) \tag{2.7}$$

**(d) Pole-Dipole:** In pole-dipole array, one of the current electrodes is place at an infinite distance away from the survey line; thus, only one current electrode and the potential electrodes are active during the measurements (Figure 2.11d). Its horizontal coverage makes pole-dipole attractive for multi-electrode resistivity meter systems with small

number of nodes. The apparent resistivity ($\rho_a$) for pole dipole electrode configuration is given as:

$$\rho_a = 2\pi n(n+1)a\frac{\Delta V}{I} \tag{2.8}$$

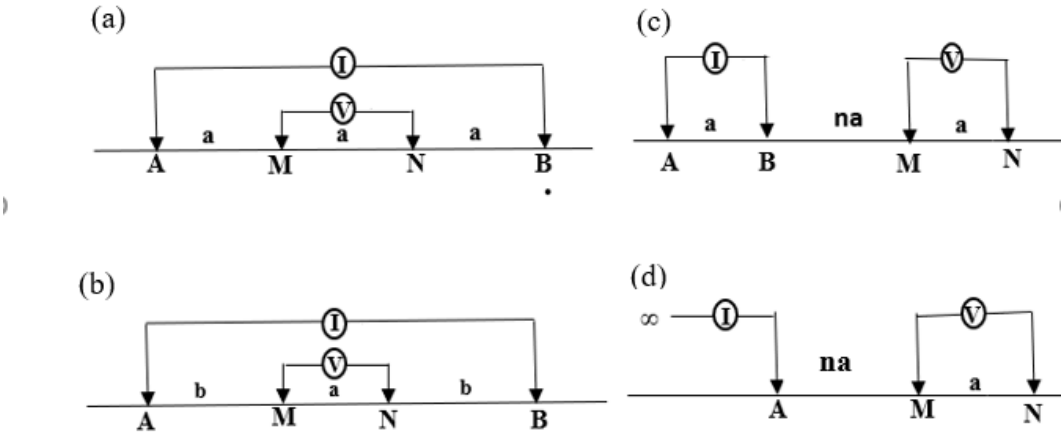


**Figure: 2.11**: Electrode configurations: (a) Wenner array of electrode configuration, (b) Schlumberger array, (c) dipole-dipole array type, and (d) pole-dipole electrode configuration

### 2.3.2.3 Related Works on Electrical Resistivity in Precision Agriculture

Electrical resistivity techniques have been modified for near-surface investigations in agricultural and environmental studies and they have been used for decades in developed countries (Golovko & Pozdnyakov, 2007). This method has been able to overcome some of the limitations of other geophysical methods in terms of calibration and profile characterisation as regards its application in agriculture and environmental sciences (Bitella et al., 2015). Compared with conventional methods of soil analysis, electrical resistivity method has been used to evaluate salt content, groundwater table, depth and thickness of horizons, time dependent change of soil water content, plant root biomass and water-plant root interactions (Amato et al., 2008; Werban, Hagrey & Rabbeh, 2008; Calamita et al., 2012; Bitella et al., 2015).

Depending on the technique used, 1D, 2D or 3D, electrical resistivity can be highly useful for soil investigations. This method enables the assessment of vertical and lateral variability in the near-surface zone (Kowalczyk, Piotr, Mieszkowski, 2015; Bitella et al., 2015). Several researchers have successfully employed electrical resistivity for various

agricultural investigations as reported in literature. Buvat et al. (2014) developed a geophysical taxonomy which was based on the vertical succession of 3 apparent resistivity values using a multi-depth resistivity dataset. They found out that the resistivity-based clusters matched well with soil unit boundaries and soil profiles. Ganiyu, Olurin, Oladunjoye & Badmus (2019) used combined 1D and 2D electrical resistivity surveys to determine the soil moisture content of topsoils in a cultivated farmland in Abeokuta. Schlumberger and Wenner arrays were used to determine the apparent resistivity along the six traverses investigated. The result revealed a range of resistivity and thickness of the topsoil, the weathered layer and the clayey sands. Effective depths of more than 30 cm were indicated by the 1D resistivity models, while the extent of the active water uptake was revealed by the 2D imaging to be about 2m depth.

On the other hand, Kowalczyk et al. (2015) and Hazreek et al. (2017) studied the relationship between electrical resistivity of non-cohesive soils and the granulated materials used in construction, with their degrees of compaction. The result revealed electrical resistivity as a potential method for the determination of the degree of compaction and soil moisture content.

Adamchuk, Hummei, Morgan and Upadhyaya (2004) reviewed the use of on-the-go sensors (real-time sensors mounted on farm equipment) to measure the physical, mechanical and chemical soil properties. The sensors are based on the concepts of optical radiometric, electrical and electromagnetic, pneumatics, mechanical and acoustic signals. Signal output provided from these sensors are used to obtain soil characteristic such as soil texture, soil salinity, soil compaction, soil pH, residual nitrate or total nitrate content, potassium content and cation exchange. Wang, Zhang and Wang (2006) also presented an overview of the recent development of wireless sensors technology applied in agriculture. The wireless sensors network is used for environmental monitoring and precision agriculture, specifically to aid food production. Measurements are taken by these sensors to a collector point, where an estimate of the field properties is calculated. Dangerous hazardous, unwired or remote areas are easily monitored with this wireless sensor.

Also, Golovko and Pozdnyakov (2007) developed two portable geophysical devices, Land-Mapper ERM-01 and ERM-02, to measure electrical conductivity, and are suitable for mapping agricultural productive fields as well as small agronomy research plots. The

electrical geophysical method permits evaluating groundwater, depths and thicknesses of soil horizons, salt content, polluted or disturbed soil when compared with the conventional methods of soil analysis. The study further demonstrated the applications of the modified geophysical methods in soil physics, precision agriculture and environmental engineering.

In a similar trend, Walsh, Grunewaldi, Turneri, Hinnel and Ferre (2014) modified a Surface Neutron Magnetic Resonance (SNMR) instrument to address the challenge of the use of Earth's field SNMR to detect and characterise water in the unsaturated zone in the western US. The SNMR experiment was performed at a managed aquifer storage and facility in Arizona. The water zones were mapped with time lapse (SNMR) prior to the flood event, quantify the spatial and temporal distribution of infiltrating water, image the influx of water in the subsurface to about 15 meters, and characterise the allotment of water in different relative pore sizes throughout the event. The data acquired at the investigation site indicated that at depths up to 30 metres, the SNMR can be used to detect and image some forms of water held in the vadose zone (Walsh et al., 2014).

Shevnin, Delgado-Rodriguez, Mousatou and Ryjov (2006) considered clay content in loose soil as the major factor influencing hydraulic conductivity. Some published experimental data on hydraulic conductivity with relation to soil lithology and clay content in the form of grain size were collected and analysed. Theoretical modelling modifying well-known formulas including clay content was also performed. Both theoretical and experimental data showed good agreement. It was deduced that clay content in soil can be estimated using soil resistivity obtained from vertical electrical sounding (VES) data interpretation and from groundwater salinity studies. Also, hydraulic conductivity can be determined from clay content.

In an irrigated field of Navarre, northern Spain, Amezketa (2007) carried out a salt control measurement to assess, map and predict soil salinity at field scle using integrated methods involving hand-held electromagnetic sensor (Geonics EM38) and electrical conductivity or salinity, sampling, assessment and prediction (ESAP) software. Salinity of the 180 locations was analyzed using the EM 38 sensor by measuring the bulk soil electrical conductivity (ECa). Also, soil core samples at 0.3 metres interval to a depth of 0.9 m were taken at 20 of the locations. The result revealed that salinity was the dominant factor influencing the EM 38 readings.

Similarly, Scudiero, Berti, Teatini and Morari (2012) monitored pore-water electrical conductivity (ECp) and soil volumetric water content using resisitivity sensors and a low-cost capacitance. Five soils and four water contents (i.e., from dry conditions to saturation) and four salinity levels of the wetting solution were probed. They estimated pore-water electrical conductivity and identified a set of fuctions for empirical prediction on soil properties such as organic matter and texture by testing four models. The models were reformulated to estimate soil characteristics and dielectric readings, performances were improved with respect to the original model. Hence, low-cost capacitance-resistance probes, if well calibrated, can be used to monitor solute and water dynamics in saline soils effectively.

Also, Brunet, Clement and Bouvier (2010) applied electrical resistivity to study the agricultural fields of Cevennes, South of France. They characterised soil parameters including soil texture, moisture, soil solution and temperature. The results of the study showed the potential of using electrical resistivity to measure water deficit and soil water content, and also described the impact porosity and soil temperature have on electrical resistivity tomography (ERT).

### 2.3.3 Geochemical Method

A Swiss Chemist, Schonbein in 1838 was the first to use the name geochemistry and defined it as earth chemistry (Fairbridge, 1998). Goldschmidt (1954) re-defined geochemistry as the study of the amount and distribution of chemical elements in rocks, minerals, soil, atmosphere and water as well as the study of the circulation of elements in nature with regards to their atoms and ionic properties. The major or trace elements which are analysed by this method are usually found in soils, groundwater and rocks in the proximity of an ore-body. Their dispersion pattern can either occur by elemental distribution during ore forming process or by the migration and distribution of elements in solution during weathering, mineral deposit erosion and oxidation (Haldar, 2013). The degree of concentration of specific elements diminishes away from the deposit logarithmically to background values of the enclosing rock (Haldar, 2013). Geochemistry may be grouped into organic and inorganic geochemistry. Organic geochemistry deals with the determination of distribution and quantity of organic compounds in the earth while inorganic geochemistry deals with the distribution and quantity of elements and their

inorganic compounds in the atmosphere, hydrosphere and the lithosphere (Banerjee, Maji & Mahapatra, 2012; Olatunde, 2016; Wu & Chen, 2018).

The science of geochemistry deals with the determination of the absolute and relative abundance of elements in the earth. Geochemistry is the study of the distribution and migration of individual elements in the different parts of the earth as well as the discovering of the principles governing this distribution and migration (Hawkes, 1957). Geochemical prospecting involves the systematic measurements of chemical properties of naturally occurring materials on the earth's surface (Hawkes, 1957; Haldar, 2013; Zhang, Xiao, Carranza, Yang & Zhao, 2019; Wang, Zhou & Xiao, 2020). The earth system, which includes the solid earth and its atmosphere, is an assemblage of atoms of about 92 natural elements. These atoms have been in the earth system since the formation of the earth, the subsequent input of materials such as meteorites and other extra-terrestrial sources notwithstanding (Schlesinger, 1997). Locating geochemical anomalies or areas where the chemical pattern indicates the presence of certain elements is the main purpose of this method. These anomalies can be formed either by the agents of weathering, surficial transportation or erosion at the earth's surface (Haldar, 2013).

In geochemistry, soil and water samples as well as sediments derived directly from the rock are analysed for their metal enrichment during mineralisation (Amor, 2013). Makkonen, Makinen and Kontoniemi (2008) and Zhao et al. (2011) affirmed that litho-geochemical study using major/trace elements are used to distinguish between certain types of barren and mineralised rocks in diagnostic exploration. In general, the fundamental principle of geochemical analysis involves testing naturally occurring media for enrichment in certain elements, and tracing those elements back to their source (Amor, 2013).

#### 2.3.3.1 Survey Mechanism in Geochemistry

Geochemical surveys have been termed as a mapping tool that gives support to a wide range of geological survey activities (Garrett, Reimann, Smith & Xie, 2008; Gong et al., 2020). Geochemical analysis of soil is required to know exactly what crops need to grow. In order to supply adequate nutrients, information about the capacity of soil can be obtained either through soil test or laboratory soil analysis. Geochemical survey can either be on a regional or local scale. The following are considered when planning soil geochemical surveys: what

elements are to be analysed, extraction and instrumentation to be used, nature of soil substrate (residual/ transported), soil profile (at what depth or horizon), local variation due to drainage, topography or parent material, size of sample (whether to sieve it or not), and spatial configuration of the sampling which may include square or offset grid, tightly spaced along widely spaced lines (Winterburn, Noble & Lawrie, 2017). Geochemical surveys are often multipurpose and multidisciplinary studies that involve several sample materials such as soil, sediment or biota and water collected at a time for various purposes (Salminen, 2018). For regional-scale surveys employed in several nations such as United Kingdom, Europe, Indonesia, Hong Kong, Slovak Republic and Barents Region, geochemical information obtained are used to describe the natural geological level of element concentrations which serves as background information for resource evaluation and environmental legislation (Muchsin, Johnson, Crow, Djumsari & Sumartono, 1997; Reimann et al., 1998; Sewell, 1999; Johnson, Breward, Ander & Ault, 2005; Salminen et al., 2005, 2018).

#### 2.3.3.2 Geochemical Analysis

Geochemical analysis of soil samples is usually carried out in the laboratory. Some laboratories employ analytical method that requires samples dissolution prior to analysis, while others use analytical instrumentation, which is energy dispersive X-ray fluorescence applied to pulverize samples (Box, Bookstrom, Ikramuddin & Lindsay, 2001). Four acids (hydrochloric, perchloric, nitric and hydrofluoric acids) and triple acids are usually used for some of the digestion procedures; others use two acids (aqua regia and nitric acids) or only concentrated nitric acids (Box et al., 2001). Dissolved samples are mostly analysed by Inductively Couples Plasma - Atomic Electron Spectroscopy (ICP-AES) or Inductively Coupled Plasma - Mass Spectrometry (ICP-MS). Flame Atomic Absorption (FAA) is used to analyse some elements such as silver (Ag) and potassium (K). Further analysis such as statistical and spatial analyses can be performed on the already obtained geochemical data of major and trace elements to support bedrock mapping (Sadeghi, Billay & Carranza, 2015), and locate pathfinder elements in ore exploration (Levitan et al., 2015). ICP-MS provides a fast screening of trace metal concentration with good precision and low detection limits (Wilschefski & Baxter, 2019). Depending on the application and instrument, ICP-MS allows the analysis of elements at concentrations as low as 1 part per trillion (ppt) or even lower (Schönbächler, 2018).

### 2.3.3.3 A Review of Geochemical Analysis of Soils

Geochemical analysis of soil sample has been used in soil management studies in developed countries for decades. A regional geochemical survey was carried out by US Geological Survey (USGS) and Geological Survey of Canada (GSC) to test and refine the protocols for soil surveys in North America (Woodruff et al., 2009). The study involved the collection of soil samples from 221 sites along two continental transects across Canada and the United States. Over forty (40) major and trace elements were analysed in the soils collected and the results indicated an abrupt change in the soil mineralogy and geochemistry along both transects as the soil parent material changes. Also, the geochemical data demonstrated that the dominance of the major factors controlling soil geochemistry can change across landscape especially at the continental scale.

Tazikeh, Khormali, Amini and Motlagh (2018) investigated the effects of parent material and pedogenic (soil formation) processes on the elements composition of some selected soils formed from sedimentary rocks of Kopet Dagh area of North East Iran. The study on the soils include geochemical, clay mineralogy and micro-morphological studies. The concentration of different elements in soils and parent materials is as a result of the abundance of the major mineral constituents such as gypsum, calcite, quartz and montmorillonite in the study area. The most common soil formation features identified in the area are the calcite features, gypsum accumulation and perturbation. The results also indicated that the dissolution and the redistribution of calcite and/or gypsum are responsible for the variations showed by the weathering characterisation of soils by the geochemical indexes. The overall result supports the influence of parent material on soil geochemistry in arid areas. Generally, management of calcareous soil is so important in dry land (Rate & Sheikh-Abdullah, 2017).

Esmaeili, Moore, Keshavarzi, Jaafarzadeh and Kermani (2014) conducted geochemical survey of heavy metals in agricultural soils of Isfahan industrial area of Iran. The results of the geochemical survey were statistically analysed using multivariate statistics. Also, Nemero's soil pollution index (Pn) was used in the evaluation of the agricultural soil quality. The results showed that the high degree of contamination in the area was as a result of the presence of Pb, Zn and Cd. High level pollution nearby and along the industrial and mining zones were revealed by the pollution indices maps (Esmaeili et al., 2014).

Also, drones imaging and wearable augmented reality technology were used to create soil maps and determine the location of soil samples in management zones in southern Finland. This soil sampling was used to get information pertaining to the fertilization of the farm fields (Huuskonen & Oksanen, 2018). Soil properties maps are particularly useful for precision farming practices as aerial images representing the soil colour can be acquired annually after tillage operations on the farm field (Huuskonen & Oksanen, 2018).

Similarly, agricultural soils of Dongchuan mining area of China were sampled and analysed to ascertain the concentration of selected trace elements (Cheng et al., 2018). Statistical analyses such as descriptive and exploratory statistics were used to identify the various sources of pollution and the relationship of the trace elements in the soil of the study area. Sources of copper (Cu) and arsenic (As) were identified in the dust, smelters and the weathering of tailings and partly agricultural fertilizers. Agricultural fertilizers were the major source of cadmium (Cd). The result also revealed that the concentrations of As, Cu and Zn at several sampling points in the study area exceeded the Yunnan background values and relatively higher than the Chinese National Standards.

Furthermore, in central Portugal, Lourenco, Sequeira, Santovaia and Gomes (2014) combined magnetic, geochemical and pedological methods to characterise the soils near Coimbra in central Portugal. Geochemical studies, scanning electron microscopy and magnetic measurements were carried out on samples collected in six (6) soil profiles in order to establish possible relationships and to interpret the environmental implications. The results showed higher values of magnetic parameters in the topsoil where there is high human activity. Chemical analyses also revealed that the concentrations of various heavy metals were higher than the mean background values for soil in Portugal.

Also, machine learning was used to investigate the spatial predictions of soil macro- and micro-nutrient content across sub-saharan Africa at 250 m spatial resolution (Hengi et al., 2017). Two machine learning algorithms were used to create an ensemble model; these random forest and gradient, boosting the ensemble model for each nutrient under investigation. Hengi et al. (2017) identified manganese (Mn), zinc (Zn), aluminium (Al), boron (B) and sodium (Na) as the most important nutrients for predicting crop yield; however, they noted some of the factors limiting the mapping of the nutrients existing data

in Africa. The limiting factors include the missing of more detailed parent material/geological maps and high spatial clustering of sampling locations.

The pollution index has been a useful tool used for ecological geochemical assessments. Qingjie, Jun, Yunchuan, Qingfei and Liqiang (2008) noted that economic development and industrialisation have introduced heavy metals into the soils and sediments via several channels including irrigation, fertilization, run-offs, rivers, refined metals by product and atmospheric deposition. Adamu, Ayuba, Murtala and Uriah (2014) used pollution index to assess the level of contamination of potentially toxic metals in the soil of Keana Brinefield in the middle Benue trough, Nigeria. The result indicated that toxic metals such as lead (Pb), nickel (Ni) and chromium (Cr) have not polluted the soil of the area. Other researchers in Nigeria and Egypt have used pollution index to assess the level of contamination of toxic metals in soils (Benson et al., 2017; Izah, Bassey & Ohimain, 2017; Odukoya, Olobaniyi & Oluseyi, 2018; Badawy, Duliu, Frontasyeva, El-Samman & Mamikhin, 2019).

Generally, without soil analysis, it is nearly impossible to tell what the soil needs to improve crop growth. Soil tests and analysis provide information about the capacity of soil to supply adequate nutrients for plant growth. Soil analysis also assists in selecting the correct mix of fertilizer and liming materials, maintain soil, and increase crop production. The use of combined geophysical methods in evaluating soil evolution and pollution history have been proved throughout time to get accurate results.

# CHAPTER THREE
# MATERIALS AND METHODS

## 3.1 Materials

The materials and equipment used to carry out this research work are listed in this section. The equipment was in good condition and well calibrated. A good and newly charged battery was used for the survey. The basic tools used for the soil sampling are clean plastic bucket, shovel, hand trowel, soil tags, measuring tape and a backpack.

### 3.1.1 Equipment

The equipment used for this research work are:

i. Aktie Bolaget Elektrisk Malmletning (ABEM) (SAS 1000/4000) Terrameter with accessories (Figure 3.1);
ii. A rechargeable 12 V lithium ion A123Systems battery with model no A123-4S1P;
iii. Garmin GPSMAP 78 color hand-held GPS device;
iv. PerkinElmer Sciex Elan 9000 Inductively Coupled Plasma Mass Spectrometer (ICP-MS) PerkinElmer Instruments, Shelton, USA ;
v. A core i5 HP laptop computer.

**Figure 3.1:** ABEM Terrameter (SAS 1000/4000)

## 3.2 Study Area and Sites Description

The study area includes two sites located at Covenant University farm, Ota, Ogun State and Landmark University farm, Omu-Aran, Kwara State, Nigeria. The map of Nigeria showing the study area is presented in Figure 3.2.

**(a) Covenant University Farm:** This farm site is located along the mandate road in Covenant University campus. It has been in existence for over 10 years with various agricultural crops such as leafy vegetables that is, okra, jute and pumpkins been cultivated in the farm. Palm trees have been recently added to the list of cultivated crops in the farm and these have served as the source of the commercial palm oil the University farm currently boasts of. Chicken litters and animal dungs are the main fertilizers used in the farm while chemical fertilizers are used sparingly.

**(b) Landmark University Farm:** The farm used for this study is one the numerous farms in Landmark University. It started operations about 7 years ago and it's located several kilometers away from the main campus. It is one of the commercial farms of the university and crops such as rice, okro and maize are usually grown on this farmland. Chemical fertilizers (NPK) are mainly used to boost crops on this farmland. Pesticides are also used to prevent pests from destroying the harvest. Irrigation facilities are available on this farmland as well. The topography of the farm is steeply undulating.

A letter of introduction from the Head, Department of Physics, introducing the research student and seeking due permission to use the farm sites was taken to the farm management of the two institutions. Detailed geographical descriptions of both study areas are presented below.

### 3.2.1 Location and Geological Setting of Covenant University Farm

The geographical coordinates of the site in Covenant University farm are 6˚40′58.39" N, 3˚9′0.24" E and 6˚41′4.82" N, 3˚10′19.51" E. Covenant University farm in Ota, Ogun State, Southwestern Nigeria falls within the Eastern Dahomey basin. Dahomey basin is basically made up of sedimentary rock sequence generally of Late Cretaceous to Early Tertiary in age (Figures 3.3) (Olabode, 2006; Aizebeokhai & Oyebanjo, 2013). Dahomey Basin stretches from Ghana through Togo and the Republic of Benin to Nigeria, combining the

inland, coastal and offshore basin of these regions. The subsurface basement high referred to as the Okitipupa Ridge sepearates it from the Niger Delta (Akinwumiju & Olorunfemi, 2016).

The stratigraphy of the area has the sequence: Cretaceous Abeokuta Formation overlain by Ewekoro Formation, Oshosun Formation and Ilaro Formation, all Tertiary in age. The Ilaro Formation is overlain by the Quaternary Benin Formation and the Deltaic plain sands (Table 3.1). The local geology consists of the coastal plain sands which are underlain by coarse sandy estuarine deltaic and continental beds sequence. A reconnaissance survey was first conducted to ascertain the actual location of the study area while the geological mapping of the study sites was later carried out.

### 3.2.2 Location and Geological Setting of Landmark University Farm

The geographical coordinates of the site at Landmark University farm, Omu-Aran, Kwara State, Northcentral Nigeria are 8˚8′47.62" N, 5˚3′34.93" E and 8˚6′45.03" N, 5˚2′58.94" E. The northcentral part of Nigeria falls within longitude 7°59′57″ E and 9°15′33″E and latitude 9°24′59″ N and 10°44′34″N (Figure 3.2).

**Table 3.1:** Stratigraphy of Dahomey Basin

| **Age** | **Formation** | **Sub-Formation** |
|---|---|---|
| Quaternary | Deltaic Plains | |
| | Benin Formation | |
| Tertiary | Ilaro | |
| | Oshosun | Ameki Formation |
| | Ewekoro | Imo Shale |
| Cretaceous | Abeokuta Formation | Araromi |
| | | Afowo |
| | | Ise |
| Precambrian | Basement | Basement |

Source: Offordile (2002).

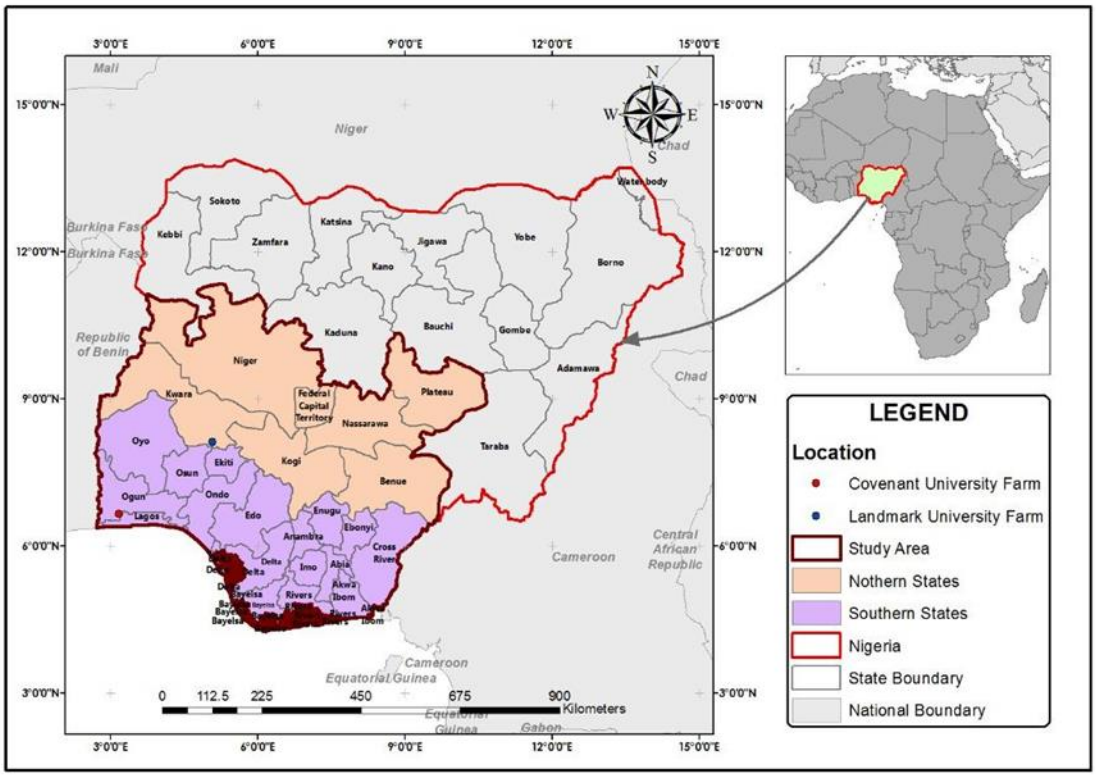


**Figure 3.2**: Map of Nigeria showing the study area (Insert: Map of Africa)

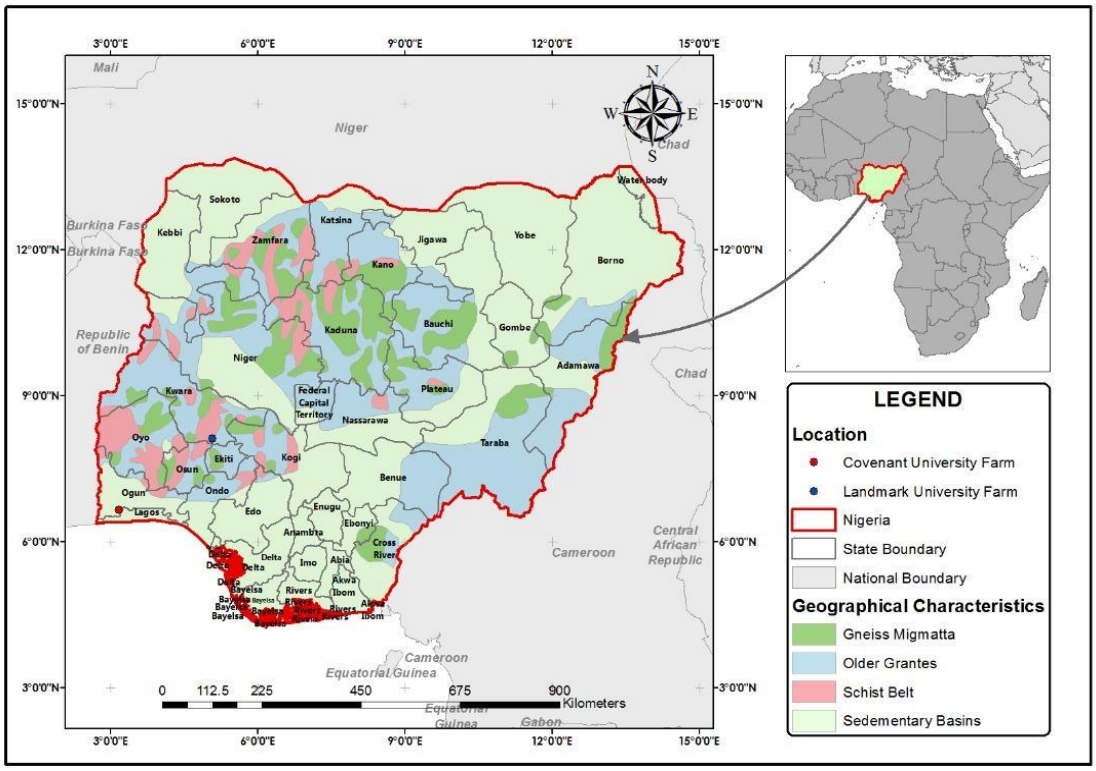


**Figure 3.3**: Geological map of Nigeria

Source: Okezie (1974) and Ugwuonah et al. (2017)

The region has elevation of over 1000 meters above mean sea level and forms a clearly defined highland area, standing above the surrounding plains. The bare grassland and the bounding scarp distinguished this region. The plateau landscape around the plains of River Benue rises steeply from 200 meters in the south to an average height of 1200 meters on the Jos plateau. Mt. Shere (1829 meters above mean sea level) is its highest point (Odunuga & Badru, 2015). The Precambrian basement complex rocks underlain three areas of Nigeria: northcentral area including the Jos Plateau; Southwest area adjacent to Benin; and southeast area adjacent to Cameroon (Obaje, 2009; Haruna, 2017). The rocks in the northcentral area are composed of granites, gneisses, schists, migmatites, quartzite and phyllites. Geological map showing both study sites is presented in Figure 3.3.

The schist belt is confined to the north-northeast (NNE)-trending zone spreading to about 300 km wide. Towards the western zone, migmatites and gneisses constitute the rocks in the area and to the east, Egbe-Isanlu schist belts which are considered as Upper Proterozoic supracrustal rocks emerging from the Pan-African granite-migmatite terrain are observed (Obaje, 2009). In all parts of the Nigerian basement complex, the Pan-African granitoids are enclosed within both the schist belts and the migmatite-gneiss complex, the extent of the Pan-African plutonism has not been fully understood though (Rahaman, 1976a, b; Ugwuonah, Tsunogae & Obiora, 2017).

The schist belts of Nigeria that extend to Kwara State have been studied extensively by researchers over the years in localities such as Iwaraja, Maru, Kazaure, Zuru, Zungeru, Isheyin, Oyan, Kushaka Iwo and Ilesha but majorly for gold mineralization (Obaje, 2009; Ugwuonah & Obiora, 2011; Kayode et al., 2015; Ugwuonah et al., 2017; Adeoti & Okonkwo, 2017; Fagbohun, Adeoti & Aladejana, 2017; Akinlalu et al., 2018). Omu-Aran falls within the Nigerian schist belt, bounded by longitudes 40.59’47.26” E and 50.29’41.667” E, and latitudes 80.0’14.8392” N and 80.30’15.5664’N. Nigerian schist belt is well developed in the southwest of Nigeria trending north-south and extending to Omu-Aran (Kayode, Nawawi, Baioumy, Khalil & Khiruddin, 2015). Minor occurrences of the schist belt are somewhat observed on the eastern flank (Obaje, 2009). Omu-Aran is underlain by granite further deformed into gneiss and quartz schists (Obaje, 2009).

## 3.3 Electrical Resistivity Method

Electrical resistivity survey involving vertical electrical sounding (VES) and two-dimensional (2D) resistivity imaging was conducted at both sites using ABEM Terrameter (SAS 1000/4000) (Figure 3.1). The surveys were carried out in the two farms for delineating the subsurface lithology and the depth to groundwater table in the study sites. The following accessories are associated with the equipment: cables, electrodes, two current cable reels, two potential cable reels, crocodile clips, sledge hammers, hand gloves, meter rules and battery. The data acquisition for Covenant University farm was carried out between April and June 2018, while that of Landmark University farm was carried out between July and August 2018, and December 2018 and January 2019. The basemaps for the survey in the study area are presented in Figures 3.4 and 3.5.

### 3.3.1 Vertical Electrical Sounding: Data Acquisition

The vertical electrical sounding was carried out to distinguish electrical resistivity differences at multiple layers in the soil profile. The Schlumberger array was used to conduct the vertical electrical sounding (VES). Five (5) VESs were conducted in the site of both farms (Covenant University and Landmark Universty Farms). The advantages the Schlumberger array have over Wenner array are that fewer electrodes are moved at each sounding points, the cable length for the potential electrodes is shorter, and greater probing depth is obtained.

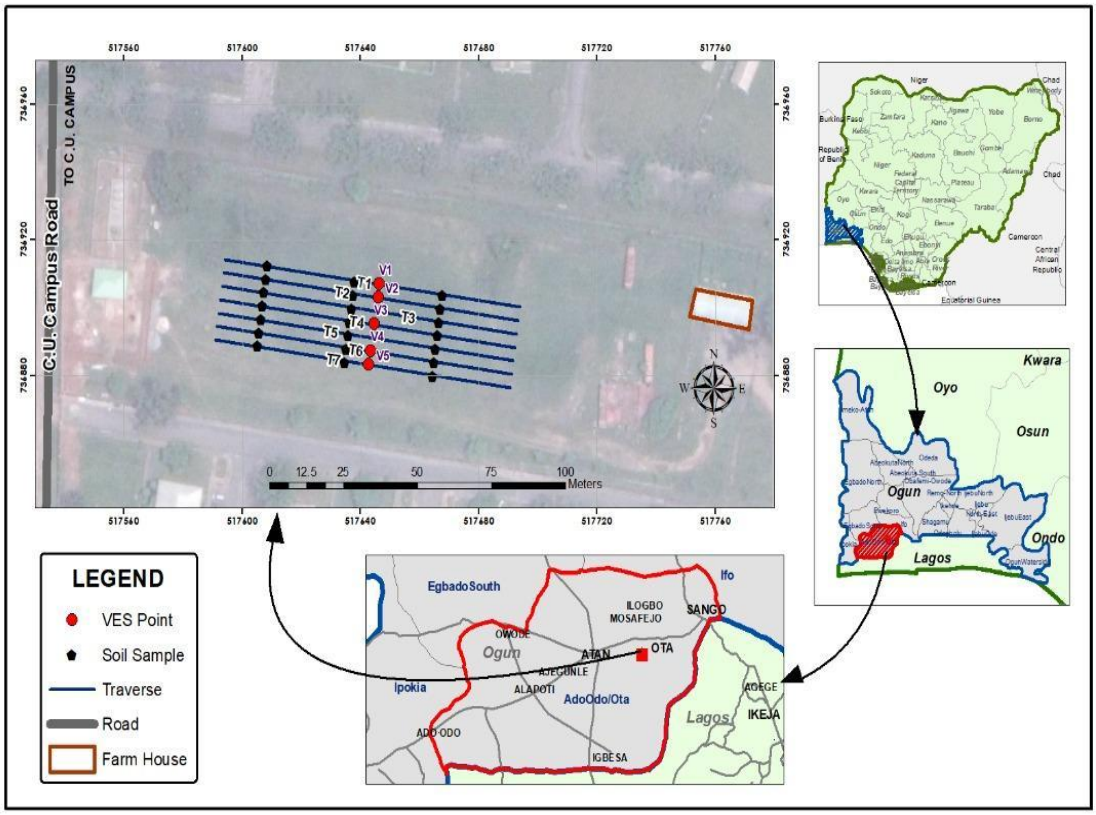


**Figure 3.4**: Basemap of traverse lines and sampling points in Covenant University farm

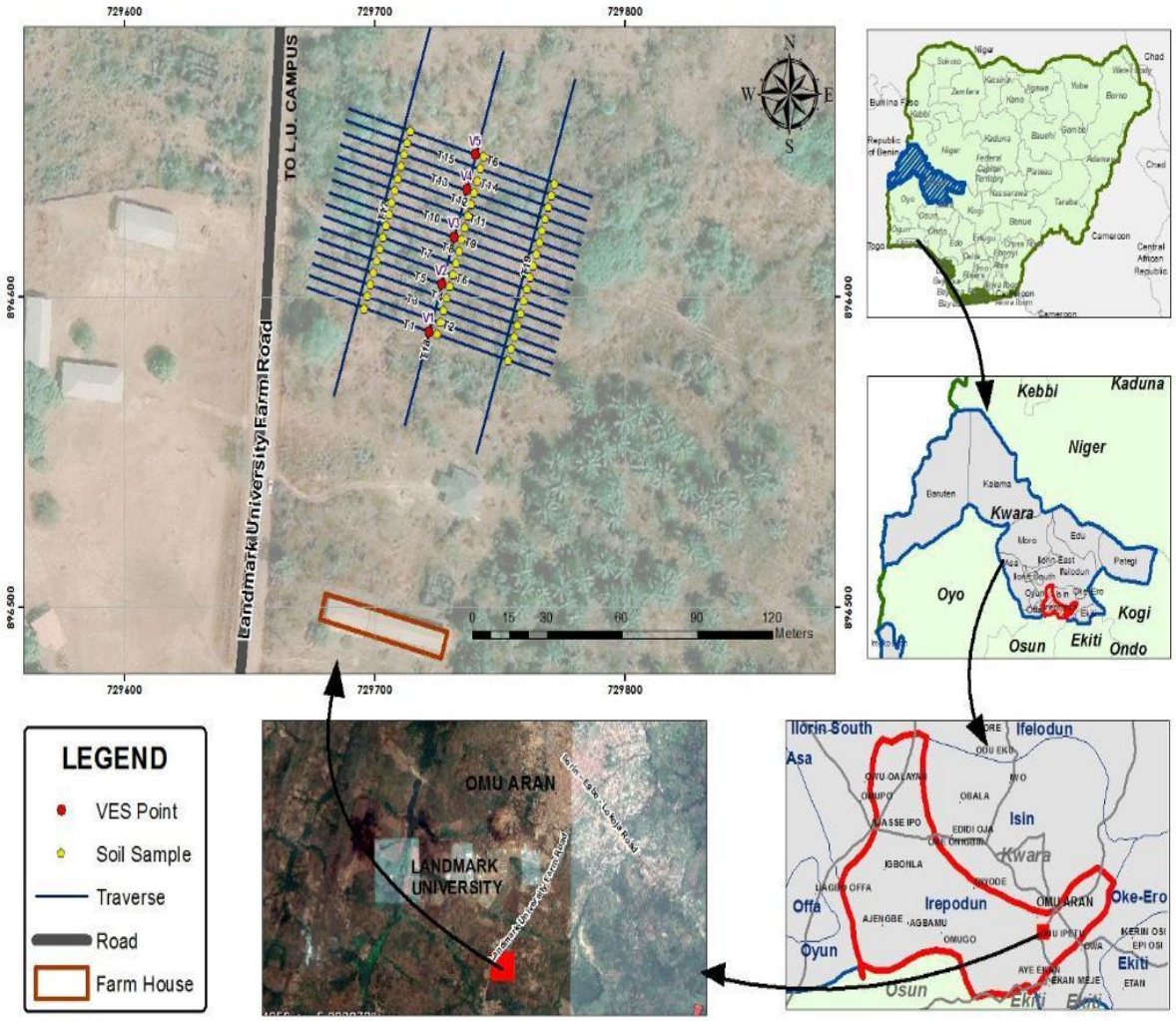


**Figure 3.5**: Basemap of traverse lines and sampling points in Landmark University farm

The current electrode spacing (AB/2) ranging from a minimum of 1.0 - 180.0 m was adopted for the resistivity sounding data measurements. The electrode spread used for the soundings was considered sufficient for the effective 2.0 m depth of investigation anticipated. The four (4) collinear electrodes were moved along the traverses with a current electrode maximum spread of 100 - 180 m. The outer two electrodes are current electrodes and the inner two electrodes are potential electrodes. The mean apparent resistivity was computed and displayed by the resistivity equipment. The potential electrodes were installed at the centre of the electrode array, while the current electrodes are progressively increased during the survey. The VESs were conducted along five main profiles for both farm sites. Care was taken to minimize electrode positioning error. Good contact was ensured at the current electrodes and water used to moisten areas around the electrodes when necessary. The root-mean squares error associated with the data measurement was minimal and it is generally less than 0.3%. Electrodes contact were re-checked and repeated when measurements have root-mean squares error up to 0.05% or more. The apparent resistivity displayed by the resistivity equipment were written down in the field book used for the survey. The target of geophysical investigation for agricultural purposes is mostly shallow, a depth of about 2 meters from the ground surface, as most root zones in tropical soil do not exceed this depth (Aditama, Widodo, Bijaksana & Sanny, 2017).

### 3.3.2 Vertical Electrical Soundings: Data Processing and Interpretation

The Schlumberger master curves were used to generate partial curve matching of the field curves to obtain estimates of the resistivity and thickness of the delineated layers. A transparent sheet was placed on the logarithm graph sheet and the apparent resistivity values was plotted against AB/2. Then the smoothened field curves were matched with the best fit on the master curves to get the geoelectric parameters. The estimated geoelectric parameters were used as initial models for the computer iteration on a Win-Resist program. The Win-Resist software was used to process the vertical electrical sounding data to obtain the one-dimensional (1D) resistivity model for each point sounded. Geoelectric parameters for each sounding points were displayed by the Win-Resist. The cross signs on the resistivity graphs indicate the observed data, while the smooth curve shows the computed data. The computed data was calculated based on the initial model supplied to the system. The misfit between the calculated and observed data was minimized through iterative

process. Therefore, the graphs show the geoelectric layers in each VES points with their estimated resistivity, thicknesses and depths.

### 3.3.3 Data Acquisition for 2D Electrical Resistivity Imaging

Two-dimensional (2D) electrical resistivity imaging was carried out at both farm sites (Covenant University farm and Landmark University farm). A total of seven (7) 2D lines, with a minimum electrode spacing of 1.0 m in all the traverses and inter-traverse spacing of 4.0 m, were carried out in the farm site. The Wenner electrode configuration was adopted with a maximum traverse length of 100 m in each 2D traverse lines. The measurements commenced at the west end with each electrode positions 1, 2, 3 and 4 in each of 2D traverses. Each electrode was then moved to a new position in an interval of 1.0 m (one unit electrode spacing), the active electrode positions being 2, 3, 4 and 5. The procedure was followed through to the end of the traverse line with the last measurement of the electrode positions being 98, 99, 100 and 101. The electrode spacing was thereafter increased by 1.0 m, as previously noted, for the next data level measurements, so that the active electrode positions were 1, 3, 5 and 7.

The field procedure was repeated and each of the electrodes was shifted a distance of 1.0 m (one unit electrode spacing) and the electrode spacing was maintained for the data level until the electrode positions of 95, 97. 99 and 101 were achieved. For this study, 5 data levels were observed from the continued procedure, giving a total of 460 data points in each of the traverses.

The seven (7) 2D traverses covered at Covenant University farm spanned a total area of 100 m x 30 m (Figure 3.4) available farm land, while a total of nineteen (19) 2D traverses were taken at Landmark University farm as shown in Figure 3.5. The total area covered by the 2D traverses in the site at Landmark University farm is 200 m x 100 m.

### 3.3.4 Electrical Resistivity Imaging: Data Processing and Inversion

The 2D resistivity data was interpreted using RES2DINV software (Loke and Baker, 1996). The 2D resistivity model of the subsurface for the apparent resistivity data imputed was automatically determined by the computer program using a nonlinear optimization technique (Aizebeokhai, Olayinka & Singh, 2010). In order to determine the subsurface

resistivity distribution, the measured apparent resistivity data were inverted to obtain the inverse model resistivity. The subsurface is divided into a number of rectangular blocks by the program in conformity with the spread of the observed data. In order to minimise the squares of the difference between the observed and calculated apparent resistivity values and invert the 2D data, least-squares inversion with standard least-square constraints was used. The smoothness constraint was applied to the model perturbation vector only based on the following equations:

$$\left[ J^T J + \mu \left( f_x f_x^T + f_z f_z^T f \right) \right] \partial = J^T g \qquad (3.1)$$

where $J^T$ is the transpose to $J$, $J$ is the Jacobian matrix of partial derivatives, $\mu$ is the damping factor, $f_x$ is the horizontal flatness, $f_z$ is the vertical flatness, $\partial$ is the model perturbation vector, and $g$ is the discrepancy vector which contains the differences between the logarithms of the measured and calculated apparent resistivity values. To normalize the sensitivity values, the calculated sensitivity values was divided with the average sensitivity for the particular model configuration. The optimum step size was located by the line search which uses quadratic interpolation, at each iteration step, for the change in apparent resistivity model blocks.

The standard Gauss-Newton optimisation with a convergent of 0.05 was used for the inversion. The forward modelling subroutine with normal mesh and 4 nodes per grid size was used to calculate the apparent resistivity values. For all iterations, the initial model was the homogeneous half space and Jacobian matrix was recalculated. The program allows users to adjust the damping factor and flatness filters in the equation above to suit the data set being inverted. The initial and minimum damping factor used for the inversion is 0.15 and 0.03, respectively. The number of iterations required for convergence was reduced by optimizing the damping factor to give the least root mean square (RMS) error; however, the time taken for each iteration increased significantly. The topographic data points were inputed into the 2D inversed models to create the topography models indicating end to end type of topographic trend.

## 3.4 Geochemical Method

### 3.4.1 Soil Sampling

Soil samples were collected at 30.0 m interval in each electrical resisitivty survey traverse line at Covenant University farm and Landmark University farm. The sample collection points were at 30.0 m, 60.0 m and 90.0 m in each 100.0 m traverse line. A cutlass and a manual soil auger with depth capacity of 5 m and a diameter of 70 mm was used for drilling the farm soil while hand trowel was used to widen the holes for easy soil sample collection. Hand gloves were worn to protect the hands. Soil samples were collected at an undisturbed depth of 30 - 50 cm to get the soil in its natural state devoid of environmental contamination and were immediately kept in air tight sampling bags (Fisher et al., 2015). All sampling bags were carefully and completely labelled with identification number of sampling location. The soil samples from Landmark University farm, Omu-Aran were labelled L1 to L16, while soil samples from Covenant University farm, Ota were labelled C1 to C19. A total of 69 soil samples (21 at Covenant University farm and 48 at Landmark University farm) were collected in both study areas during the rainy season. The soil samples were collected at Landmark University farm during the rainy season (August 2018) when fertilizers have not been applied on the soil. In the Covenant University farm, the soil samples were collected also during the rainy season between June and July 2018.

### 3.4.2 Geochemical Target Elements

Soil samples were collected from both study areas (Covenant University and Landmark University farms) for geochemical analysis of macro-, micro- (trace elements) and rare earth elements contained in the soil. Thirty (30) target elements which include macro-elements such as aluminium, (Al), calcium (Ca), iron (Fe), manganese (Mn), magnesium (Mg), titanium (Ti), silicon (Si), sodium (Na), phosphorus (P) and potassium (K), and micro (trace elements) such as chromium (Cr), zircon (Zr), beryllium (Be), copper (Cu), cobalt (Co), lead (Pb), zinc (Zn), nickel (Ni), barium (B), molybdenum (Mo), arsenic (As), manganese (Mn), cadmium (Cd) . Rare earth elements (REEs) such as gadolinium (Gd), lanthanium (La), cerium (Ce), praseodymium (Pr), samarium (Sm), europium (Eu) and vanadium (V) in the study area were also quantified by Inductively Coupled Plasma Mass Spectrometry (ICP-MS), one of the most superior technique used to quantify REE in soil samples as reported by Li et al. (2017).

### 3.4.3 Geochemical Analysis

The soil samples were analysed for a range of trace elements, macro elements and other rare earth elements using a Perkin Elmer Elan 9000 Inductively Coupled Plasma Mass Spectrometer (ICP-MS). The soil samples in the sampling containers were sealed and shipped to Bureau Veritas Laboratory, Canada for trace element analysis. Elan 9000 1CP-MS equipment was used for the elemental analysis. Elan 9000 has speed and performance advantage over other absorption spectroscopy and significantly improves sample turnaround times. Analysis for the soil parameters followed the standard procedures (Enamorado-Baez, Abril & Gomez-Guzman, 2013; Finch, Roldan, Walsh, Kelly & Amor, 2018; Wilschefski & Baxter, 2019). The concentration is presented in ppm and %; the micro (or trace) elements are in ppm while macro (or major) elements are in %. The units of ppm and % for both micro elements and macro elements respectively are standards of the analytical package used for the analysis. Conversion from ppm to mg/kg is such that 1 ppm equals 1 mg/kg. Also, 1 µg/kg or 1 µg/L equals 1 ppb, and 1 ppb equals 0.001 ppm; therefore, 1 µg/kg equals 0.001 ppm.

The soil samples were dried in the oven at 40˚C, disaggregated with the aid of a hammer to reduce agglomeration, disintegrated and homogenised in a porcelain mortal and then passed through a 2 mm sieve. Each sample was thereafter splitted into three (3) portions, one of which was archived for further studies and the second was submitted for engineering properties analysis including particle size analysis, bulk density and percentage void. The third portion was pulverized and divided into bottles and was submitted to the analytical laboratory. The element concentration for all the samples were determined after a multi-acid digestion with perchloric and HF. The MA250 analytical packet (ICP-MS chemical analysis of multi-acid digested samples) at bureau veritas mineral laboratory (BVML) was used for the total digestion of samples. A 0.25 g split of sample was heated in $HNO_3$-$HClO_4$-HF (Tripple acid digestion) to fuming and was then dried. The residue was then dissolved in 50% HCl solution (Tejada et al., 2016; Cecconi et al., 2019). Strong oxidizing agents ($HNO_3$ and $HClO_4$) were used for total removal of the organic matter, while the use of HF enables the dissolution of silicates, allowing the near-total dissolution of the mineral fraction. Other laboratory analysis was conducted at the Civil Engineering geotechnical laboratory in Covenant University.

### 3.4.4 Quality Control

All glasswares used in the laboratory were washed and rinsed with distilled water and air-dried before the analysis. Appropriate solvents were also used to rinse dry glasswares before use. In other for uniformity of comparisons similar masses (0.25 g) of soil samples were analysed. Samples were carefully labelled through the process. Accuracy of the analytical methods was monitored by repeated analysis of standard reference materials, STD OREAS25A-4A and OREAS45E, together with batches of soil samples. The detection limits for the trace and major elements analysed are presented in Table 3.2.

### 3.4.5 Toxic Elements Contamination Assessment

Contamination factor ($Cf$) and Pollution Load Index (PLI) were used to assess the degree of contamination in the study area. Contamination factor ($Cf$) was calculated using the equation:

$$Cf = \frac{C_n}{B_n} \tag{3.2}$$

where $C_n$ the concentration of metal and $B_n$ is the background/crustal average value of the element. The classification of contamination factor is presented in Table 3.3. The pollution load index (PLI) otherwise called the Tomlinson's pollution index and the Nemerow integrated pollution index (NIPI) have been used to assess the overall pollution status for samples (Tomlinson, et al., 1980; Nemerow, 1985; Lu, Zhang, Li & Chen, 2014; Odukoya, Olobaniyi & Oluseyi, 2018). The PLI was calculated using the equation:

$$PLI = \sqrt[n]{Cf_1} \times Cf_2 ... Cf_n \tag{3.3}$$

where PLI is pollution load index, n is the number of samples, $Cf_n$ is the $Cf$ value of metal n. According to the equation, PLI value of $\leq 1$ indicates no pollution, $1 \succ PLI \leq 2$ unpolluted to moderate pollution, $2 \succ PLI \leq 3$ moderately polluted, $3 \succ PLI \leq 4$ moderate to high pollution and $4 \succ PLI \leq 5$ is highly polliuted (Tomlinson, et al., 1980; Adamu et al., 2014 & Benson et al., 2018). The Nemerow integrated pollution index (NIPI) is calculated using the equation:

$$NIPI = \sqrt{0.5}(I_{mean}^2 + I_{\max}^2) \tag{3.4}$$

where $I_{mean}$ is the mean value of all CF and $I_{\max}$ is the maximum value.

**Table 3.2**: Trace elements detection limits using ICP-MS

| *S/N* | Trace elements | Detection limit |
|---|---|---|
| 1 | As | 0.2 ppm |
| 2 | Na | 0.001 % |
| 3 | Mg | 0.01 % |
| 4 | Be | 0.1 ppm |
| 5 | Ni | 0.1 ppm |
| 6 | P | 0.01% |
| 7 | Pb | 0.02 ppm |
| 8 | Pr | 0.1 ppm |
| 9 | Gd | 0.1 ppm |
| 10 | Ce | 0.02 ppm |
| 11 | K | 0.01% |
| 12 | Ca | 0.01% |
| 13 | Fe | 0.01 % |
| 14 | Se | 0.3 ppm |
| 15 | Sm | 0.1 ppm |
| 16 | Sn | 0.1 ppm |
| 17 | Sr | 1 ppm |
| 18 | Zr | 0.2 ppm |
| 19 | Tb | 0.1 ppm |
| 20 | B | 0.05 ppm |
| 21 | Th | 0.1 ppm |
| 22 | Ti | 0.001 % |
| 23 | TI | 0.05 ppm |
| 24 | Co | 0.2 ppm |
| 25 | Mo | 0.05 ppm |
| 26 | V | 1 ppm |
| 27 | W | 0.1 ppm |
| 28 | Cu | 0.1 ppm |
| 29 | Yb | 0.1 ppm |
| 30 | Zn | 0.2 ppm |
| 31 | Cr | 1.0 ppm |
| 32 | Mn | 1 ppm |
| 33 | Cd | 0.02 ppm |

The pollution load index (PLI) and Nemerow integrated pollution index classification is presented in Table 3.4. The degree of contamination $C_d$ was proposed by Hakanson (1980) to facilitate pollution control. Cd is determined as the sum of Cf for each sample and calculated using the equation:

$$C_d = \sum_{i=1}^{i=n} Cf \tag{3.5}$$

The $C_d$ is a measure of the degree of overall contamination in surface layers in core or sampling site. The classification of degree of contamination in sediment as proposed by Hakanson (1980) is $C_d$ <6 is low degree contamination, $6 \prec C_d \prec 12$ moderate degree of contamination, $12 \prec C_d \prec 24$ considerate degree of contamination and $C_d \succ 24$ high degree of contamination. To estimate the overall degree of contamination at a given site a modified degree of contamination $mC_d$ was introduced by Abraham and Parker (2008) and was calculated by this equation:

$$mC_d = \frac{(\sum_{i=1}^{i=n} CF)}{n} \tag{3.6}$$

where n is the number of analysed samples, i is the ith element (or pollutant) and CF is the contamination factor. This modified equation defines the degree of contamination as the sum of all the contamination factors (CF) for a given set of sediment pollutants divided by the number of analysed pollutants. The proposed gradation for modified contamination degree (mCd) in the sediment is $mC_d \prec 1.5$ nil to very low degree of contamination, $1.5 \leq mC_d \prec 2$ is a low degree contamination, $2 \leq mC_d \prec 4$ is a moderate egree of contamination, $4 \leq mC_d \prec 8$ is a high degree of contamination and $8 \leq mC_d \prec 16$ is a very high contamination and $16 \leq mC_d \prec 32$ is extremely high contamination.

Geoaccumulation index ($I_{geo}$) introduced by Muller (1969) was used to assess pollution of metals in soils and is calculated using the equation:

$$I_{geo} = Log_2 \frac{Cn}{1.5Bn} \tag{3.7}$$

where Cn is the concentration of metal, 1.5 factor is introduced into the expression to account for variations in background values as a result of lithogenic effects. The geoaccumulation index is graded from unpolluted $(I_{geo} \prec 1)$; very low and low polluted $(1 \prec I_{geo} \prec 3)$; moderately polluted $(3 \prec I_{geo} \prec 4)$; highly polluted $(4 \prec I_{geo} \prec 5)$; to very highly polluted $(5 \prec I_{geo} \prec 6)$. The highest-grade (6) indicates a 100-fold enrichment, above the background data.

The ecological risk index proposed by Hakanson (1980) was used to assess the overall degree of toxic elements contamination in soils and its short to long term response to the environment. This risk index ($R_i$) is calculated using the equation:

$$R_i = \sum\sum f^i \qquad (3.8)$$

$$\sum f^i = \sum T_r^i \left(\frac{C^i}{C_n}\right) \qquad (3.9)$$

Where $R_i$ is the sediment risks factor considering all sediment bound elements, $\sum f^i$ is the potential ecological risk index for each single element i, $C_i$ is the observed concentration of element i in soil samples, $C_n$ is the background values of element i and $T_r^i$ is the toxicity coefficient for As, Cd, Cr, Cu, Pb, Ni and Zn are 10, 30, 2, 5, 5, 5 and 1 respectively (Hakanson, 1980, Benson et al., 2017). The gradation for the ecological risk index is presented in Table 3.5.

**Table 3.3**: Classification of Contamination factor

| Contamination factor | Level of Contamination |
|---|---|
| $PI \leq 1$ | Low Contamination |
| $1 < PI \leq 3$ | Middle Contamination |
| $PI > 3$ | High Contamination |

**Table 3.4**: Pollution load index (PLI) and Newerow integrated pollution index (NIPI) classification

| Contamination factor and level of pollution | | |
|---|---|---|
| PLI = 0 Background Contamination | NIPI = 0.7 | Safe |
| 0 < PLI = 1 Unpolluted | 0.7< NIPI = 1 | Precaution |
| 1 < PLI = 2 Unpolluted to moderately polluted | 1< NIPI = 2 | Slight Pollution |
| 2 < PLI = 3 Moderately polluted | >NIPI = 3 | Moderate pollution |
| 3 < PLI = 4 Moderately to highly polluted | NIPI > 3 | Heavy Pollution |
| 4 < PLI = 5 Highly polluted | | NIPI = 0.7 Safe |
| PLI > 5 Very highly polluted | | |

Source: Zhang et al. (2007).

**Table 3.5:** Multi-elemental potential ecological risk index

| $R^i$ | Degree of Risk |
|---|---|
| $R_i < 95$ | Low Risk |
| $95 \leq R_i < 190$ | Moderate Risk |
| $190 \leq R_i < 380$ | High Risk |
| $R_i \geq 380$ | Very High Risk |

### 3.4.6 Geostatistical Analysis

Geostatistical analysis is used to analyse and predict values associated with spatial phenomena. It is specifically used in precision agricultural evaluations. The data obtained from soil geochemical analysis from the two sites (Covenant University and Landmark University farms) were analysed; the mean, median distribution and correlation between datasets of the two farm sites were studied using the IBM statistical package for social sciences (SPSS) version 23.0. The average of each variable as described in the results section was used for the interpretation. Toxic elements and essential elements data needed for soil fertility determination of the two study areas were subjected to correlation matrix at 0.05 significance levels.

### 3.4.7 Geospatial Mapping

The soil samples were geo-referenced with the aid of ground positioning system (GPS) at the collection points in the studied sites in both Covenant University and Landmark University farms (Tables 3.4 and 3.5). The geochemical soil analytical results with sample coordinates at both farm sites were used to produce the map in ArcGIS 10.6 version. The georeferenced sampling points with elemental concentration values were entered into ArcGIS 10.6 version to generate the 2D geospatial maps.

### 3.4.8 Soil Bulk Density

The bulk density and percentage void (soil porosity) test of undisturbed soil samples in the study areas were determined in the Covenant University geotechnical laboratory. The tools used for measuring bulk density include a steel ring, a shovel, oven proof dish, calculator, oven, marker pen, ruler and kitchen scale or balance in grams. The measurements of the volume and mass of the soil sample were taken in the laboratory and the mass of the soil sample was obtained by weighing. After weighing soil sample, it was dried at $105^{\circ}C$ until a constant weight is achieved. The bulk density was estimated by dividing the dry weight of the soil ($W_d$) by the volume of soil solids and pores ($V_s$). The result was collected and recorded. These methods depend on measurements of the volume and mass of the soil, including air and moisture (Al-Shammary et al., 2018). The bulk density of dry soil can be calculated using the equation:

$$\rho_b = \frac{W_d}{V_s} \tag{3.4}$$

where $\rho_b$ is bulk density in $mg/\mathrm{m}^3$, $W_d$ is the weight of dry soil in mg and $V_s$ is the volume of the dry soil sample in $m^3$.

### 3.4.9 Soil Porosity or Percentage Void

Particle density is equal to oven dry soil weight divided by volume of soil solids. The soil porosity or percentage void of the soil samples was then calculated using the equation:

$$\text{Soil porosity} = 100 - \frac{Bulk\ density}{Particle\ density} \tag{3.5}$$

## 3.5 Remote Sensing and GIS

The Modern-era Retrospective Analysis for Research and Applications (MERRA) of land surface variables from National Aeronautics and Space Administration (NASA) were used for the estimation of the soil temperature and soil moisture content in both sites. The monthly MERRA soil temperature and soil moisture content satellite datasets for the study areas were retrieved for this study. Also, Landsat-8 imagery obtained from the United State Geological Survey (USGS) site was used to estimate the soil salinity in the study area. The specific path and row of each image scene were specified. Tiles of Landsat-8 imagery covering the study areas were used (Figure 3.6). ArcGIS software was used to analyse the satellite imagery.

### 3.5.1 Remote Sensing Data Acquisition

Monthly MERRA soil temperature and soil moisture content for the study areas (Covenant University farm and Landmark University farm) were extracted from the NASA data set website (https://esgf.nccs.nasa.gov/projects/create-ip/). The soil temperature data spanned from 2017 to 2019 covering periods before and after the electrical resistivity survey was carried out at both selected farms. Monthly MERRA 2017 - 2019 soil moisture content (SMC) data of the study areas were used in the study. This dataset was treated using the Hierarchical Data Format (HDF) software and excel spread sheets. The averages of dataset sets were calculated at shallow depth of investigation of 15 cm.

Twenty (20) sheets/tiles of Landsat-8 imagery covering the southern and northcentral states of Nigeria were obtained from the United States Geological Survey website (https://www.usgs.gov/land-resources/nli/landsat/landsat-8) (Figure 3.7). The Landsat-8 satellite multispectral image has 11 bands, each measuring different range of frequencies along the electromagnetic spectrum (visible and invisible colour ranges). Some areas covered by cloud and shadows were not captured by the imager; such areas were excluded from the estimation process. Each band of the tiles of Landsat-8 used for the study was mosaiced in ArcGIS and the study area clipped before the map was produced.

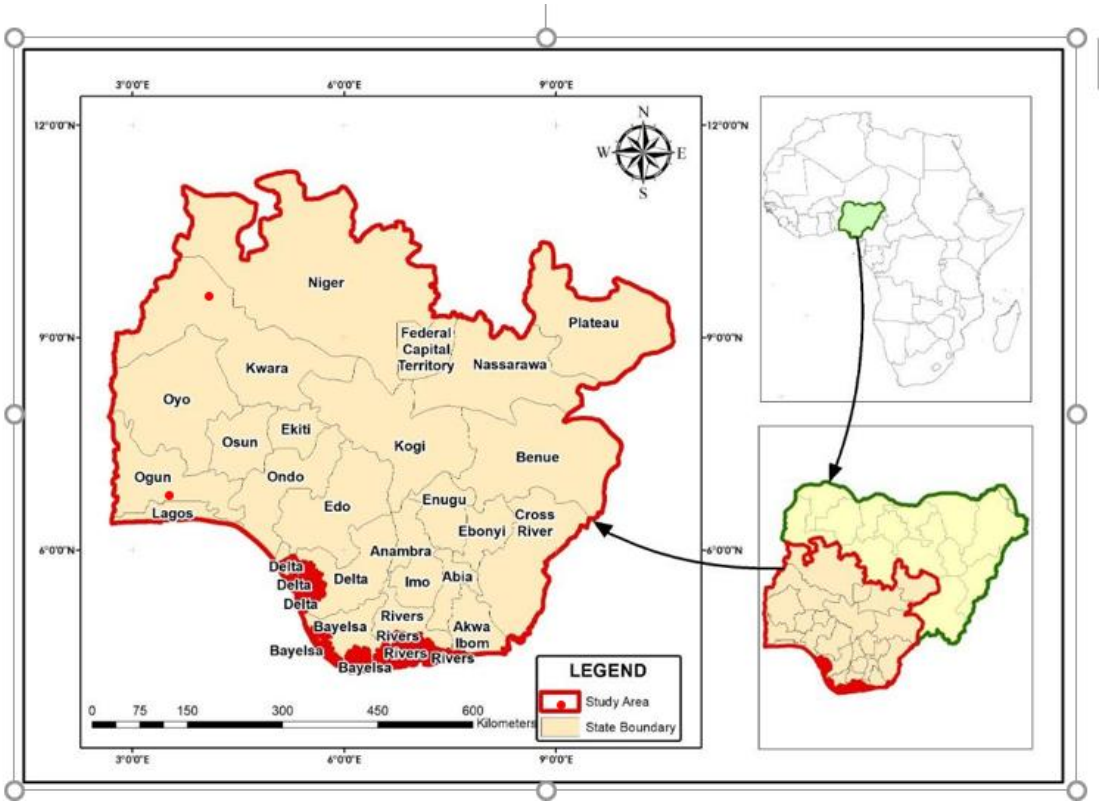


**Figure 3.6**: Map of the southern and northcentral Nigeria covered by the Landsat-8 imagery

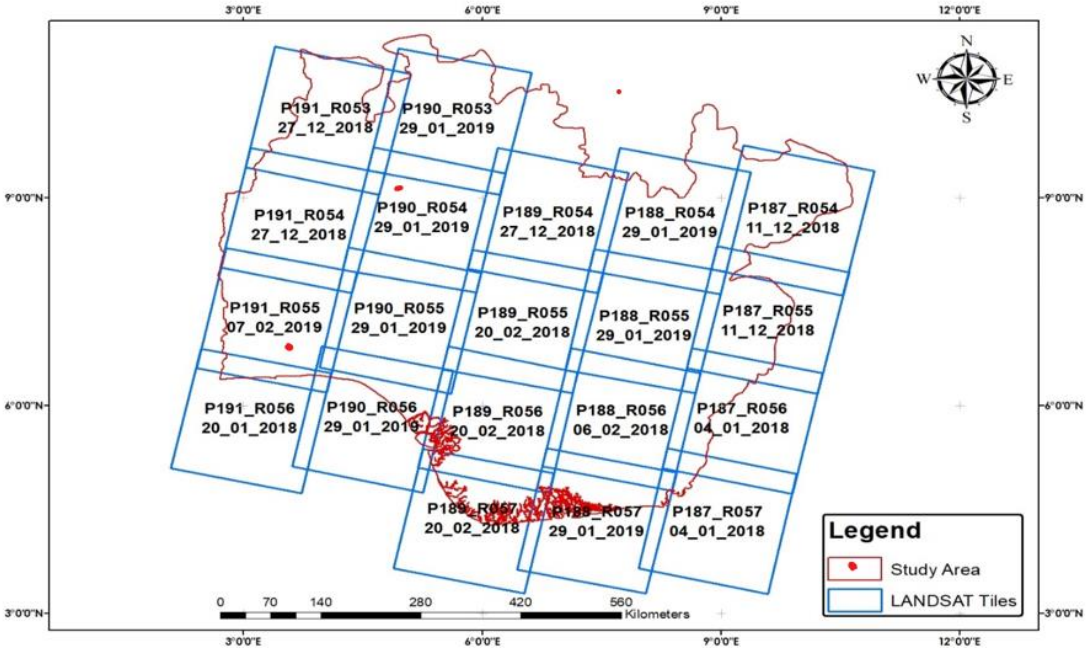


**Figure 3.7**: Layout of Landsat-8 dataset used for the study

Reflectance rescaling degrees were used to mutate the digital rate (DN) to topmost of atmosphere (TOA) planetary physical units (reversal) in the Landsat-8 operational land imager (OLI) sensor (Zanter, 2019). The DN values were mutated to reflectance for OLI data using this equation:

$$\rho\lambda = \frac{M\rho \times \mathbb{Q}_{cal} + A\rho}{Sin(\theta)} \tag{3.6}$$

$M\rho$ is the reversal multiplicative factor for the band, $A\rho$ is reflectance additive scaling factor for the band, $\mathbb{Q}_{cal}$ is the pixel value in DN, $\rho\lambda$ is TOA planetary reversal and $\theta$ is the sun altitude Angle. Following the procedures of Zanter (2019), the near infra-red (NIR) band 5, which is basically used to detect biomass content and shoreline, is also suitable for detecting soil salinity when the red and green bands of the visible spectrums are combined using the equation:

$$SI = \frac{NIR - RED}{GREEN} \tag{3.7}$$

where SI is the salinity index.

The processing steps to mapping soil salinity from Landsat-8 Imagery followed the steps highlighted by previous researchers (Mustafa & Hatem, 2019; Zanter, 2019; Nguyen, Liou, Tran, Hoang & Nguyen, 2020). Firstly, the satellite images were converted from DN to reflectance physical units where the Landsat-8 image is placed within the range of 0 to maximum value. The region of interest (ROI) and samples are selected based on SWIR2, NIR and Green combination bands. Image was classified by maximum likelihood method and bare soil class was segmented from the classes of the images. Also, soil indicator used in the research that is, soil salinity was introduced at this stage. The segment image shows the resulting soil salinity images. Then, find the associated salinity index values associated with the Gray scale values for each of the images already obtained. A plot is subsequently made for each of the extracted salinity values with corresponding soil indicator (grassland) images to find the minimum and maximum values. Lastly, the spatial analysis tools in ArcGIS 10.6 software were used to compute indices and analyze the indices.

# CHAPTER FOUR
# RESULTS

## 4.1 Soil Profile Delineation Using Geoelectrical Resistivity Techniques

The resistivity models of the vertical electrical sounding (VES) data for the sites at Covenant University farm and Landmark University farm obtained using the Win-Resist software are presented in Figures 4.1 - 4.5. The vertical electrical sounding models obtained for the site at Covenant University farm are shown in Figures 4.1 - 4.3a, while the VES models for Landmark University farm are presented in Figure 4.3b - 4.5. The cross signs in the resistivity models indicate the observed data and the smooth curves indicate the computed data. The geoelectric parameters and corresponding lithology inferred for resistivity soundings conducted on both sites are presented in Tables 4.1 and 4.2. The geoelectric parameters include inferred lithology, varying thicknesses and depths obtained from the resistivity soundings. The weathering profile of Landmark University farm (Table 4.2) has revealed four (4) main lithology which include the topsoil (Stone zone), the upper and lower saprolite layers which represent the weathered zone comprising of the sandy and gravelly sand, and the fractured/fresh basement units.

**Table 4.1**: Geoelectric parameters from the VESs in Covenant University farm

| VES no | Layer | Resistivity | Thickness | Depth (m) | Inferred Lithology |
|---|---|---|---|---|---|
| 1 | 1 | 158 | 2.0 | 2.0 | Topsoil (Sandy Clay) |
| | 2 | 212 | 3.1 | 5.1 | Sandy Clay |
| | 3 | 1340 | 28.3 | 33.4 | Lateritic Clay |
| | 4 | 400 | - | - | Clayey Sand |
| 2 | 1 | 245 | 1.8 | 1.8 | Topsoil (Sandy Clay) |
| | 2 | 355 | 6.8 | 8.6 | Clayey Sand |
| | 3 | 1723 | 4.2 | 12.8 | Lateritic Clay |
| | 4 | 1920 | 17.1 | 29.9 | Lateritic Clay (Compacted) |
| | 5 | 1977 | 24.9 | 54.8 | Kaolinitic Clay |
| | 6 | 474 | - | - | Clayey Sand |
| 3 | 1 | 236 | 1.6 | 1.6 | Topsoil (Sandy Clayey) |
| | 2 | 672 | 8.3 | 13.3 | Sandy mudstone |
| | 3 | 629 | 3.4 | 19.3 | Sandy mudstone |
| | 4 | 418 | 10.0 | 23.3 | Clayey Sand |
| | 5 | 4655 | 27.2 | 50.5 | Kaolinitic Clay |
| | 6 | 578 | - | - | Clayey Sand |
| 4 | 1 | 161 | 0.8 | 0.8 | Topsoil (Sandy Clay) |
| | 2 | 466 | 18.5 | 9.3 | Sandy mudstone |
| | 3 | 891 | 5.9 | 15.1 | Lateritic Clay |
| | 4 | 674 | 8.6 | 23.1 | Sandy mudstone |
| | 5 | 5418 | 33.3 | 57 | Kaolinitic Clay |
| | 6 | 494 | - | - | Clayey Sand |
| 5 | 1 | 156 | 1.9 | 1.9 | Topsoil (Sand Clay) |
| | 2 | 155 | 6.0 | 7.9 | Sandy Clay |
| | 3 | 2385 | 11.4 | 19.3 | Lateritic Clay (Compacted) |
| | 4 | 3695 | 21.9 | 41.2 | Kaolinitic Clay |
| | 5 | 2479 | 14.2 | 55.4 | Lateritic Clay |
| | 6 | 592 | - | - | Clayey Sand |

**Table 4.2**: Geoelectric parameters and inferred lithology obtained from VESs in Landmark University farm

| VES no | Layer | Resistivity (Ωm) | Thickness (m) | Depth (m) | Inferred Lithology |
|---|---|---|---|---|---|
| 1 | 1 | 152 | 2.7 | 2.7 | Topsoil (Clayey) |
| | 2 | 599 | 7.1 | 9.8 | Upper Saprolite |
| | 3 | 966 | 33.6 | 43.4 | Fractured Basement |
| | 4 | 424 | - | - | Fractured Basement |
| 2 | 1 | 884 | 2.6 | 2.6 | Topsoil (Stone zone) |
| | 2 | 494 | 2.9 | 5.5 | Upper Saprolite |
| | 3 | 906 | 9.8 | 15.3 | Lower Saprolite |
| | 4 | 6326 | - | - | Fresh Basement |
| 3 | 1 | 614 | 2.1 | 2.1 | Topsoil (Stone zone) |
| | 2 | 1575 | 13.7 | 15.8 | Upper Saprolite |
| | 3 | 294 | 5.0 | 20.8 | Lower Saprolite |
| | 4 | 1793 | - | - | Fractured basement |
| 4 | 1 | 1075 | 2.0 | 2.0 | Topsoil (Stone zone) |
| | 2 | 1440 | 14.0 | 16.0 | Upper Saprolite |
| | 3 | 858 | 10.0 | 26.0 | Lower Saprolite |
| | 4 | 3045 | - | - | Fresh Basement |
| 5 | 1 | 830 | 2.0 | 2.0 | Topsoil (Stone zone) |
| | 2 | 977 | 14 | 16 | Upper Saprolite |
| | 3 | 484 | 21 | 37 | Lower Saprlite |
| | 4 | 1250 | - | - | Fractured Basement |

a)

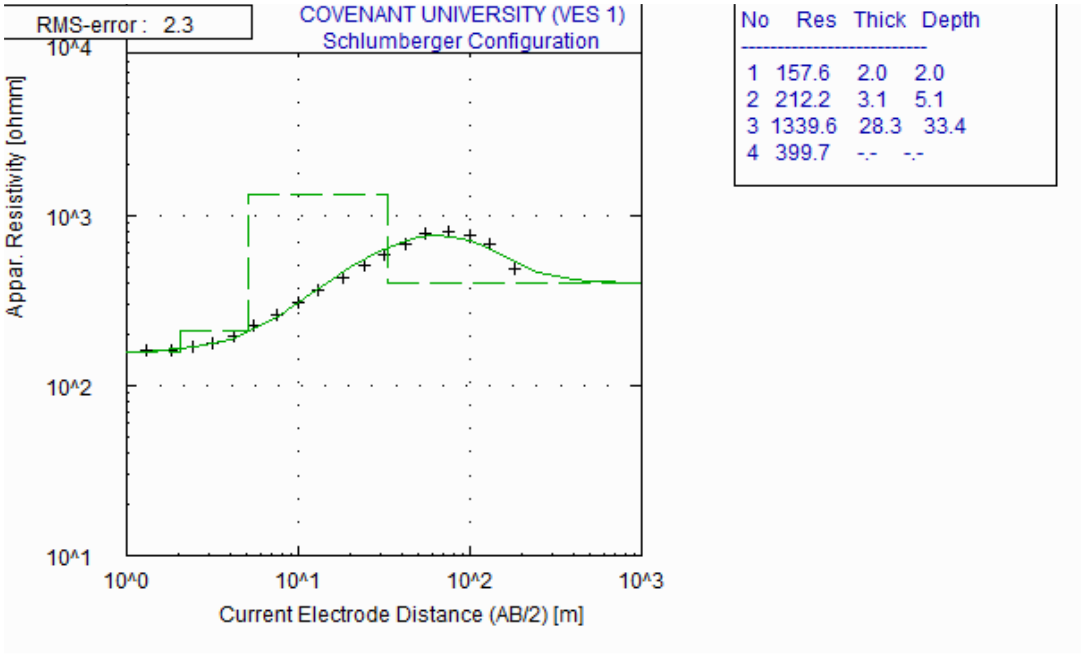


b)

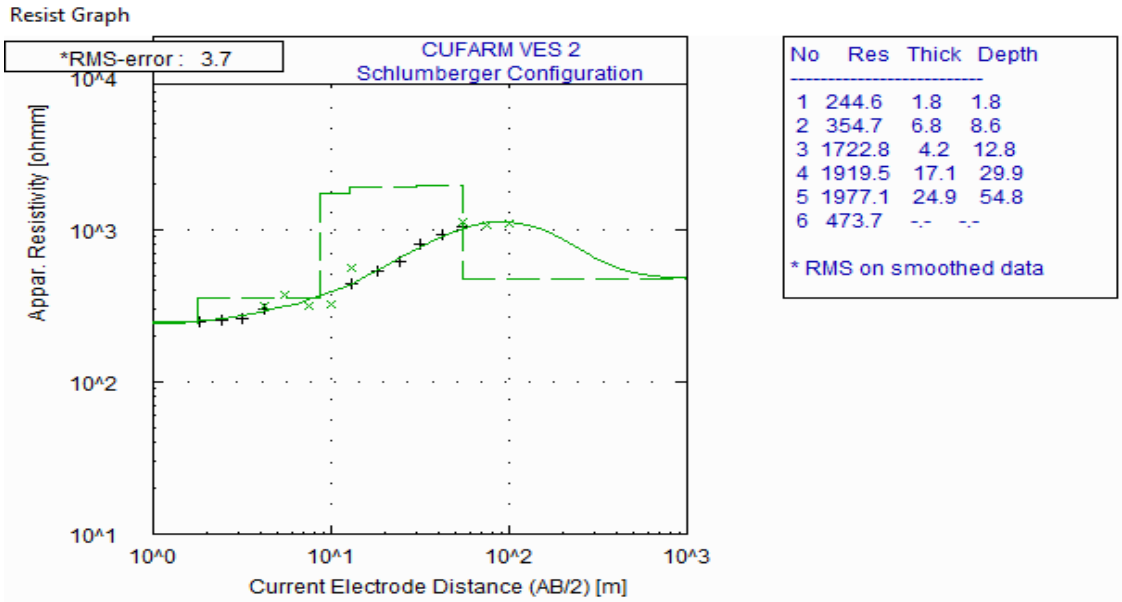


**Figure 4.1**: Resistivity models in Covenant University farm for: (a) VES 1, and (b) VES 2

a)

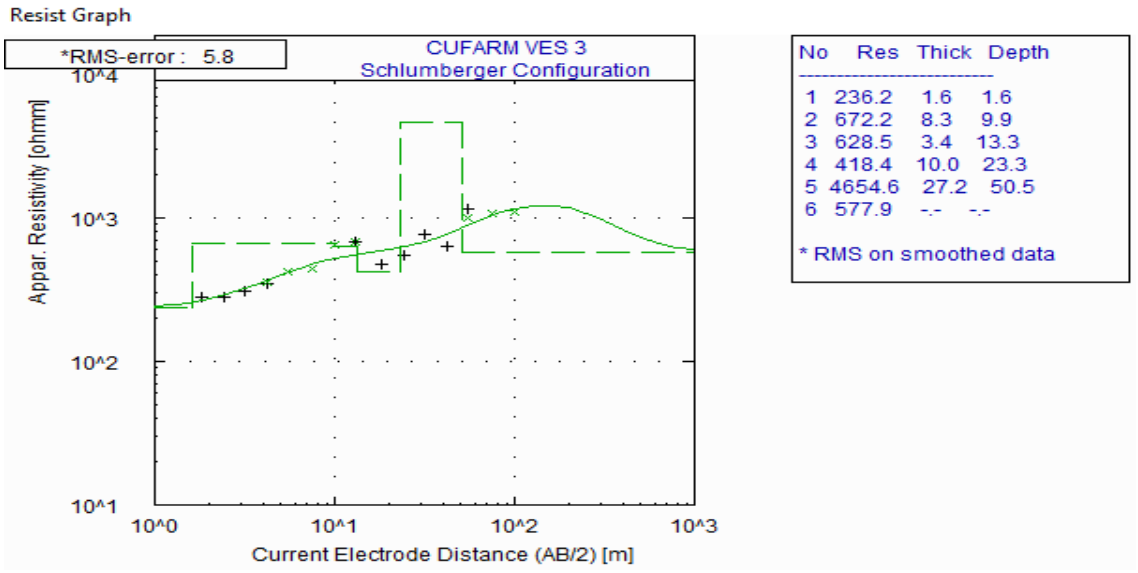


b)

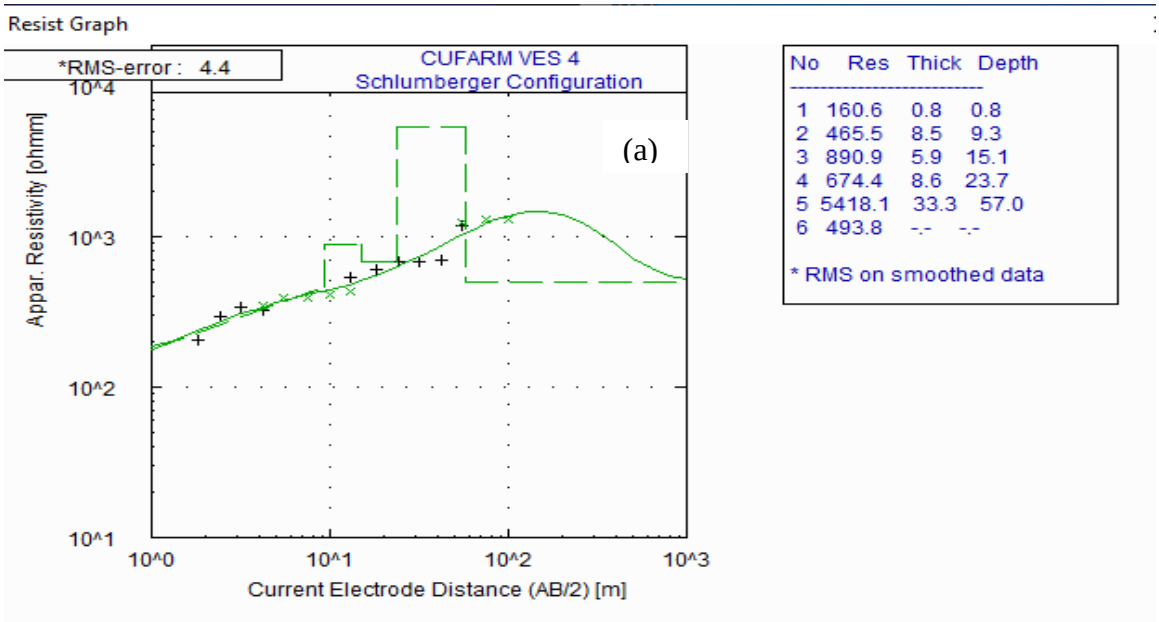


**Figure 4.2**: Resistivity models in Covenant University farm for: (a) VES 3, and (b) VES 4

a)

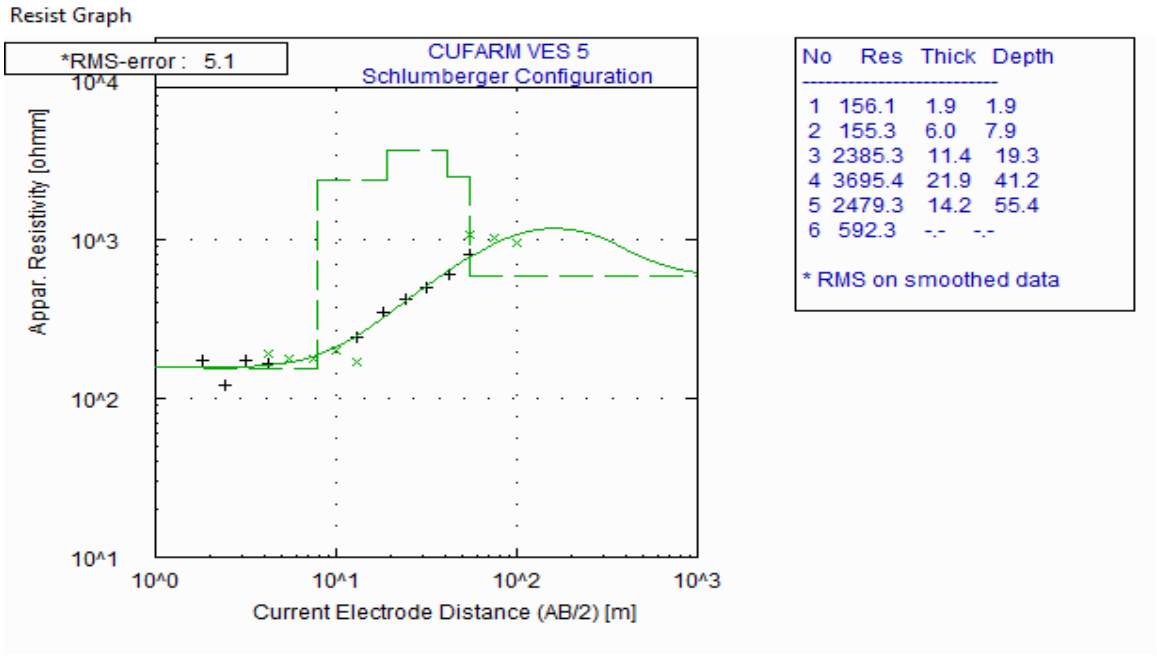


b)

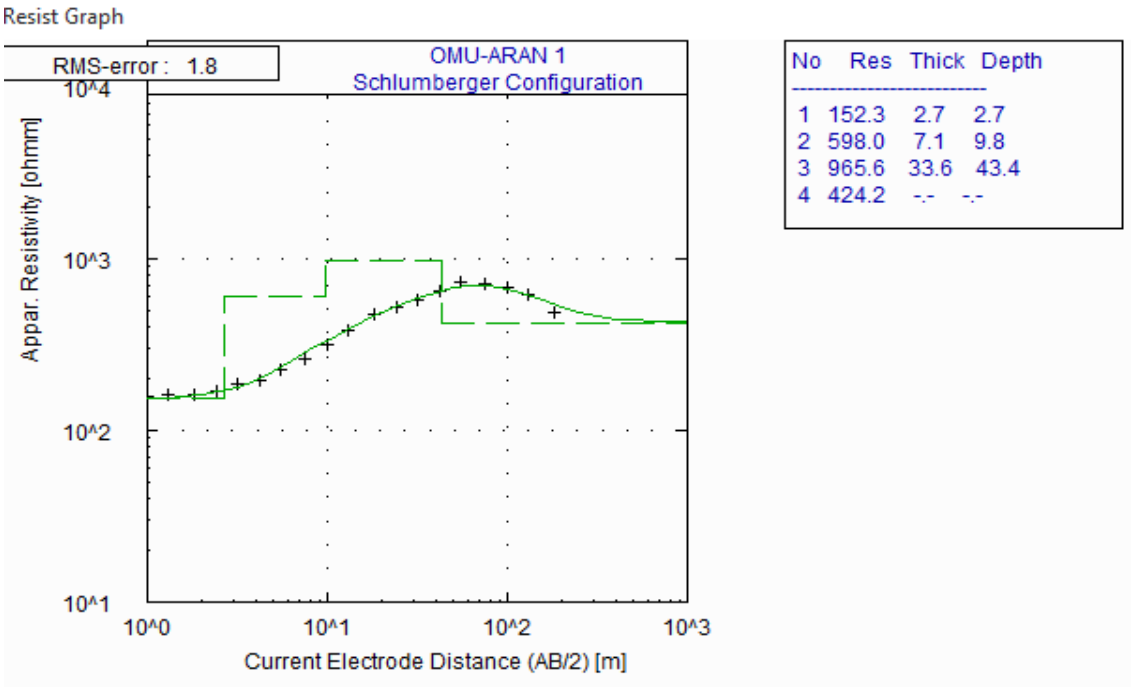


**Figure 4.3**: Resistivity models for: (a) VES 5 in Covenant University farm, and (b) VES 1 in Landmark University farm

a)

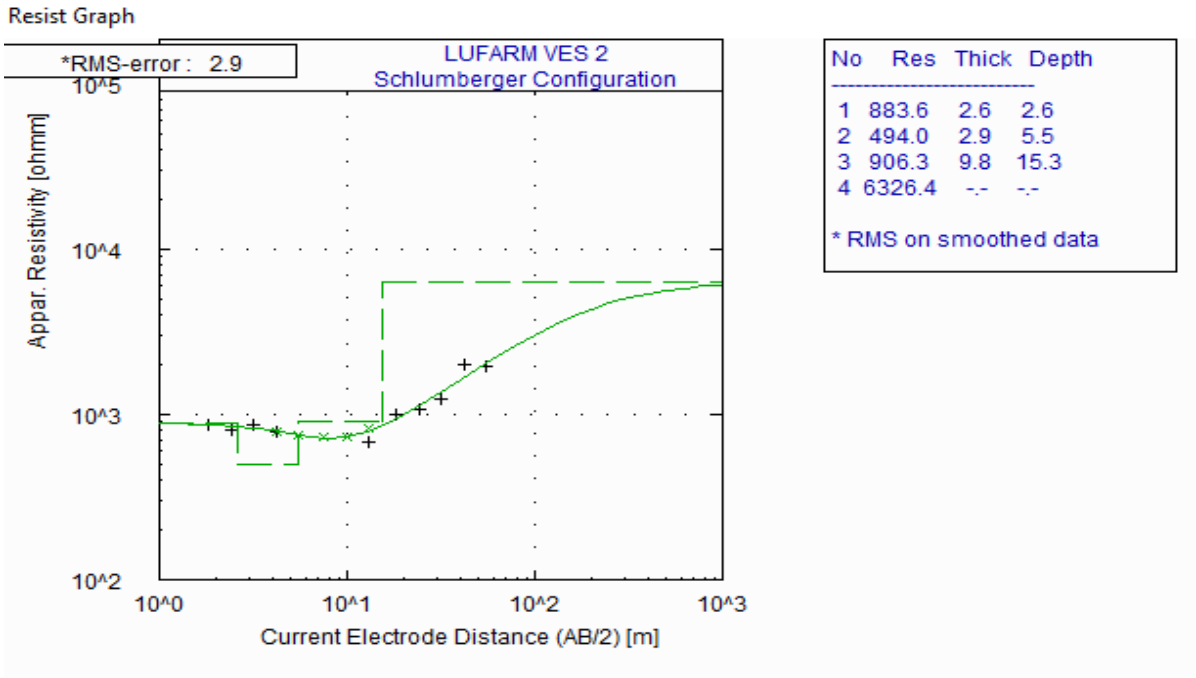


b)

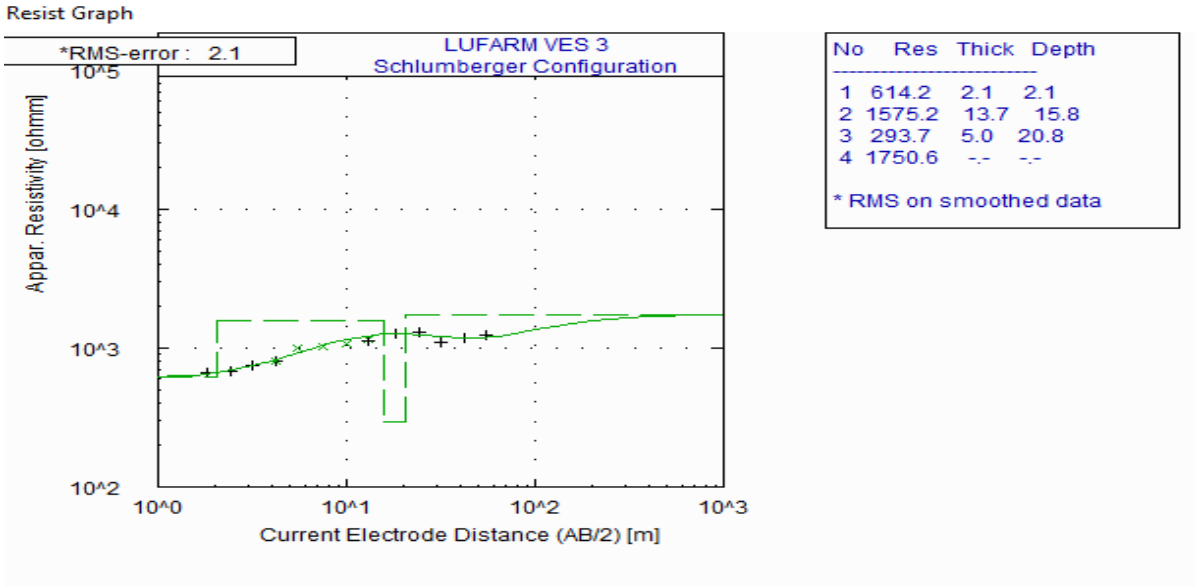


**Figure 4.4:** Resistivity models in Landmark University farm for: (a) VES 2, and (b) VES 3

a)

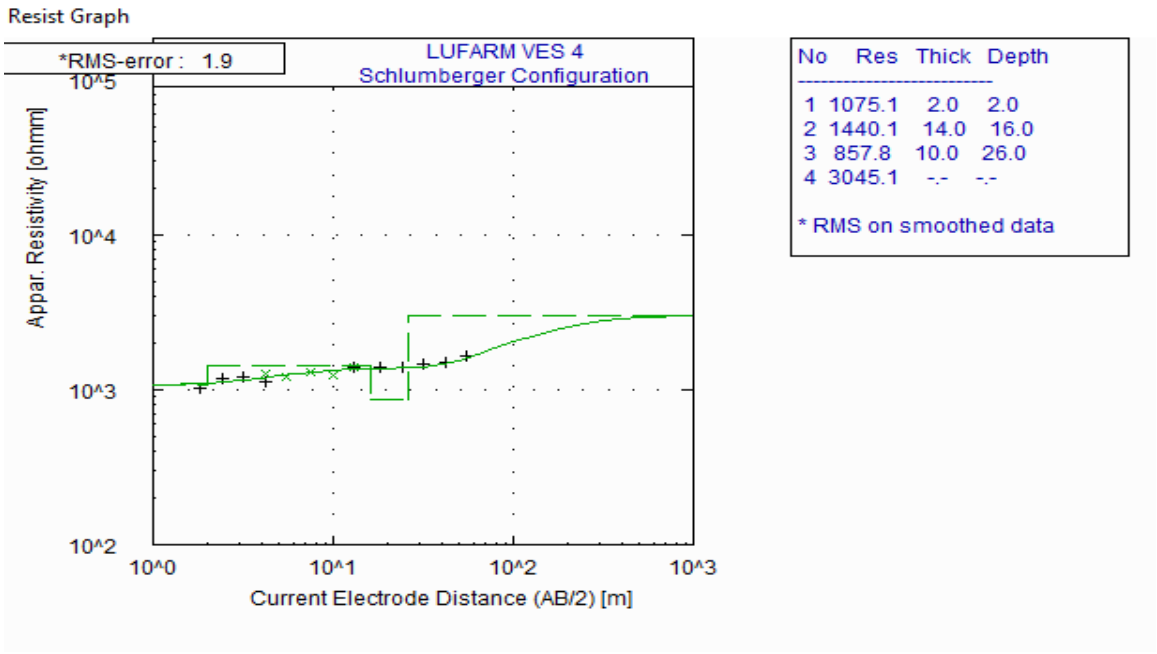


b)

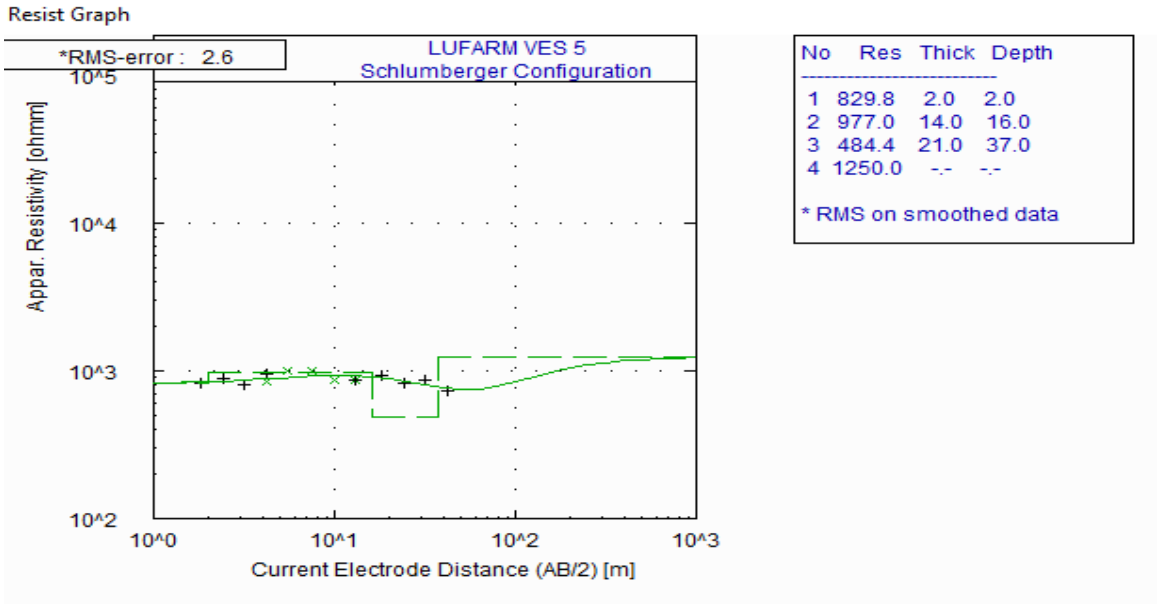


**Figure 4.5**: Resistivity models in Landmark University farm for: (a) VES 4, and (b) VES 5

## 4.2 Resistivity Inversion Models

The 2D resistivity inversion models with elevations for the sites at Covenant University farm and Landmark University farm are presented in Figures 4.6 - 4.14. The root mean square (RMS) errors achieved for the inversion models ranged from 4.9 to 9.4. The depth of investigation of the 2D images is about or approximately 3 m. The values displayed on the vertical side of the sections represent the elevation of each of the traverse lines at the two study sites. The measured apparent resistivity, the calculated and the resulting inverse model resistivity sections for both sites are presented in the Appendix A and B.

### 4.2.1 Resistivity Inverse Models in the Site at Covenant University Farm

The inverse resistivity models at Covenant University farm are generally characterised with low resistivity values in all the traverses, ranging from 32 to 1190.0 Ωm (Figures 4.6 - 4.8a). The low resistivity (<100 Ωm) values are somewhat pronounced at the topsoil to a depth of about 2.1 m, while the higher resistivity (>100 Ωm) values observed at the depth of ≥2.2m in the models are as a result of different degrees of compaction in the soil of the areas.

a)

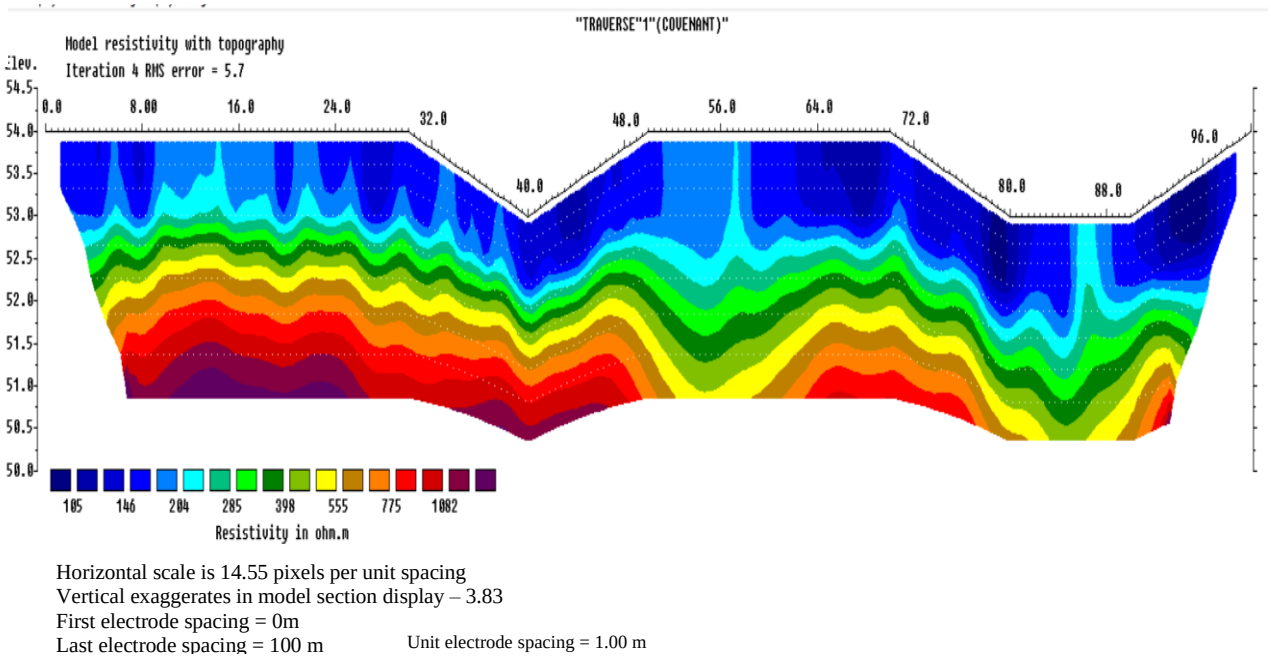


Horizontal scale is 14.55 pixels per unit spacing
Vertical exaggerates in model section display – 3.83
First electrode spacing = 0m
Last electrode spacing = 100 m Unit electrode spacing = 1.00 m

b)

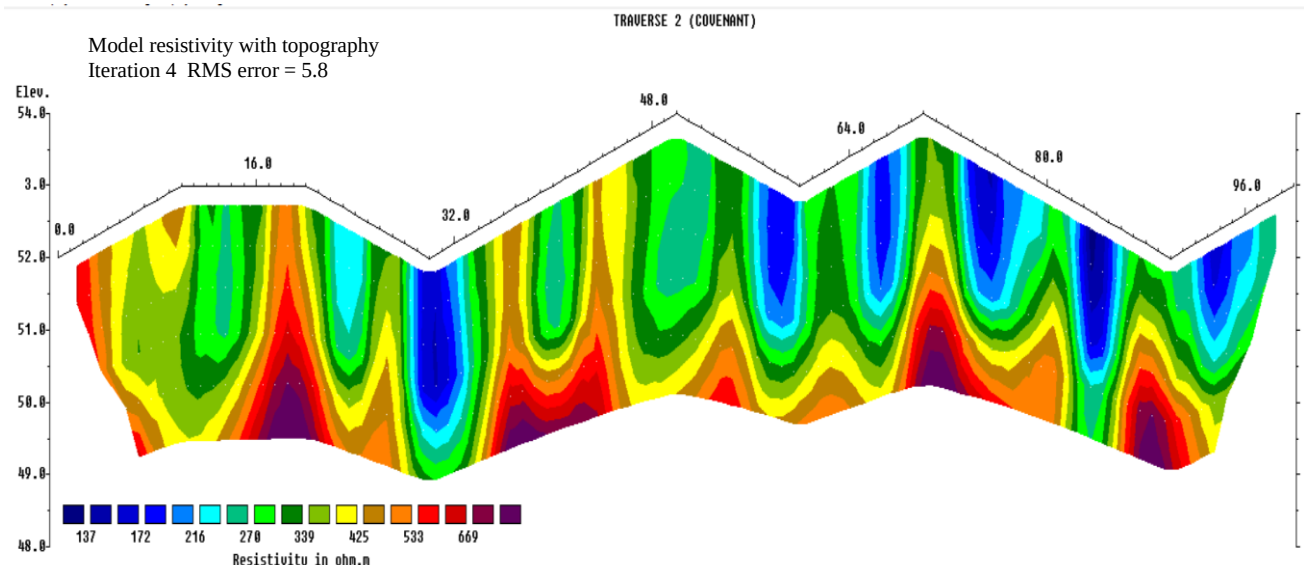


Horizontal scale is 14.55 pixels per unit spacing
Vertical exaggerates in model section display =3.83
First electrode is located at 0.0 m, Last electrode location = 100.0 m Unit electrode spacing = 1.00 m

**Figure 4.6**: 2D resistivity inverse model at the site in Covenant University farm for: (a) Traverse 1, and (b) Traverse 2

a)

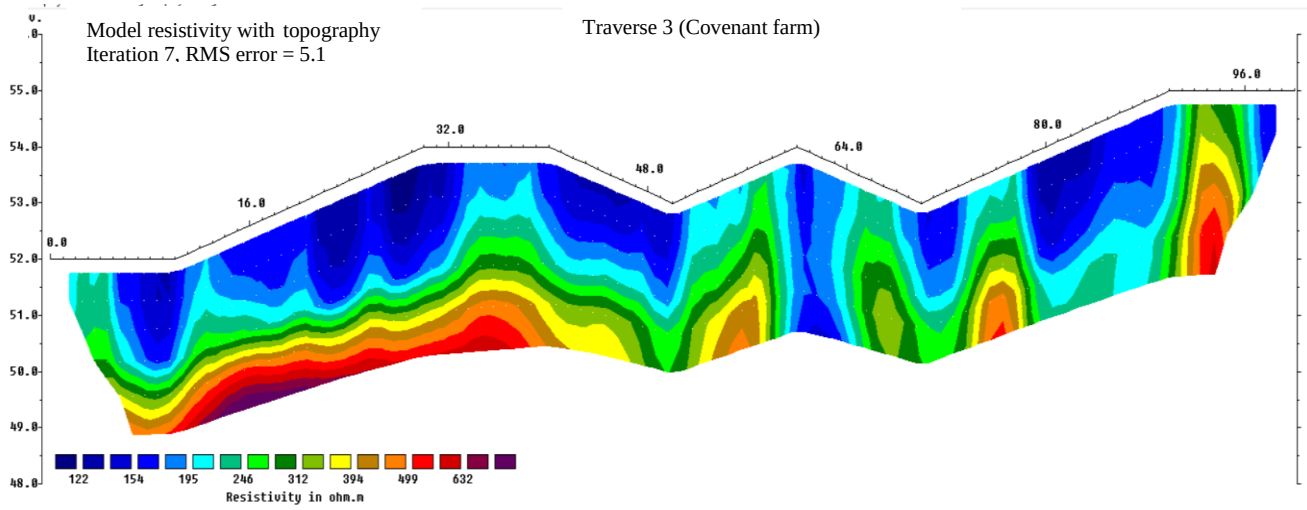


b)

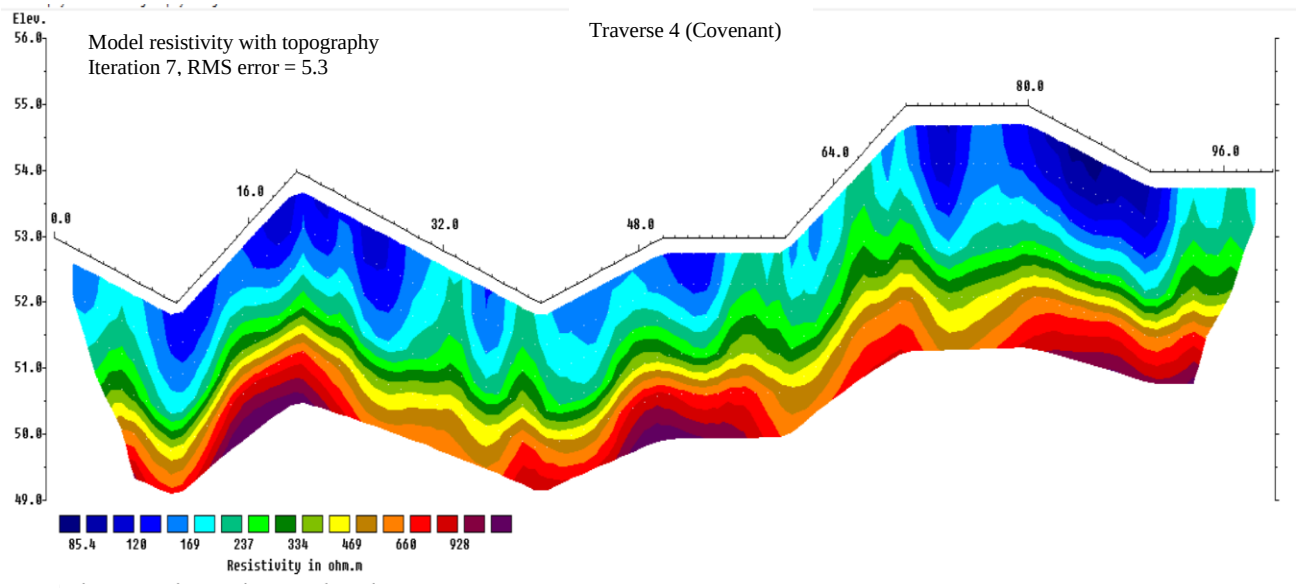


**Figure 4.7**: 2D resistivity inverse model at the site in Covenant University farm for: (a) Traverse 3, and (b) Traverse 4

a)

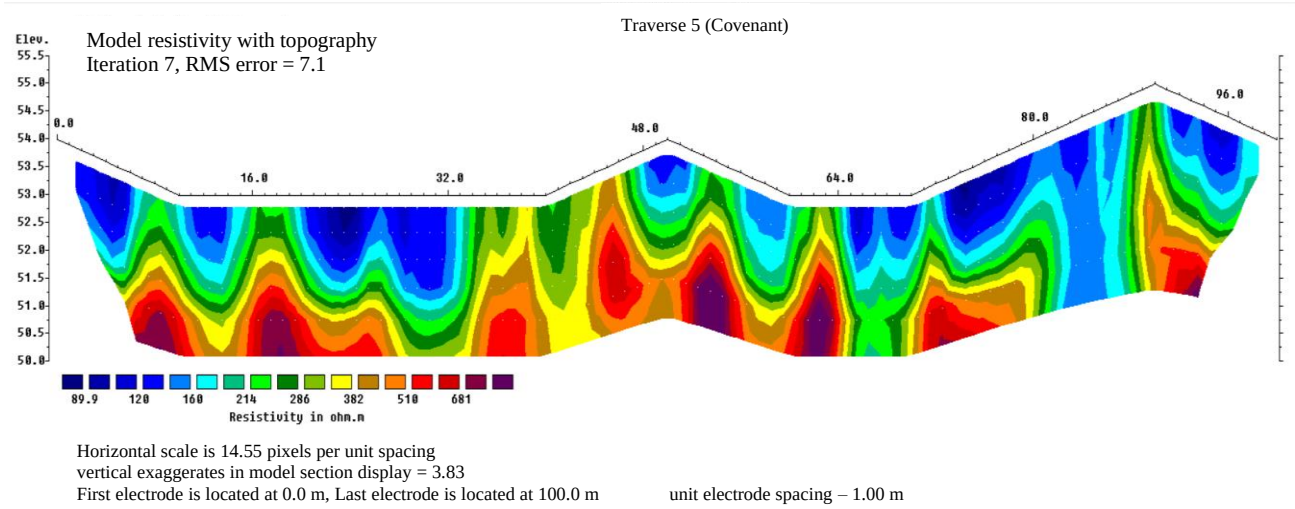


b)

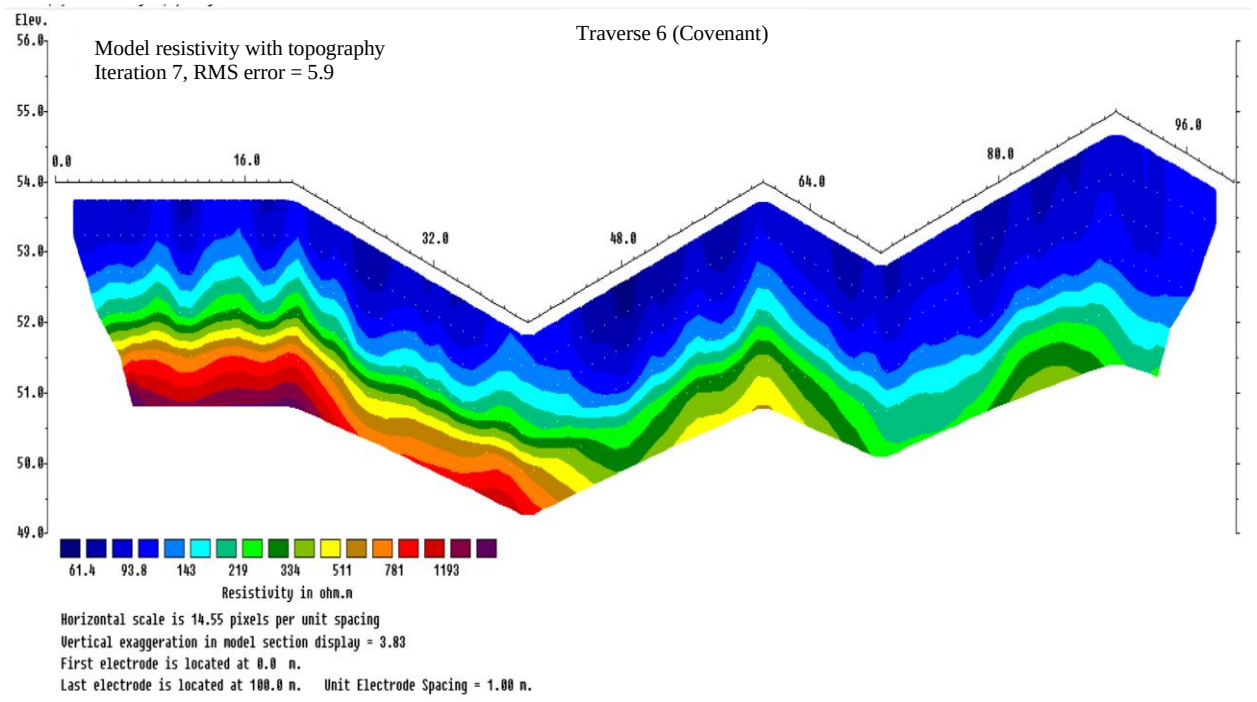


**Figure 4.8**: 2D resistivity inverse model at the site in Covenant University farm for: (a) Traverse 5, and (b) Traverse 6

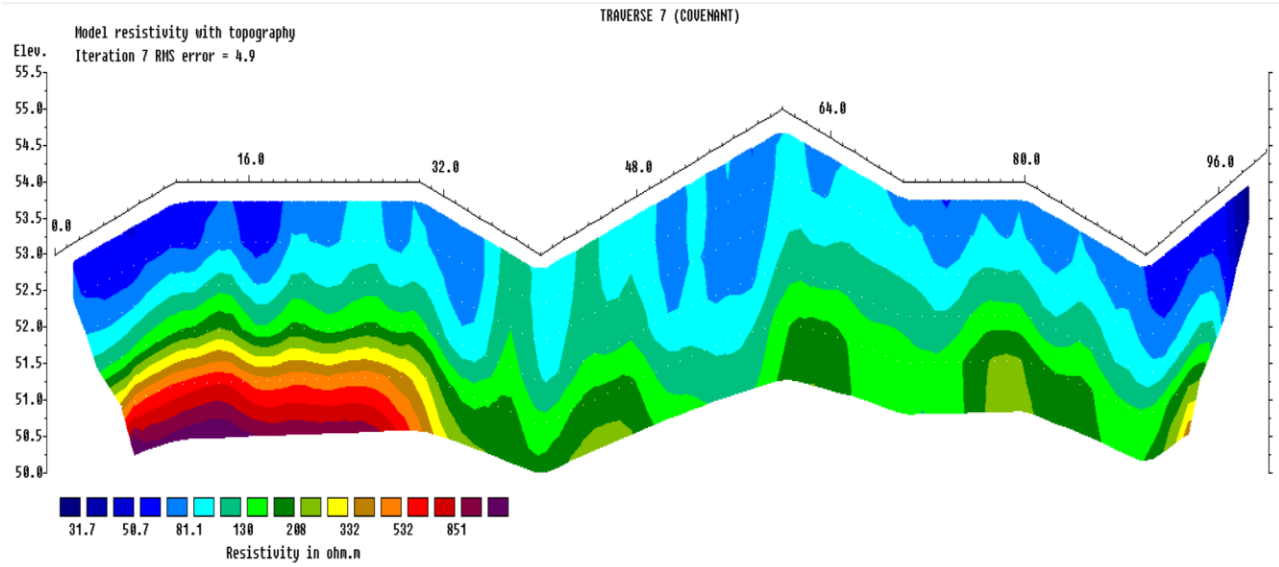


**Figure 4.9**: 2D resistivity inverse model for Traverse 7 at the site in Covenant University farm

### 4.2.2 Resistivity Inverse Models in the Site at Landmark University Farm

In the site at Landmark University farm, the inverse resistivity models for all the traverses have resistivity values ranged from 21.0 to 3145 Ωm (Figures 4.10 – 4.19 and Appendix B). The inverse resistivity models in this farm site are generally characterised with high resistivity (>300 Ωm) values and this is observed for all the traverses. Patches of low resistivity (< 100 Ωm) values are observed at depths below 2 m for all the traverses in the site at Landmark University farm. However, relatively higher model resistivity values are observed in Traverses 17 – 19.

a)

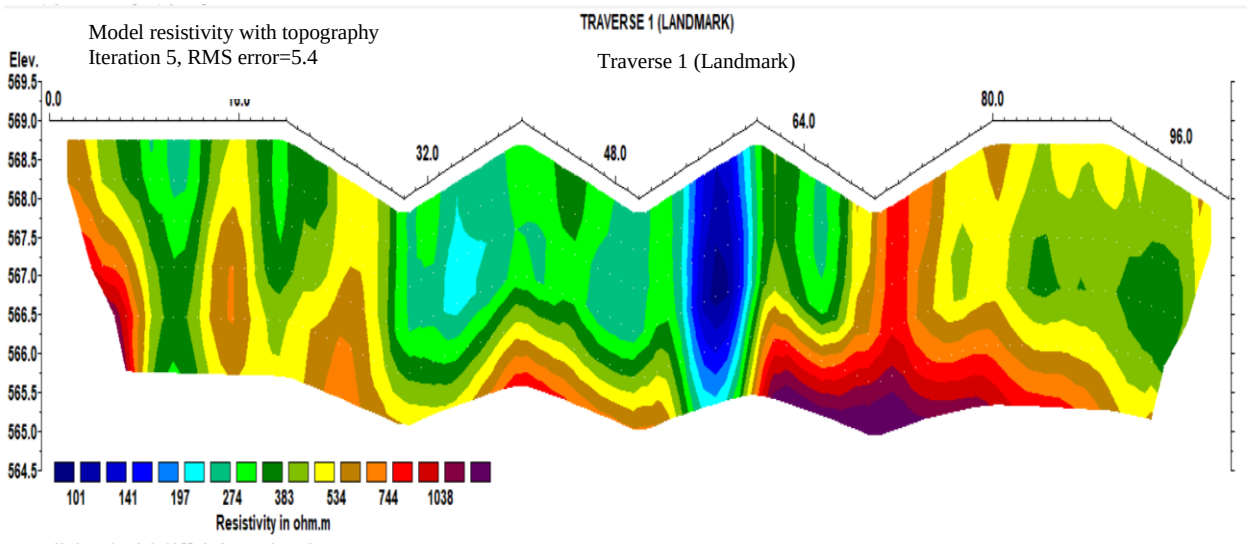


Horizontal scale is 14.55 pixels per unit spacing
Vertical exaggerates in model section display = 3.83
First electrode is located at 0.0 m, Last electrode is located at 100.0 m unit electrode spacing = 1.00 m

b)

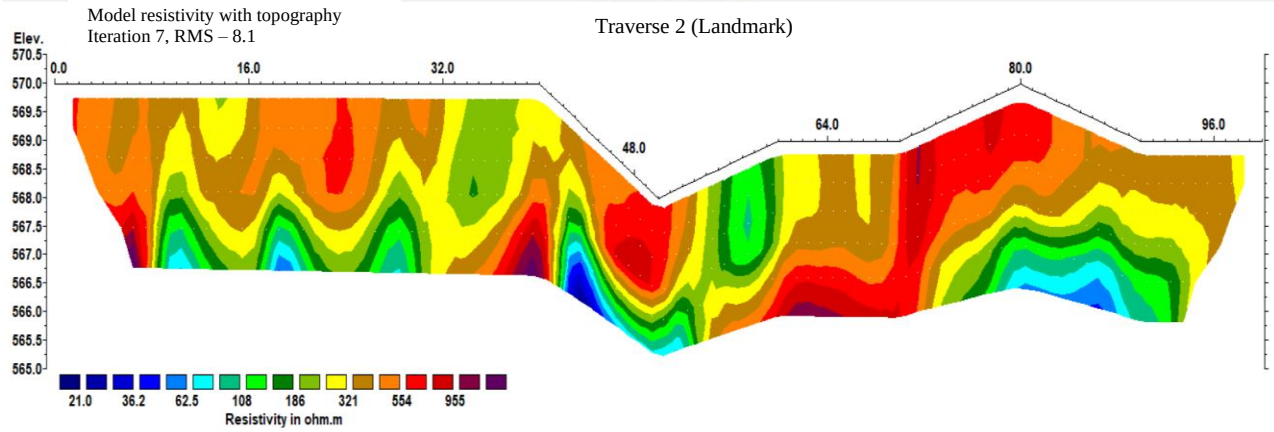


Horizontal scale is 14.55 pixels per unit spacing
Vertical exaggerates in model section display = 3.83
First electrode is located at 0.0 m, Last electrode is located at 100.0 m unit electrode spacing = 1.00 m

**Figure 4.10:** 2D resistivity inverse models at the site in Landmark University farm for: (a) Traverse 1, and (b) Traverse 2

a)

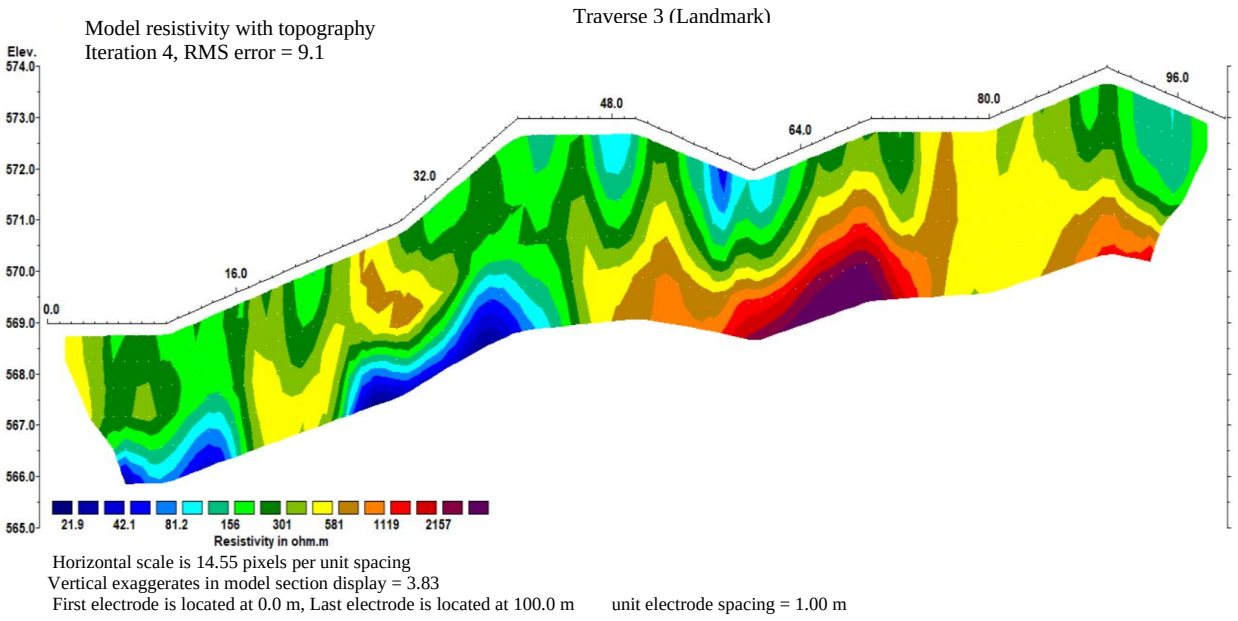


b)

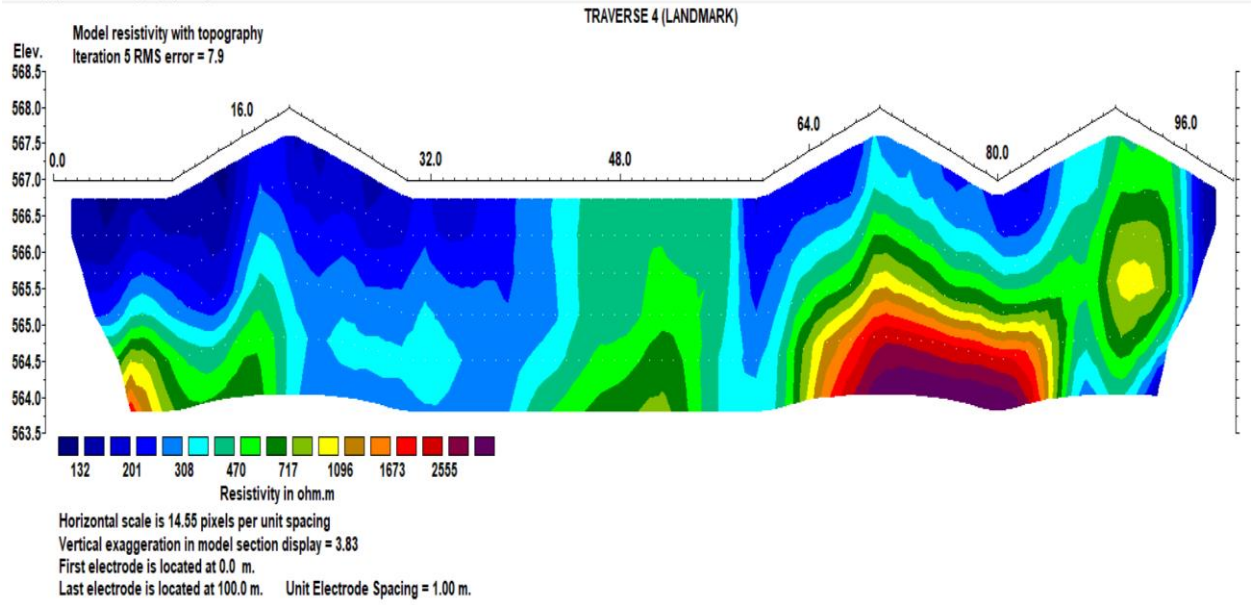


**Figure 4.11**: 2D resistivity inverse model at the site in Landmark University farm for: (a) Traverse 3, and (b) Traverse 4

a)

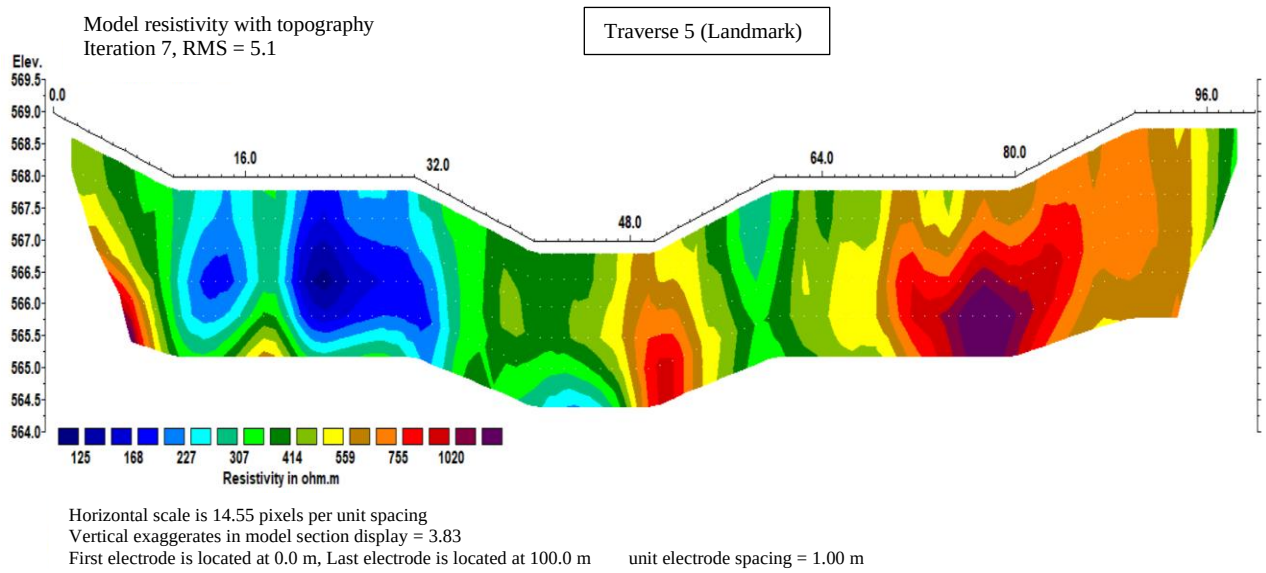


.

b)

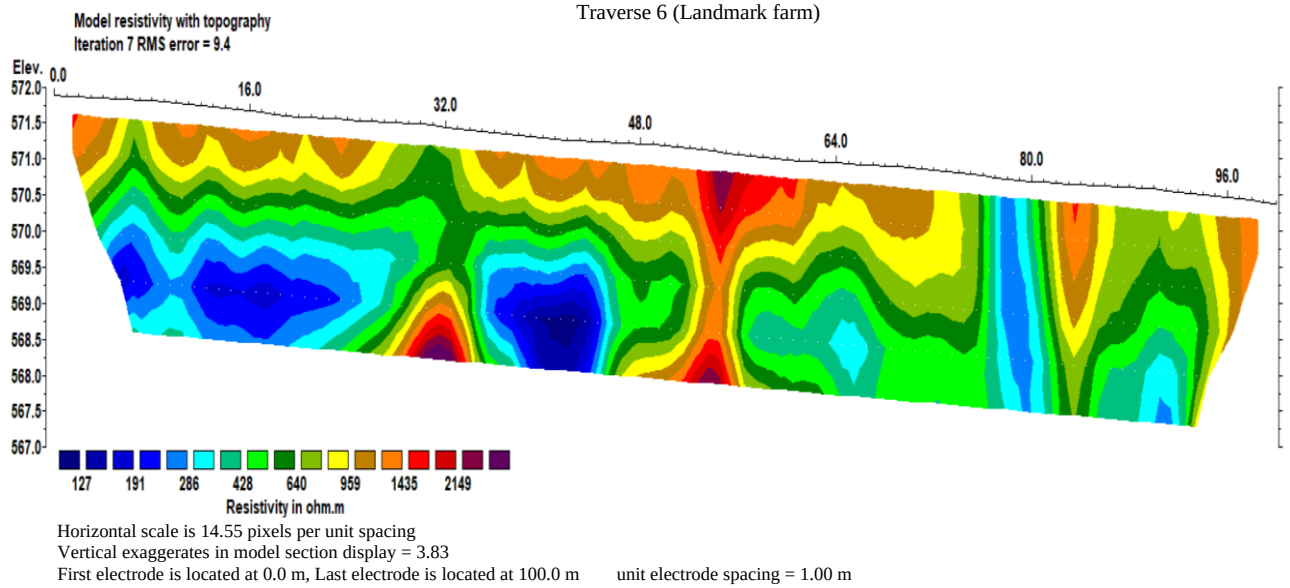


**Figure 4.12:** 2D resistivity inverse model at the site in Landmark University farm for: (a) Traverse 5, and (b) Traverse 6

a)

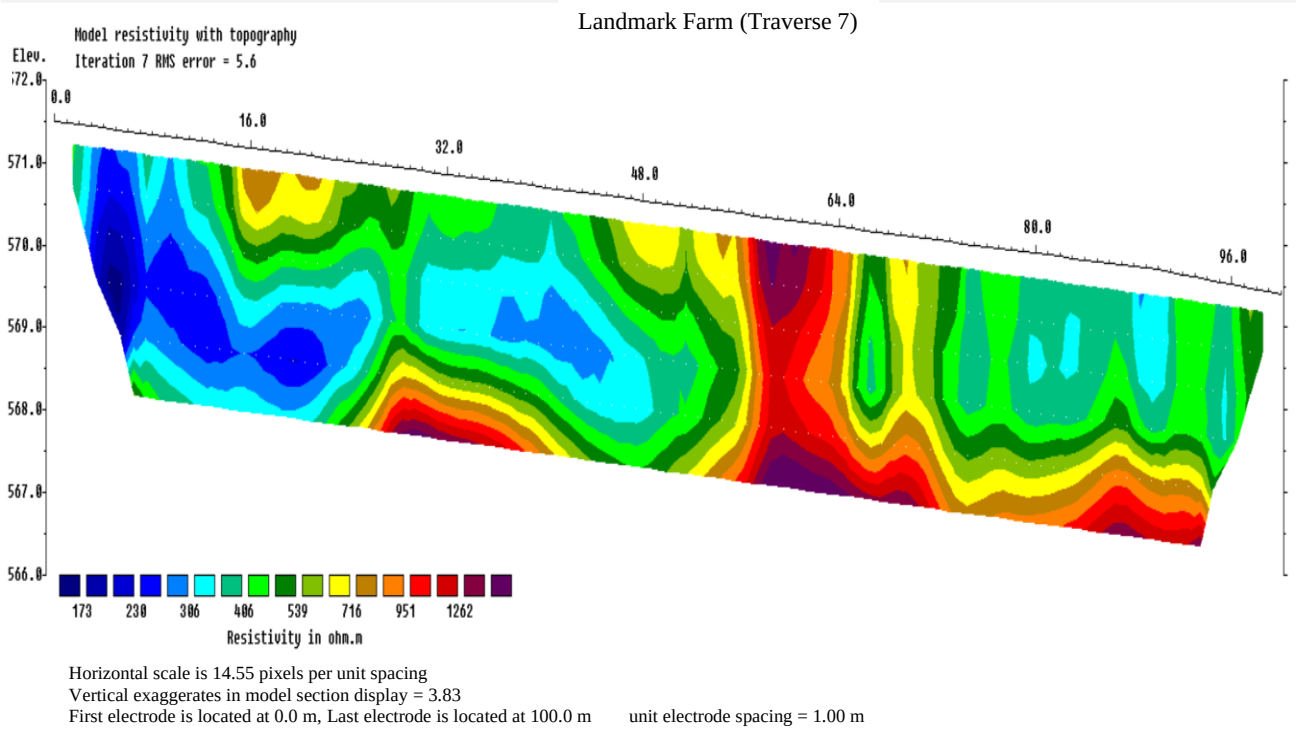


b)

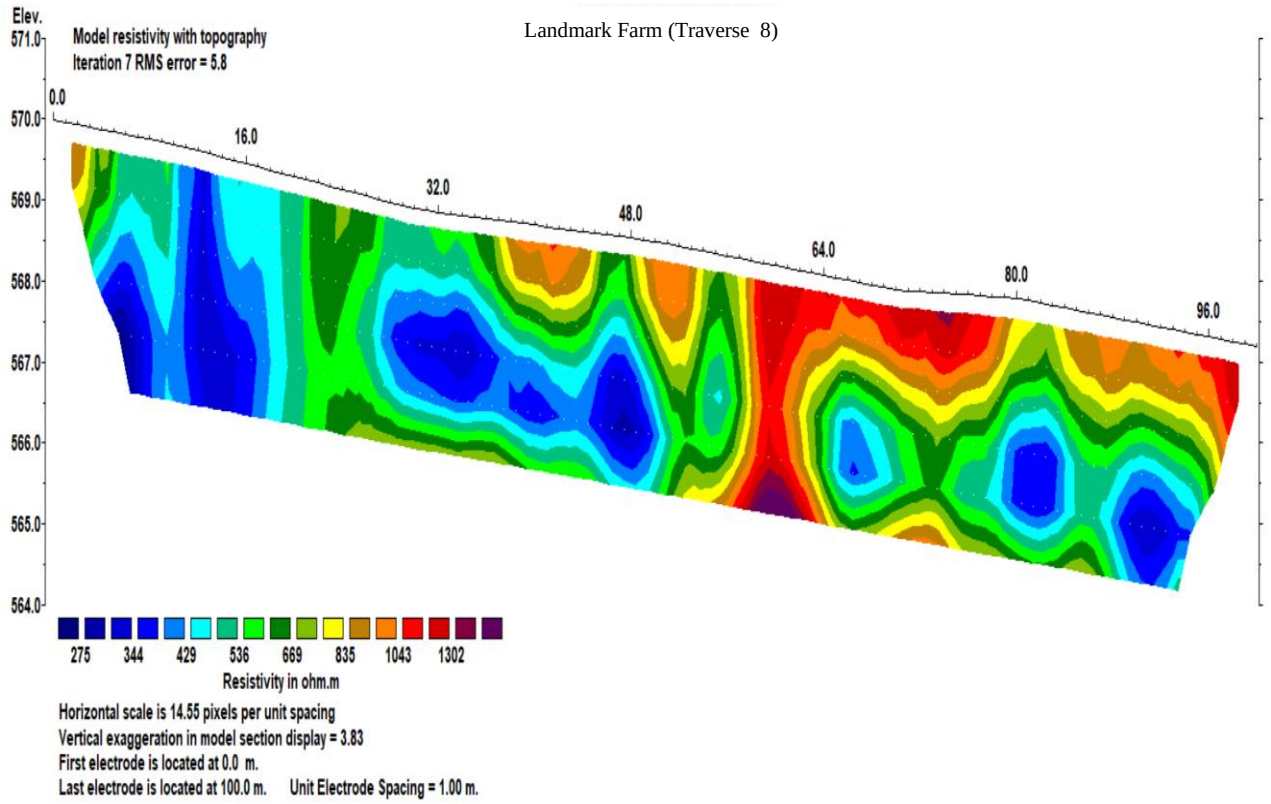


**Figure 4.13**: 2D resistivity inverse model at the site in Landmark University farm for: (a) Traverse 7, and (b) Traverse 8

a)

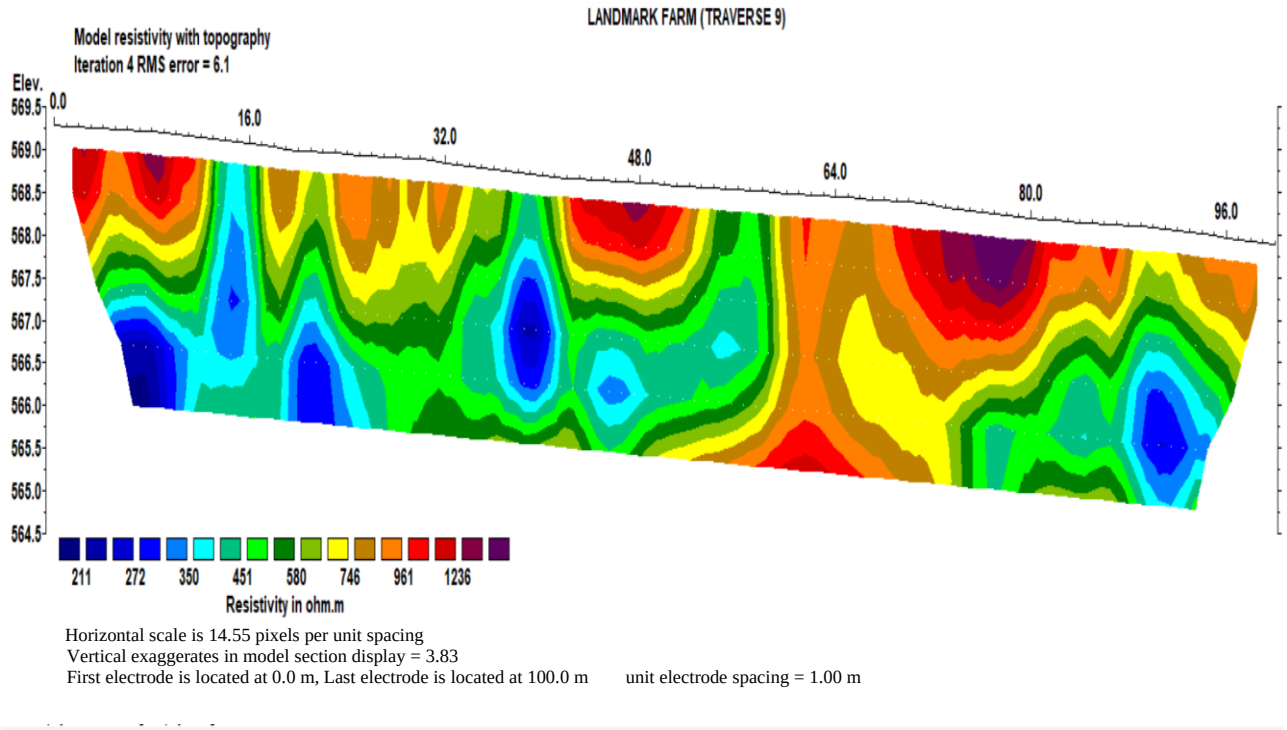


b)

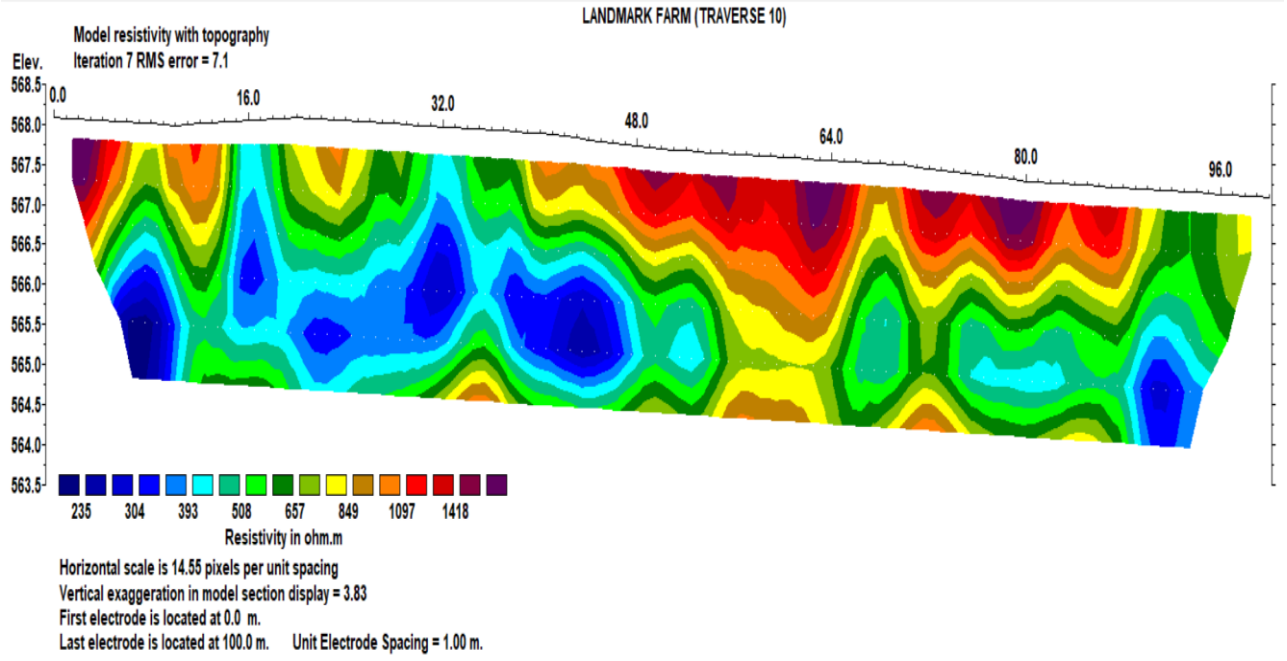


**Figure 4.14**: 2D resistivity inverse model at the site in Landmark University farm for: (a) Traverse 9, and (b) Traverse 10

a)

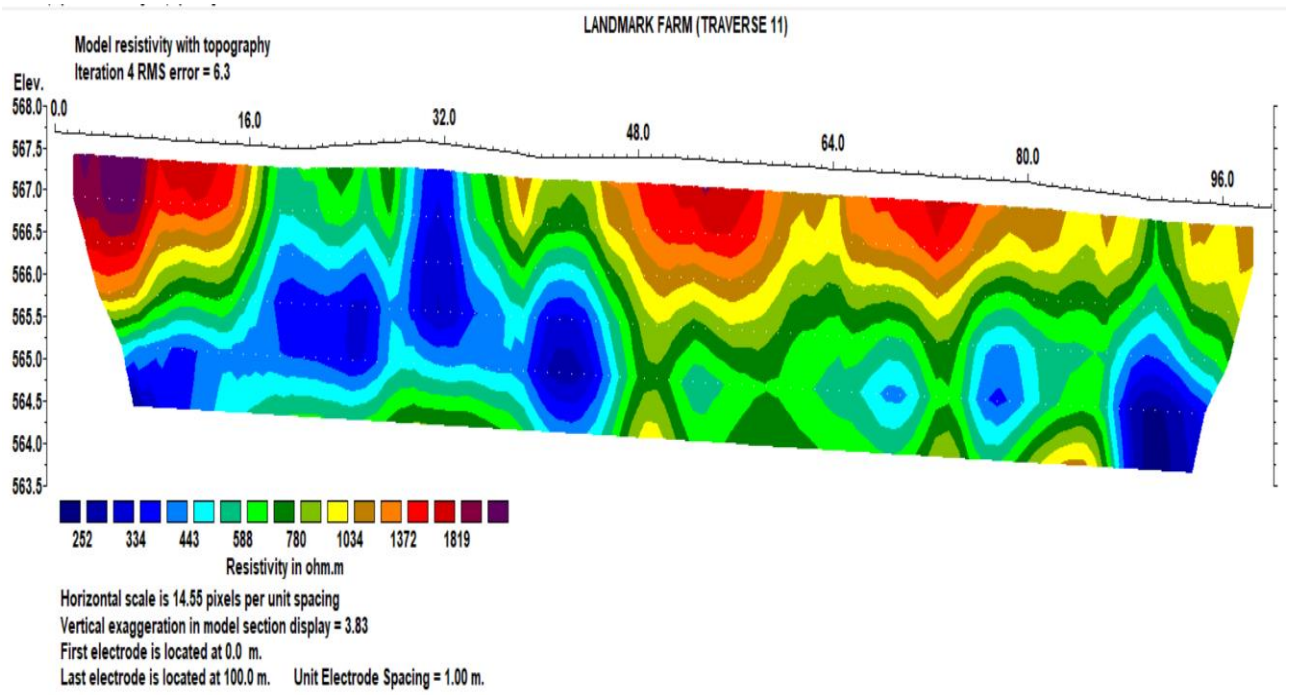


b)

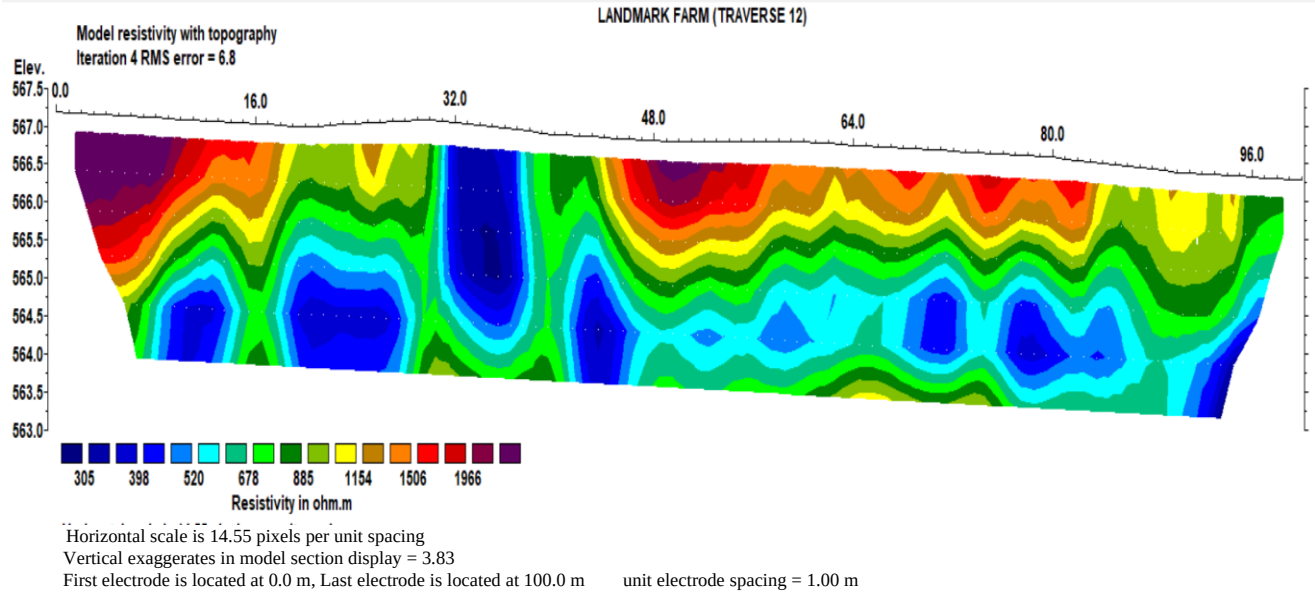


**Figure 4.15**: 2D resistivity inverse model for the site at Landmark University farm for: (a) Traverse 11, and (b) Traverse 12

a)

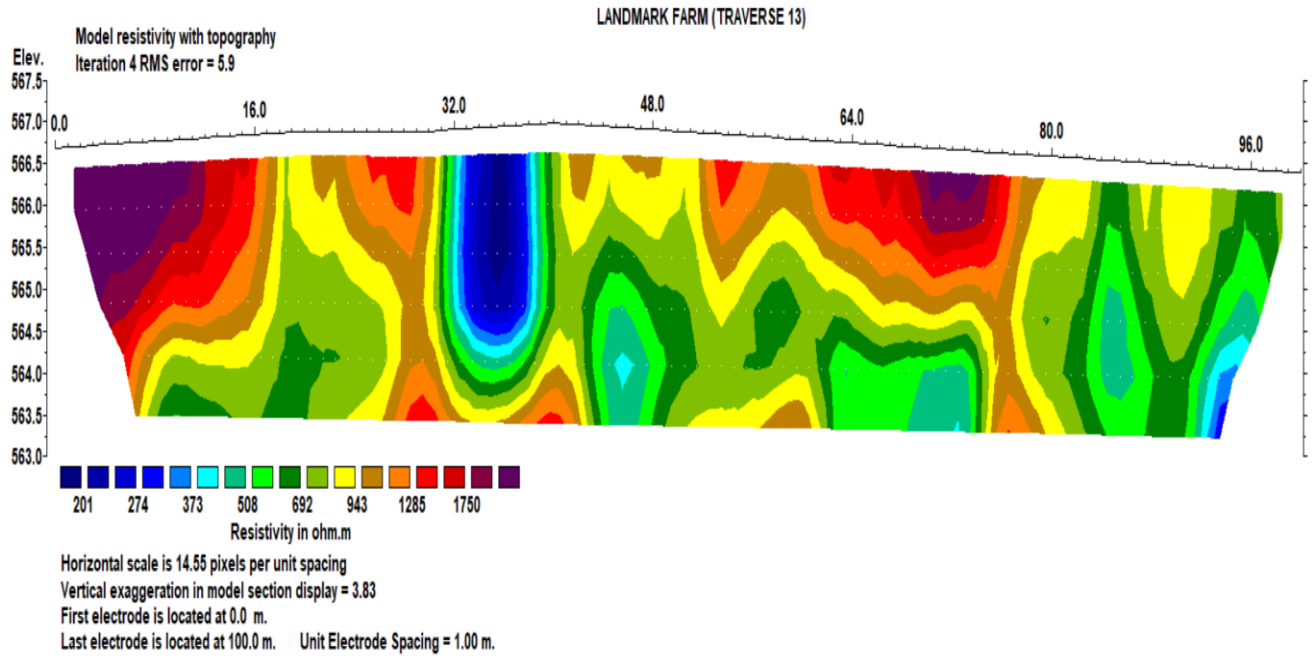


b)

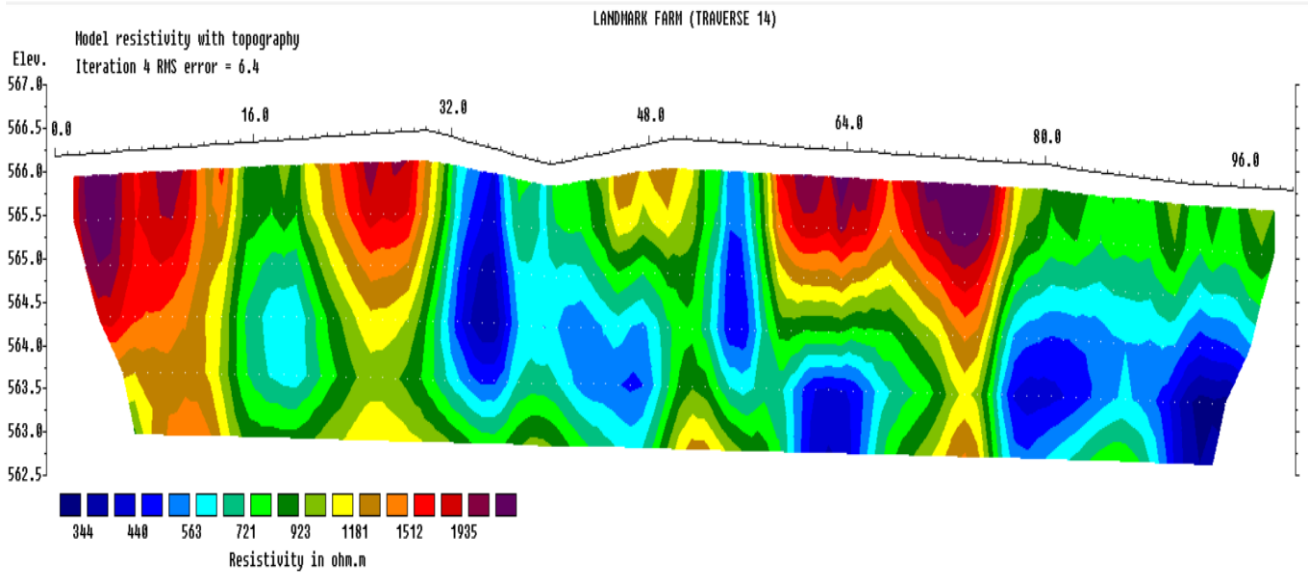


Horizontal Scale is 4.55 pixels per unit spacing
Vertical exaggeration in model section display = 3.83
First electrode is located at 0.0 m
Last electrode is located at 100.0 m Unit electrode spacing = 1.00 m

**Figure 4.16**: 2D resistivity inverse model at the site in Landmark University farm for: (a) Traverse 13, and (b) Traverse 14

a)

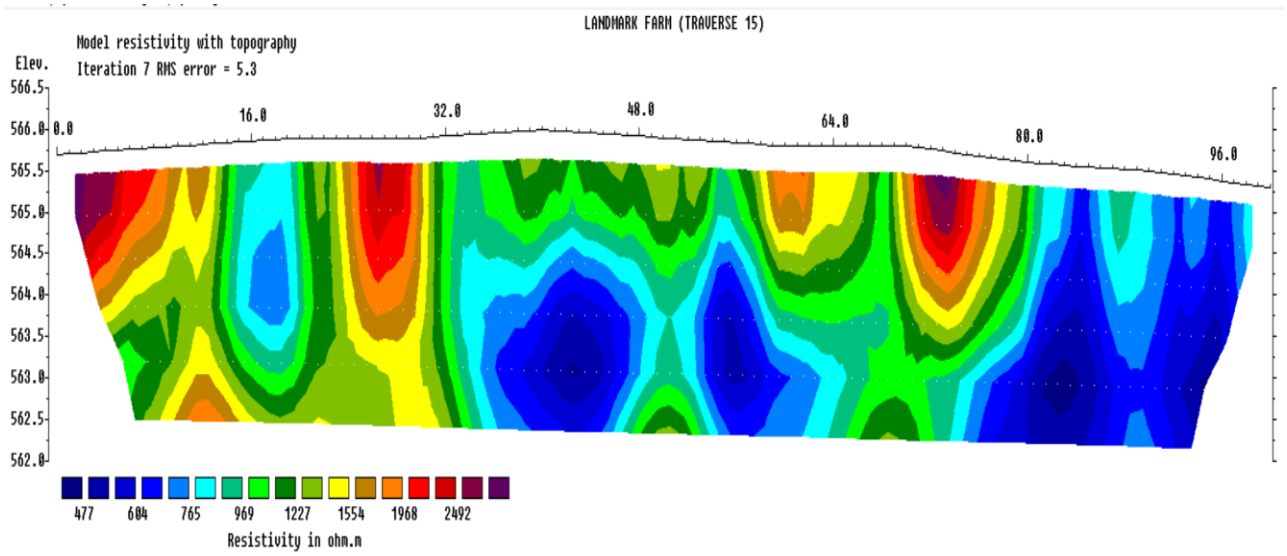


Horizontal scale is 14.55 pixels per unit spacing
Vertical exaggerates in model section display = 3.83
First electrode is located at 0.0 m, Last electrode is located at 100.0 m unit electrode spacing = 1.00 m

b)

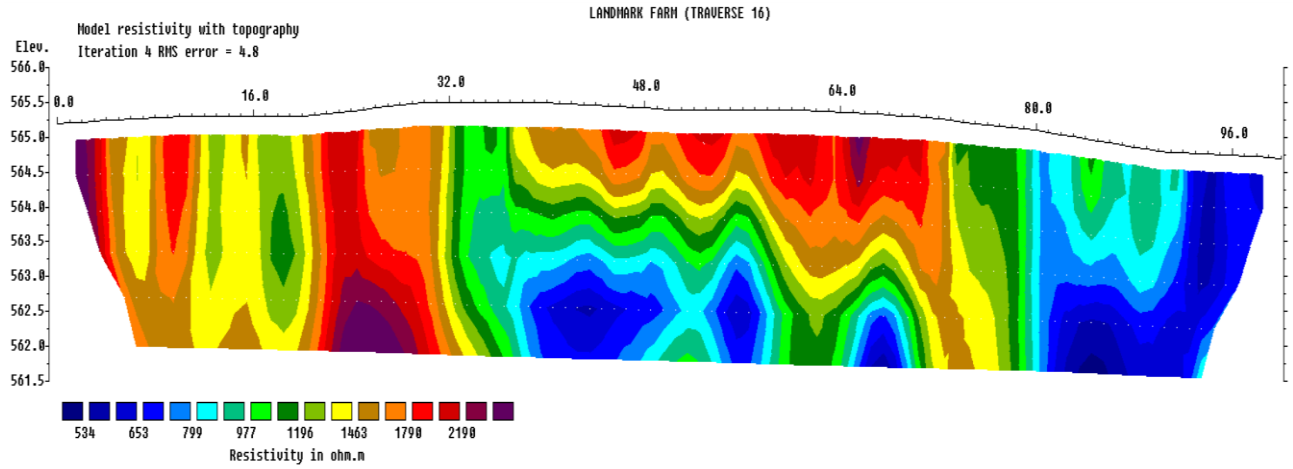


Horizontal scale is 14.55 pixels per unit spacing
Vertical exaggerates in model section display = 3.83
First electrode is located at 0.0 m, Last electrode is located at 100.0 m unit electrode spacing = 1.00 m

**Figure 4.17:** 2D resistivity inverse model at the site in Landmark University farm for: (a) Traverse 15, and (b) Traverse 16

a)

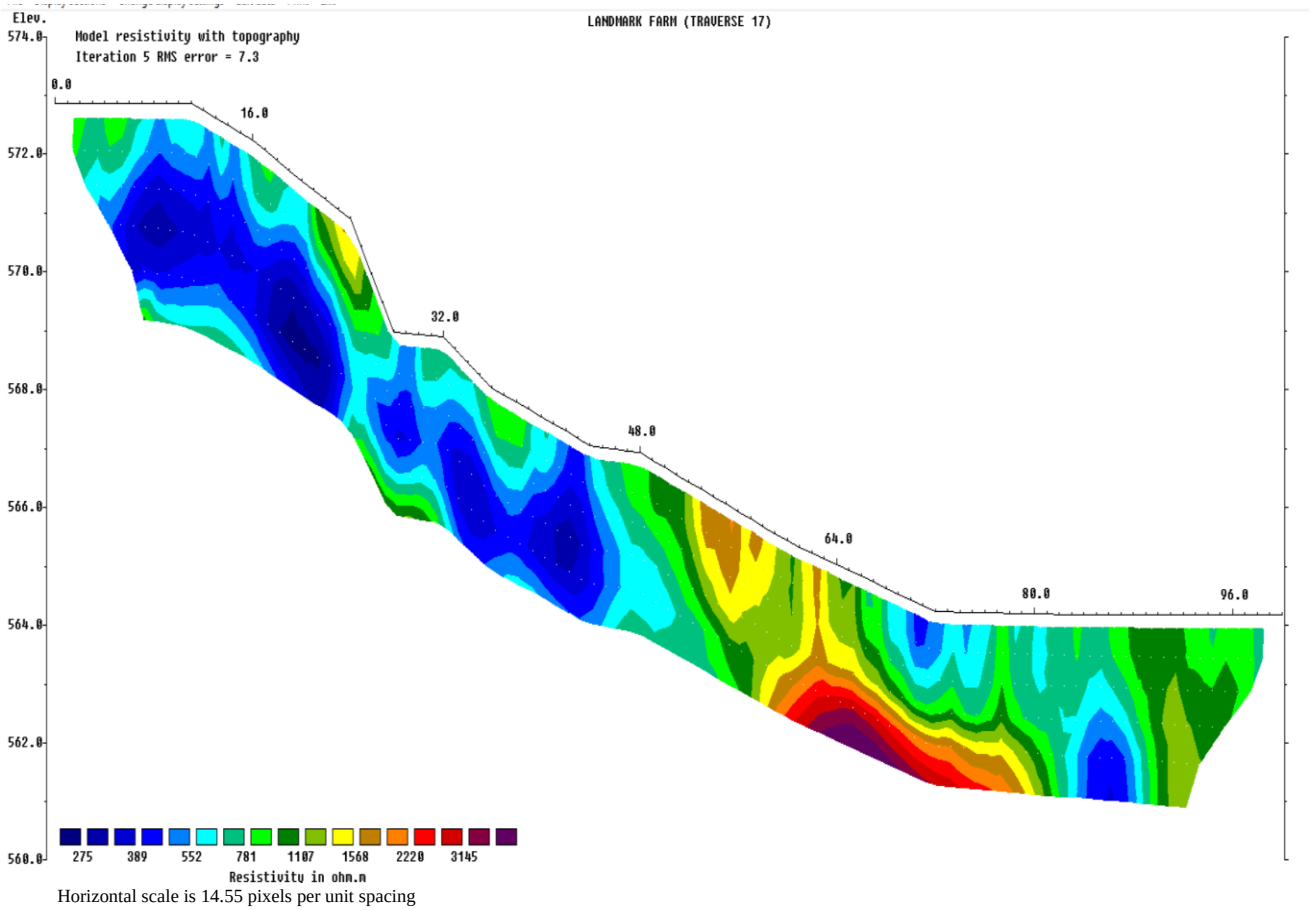


Horizontal scale is 14.55 pixels per unit spacing
Vertical exaggerates in model section display = 3.83
First electrode is located at 0.0 m, Last electrode is located at 100.0 m unit electrode spacing = 1.00 m

b)

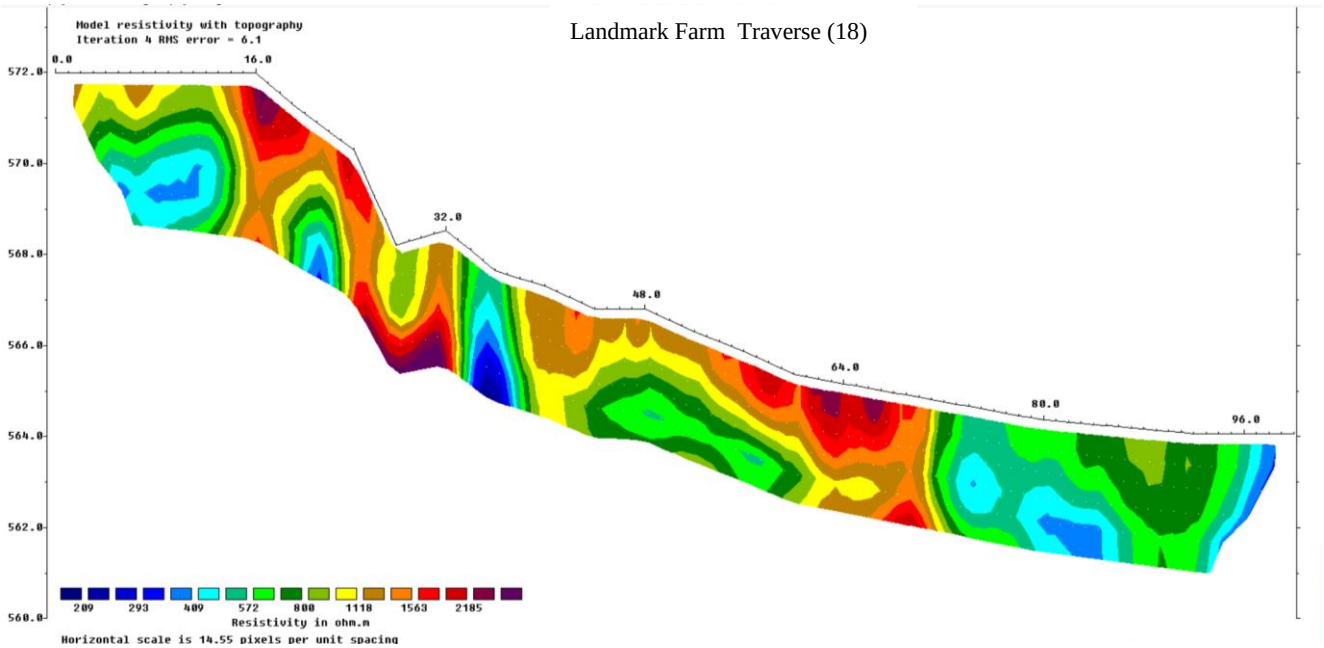


Horizontal scale is 14.55 pixels per unit spacing
Vertical exaggerates in model section display = 3.83
First electrode is located at 0.0 m, Last electrode is located at 100.0 m unit electrode spacing = 1.00 m

**Figure 4.18**: 2D resistivity inverse model for the site at Landmark University farm for: (a) Traverse 17, and (b) Traverse 18

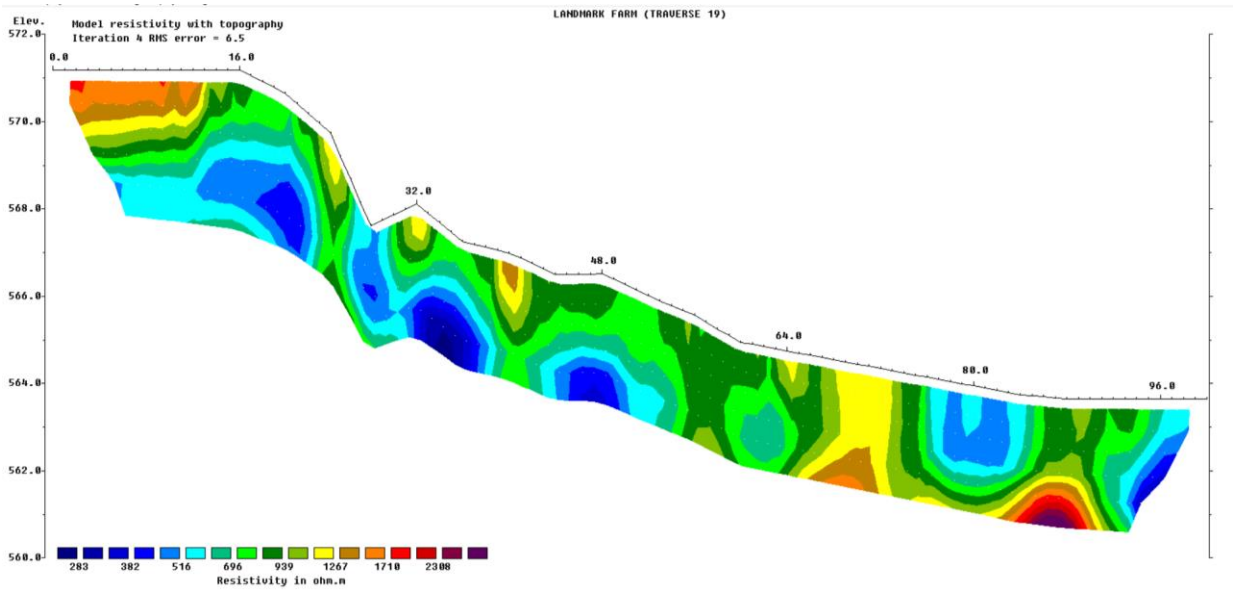


Horizontal scale is 14.55 pixels per unit spacing
Vertical exaggerates in model section display = 3.83
First electrode is located at 0.0 m, Last electrode is located at 100.0 m unit electrode spacing = 1.00 m

**Figure 4.19**: 2D resistivity inverse model of the site at Landmark University farm for Traverse 19

## 4.3 Soil Parameters Derived from Remote Sensing Satellite Data

Soil properties including temperature, moisture content and salinity, were obtained from the Modern-era Retrospective Analysis for Research and Applications (MERRA) dataset and Landsat-8 satellite imagery of National Aeronautical and Space Administration (NASA). The soil temperature (ST) graphs of the study sites (Covenant University farm and Landmark University farm) are presented in Figures 4.20 - 4.23. Soil moisture content for the two farm sites are presented in Figures 4.24 and 4.27, while soil salinity graphs are presented in Figures 4.28 and 4.29.

### 4.3.1 Soil Temperature (ST)

The three years soil temperatures for the site at Covenant University farm from January 2017 to January 2020 ranged from 296 K to 315 K as presented in Figures 4.20 and 4.21. Figure 4.20 presents the upper and lower limits of soil temperature variations at 0 – 10 cm and 10 – 40 cm underground at the site in Covenant University farm from January 2017 to January 2018. The soil temperature recorded at this site from January to September 2017 ranged from 296 K to 314 K and the highest was recorded in March and April of the same year. Figure 4.21 presents the ST distribution for 2018 and 2019 in the site at Covenant University farm and this ranged from 289 K to 315 K with the highest record of 315 K observed between in February and March, 2018. For the three (3) consecutive years studied, the highest ST of 315 K was recorded between February and March, 2018, with the lowest ST of 297 K recorded between July and September of the three (3) years.

Figures 4.22 and 4.23 displayed the soil temperature variations ranged from 289 K to 317 K at the in Landmark University farm between January 2017 to December 2019. The highest ST of 316 K for this period was observed between February and March, 2018. The soil temperatures from January to December, 2017 in this site ranged from 289 K to 316 K and the highest ST of 316 K was observed between February and March, 2017 as presented in Figure 4.22b. Soil temperatures were stable at 295 K between July and September, 2017. The soil temperatures from January to December, 2018 ranged from 290 K to 317 K and the highest value of 317 K was observed in April, 2018. There was stable soil temperature of 294 K between July and September, 2018. The soil temperature for the depth at 10 – 40 cm in 2018 as presented in Figure 4.23b ranged from 297 K to 305 K. In 2019, soil temperature between January and December, 2019 ranged from 287 K to 316 K and the

highest ST of 316 K was observed between February and March, 2019. Soil temperature variation for 2019 at the depth of 10 – 40 cm ranged from 297 K to 305 K. ST was stable at 294 K between July and September, 2019.

a)

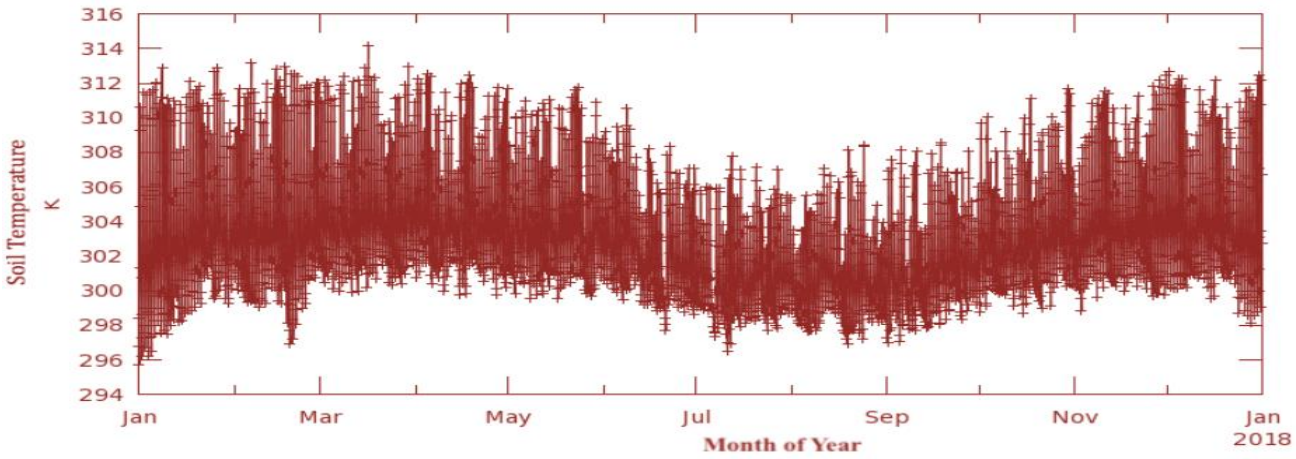


b)

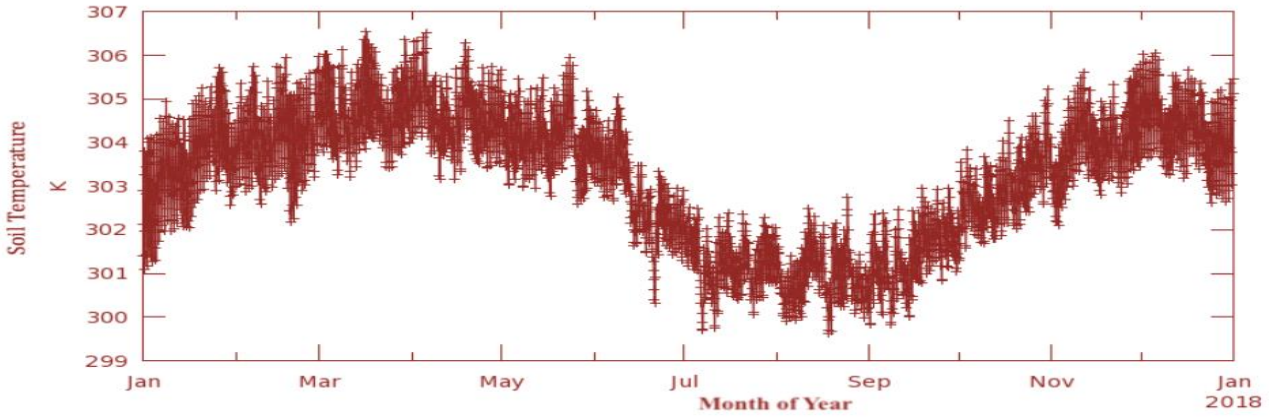


**Figure 4.20**: Soil temperature for the site at Covenant University farm for: (a) 2017 at 0 – 10 cm, and (b) 10 – 40 cm

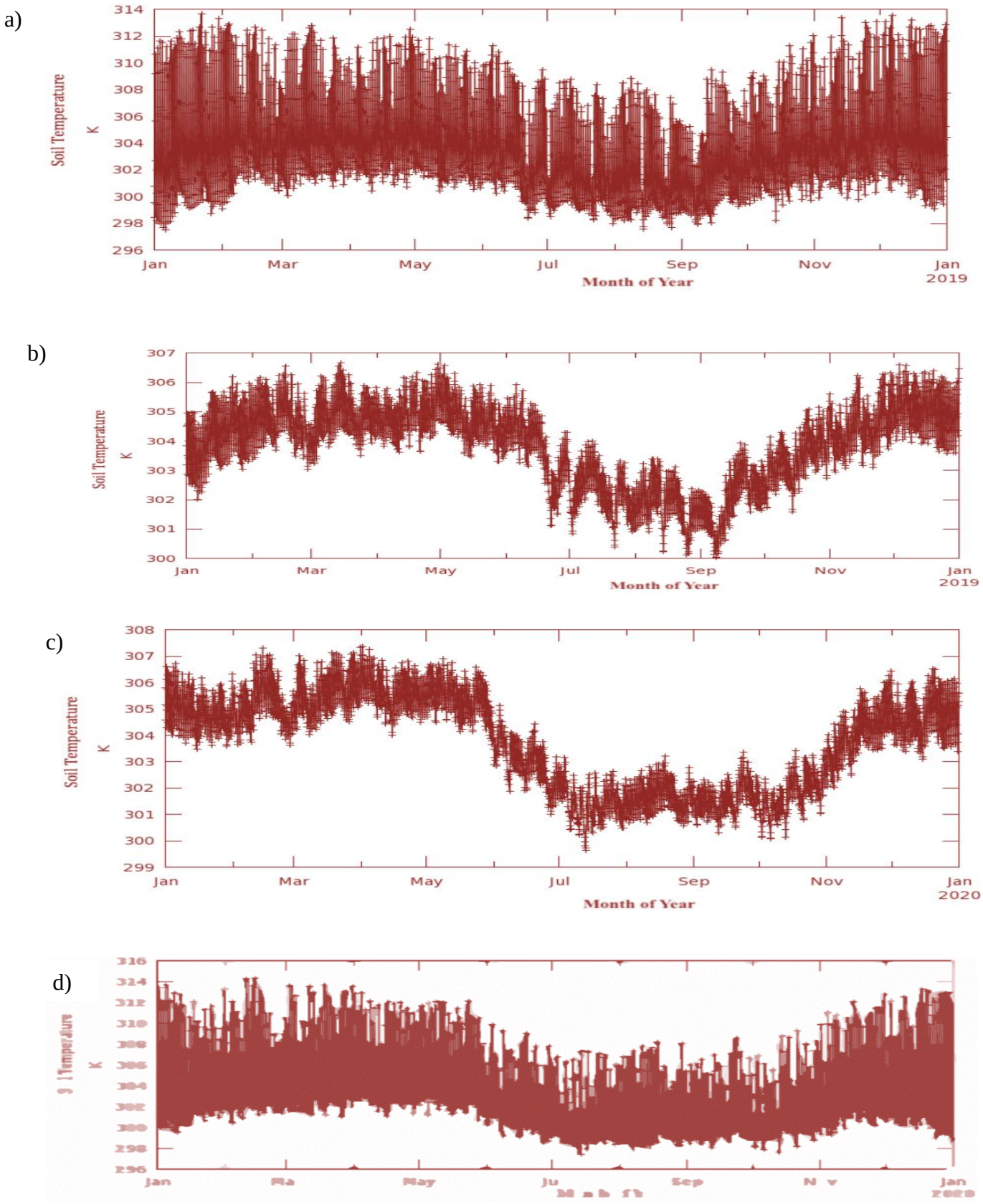


**Figure 4.21**: Soil temperatures for the site at Covenant University farm for: (a) 2018 at 0 – 10 cm, (b) 2018 at 10 – 40 cm, (c) 2019 at 0 – 10 cm, and (d) 2019 at 10 – 40 cm

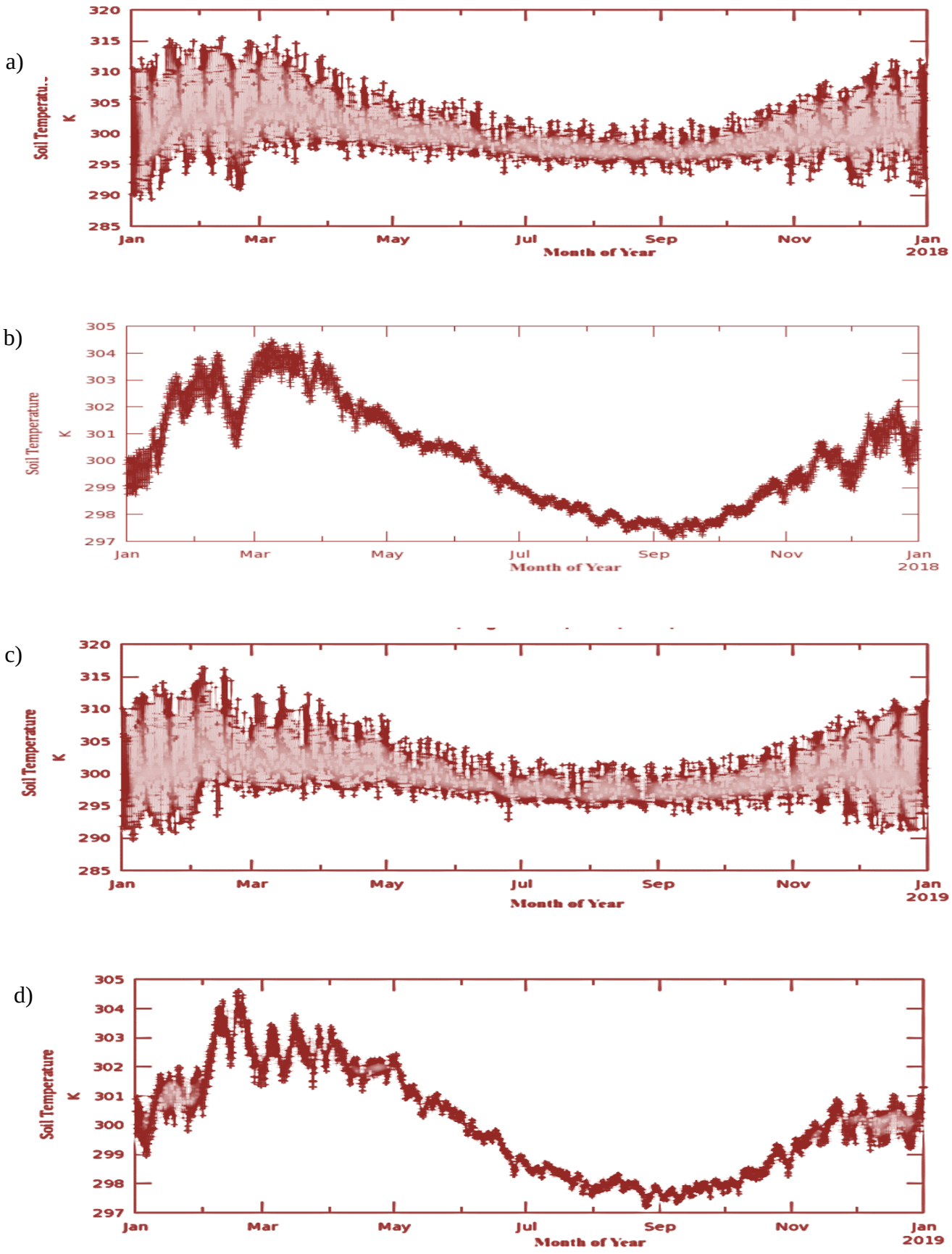


**Figure 4.22**: Soil temperatures for the site at Landmark University farm for: (a) 2017 at 0 – 10 cm, (b) 2017 at 10 – 40 cm, (c) 2018 at 0 – 10 cm, and (d) 2018 at 10 – 40 cm

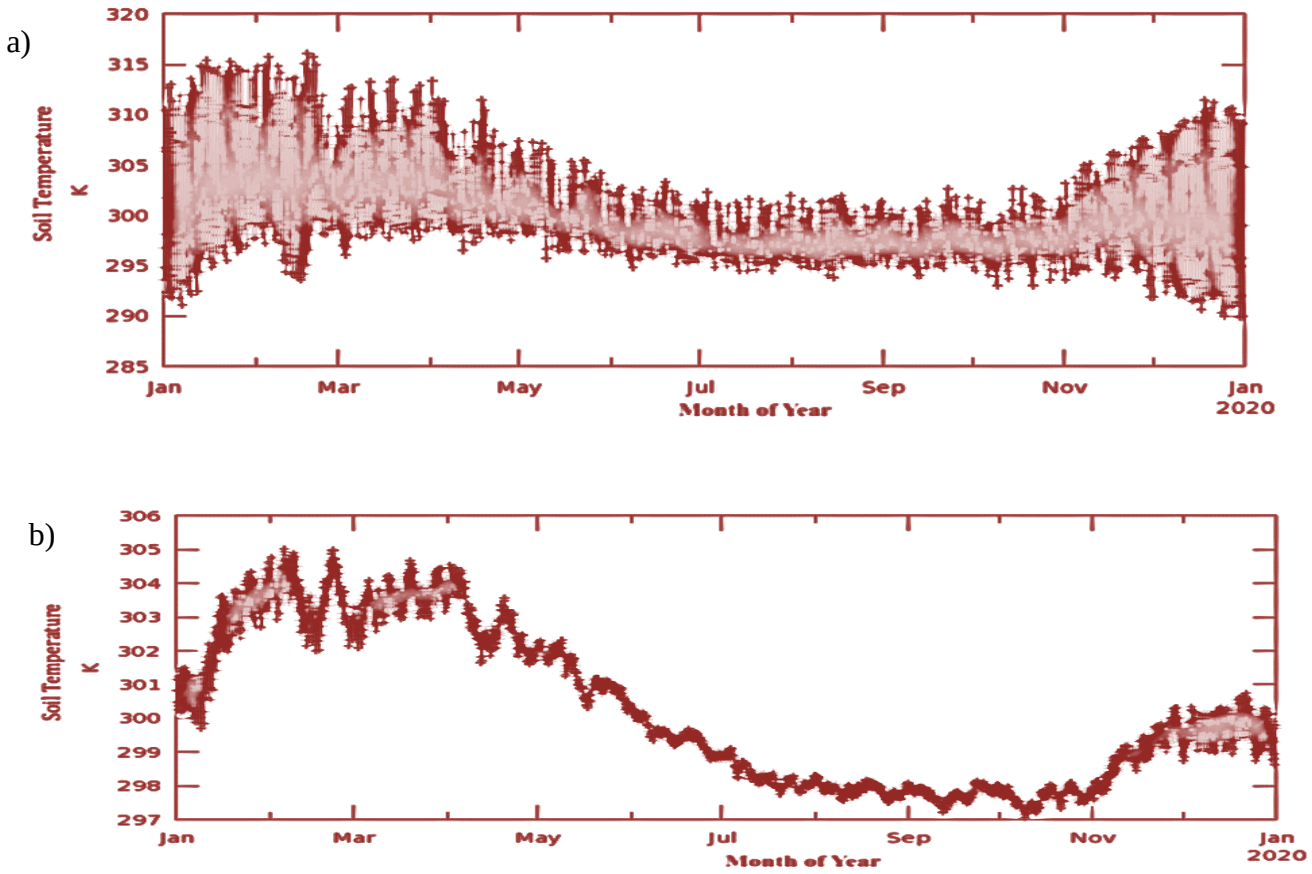


**Figure 4.23:** Soil temperature at Landmark University farm for: (a) 2019 at 0 – 10 cm, and (b) 2019 at 10 – 40 cm

### 4.3.2 Soil Moisture Content (SMC)

The soil moisture content (SMC) for 2017 – 2019 at Covenant University farm ranged from $10-40\,m^3/m^3$ at depth of 0 – 10 cm and 60 $m^3/m^3$ to 112 $m^3/m^3$ at depth of 10 – 40 cm underground for the three (3) consecutive years studied (Figures 4.24 and 4.25). The upper and lower limits of SMC at the site in Covenant University farm showed the variability in SMC for the three (3) consecutive years. The SMC for 2017 ranged from 23 $m^3/m^3$ to 29 $m^3/m^3$ at depth of 0 – 10 cm with the highest observed between late May and mid July, 2017. At depth of 1 – 40 cm, SMC ranged from $75\,m^3/m^3$ to 112 $m^3/m^3$ in 2017. In 2018, SMC at depth of 0 – 10 cm ranged from 22 $m^3/m^3$ to $39\,m^3/m^3$ with the highest SMC of $39\,m^3/m^3$ observed between July and September. At depth of 10 – 40 cm, SMC for the site in Covenant University farm ranged from 75 $m^3/m^3$ to 110 $m^3/m^3$ for 2018. For 2019, SMC ranged from 10 $m^3/m^3$ to 40 $m^3/m^3$ with the highest SMC of $40\,m^3/m^3$ observed in September, 2019. Low SMC that ranged from 10 $m^3/m^3$ to 24 $m^3/m^3$ was observed between January and March of the three (3) years studied.

Figures 4.26 and 4.27 show the SMC values in the site at Landmark University farm for the three (3) years studied. In 2017, SMC in the site at Landmark University farm ranged from 10 $m^3/m^3$ to 30 $m^3/m^3$ at depth 0 – 10 cm and 60 $m^3/m^3$ to 110 $m^3/m^3$ at depth of 10 – 40 cm. In 2018, SMC ranged from $10\,m^3/m^3$ to 39 $m^3/m^3$ at depth 0 – 10 cm and 60 $m^3/m^3$ to 109 $m^3/m^3$ at depth of 10 – 40 cm. The monthly SMC at the farm site ranged from 10 $m^3/m^3$ to 39 $m^3/m^3$ at the depth of 0 – 10 cm and 60 $m^3/m^3$ to 109 $m^3/m^3$ at depth 10 – 40 cm in 2019. Highest SMC of 40 $m^3/m^3$ was observed in September, 2017 for the three years studied. Low SMC that ranged from 10 $m^3/m^3$ to 19 $m^3/m^3$ was observed between January and March, 2017 – 2019.

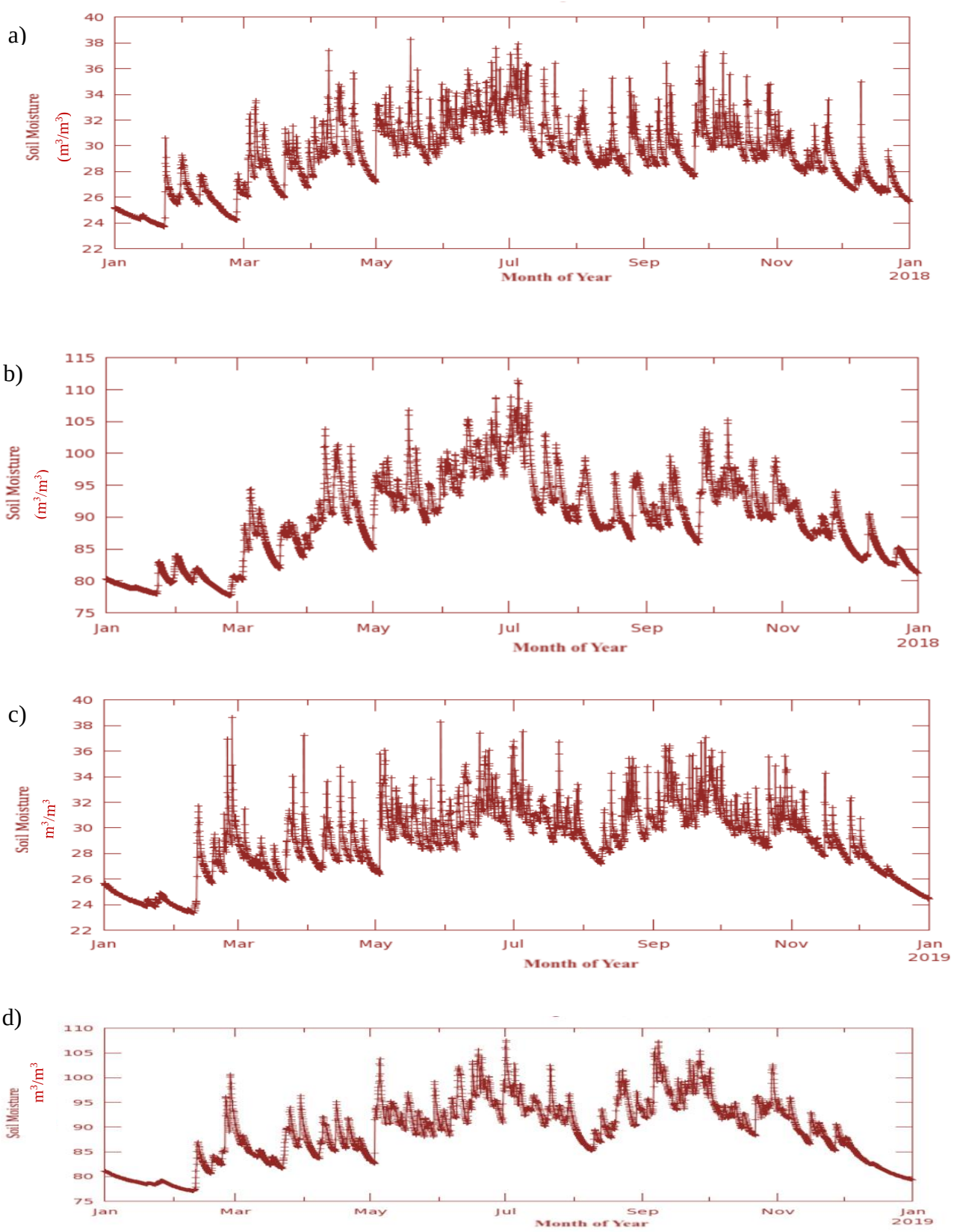


**Figure 4.24**: Monthly soil moisture content for the site at Covenant University farm for: (a) 2017 at 0 – 10 cm, (b) 2017 at 10 – 40 cm, (c) 2018 at 0 – 10 cm, and (d) 2018 at 10 – 40 cm

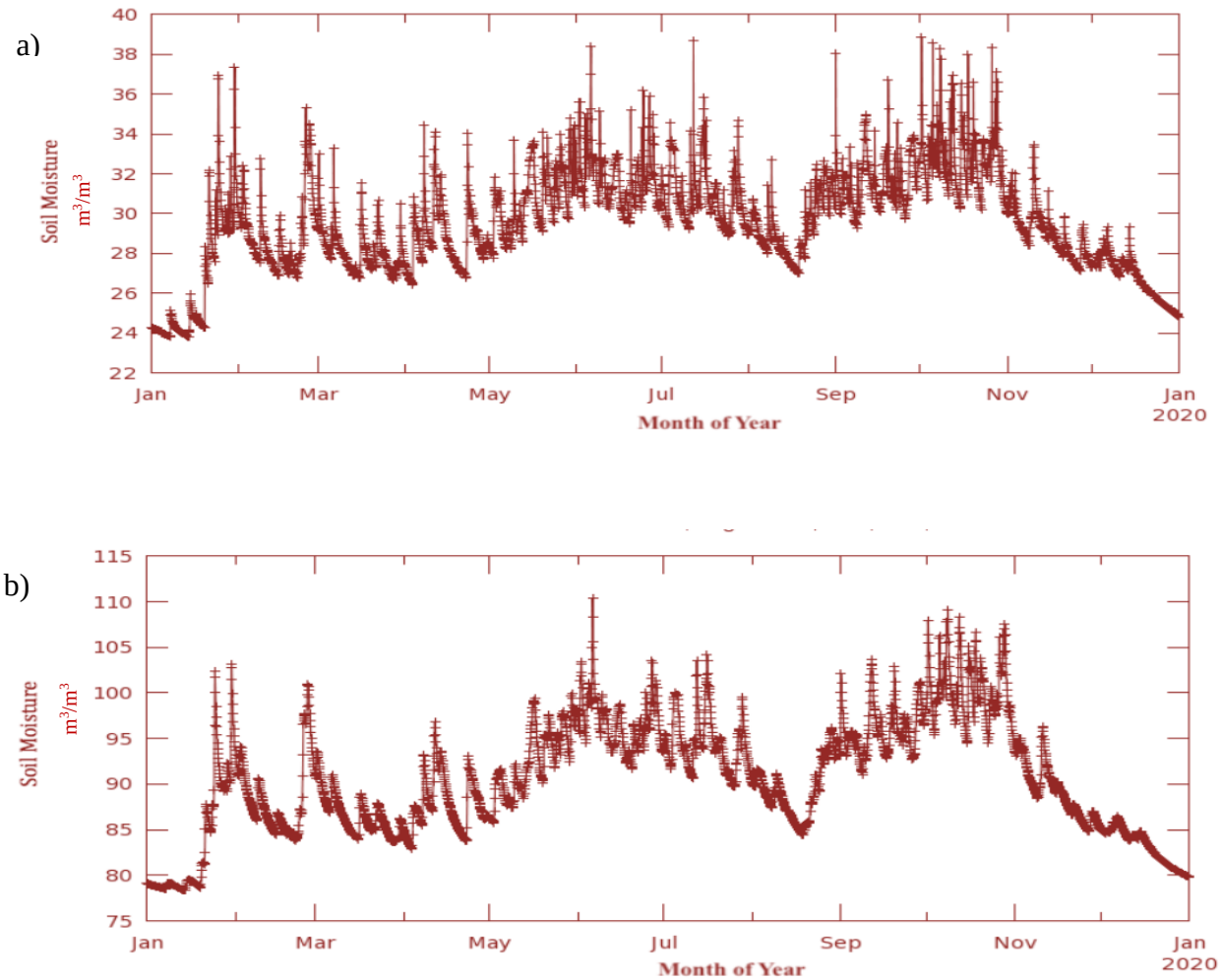


**Figure 4.25:** Monthly soil moisture for the site at Covenant University farm for: (a) 2019 at 0 – 10 cm, and (b) 2019 at 10 – 40 cm

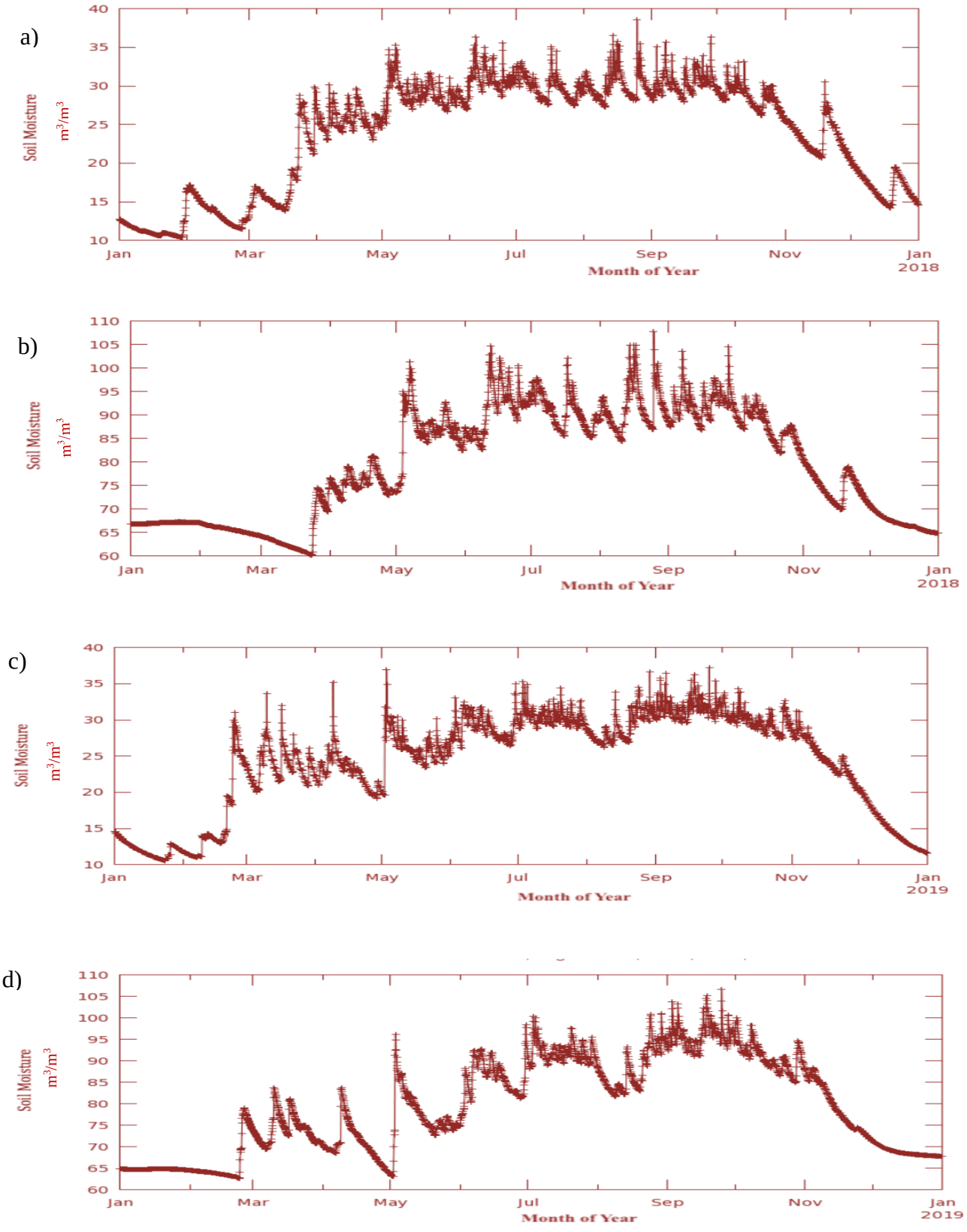


**Figure 4.26**: Monthly soil moisture content for the site at Landmark University farm for: (a) 2017 at 0 – 10 cm, (b) 2017 at 10 – 40 cm, (c) 2018 at 0 – 10 cm, and (d) 2018 at 10 – 40 cm

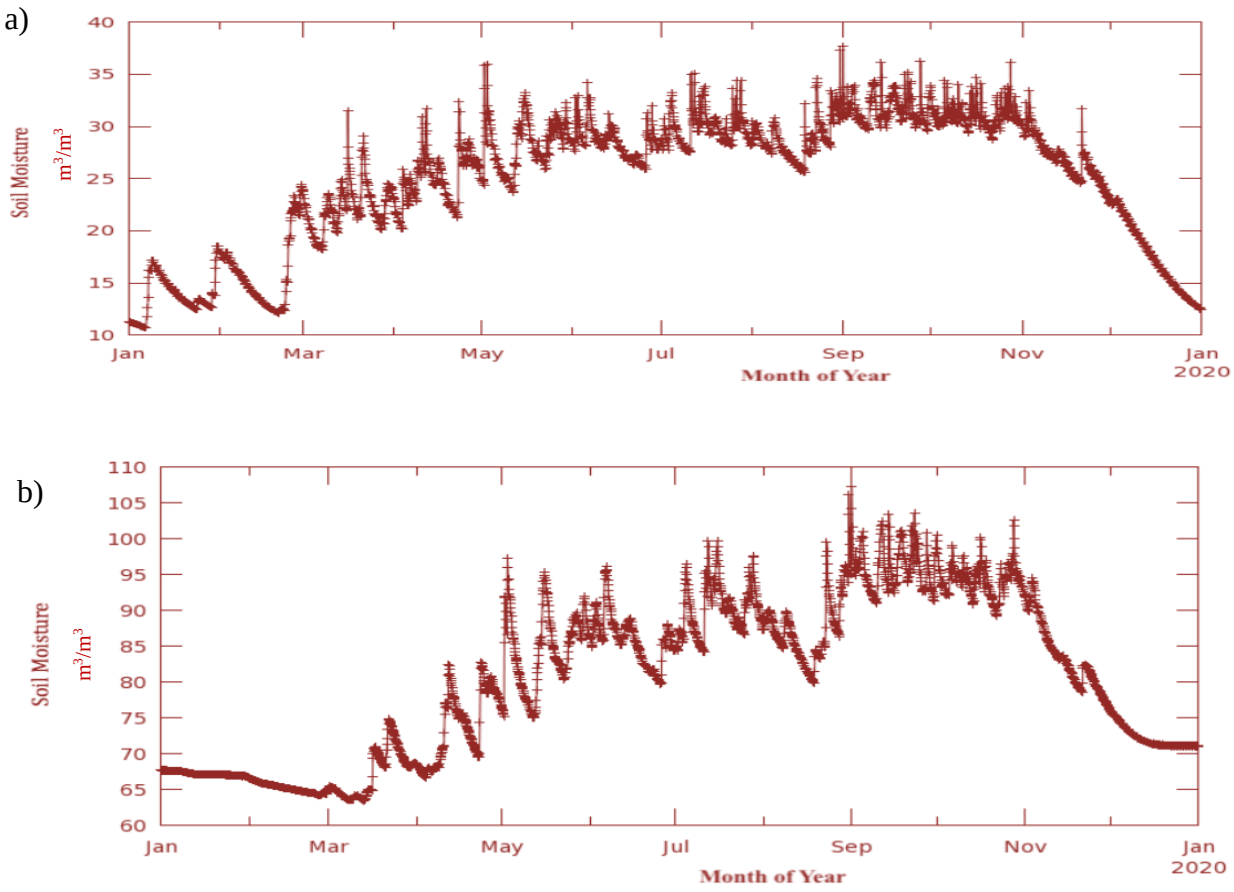


**Figure 4.27**: Soil moisture at Landmark University for: (a) 2019 at 0 -10 cm, and (b) 2019 at 10 – 40 cm

### 4.3.3 Soil Salinity Index

The soil salinity index map for southern and north-central states of Nigeria (Figure 4.28a) showed that high and low salt affected parts of the study sites. High soil salinity was observed towards the north-central part of Nigeria covering states such as; Niger, Plateau, some part of Benue, FCT and Kwara. The riverine area of south-south Nigeria, consisting of Bayelsa, Rivers, Delta, Akwa-Ibom and Cross River have low soil salinity. Other states in south-south such as Edo, north-eastern part of Cross River and Benue states have areas affected by soil salinity at low to medium level. Lagos, Ogun, Ekiti and some parts of Oyo states also have low to moderate soil salinity index while Abia, Imo, Enugu and some parts of Anambra and Ebonyi indicated low to moderate soil salinity.

Soil salinity maps of Covenant University and Landmark University farms are presented in Figures 4.28b and 4.29. The salinity index for Covenant University farm (Figure 4.28b) showed high soil salinity towards the northern, southwestern and southern portions of the farmland. The northeastern part of the farmland has low soil salinity as observed in Figure 4.28b. However, a large portion of the farm area at the site in Landmark University farm exhibited high soil salinity as observed in the satellite imagery (Figure 4.29).

a)

b)

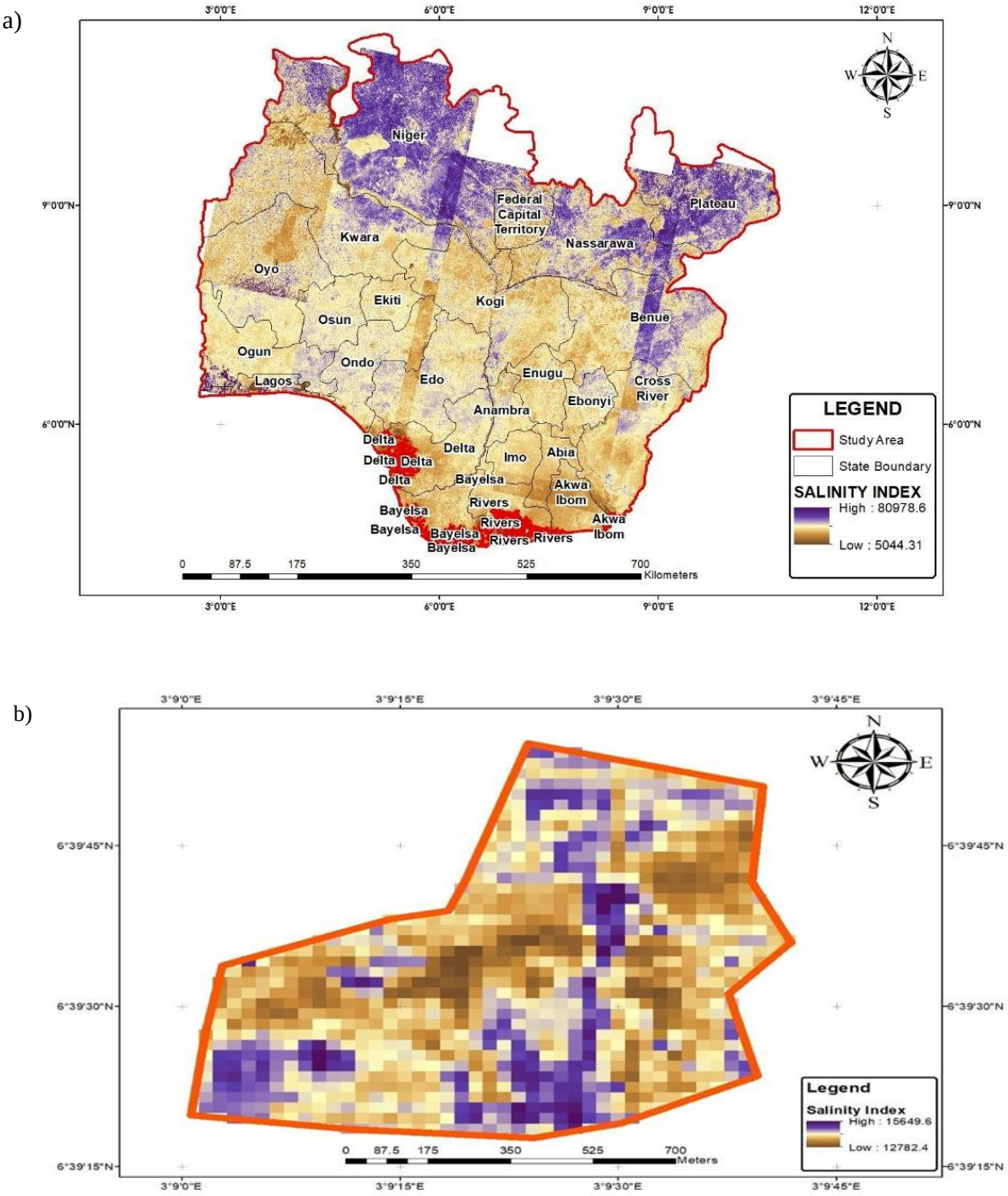


**Figure 4.28:** Salinity index maps for: (a) southern and northcentral states of Nigeria, and (b) at Covenant University farm

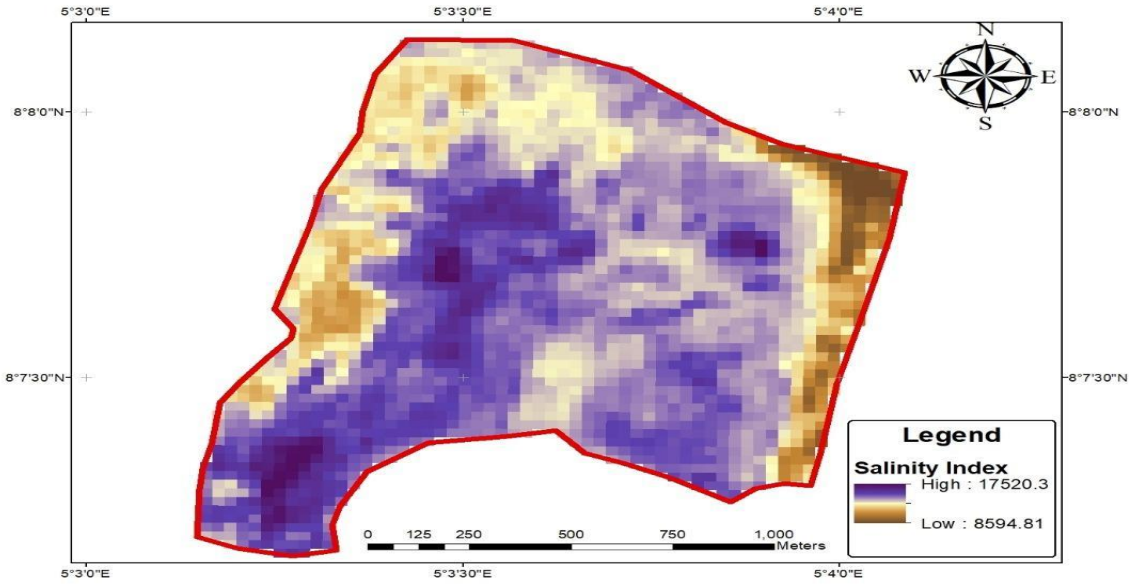


**Figure 4.29**: Soil salinity extracted from Landsat-8 for the site at Landmark University farm

## 4.4 Elemental Composition of the Analysed Soil Samples

The major, trace and rare earth elemental geochemical composition of the analysed soil samples in the study area are presented in Tables 4.3 – 4.6, 4.18 and 4.22. The results of the trace elements analysis were compared with WHO (2001) and European Union Standard (2002) as presented in Tables 4.3 and 4.5. Tables 4.4 and 4.6 present the rare earth elements (REEs) that acts as contaminants in the soil samples of the study sites, and these include lanthanum (La), terbium (Tr), thorium (Th), samarium (Sm), gadolinium (Gd), Praseodymium (Pr) and cerium (Ce).

Table 4.3 presents the trace elements concencentration at Covenant University farm. As, Cr, Co, Cu, Mn and Zn have concentrations higher in some of the soil samples than FAO/WHO standard limits in agricultural soils. Cd and Pb concentrations in the soils of this site are considerably minimal, that is within the limits recommended for agricultural soils by WHO/FAO but Pb have concentration in some of the soil samples higher than the European Union standard limits (16 mg/kg). Table 4.4 showed higher concentrations of rare earth elements and radionuclides such as, Ce, Sr, La and V at Covenant University farm.

The trace elements concentrations at Landmark University farm are presented in Table 4.5. As, Cd, Mo, Ni, Sb, S, and Zn concentrations in the farm site are considerably low as compared to FAO/WHO (2001) but Cr and Mn have concentrations higher than the permissible limits by European Union (2002). Table 4.6 presents the concentration of rare elements and radionuclides at Landmark University farm; Ce, La, Sr, V and Th have higher concentration in the farm site. The major elemental composition values and coordinates are presented in Tables 4.7 and 4.8.

**Table 4.3**: Trace elements concentration (mk/kg) in Covenant University farm (n=10)

| *Elements mg/kg* | *WHO/FAO (2001)* | *EU (2002)* | *Crustal Average (1964)* | *C1* | *C2* | *C3* | *C4* | *C5* | *C6* | *C7* | *C8* | *C9* | *C10* |
|---|---|---|---|---|---|---|---|---|---|---|---|---|---|
| As | 10 | N/A | 1.50 | 10.1 | 12.4 | 14 | 7.3 | 8.9 | 8.2 | 3.1 | 3.0 | 5.4 | 9.7 |
| Cd | 0.2 | 0.2 | 0.1 | 0.01 | 0.01 | 0.01 | 0.01 | 0.01 | 0.01 | 0.01 | 0.01 | 0.02 | 0.02 |
| Co | N/A | 50 | 17.0 | 4.70 | 4.20 | 4.60 | 4.9 | 4.0 | 4.60 | 10.1 | 18.0 | 75.2 | 59.4 |
| Cr | 20 | 1.0 | 83.0 | 136 | 161 | 187 | 92.0 | 148 | 138 | 22.0 | 41.0 | 444 | 193 |
| Cu | 40 | 20 | 25.0 | 22.7 | 36.3 | 34.4 | 25.8 | 29.2 | 34.0 | 9.6 | 15 | 45.1 | 36.4 |
| Mn | N/A | 500 | 600 | 227 | 167 | 159 | 132 | 141 | 154 | 454 | 720 | 1897 | 2359 |
| Ni | 68.0 | N/A | 44.0 | 18.8 | 18.0 | 21.7 | 22.8 | 20.4 | 26.3 | 10.9 | 18.3 | 240 | 74.2 |
| Pb | 50.0 | 16 | 17.0 | 24.04 | 28.8 | 25.7 | 23.8 | 23.2 | 22.4 | 16.9 | 26.3 | 39.6 | 81.0 |
| Se | N/A | N/A | 0.05 | 1.40 | 1.20 | 1.10 | 0.50 | 0.5 | 0.8 | 0.2 | 0.3 | 1.0 | 0.8 |
| Mo | 5.0 | N/A | 1.50 | 3.97 | 4.04 | 4.77 | 2.97 | 3.37 | 3.07 | 0.49 | 0.89 | 2.31 | 2.29 |
| Sb | N/A | 10 | 0.20 | 0.52 | 0.61 | 0.71 | 0.43 | 0.50 | 0.49 | 0.13 | 0.19 | 0.41 | 0.56 |
| Sr | 200 | N/A | 375.0 | 22.0 | 20.0 | 18.0 | 20.0 | 25.0 | 22.0 | 66 | 107 | 66 | 87.0 |
| Zn | 60 | 50.0 | 71.0 | 23.5 | 26.8 | 28.1 | 22.7 | 28.2 | 29.0 | 28.4 | 49.6 | 83.6 | 85.4 |

N/A- Not Available , C – Sample Location

**Table 4.4:** Rare earth elements (REEs) concentration (mg/kg) in Covenant University farm (n=10)

| *Samples* | *Sm* | *Eu* | *Gd* | *Tb* | *Pr* | *La* | *Ce* | *Sr* | *V* | *Th* |
|---|---|---|---|---|---|---|---|---|---|---|
| C1 | 3.7 | 0.8 | 2.5 | 0.3 | 6.9 | 35.0 | 79.65 | 22.0 | 231.0 | 17.3 |
| C2 | 3.6 | 0.7 | 2.7 | 0.4 | 7.6 | 42.1 | 68.01 | 20.0 | 309.0 | 20.4 |
| C3 | 3.2 | 0.7 | 2.3 | 0.3 | 5.5 | 30.1 | 57.49 | 18.0 | 315.0 | 21.1 |
| C4 | 3.3 | 0.6 | 2.1 | 0.3 | 6.3 | 35.3 | 65.94 | 20.0 | 159.0 | 16.0 |
| C5 | 6.4 | 1.3 | 4.4 | 0.4 | 12.7 | 57.5 | 87.55 | 25.0 | 198.0 | 17.9 |
| C6 | 4.0 | 0.8 | 3.2 | 0.4 | 8.1 | 43.5 | 78.76 | 22.0 | 169.0 | 18.4 |
| C7 | 4.6 | 0.8 | 3.2 | 0.5 | 6.6 | 27.7 | 57.21 | 66.0 | 26.0 | 9.60 |
| C8 | 6.5 | 1.2 | 4.9 | 0.6 | 10.8 | 48.4 | 99.45 | 107.0 | 52.0 | 15.7 |
| C9 | 8.1 | 1.9 | 5.2 | 0.8 | 12.8 | 56.2 | 141.95 | 66.0 | 228.0 | 13.1 |
| C10 | 7.7 | 1.7 | 5.7 | 0.7 | 11.9 | 54.7 | 134.08 | 87.0 | 148.0 | 15.0 |

**Table 4.5**: Trace elements concentration (mg/kg) in Landmark University farm (n=8)

| *Elements* | *WHO/FAO (2001)* | *EU (2002)* | *Crustal Average (1964)* | *L1* | *L2* | *L3* | *L4* | *L5* | *L6* | *L7* | *L8* |
|---|---|---|---|---|---|---|---|---|---|---|---|
| As | 10 | N/A | 1.5 | 4.3 | 2.6 | 4.2 | 4.6 | 4.6 | 4.3 | 2 | 1.2 |
| Cd | 0.2 | 0.2 | 0.1 | 0.01 | 0.01 | 0.01 | 0.01 | 0.01 | 0.01 | 0.12 | 0.09 |
| Co | N/A | 50 | 17.0 | 6.10 | 5.10 | 5.5 | 6.6 | 6.20 | 6.50 | 17.4 | 9.70 |
| Cr | 20 | 1.0 | 83.0 | 56.0 | 55.0 | 60.0 | 67.0 | 72.0 | 71.0 | 58.0 | 38.0 |
| Cu | 40 | 20 | 25.0 | 19.3 | 16.4 | 22.2 | 22.0 | 21.2 | 23.9 | 24.5 | 16.8 |
| Mn | N/A | 500 | 600 | 360 | 292 | 402 | 329 | 393 | 323 | 1137 | 554 |
| Ni | 68 | N/A | 44.0 | 21.4 | 17.3 | 21.9 | 25.0 | 21.8 | 26.1 | 19.7 | 12.3 |
| Pb | 50 | 16 | 17.0 | 18.46 | 15.58 | 19.37 | 19.73 | 19.22 | 21.3 | 49.9 | 36.5 |
| Se. | N/A | N/A | 0.05 | 0.3 | 0.50 | 0.20 | 0.70 | 0.5 | 0.7 | 0.2 | 0.70 |
| Mo | 5.0 | N/A | 1.50 | 1.42 | 1.07 | 1.41 | 1.53 | 1.34 | 1.54 | 2.16 | 1.48 |
| Sb | N/A | 10 | 0.20 | 0.31 | 0.25 | 0.28 | 0.32 | 0.3 | 0.30 | 0.39 | 0.24 |
| Sr | 200 | N/A | 375.0.0 | 21 | 17.0 | 21 | 22.0 | 22 | 22.0 | 167 | 212 |
| Zn | 60 | 50 | 71.0 | 28.6 | 23.2 | 29.5 | 30.1 | 28.7 | 34.1 | 156.9 | 96.0 |

N/A-Not Available

**Table 4.6**: Rare earth elements (REE) concentration (mg/kg) at Landmark University farm (n=8)

| *Samples* | *Sm* | *Eu* | *Gd* | *Tb* | *Pr* | *La* | *Ce* | *Sr* | *V* | *Th* |
|---|---|---|---|---|---|---|---|---|---|---|
| L1 | 2.1 | 0.4 | 1.8 | 0.2 | 5.0 | 26.7 | 79.37 | 21.0 | 71.0 | 12.7 |
| L2 | 2.0 | 0.4 | 1.3 | 0.2 | 4.2 | 22.8 | 71.49 | 17.0 | 58.0 | 11.6 |
| L3 | 3.1 | 0.5 | 1.8 | 0.3 | 5.5 | 30.2 | 89.2 | 21.0 | 73.0 | 13.8 |
| L4 | 3.0 | 0.5 | 2.2 | 0.3 | 5.4 | 30.2 | 87.66 | 22.0 | 75.0 | 14.0 |
| L5 | 2.8 | 0.5 | 1.8 | 0.3 | 5.0 | 28.3 | 84.92 | 22.0 | 70.0 | 13.2 |
| L6 | 2.8 | 0.5 | 1.9 | 0.3 | 5.9 | 32.0 | 97.86 | 22.0 | 83.0 | 14.9 |
| L7 | 8.1 | 1.5 | 6.1 | 0.8 | 15.4 | 73.5 | 183.63 | 167.0 | 80.0 | 26.3 |
| L8 | 5.4 | 0.9 | 4.1 | 0.5 | 9.8 | 48.8 | 115.91 | 212.0 | 54.0 | 16.9 |

**Table 4.7** ordinates and values of elemental composition of samples in Covenant University farm

| CU | Longitudes (N) | Latitudes (E) | Na | P | Ca | Mg | K | Fe | Ti | Al |
|---|---|---|---|---|---|---|---|---|---|---|
| C1 | 06 39 83.9 | 03 09 53.6 | 0.013 | 0.049 | 0.06 | 0.07 | 0.23 | 0.23 | 0.346 | 7.63 |
| C2 | 06 39 83.4 | 03 09 56.7 | 0.009 | 0.039 | 0.01 | 0.05 | 0.19 | 0.19 | 0.323 | 8.29 |
| C3 | 06 39 83.8 | 03 09 55.3 | 0.008 | 0.046 | 0.02 | 0.05 | 0.15 | 0.15 | 0.348 | 8.01 |
| C4 | 06 39 84.0 | 03 09 56.9 | 0.01 | 0.031 | 0.05 | 0.07 | 0.21 | 0.21 | 0.375 | 8.32 |
| C5 | 06 39 84.8 | 03 09 53.8 | 0.009 | 0.039 | 0.02 | 0.06 | 0.23 | 0.23 | 0.349 | 8.56 |
| C6 | 06 39 84.2 | 03 09 57.1 | 0.008 | 0.033 | 0.02 | 0.06 | 0.17 | 0.17 | 0.37 | 8.17 |
| C7 | 06 39 85.1 | 03 09 53.9 | 0.714 | 0.016 | 0.07 | 0.06 | 0.53 | 0.53 | 0.269 | 3.32 |
| C8 | 06 39 84.7 | 03 09 55.4 | 0.525 | 0.031 | 0.08 | 0.15 | 0.8 | 0.8 | 0.586 | 4.17 |
| C9 | 06 39 84.5 | 03 09 57.1 | 0.208 | 0.072 | 0.18 | 0.39 | 0.75 | 0.75 | 0.993 | 7.59 |
| C10 | 0639 84.8 | 03 09 57.2 | 0.2 | 0.052 | 0.18 | 0.25 | 0.79 | 0.79 | 0.49 | 6.56 |

**Table 4.8** ordinates and values of elemental composition of samples in Landmark University farm

| Soil | Longitude N | Latitude E | Na | P | Ca | Mg | K | Fe | Ti | Al |
|---|---|---|---|---|---|---|---|---|---|---|
| L1 | 08 07 72.8 | 05 03 59.9 | 0.012 | 0.0024 | 0.06 | 0.07 | 0.04 | 2.75 | 0.548 | 5.47 |
| L2 | 08 07 73.4 | 05 03 58.4 | 0.007 | 0.019 | 0.05 | 0.06 | 0.03 | 2.29 | 0.48 | 4.46 |
| L3 | 08 07 71.9 | 05 03 61.4 | 0.008 | 0.023 | 0.04 | 0.06 | 0.04 | 2.81 | 0.62 | 5.61 |
| L4 | 08 07 73.0 | 05 03 58.4 | 0.007 | 0.022 | 0.05 | 0.07 | 0.04 | 2.98 | 0.603 | 6.5 |
| L5 | 08 07 71.5 | 05 03 61.4 | 0.008 | 0.021 | 0.07 | 0.07 | 0.04 | 2.75 | 0.583 | 5.78 |
| L6 | 08 07 12.859 | 05 06. 003 | 0.008 | 0.026 | 0.04 | 0.07 | 0.04 | 3.24 | 0.591 | 6.99 |
| L7 | 08 07 12. 848 | 05 06.002 | 0.493 | 0.069 | 0.44 | 0.25 | 2.46 | 4.19 | 0.599 | 9.33 |
| L8 | 08 07 12.45 | 05 05 970 | 0.767 | 0.049 | 0.52 | 0.2 | 2.9 | 2.66 | 0.408 | 7.29 |

### 4.4.1 Toxic Elements Contamination Assessment

Tables 4.9 - 4.18 show the pollution indices and degree of contamination of the toxic elements at Covenant University farm and Landmark University farm. For the site at Covenant University farm, arsenic concentration was the highest contaminant with contamination factor ranging from 2.0 - 9.3 (Table 4.9). Cadmium (Cd) concentration was the highest contaminant at Landmark University farm having contamination factor ranging from 2.5 – 3.9. The pollution load index (PLI) in the two farm sites indicates unpolluted to highly polluted soils. Tables 4.17 and 4.18 showed a very high risk of arsenic in Covenant University farm and a moderate risk at Landmark University farm.

**Table 4.9:** Contamination factor at Covenant University farm

| *Toxic elements* | *Contamination Factor (Range)* | *Contamination Factor* | *Interpretation* |
|---|---|---|---|
| As | 2.0 - 9.3 | 5.31 | Moderate to Highly Contamination |
| Cd | 0.1 - 0.2 | 1.11 | Low Contamination |
| Co | 0.06 – 4.42 | 1.02 | Low to High Contamination |
| Cr | 0.27 – 5.35 | 1.88 | Low to High Contamination |
| Cu | 0.36 – 1.80 | 1.15 | Low to Moderate Contamination |
| Ni | 0.25 – 5.47 | 1.07 | Low to High Contamination |
| Mn | 0.22 – 3.94 | 1.07 | Low to High Contamination |
| Pb | 0.99 – 4.76 | 1.84 | Low to High Contamination |
| Zn | 0.33 – 1.20 | 0.57 | Low to Moderate Contamination |

**Table 4.10:** Contamination factor at Landmark University farm

| *Toxic elements* | *Contamination Factor (Range)* | *Contamination Factor* | *Interpretation* |
|---|---|---|---|
| As | 0.80 - 2.87 | 2.33 | Low to Moderate Contamination |
| Cd | 0.10 – 0.20 | 0.34 | Low to Moderate Contamination |
| Co | 0.30 - 1.02 | 0.46 | Low to Moderate Contamination |
| Cr | 0.46 - 0.87 | 0.72 | Low Contamination |
| Cu | 0.66 - 1.29 | 0.88 | Low to Moderate Contamination |
| Ni | 0.28 – 0.6 | 0.47 | Low Contamination |
| Mn | 0.49 - 1.90 | 0.79 | Low to Moderate Contamination |
| Pb | 0.92 - 2.93 | 1.47 | Low to Moderate Contamination |
| Zn | 0.33 – 2.21 | 0.75 | Low to Moderate Contamination |

**Table 4.11:** Pollution load index (PLI and NIPI) at Covenant University farm

| *Toxic elements* | *Pollution load index (PLI)* | *Nemerow integrated pollution index (NIPI)* | *Interpretation* |
|---|---|---|---|
| As | 4.01 | 7.65 | High to Very HIgh Pollution |
| Cd | 0.69 | 0.21 | Unpolluted |
| Co | 0.57 | 0.79 | Unpolluted |
| Cr | 1.69 | 18.67 | Moderate to Ultra High Pollution |
| Cu | 1.06 | 1.51 | Moderate Pollution |
| Ni | 0.64 | 7.51 | Unpolluted to Very High Pollution |
| Mn | 0.58 | 5.78 | Unpollited to Very High Pollution |
| Pb | 1.59 | 3.60 | Moderate to High Pollution |
| Zn | 0.50 | 0.93 | No Pollution |

**Table 4.12:** Pollution load index (PLI and NIPI) at Landmark University farm

| *Toxic elements* | *Pollution load index (PLI)* | *Nemerow integrated pollution index (NIPI)* | *Interpretation* |
|---|---|---|---|
| As | 2.12 | 0.93 | Unpolluted to Moderate Pollution |
| Cd | 0.18 | 0.21 | Unpolluted |
| Co | 0.42 | 0.79 | Unpolluted |
| Cr | 0.71 | 0.79 | Unpolluted |
| Cu | 0.83 | 0.91 | Unpolluted |
| Ni | 0.46 | 0.53 | Unpolluted |
| Mn | 0.71 | 0.71 | Unpolluted |
| Pb | 1.36 | 2.33 | Moderate Pollution |
| Zn | 0.58 | 1.64 | Unpolluted to Moderate Pollution |

**Table 4.13:** Degree of contamination and modified degree of contamination ($C_d$ and $mC_d$) at Covenant University farm

| *Toxic elements* | *Degree of Contamination ($C_d$)* | *Modified Degree of Contamination ($mC_d$)* | *Interpretation* |
|---|---|---|---|
| As | 54.71 | 5.47 | High Degree of Contamination |
| Cd | 0.12 | 0.01 | Nil to Low Contamination |
| Co | 11.20 | 1.12 | Nil to Moderate Contamination |
| Cr | 39.60 | 3.96 | Moderate to High Contamination |
| Cu | 11.54 | 1.15 | Low to Moderate Contamination |
| Ni | 10.70 | 1.07 | Low to Moderate Contamination |
| Mn | 10.70 | 1.07 | Low to Moderate Contamination |
| Pb | 18.23 | 1.82 | Low to Considerate Contamination |
| Zn | 5.70 | 0.57 | Nil to Low Degree of Contamination |

**Table 4.14:** Degree of contamination and modified degree of contamination ($C_d$ and $mC_d$) at Landmark University farm

| *Toxic elements* | *Degree of Contamination ($C_d$)* | *Modified Degree of Contamination ($mC_d$)* | *Interpretation* |
|---|---|---|---|
| As | 08.60 | 1.08 | Low to Moderate Contamination |
| Cd | 01.99 | 0.25 | Nil to Low Contamination |
| Co | 03.69 | 0.46 | Nil to Low Contamination |
| Cr | 05.74 | 0.72 | Nil to Low Degree of Contamination |
| Cu | 06.67 | 0.83 | Nil to Low Degree of Contamination |
| Ni | 03.73 | 0.47 | Nil to Low Degree of Contamination |
| Mn | 06.32 | 0.80 | Nil to Low Degree of Contamination |
| Pb | 11.78 | 1.47 | Low to Modearte Contamination |
| Zn | 06.01 | 0.75 | Nil to Low Degree of Contamination |

**Table 4.15:** The geoaccumulation index ($I_{geo}$) at Covenant University farm

| *Toxic elements* | *Range of $I_{geo}$ Contamination* | *Soil Quality Interpretation* |
|---|---|---|
| As | 0.41-2.64 | Very Low to Low Pollution |
| Cd | 0.00-0.00 | Unpolluted |
| Co | 1.22-1.56 | Low Pollution |
| Cr | 0.00 -1.80 | Unpolluted to Low Pollution |
| Cu | 0.00-0.26 | Unpolluted |
| Ni | 0.16-1.86 | Low Pollution |
| Mn | 0.00-1.39 | Very Low to Low Pollution |
| Pb | 0.01-1.67 | Very Low to Low Pollution |
| Zn | 0.00-0.00 | Unpolluted |

**Table 4.16:** The geoaccumulation index ($I_{geo}$) at Landmark University farm

| *Toxic elements* | *Range of $I_{geo}$ Contamination* | *Soil Quality Interpretation* |
|---|---|---|
| As | 0.00-1.03 | Very Low to Low Pollution |
| Cd | 0.00-0.00 | Unpolluted |
| Co | 0.00-0.00 | Unpolluted |
| Cr | 0.00 -0.00 | Unpolluted |
| Cu | 0.00-0.00 | Unpolluted |
| Ni | 0.00-0.00 | Unpolluted |
| Mn | 0.00-0.00 | Unpolluted |
| Pb | 0.00-1.00 | Unpolluted to Low Pollution |
| Zn | 0.00-0.50 | Unpolluted to Low Pollution |

**Table 4.17:** The potential ecological risk index at Covenant University farm

| *Toxic elements* | *Degree of Risk* | *Interpretation* |
|---|---|---|
| As | 547.1 | Very High Risk |
| Cd | 36 | Low Risk |
| Cr | 79.01 | Low Risk |
| Ni | 53.5 | Low Risk |
| Cu | 52.7 | Low Risk |
| Pb | 91.15 | Low Risk |
| Zn | 5.7 | Low Risk |

**Table 4.18:** The potential ecological risk index at Landmark University farm

| *Toxic elements* | *Degree of Risk* | *Interpretation* |
|---|---|---|
| As | 185.4 | Moderate Risk |
| Cd | 81.0 | Low Risk |
| Cr | 11.48 | Low Risk |
| Cu | 33.35 | Low Risk |
| Ni | 18.65 | Low Risk |
| Pb | 53.25 | Low Risk |
| Zn | 6.01 | Low Risk |

### 4.4.2 Geospatial Maps of Geochemical Compositions

The elemental geospatial maps of the site at Covenant University farm are presented in Figures 4.30 - 4.33 while that of the site at Landmark University farm are presented in Figures 4.34 - 4.37. The geospatial maps are presented in percentage (%) composition. The geospatial maps show the distribution of essential elements/macronutrients including calcium (Ca), sodium (Na), potassium (K), magnesium (Mg), phosphorus (P), iron (Fe), aluminium (Al) and titanium (Ti) in both farm sites. With the aid of the geospatial maps, areas with high accumulation and deficiency of essential/macro elements in the two farm sites can easily be detected.

a)

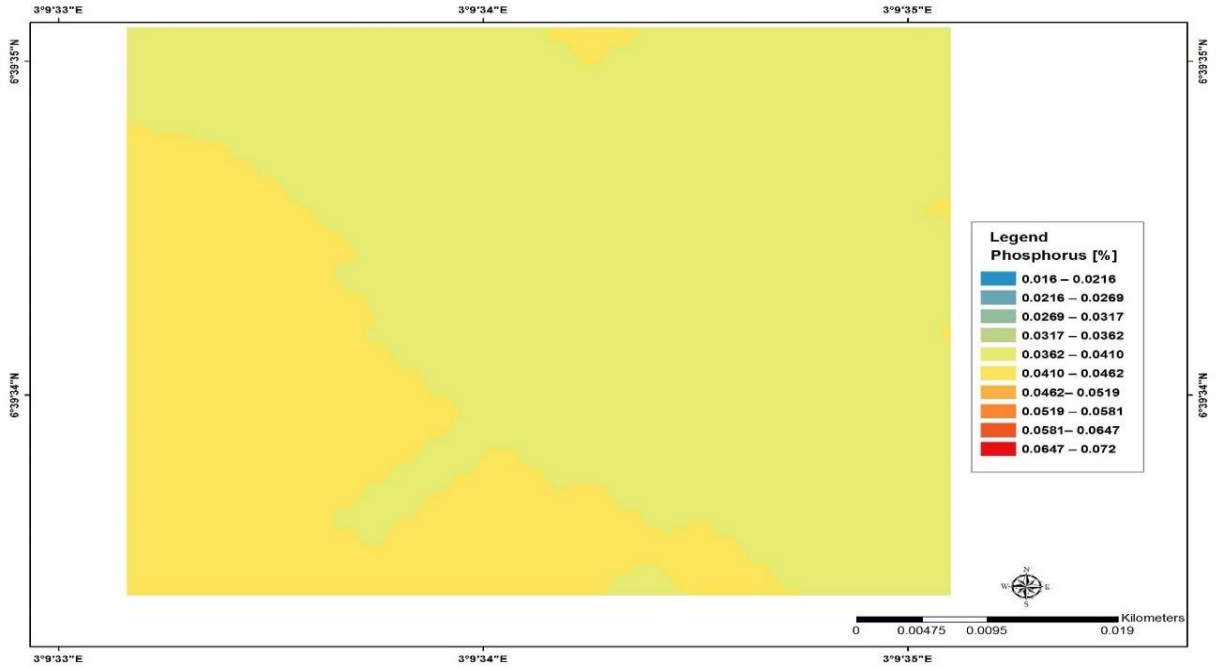


b)

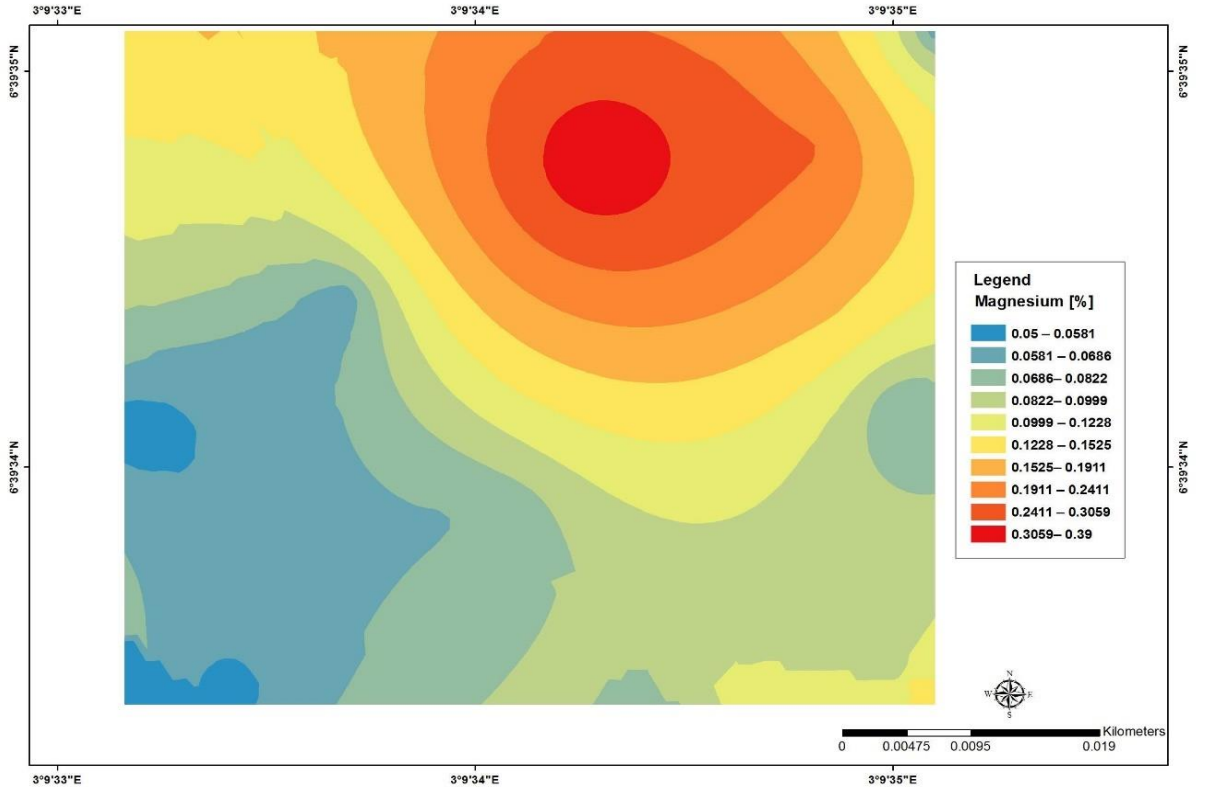


**Figure 4.30:** Geospatial map of the concentration of: (a) phosphorus, and (b) magnesium at Covenant University farm

a)

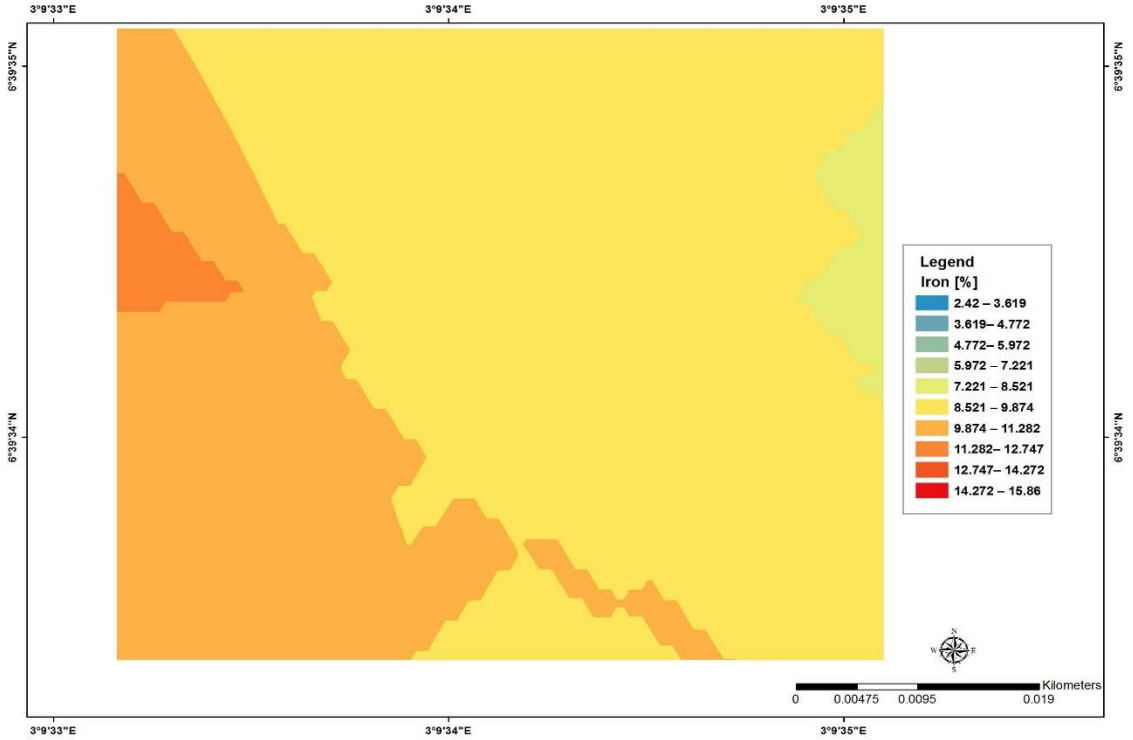


b)

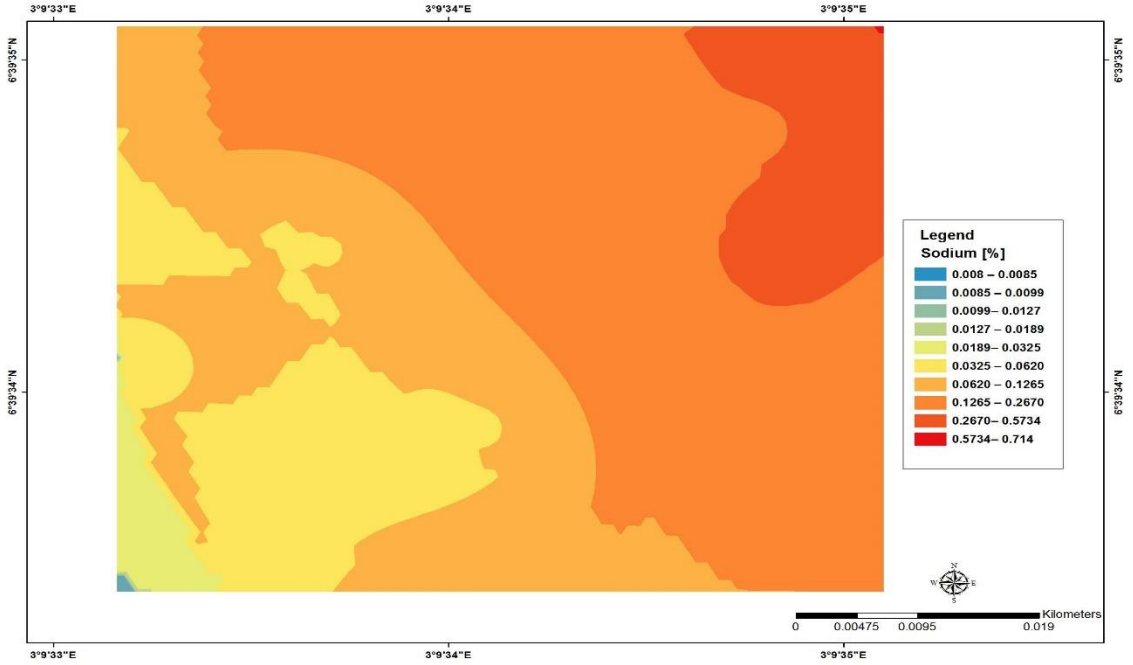


**Figure 4.31**: Geospatial map of the concentration of: (a) iron (Fe), and (b) sodium (Na) at Covenant University farm

a)

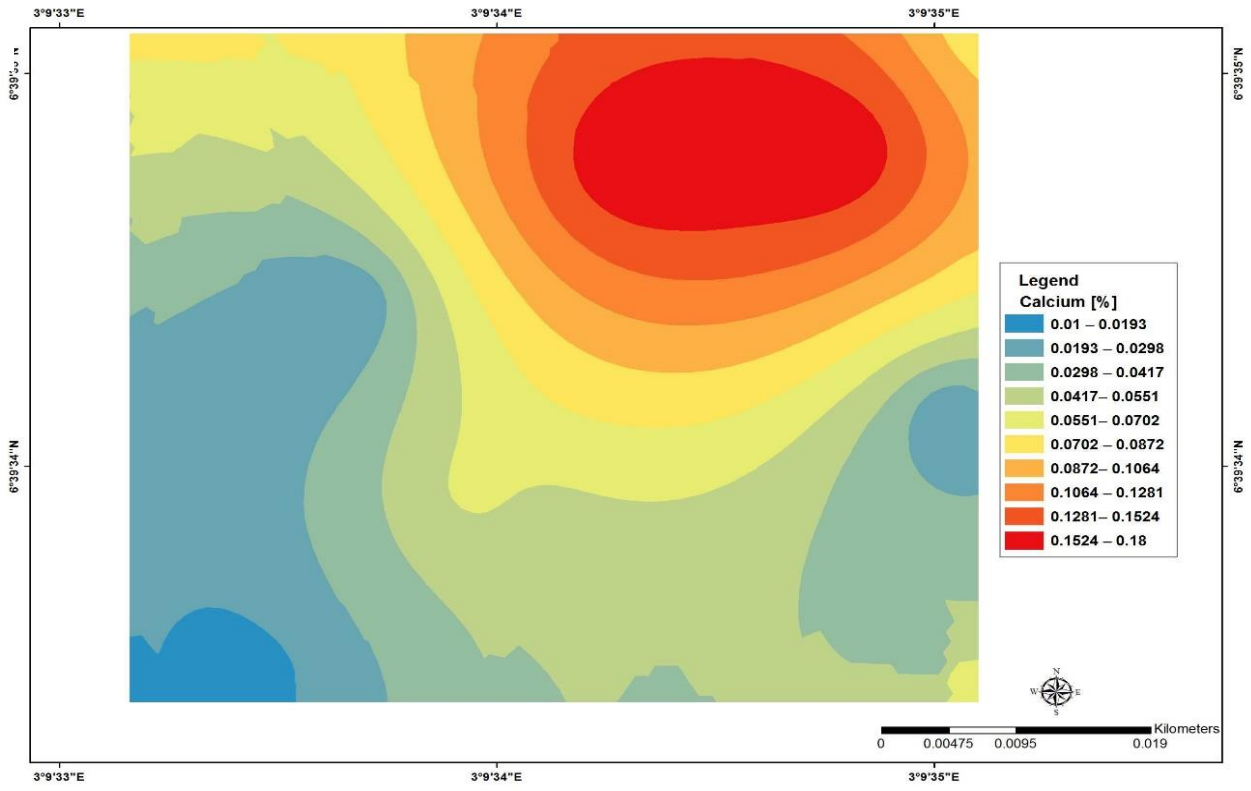


b)

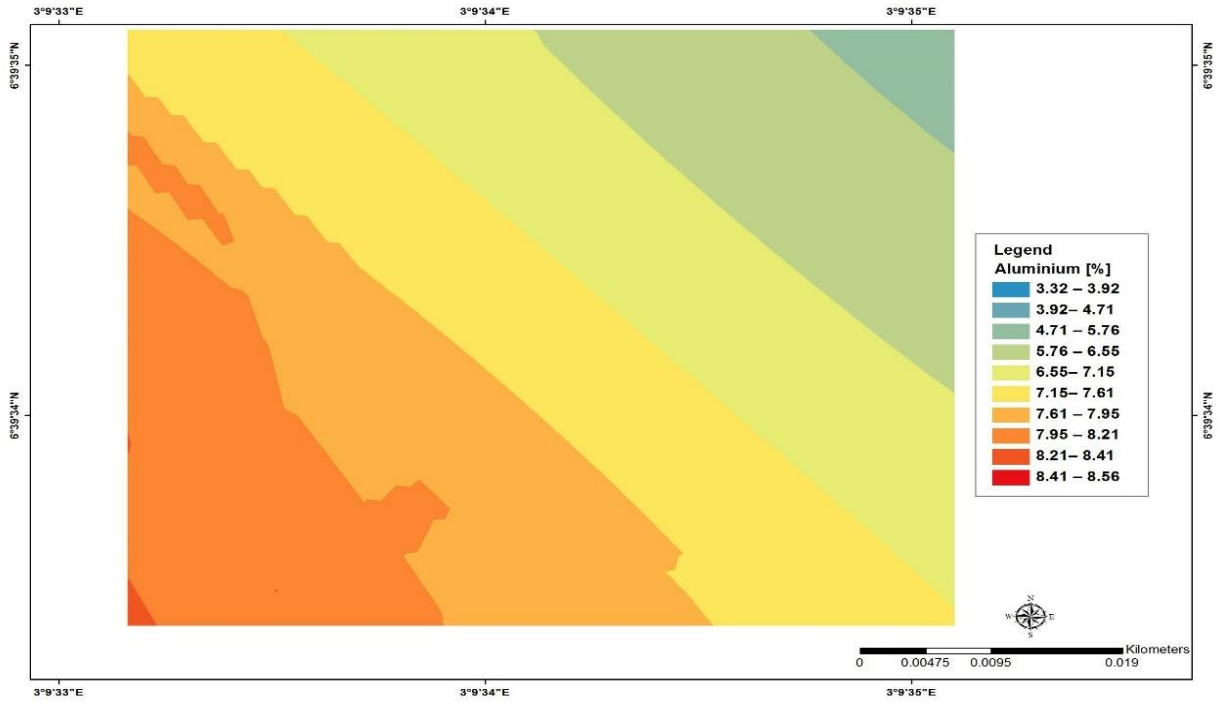


**Figure 4.32**: Geospatial maps of the concentraton of: (a) calcium (Ca), and (b) aluminium (Al) at Covenant University farm

a)

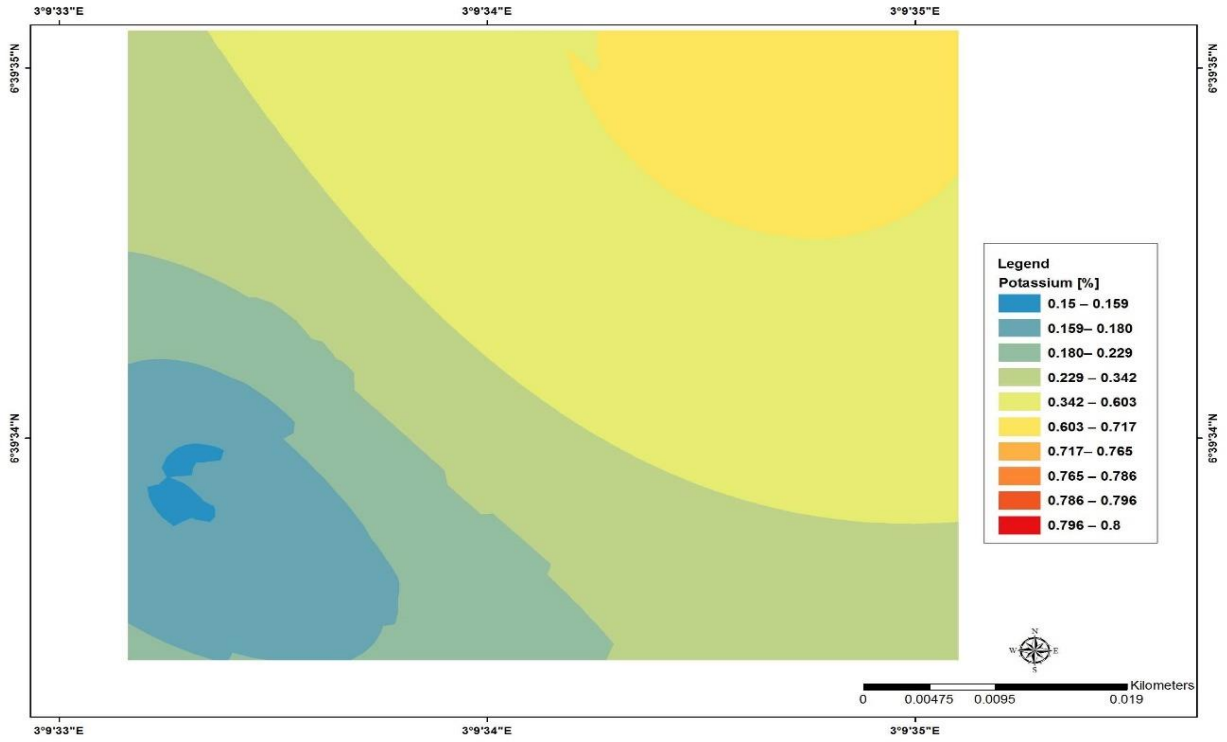


b)

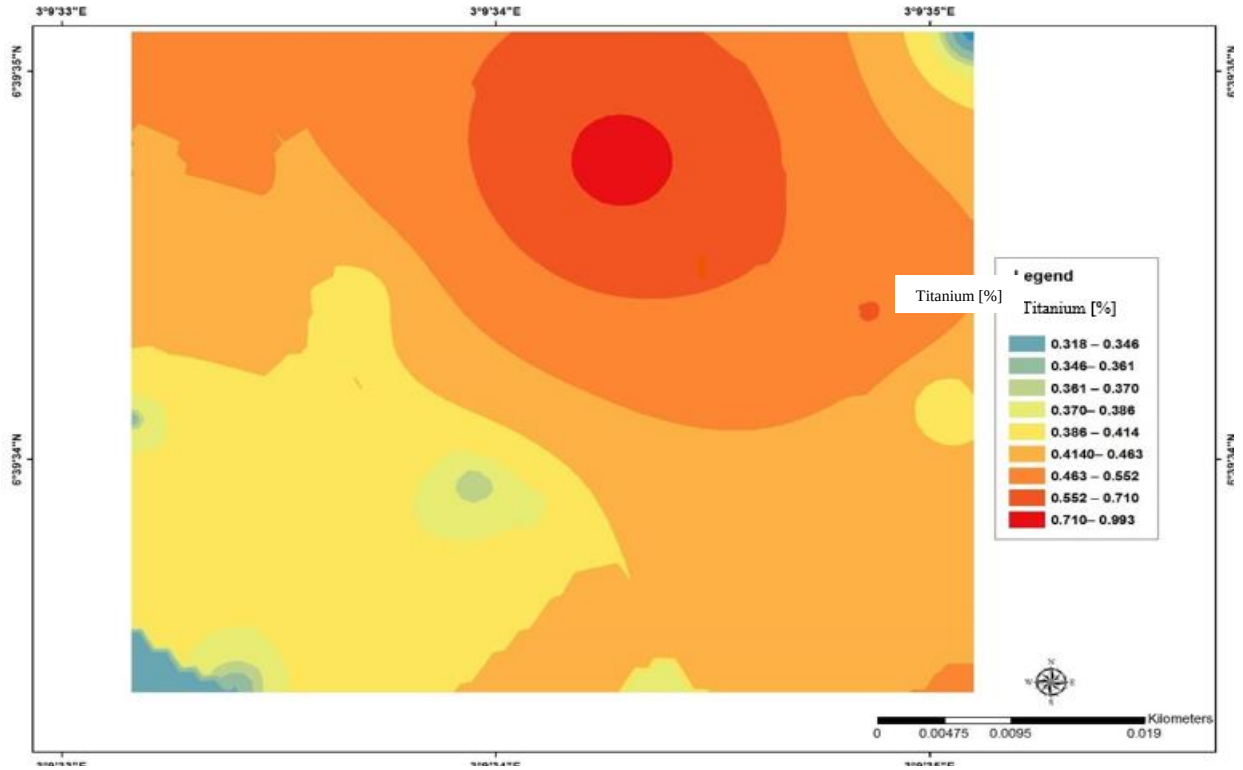


**Figure 4.33**: Geospatial maps of the concentration of: (a) potassium (K), and (b) titanium (Ti) at Covenant University farm

The percentage geospatial maps of macronutrients concentration for the site at Landmark University farm is presented in Figures 4.34 – 4.37. Zones of high accumulations of essential elements and deficiencies have been identified from the results. The macronutrients concentration include magnessium (Mg), calcium (Ca), potassium (K), sodium (Na), phosphorus (P), alumnium Al), iron (Fe) and titanium (Ti).

a)

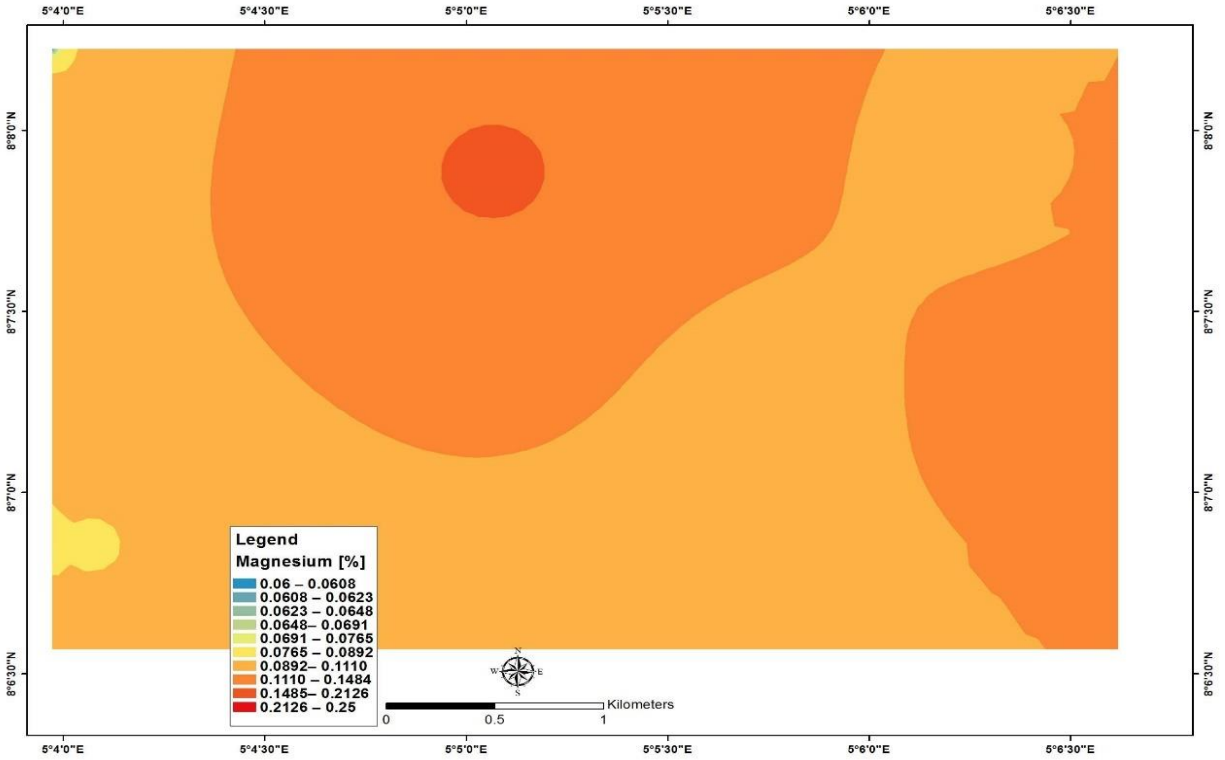


b)

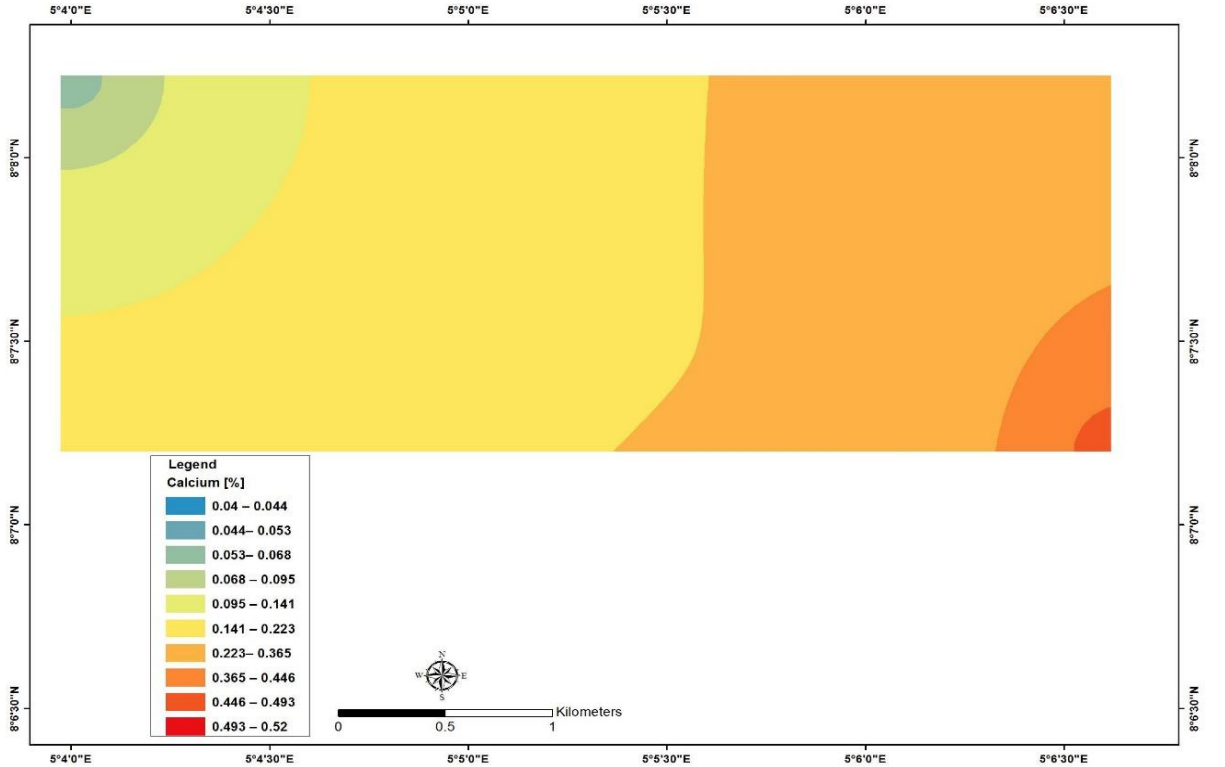


**Figure 4.34**: Geospatial maps of: (a) magnesium (Mg), and (b) calcium (Ca) at Landmark University farm

a)

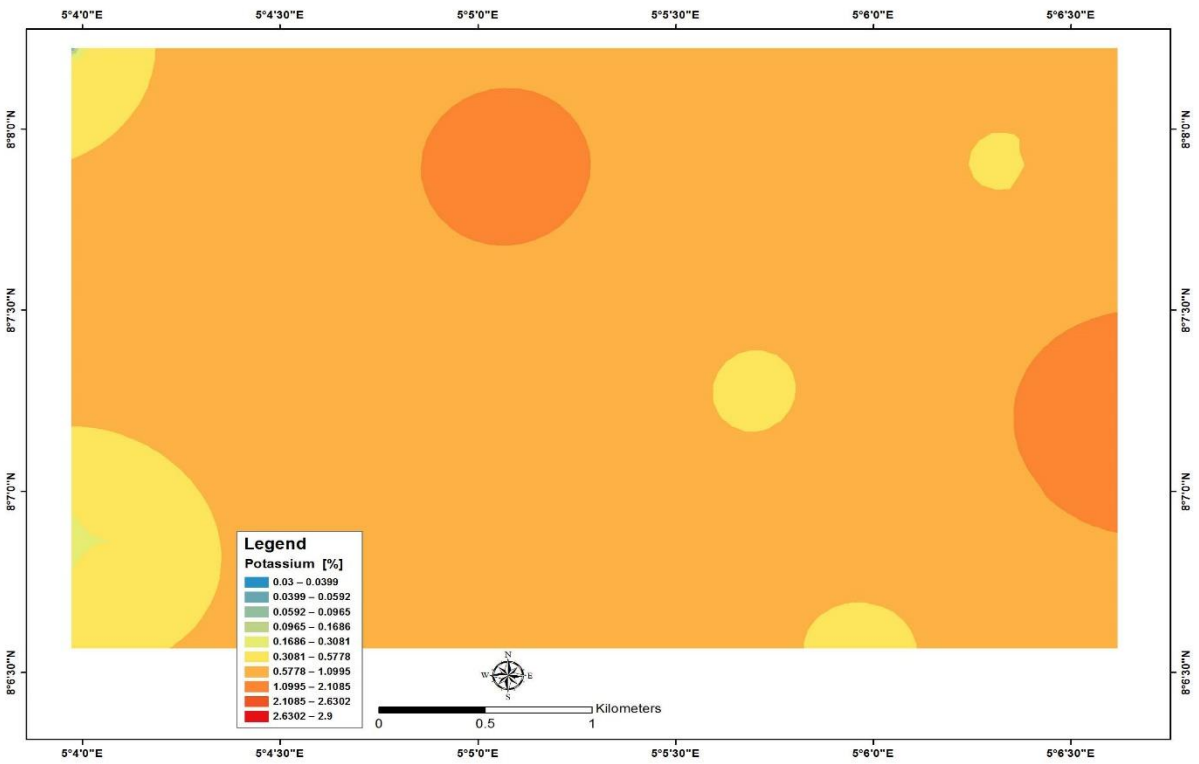


b)

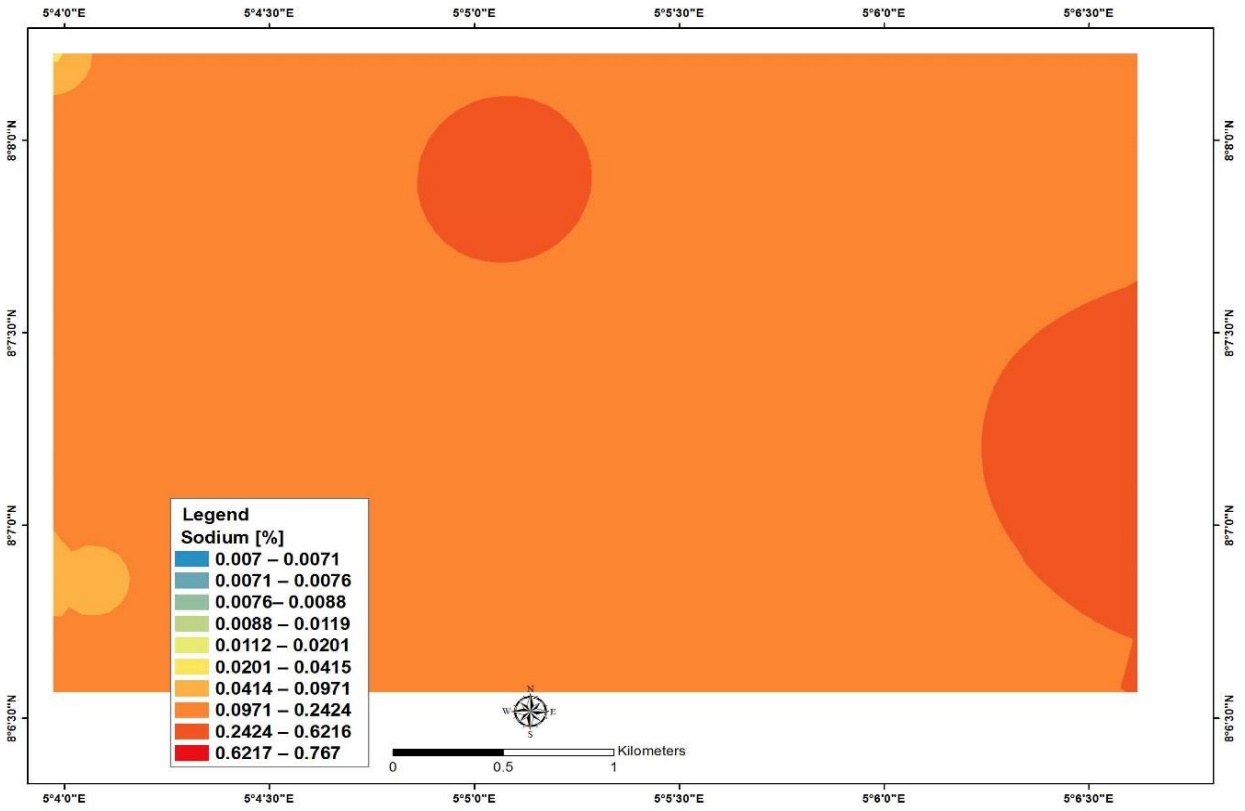


**Figure 4.35**: Geospatial maps of the concentration of: (a) potassium (K), and (b) sodium (Na) at Landmark University farm

a)

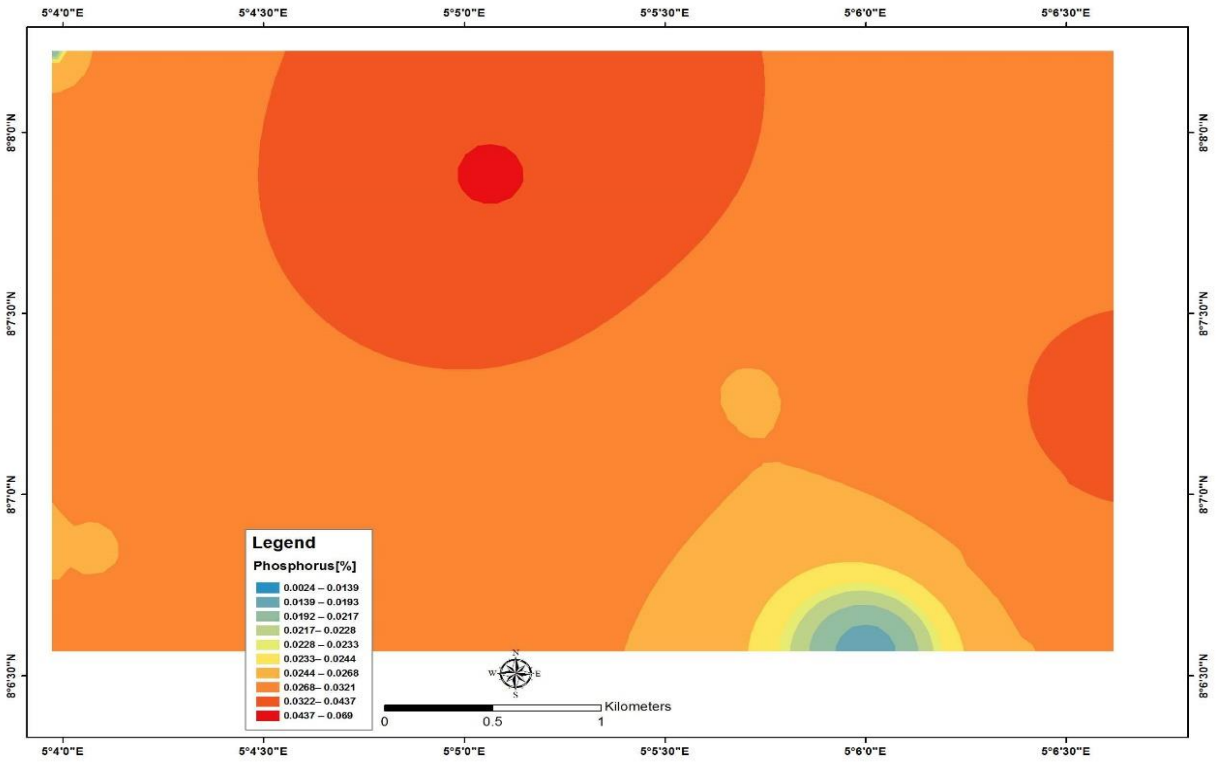


b)

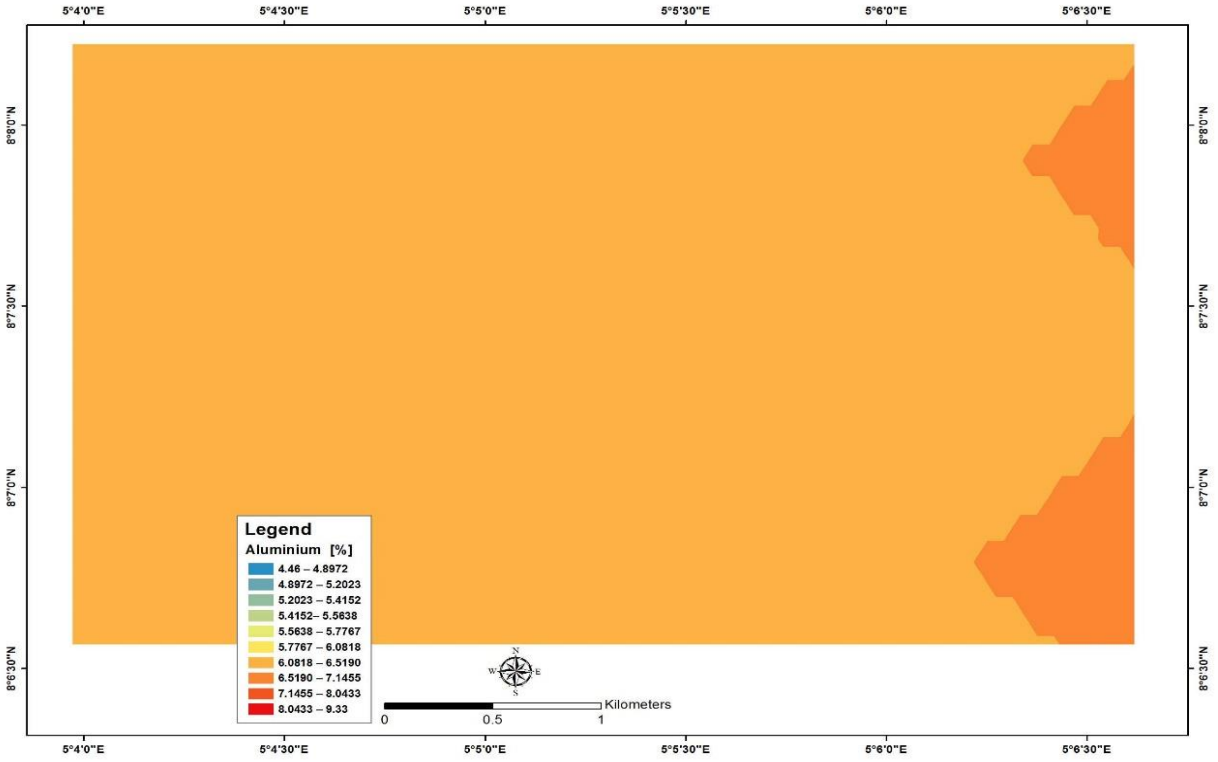


**Figure 4.36**: Geospatial maps of the concentration of: (a) phosphorus (P), and (b) aluminium (Al) at Landmark University farm

a)

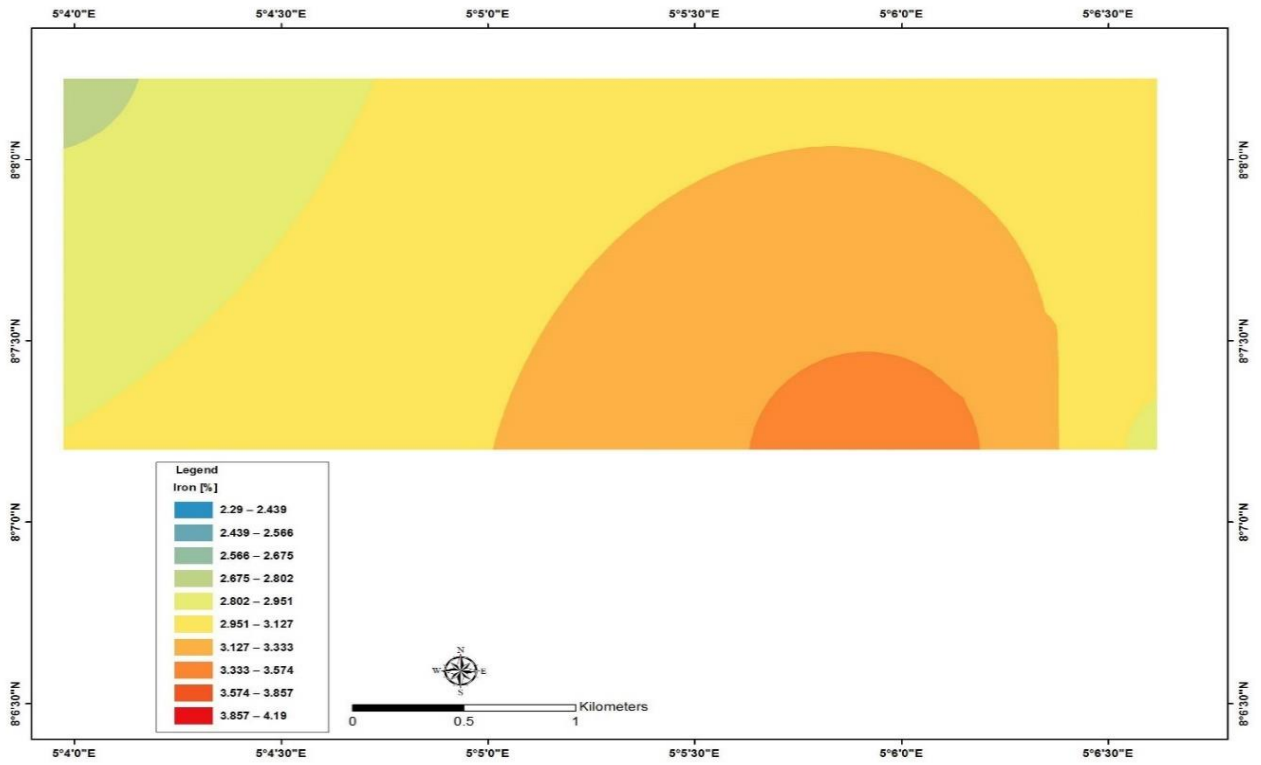


b)

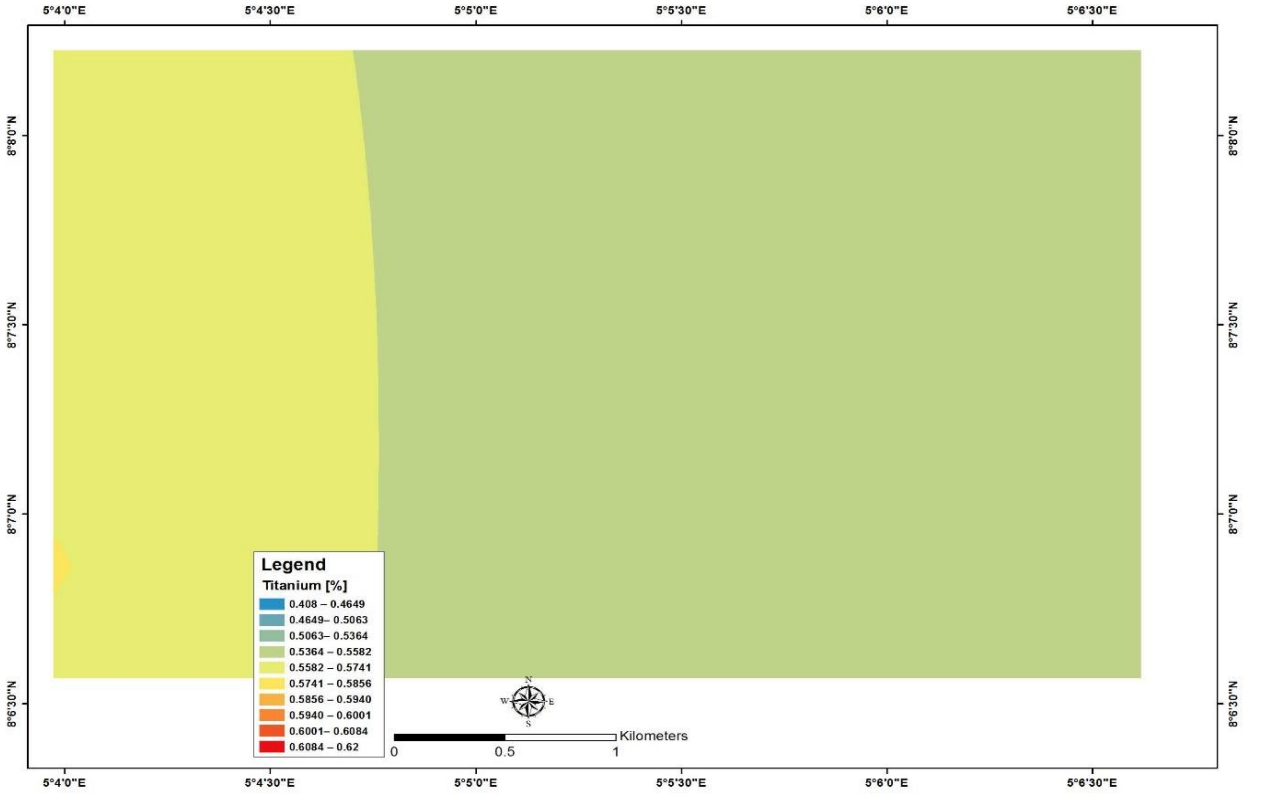


**Figure 4.37:** Geospatial maps of the concentration of: (a) Iron (Fe), and (b) Titanium (Ti) at Landmark University farm

## 4.5 Geostatistical Analysis of Geochemical Compositions

### 4.5.1 Major Elements or Macronutrients

The results of the geochemical analysis for macronutrients in the soil samples of the sites at Landmark University farm and Covenant University farm are presented in Tables 4.17 and 4.21, respectively. Statistical analysis of the macronutrients and micronutrients concentration, using the statistical package for social science (SPSS) version 23 for the two sites are presented in Tables 4.18 - 4.20 and Tables 4.22 - 4.24 respectively. The macro elements/nutrients analysed include calcium (Ca), phosphorus (P), magnesium (Mg), titanium (Ti), aluminium (Al), sodium (Na), iron (Fe) and potassium (K). The P-test for mean and Mann Whitney test for median were used for the comparison of the micro and macro elements concentrations in both farm sites. P value <0.05 indicates that there is correlation between two elements for comparison.

Table 4.18 presents the descriptive statistics of the macro elements at Landmark University farm. The close values of all mean (arithmetric, geometric, harmonic, quadratic) indicate that P, Ti and Al are evenly distributed with no significant extreme values in the study area. Other elements such as Ca, Mg, Na, Fe and K are unevenly distributed in the study area. The mean distribution of Ti at Landmark University is less than the median, this is responsible for the negative (-ve) value of the skewness. This negative value of Ti in Figure 4.19 further indicates that Ti is highly evenly distributed in the study area. Correlation result for Landmark University farm in Table 4.19 indicates that the p-values are less than 0.05 for Ca/Ti, P/Ti, Mg/Ti, Ti/Na and Ti/K. The negative (-ve) values in Table 4.19 mean that the pair elements (Ca/Ti, P/Ti, Mg/Ti, Ti/Na and Ti/K) are negatively correlated and Ti is negatively correlated with other elements except Al and Fe. The correlation result for Covenant University farm (Table 4.23) indicates that the p-values are less than 0.05 for Ca/Al, P/Na, Ti/Al, Al/Na, Al/K and Na/Fe. The highlighted values in Table 4.20 indicate that the p-value is less than 0.05 for Ca/P, Ca/Mg, Ca/Al, Ca/K, P/Mg, P/Al, P/Na, P/Fe, P/K, Mg/Al. Mg/Na, Mg/K, Al/Fe, Al/K and Na/K. All paired elements are significantly correlated with each other. All values less than 0.05 (this include 0.00 and other negative values) as presented in Figure 4.19 imply that the pair of the macro elements are either positively or negatively significantly correlated.

**Table 4.19:** Macro-nutrients concentrations at Landmark University farm

| Analytes (%) | Ca | P | Mg | Ti | Al | Na | Fe | K |
|---|---|---|---|---|---|---|---|---|
| MDL | 0.01 | 0.01 | 0.01 | 0.00 | 0.01 | 0.001 | 0.01 | 0.01 |
| L1 | 0.06 | 0.02 | 0.07 | 0.55 | 5.47 | 0.012 | 2.75 | 0.04 |
| L2 | 0.05 | 0.02 | 0.06 | 0.48 | 4.46 | 0.007 | 2.29 | 0.03 |
| L3 | 0.04 | 0.02 | 0.06 | 0.62 | 5.61 | 0.008 | 2.81 | 0.04 |
| L4 | 0.05 | 0.02 | 0.07 | 0.60 | 6.50 | 0.007 | 2.98 | 0.04 |
| L5 | 0.07 | 0.02 | 0.07 | 0.58 | 5.78 | 0.008 | 2.75 | 0.04 |
| L6 | 0.04 | 0.03 | 0.07 | 0.59 | 6.99 | 0.008 | 3.24 | 0.04 |
| L7 | 0.44 | 0.07 | 0.25 | 0.59 | 9.33 | 0.493 | 4.19 | 2.46 |
| L8 | 0.52 | 0.05 | 0.20 | 0.42 | 7.29 | 0.767 | 2.66 | 2.90 |

MDL – measurement detection limit

**Table 4.20:** Descriptive statistics of macro-elements concentrations at Landmark University farm

| Statistic | Ca | P | Mg | Ti | Al | Na | Fe | K |
|---|---|---|---|---|---|---|---|---|
| Arithmetic mean | 0.16 | 0.03 | 0.11 | 0.55 | 6.43 | 0.14 | 2.95 | 0.69 |
| Geometric mean | 0.09 | 0.03 | 0.09 | 0.55 | 6.29 | 0.02 | 2.91 | 0.11 |
| Harmonic mean | 0.06 | 0.03 | 0.08 | 0.54 | 6.16 | 0.01 | 2.87 | 0.05 |
| Quadratic mean | 0.24 | 0.04 | 0.13 | 0.56 | 6.58 | 0.32 | 3.00 | 1.34 |
| Median | 0.05 | 0.02 | 0.07 | 0.59 | 6.14 | 0.01 | 2.78 | 0.04 |
| SD | 0.19 | 0.02 | 0.07 | 0.07 | 1.48 | 0.29 | 0.56 | 1.22 |
| Skewness | 1.48 | 1.75 | 1.56 | -1.41 | 0.93 | 1.69 | 1.62 | 1.47 |

**Table 4.21:** Correlation matrix for macro-nutrients at Landmark University farm

| Element | P | Mg | Ti | Al | Na | Fe | K |
|---|---|---|---|---|---|---|---|
| Ca | 0.906 | 0.957 | -0.502 | 0.732 | 0.989 | 0.42 | 0.999 |
| P | | 0.987 | -0.156 | 0.895 | 0.844 | 0.744 | 0.914 |
| Mg | | | -0.281 | 0.855 | 0.908 | 0.646 | 0.961 |
| Ti | | | | 0.141 | -0.582 | 0.499 | -0.487 |
| Al | | | | | 0.669 | 0.894 | 0.746 |
| Na | | | | | | 0.315 | 0.988 |
| Fe | | | | | | | 0.438 |

**Table 4.22:** Significance table of macro-nutrients concentrations at Landmark University farm

| p value | P | Mg | Ti | Al | Na | Fe | K |
|---|---|---|---|---|---|---|---|
| Ca | **0.002** | **0.000** | 0.205 | **0.039** | **0.000** | 0.300 | **0.000** |
| P | | **0.000** | 0.712 | **0.003** | **0.008** | **0.034** | **0.001** |
| Mg | | | 0.500 | **0.007** | **0.002** | 0.084 | **0.000** |
| Ti | | | | 0.739 | 0.130 | 0.208 | 0.221 |
| Al | | | | | 0.070 | **0.003** | **0.034** |
| Na | | | | | | 0.448 | **0.000** |
| Fe | | | | | | | 0.278 |

**Table 4.23:** Macro-nutrients concentration at Covenant University farm

| Analytes (%) | Ca | P | Mg | Ti | Al | Na | Fe | K |
|---|---|---|---|---|---|---|---|---|
| C 1 | 0.06 | 0.05 | 0.07 | 0.35 | 7.63 | 0.01 | 10.13 | 0.23 |
| C 2 | 0.01 | 0.04 | 0.05 | 0.32 | 8.29 | 0.01 | 13.64 | 0.19 |
| C 3 | 0.02 | 0.05 | 0.05 | 0.35 | 8.01 | 0.01 | 13.8 | 0.15 |
| C 4 | 0.05 | 0.03 | 0.07 | 0.38 | 8.32 | 0.01 | 7.20 | 0.21 |
| C 5 | 0.02 | 0.04 | 0.06 | 0.35 | 8.56 | 0.01 | 9.15 | 0.23 |
| C 6 | 0.02 | 0.03 | 0.06 | 0.37 | 8.17 | 0.01 | 7.45 | 0.17 |
| C 7 | 0.07 | 0.02 | 0.06 | 0.27 | 3.32 | 0.71 | 2.42 | 0.53 |
| C 8 | 0.08 | 0.03 | 0.15 | 0.59 | 4.17 | 0.51 | 3.72 | 0.80 |
| C 9 | 0.18 | 0.07 | 0.39 | 0.99 | 7.59 | 0.21 | 11.71 | 0.75 |
| C 10 | 0.18 | 0.05 | 0.25 | 0.49 | 6.56 | 0.20 | 15.86 | 0.79 |

**Table 4.24:** Descriptive statistics of macro-elements at Covenant University farm

| Statistic | Ca | P | Mg | Ti | Al | Na | Fe | K |
|---|---|---|---|---|---|---|---|---|
| Arithmetic mean | 0.06 | 0.04 | 0.11 | 0.45 | 6.07 | 0.12 | 7.97 | 0.34 |
| Geometric mean | 0.04 | 0.03 | 0.08 | 0.43 | 5.60 | 0.02 | 6.11 | 0.23 |
| Harmonic mean | 0.03 | 0.03 | 0.07 | 0.41 | 5.06 | 0.01 | 4.32 | 0.12 |
| Quadratic mean | 0.08 | 0.04 | 0.14 | 0.49 | 6.46 | 0.24 | 9.29 | 0.43 |
| Median | 0.05 | 0.03 | 0.06 | 0.37 | 7.07 | 0.01 | 8.30 | 0.23 |
| SD | 0.05 | 0.02 | 0.09 | 0.18 | 2.28 | 0.22 | 4.96 | 0.26 |
| Skewness | 1.50 | 0.71 | 2.34 | 1.98 | -0.39 | 2.04 | 0.01 | 0.79 |

Table 4.25 gave the result of negatively correlated pair of elements Ca/Al, P/Na, Ti/Al, Al/Na, Al/K and Na/Fe at Covenant University farm, while the remainng paired element are positively correlated. The highlighted values in Table 4.25 imply that the p-value is less than 0.05 for Ca/Mg, Ca/Ti, Ca/K, P/Ti, P/Fe, Mg/Ti, Mg/K, Ti/K, Al/Fe and Na/K at Covenant University farm. Mann-Whitney median test (Table 4.27) showed that the median of Ti concentration at Landmark University farm and Covenant University farm are different but same for other macro elements analysed. The t-test (Table 4.27) showed that the mean distribution of Fe is different in both farm sites but the same for other elements analysed at the two farm sites.

**Table 4.25:** Correlation matrix of macro-elements at Covenant University farm

| Element | P | Mg | Ti | Al | Na | Fe | K |
|---|---|---|---|---|---|---|---|
| Ca | 0.333 | 0.879 | 0.623 | -0.126 | 0.363 | 0.177 | 0.734 |
| P | | 0.625 | 0.558 | 0.410 | -0.200 | 0.776 | 0.319 |
| Mg | | | 0.838 | 0.135 | 0.263 | 0.390 | 0.767 |
| Ti | | | | -0.059 | 0.085 | 0.118 | 0.587 |
| Al | | | | | -0.386 | 0.706 | -0.088 |
| Na | | | | | | -0.270 | 0.681 |
| Fe | | | | | | | 0.185 |

**Table 4.26:** Significance table of macro-elements concentrations at Covenant University farm

| p value | P | Mg | Ti | Al | Na | Fe | K |
|---|---|---|---|---|---|---|---|
| Ca | 0.245 | **0.000** | **0.017** | 0.668 | 0.203 | 0.544 | **0.003** |
| P | | **0.017** | **0.038** | 0.145 | 0.493 | **0.001** | 0.266 |
| Mg | | | **0.000** | 0.646 | 0.364 | 0.167 | **0.001** |
| Ti | | | | 0.841 | 0.772 | 0.688 | **0.027** |
| Al | | | | | 0.173 | **0.005** | 0.765 |
| Na | | | | | | 0.351 | **0.007** |
| Fe | | | | | | | 0.527 |

**Table 4.27:** Statistical comparison of macro-elements at Landmark University farm and Covenant University farm

| Element | T | p value | U score | p value |
|---|---|---|---|---|
| Ca | 1.31 | 0.231 | 105 | 0.3936 |
| P | -0.87 | 0.397 | 79.5 | 0.4128 |
| Mg | 0.03 | 0.974 | 108.5 | 0.2748 |
| Ti | 1.7 | 0.107 | 126 | **0.0222** |
| Al | 0.44 | 0.668 | 94 | 0.9185 |
| Na | 0.32 | 0.756 | 80 | 0.4325 |
| Fe | -3.74 | **0.002** | 67 | 0.0945 |
| K | 0.81 | 0.447 | 75 | 0.2601 |

## 4.5.2 Micro-nutrient orTrace Elements

The results of the geostatistical analysis of micro-nutrients in both farm sites (Covenant University and Landmark University farms) are presented in Tables 4.28 - 4.36. The following trace elements namely: cadmium (Cd), cobalt (Co), chromium (Cr), copper (Cu), manganese, Mn, nickel (Ni), lead (Pb), selenium (Se), molybdenum (Mo), strontium (Sr) and zinc (Zn) were statistically analysed in the soil samples of the two farm sites. Table 4.29 shows the result of the arithmetic, geometric, harmonic and quadratic means of the trace elements at Covenant University farm, revealed an even distribution of cadmium (Cd) at the farm site. The correlation result at Covenant University farm in Table 4.30 indicate that the following paired elements As/Se, As/Mo, Cd/Co, Cd-Cr, Cd/Mn, Cd/Ni, Cd/Pb, Cd/Zn, Co/Mn, Co/Ni, Co/Zn, Cr/Cu, Cr/Ni, Mn/Pb, Mn/Sr, Mn/Zn, Ni/Zn, Pb/Zn, Se/Mo and Sr/Zn are positively correlated.

The correlation result of micro/trace elements at Landmark University farm (Table 4.34) indicate positive correlation of the following paired elements As/Cr, As/Ni, Cu/Cd, Mo/Cd, Co/Mn, Co/Pb, Co/M0, Co/Sr, Co/Zn, Cr/Ni, Cu/Ni, Mn/Pb, Mn/Mo, Mn/Sr, Mn/Zn, Pb/Mo, Pb/Sr and Pb/Zn. Table 4.35 presents the signifance table for the correlation matrix of micro-nutrients at Landmark University farm and the result indicates p-values less than 0.05 for As/Cr, As/Ni, As/Pb, As/Sr, As/Zn, Cd/Cu, Cd/Mo, Co/Mo, Co/Pb, Co/Mo, Co/Sr, Co/Zn, Cr/Ni, Cr/Sr, Cu/Ni, Mn/Pb, Mn/Mo, Mn/Sr, Mn/Zn, Ni/Sr, Pb/Mo, Pb/Sr, Pb/Zn,, Mo/Zn, Sr/Zn. The negative values in Table 4.34 indicate that the mean of micro-elements

concentrations at Landmark University farm is smaller than the mean for the site at Covenant University farm. The median test (Mann-Whitney) in Table 4.36 shows that the median distribution of micro- elements analysed in both farm sites are different for As, Cd, Cr and Mo, however, it is the same for Co, Cu, Mn, Ni, Pb, Se, Sr and Zn.

**Table 4.28**: Micro-nutrients/trace elements at Covenant University farm

| Analytes (%) | As | Cd | Co | Cr | Cu | Mn | Ni | Pb | Se | Mo | Sr | Zn |
|---|---|---|---|---|---|---|---|---|---|---|---|---|
| C1 | 10.1 | 0.01 | 4.7 | 136.0 | 22.7 | 227.0 | 18.8 | 24.04 | 1.4 | 3.97 | 22.0 | 23.5 |
| C2 | 12.4 | 0.01 | 4.2 | 161.0 | 36.3 | 167.0 | 18.0 | 28.80 | 1.2 | 4.04 | 20.0 | 26.8 |
| C3 | 14.0 | 0.01 | 4.6 | 187.0 | 34.4 | 159.0 | 21.7 | 25.70 | 1.1 | 4.77 | 18.0 | 28.1 |
| C4 | 7.3 | 0.01 | 4.9 | 92.0 | 25.8 | 132.0 | 22.8 | 23.80 | 0.5 | 2.97 | 20.0 | 22.7 |
| C5 | 8.9 | 0.01 | 4.0 | 148.0 | 29.2 | 141.0 | 20.4 | 23.20 | 0.5 | 3.37 | 25.0 | 28.2 |
| C6 | 8.2 | 0.01 | 4.6 | 138.0 | 34.0 | 154.0 | 26.3 | 22.40 | 0.8 | 3.07 | 22.0 | 29.0 |
| C7 | 3.1 | 0.01 | 10.1 | 22.0 | 9.6 | 454.0 | 10.9 | 16.90 | 0.2 | 0.49 | 66.0 | 28.4 |
| C8 | 3.0 | 0.01 | 18.0 | 41.0 | 15.0 | 720.0 | 18.3 | 26.60 | 0.3 | 0.89 | 107.0 | 49.6 |
| C9 | 5.4 | 0.02 | 75.2 | 444.0 | 45.1 | 1897.0 | 240.0 | 39.60 | 1.0 | 2.31 | 66.0 | 83.6 |
| C10 | 9.70 | 0.02 | 59.4 | 193.0 | 36.4 | 2359.0 | 74.2 | 81.00 | 0.8 | 2.29 | 87.0 | 85.4 |

**Table 4.29:** Descriptive statistics for micro elements concentrations at Covenant University farm

| Analytes (%) | As | Cd | Co | Cr | Cu | Mn | Ni | Pb | Se | Mo | Sr | Zn |
|---|---|---|---|---|---|---|---|---|---|---|---|---|
| Arithmetic mean | 8.21 | 0.01 | 18.97 | 156.20 | 28.85 | 641.0 | 47.14 | 31.20 | 0.77 | 2.81 | 45.30 | 40.53 |
| Geometric mean | 7.34 | 0.01 | 9.60 | 119.52 | 26.51 | 346.9 | 28.21 | 28.19 | 0.67 | 2.36 | 35.88 | 35.63 |
| Harmonic mean | 6.38 | 0.01 | 6.56 | 82.60 | 23.61 | 235.92 | 22.23 | 26.36 | 0.55 | 1.75 | 29.62 | 32.45 |
| Quadratic mean | 8.91 | 0.01 | 31.19 | 191.14 | 30.61 | 1002.68 | 81.45 | 35.77 | 0.87 | 1.09 | 55.18 | 46.65 |
| Median | 8.55 | 0.01 | 4.80 | 143.00 | 31.60 | 197.00 | 21.05 | 24.87 | 0.80 | 3.02 | 23.50 | 28.30 |
| SD | 3.64 | 0.00 | 26.10 | 116.12 | 10.77 | 812.74 | 70.01 | 18.44 | 0.39 | 1.36 | 33.21 | 24.34 |
| Skewness | -0.05 | 1.78 | 1.76 | 1.75 | -0.51 | 1.65 | 2.84 | 2.63 | 0.01 | -0.49 | 0.91 | 1.45 |

**Table 4.30**: Correlation matrix for the pair of nutrients at Covenant University farm

| Elements | Cd | Co | Cr | Cu | Mn | Ni | Pb | Se | Mo | Sr | Zn |
|---|---|---|---|---|---|---|---|---|---|---|---|
| As | -0.096 | -0.253 | 0.196 | 0.541 | -0.220 | -0.211 | 0.155 | 0.743 | 0.928 | -0.664 | -0.242 |
| Cd | | 0.976 | 0.737 | 0.582 | 0.964 | 0.828 | 0.832 | 0.158 | -0.200 | 0.495 | 0.952 |
| Co | | | 0.734 | 0.500 | 0.959 | 0.883 | 0.735 | 0.074 | -0.325 | 0.602 | 0.972 |
| Cr | | | | 0.850 | 0.562 | 0.909 | 0.382 | 0.518 | 0.276 | -0.019 | 0.628 |
| Cu | | | | | 0.395 | 0.620 | 0.460 | 0.607 | 0.554 | -0.264 | 0.454 |
| Mn | | | | | | 0.717 | 0.869 | 0.015 | -0.375 | 0.691 | 0.980 |
| Ni | | | | | | | 0.397 | 0.214 | -0.133 | 0.302 | 0.776 |
| Pb | | | | | | | | 0.155 | -0.080 | 0.472 | 0.813 |
| Se | | | | | | | | | 0.779 | -0.484 | 0.011 |
| Mo | | | | | | | | | | -0.815 | -0.362 |
| Sr | | | | | | | | | | | 0.704 |

**Table 4.31**: Significance table for the correlation matrix at Covenant University farm (%)

| p value | Cd | Co | Cr | Cu | Mn | Ni | Pb | Se | Mo | Sr | Zn |
|---|---|---|---|---|---|---|---|---|---|---|---|
| As | 0.793 | 0.480 | 0.588 | 0.107 | 0.541 | 0.558 | 0.669 | **0.014** | **0.000** | **0.036** | 0.500 |
| Cd | | **0.000** | **0.015** | 0.077 | **0.000** | **0.003** | **0.003** | 0.662 | 0.579 | 0.146 | **0.000** |
| Co | | | 0.016 | 0.141 | **0.000** | **0.001** | **0.015** | 0.838 | 0.360 | 0.065 | **0.000** |
| Cr | | | | **0.002** | 0.091 | **0.000** | 0.276 | 0.125 | 0.440 | 0.958 | 0.052 |
| Cu | | | | | 0.259 | 0.056 | 0.181 | 0.063 | 0.096 | 0.462 | 0.188 |
| Mn | | | | | | **0.020** | **0.001** | 0.967 | 0.286 | **0.027** | **0.000** |
| Ni | | | | | | | 0.256 | 0.553 | 0.715 | 0.396 | **0.008** |
| Pb | | | | | | | | 0.669 | 0.826 | 0.168 | **0.004** |
| Se | | | | | | | | | **0.008** | 0.157 | 0.976 |
| Mo | | | | | | | | | | **0.004** | 0.305 |
| Sr | | | | | | | | | | | **0.023** |

**Table 4.32:** Micronutrients/trace elements at Landmark University farm

| Analytes (%) | As | Cd | Co | Cr | Cu | Mn | Ni | Pb | Se | Mo | Sr | Zn |
|---|---|---|---|---|---|---|---|---|---|---|---|---|
| L1 | 3.90 | 0.01 | 6.10 | 56.00 | 19.300 | 360.00 | 21.40 | 18.46 | 0.30 | 1.42 | 21.00 | 28.60 |
| L2 | 2.20 | 0.01 | 5.10 | 55.00 | 16.40 | 292.00 | 17.30 | 15.58 | 0.50 | 1.07 | 17.00 | 23.20 |
| L3 | 3.80 | 0.01 | 5.50 | 60.00 | 22.20 | 402.00 | 21.90 | 19.37 | 0.20 | 1.41 | 21.00 | 29.50 |
| L4 | 4.20 | 0.01 | 6.60 | 67.00 | 22.00 | 329.00 | 25.00 | 19.73 | 0.70 | 1.53 | 22.00 | 30.10 |
| L5 | 4.20 | 0.01 | 6.20 | 72.00 | 21.20 | 393.00 | 21.80 | 19.22 | 0.50 | 1.34 | 22.00 | 28.70 |
| L6 | 3.90 | 0.01 | 6.50 | 71.00 | 23.90 | 323.00 | 26.10 | 21.30 | 0.70 | 1.54 | 22.00 | 34.10 |
| L7 | 1.60 | 0.12 | 17.40 | 58.00 | 24.50 | 1137.00 | 19.70 | 49.90 | 0.20 | 2.16 | 167.00 | 156.90 |
| L8 | 0.80 | 0.09 | 9.70 | 38.00 | 16.80 | 554.00 | 12.30 | 36.50 | 0.70 | 1.48 | 212.000 | 96.00 |

0

**Table 4.33:** Descriptive statistics at Landmark University farm

| Analytes (%) | As | Cd | Co | Cr | Cu | Mn | Ni | Pb | Se | Mo | Sr | Zn |
|---|---|---|---|---|---|---|---|---|---|---|---|---|
| Arithmetic mean | 3.48 | 0.01 | 7.89 | 59.63 | 20.79 | 473.75 | 20.69 | 25.01 | 0.48 | 1.49 | 63.00 | 53.39 |
| Geometric mean | 3.17 | 0.01 | 7.26 | 58.62 | 20.59 | 427.31 | 20.22 | 23.13 | 0.42 | 1.47 | 36.01 | 41.43 |
| Harmonic mean | 2.80 | 0.01 | 6.85 | 57.49 | 20.38 | 398.91 | 19.68 | 21.79 | 0.37 | 1.45 | 26.57 | 35.38 |
| Quadratic mean | 3.69 | 0.01 | 8.76 | 60.50 | 20.98 | 541.19 | 21.09 | 27.37 | 0.52 | 1.52 | 97.12 | 69.78 |
| Median | 4.25 | 0.01 | 6.35 | 59.00 | 21.60 | 376.50 | 21.60 | 19.55 | 0.50 | 1.45 | 22.00 | 29.80 |
| SD | 1.34 | 0.05 | 4.09 | 10.97 | 3.03 | 279.71 | 4.37 | 11.89 | 0.22 | 0.31 | 79.02 | 48.03 |
| Skewness | -0.89 | 1.82 | 2.28 | -0.94 | -0.44 | 2.42 | -0.88 | 1.73 | -0.23 | 1.41 | 1.54 | 1.88 |

**Table 4.34**: Correlation matrix for the pair of nutrients at Landmark University farm

| Elements | Cd | Co | Cr | Cu | Mn | Ni | Pb | Se | Mo | Sr | Zn |
|---|---|---|---|---|---|---|---|---|---|---|---|
| As | -0.82 | -0.61 | 0.82 | 0.41 | -0.58 | 0.87 | -0.72 | -0.002 | -0.27 | -0.87 | -0.74 |
| Cd | | 0.69 | 0.43 | 0.80 | 0.69 | 0.46 | 0.53 | -0.42 | 0.85 | 0.12 | 0.53 |
| Co | | | -0.26 | 0.38 | 0.98 | -0.27 | 0.97 | -0.31 | 0.91 | 0.77 | 0.98 |
| Cr | | | | 0.67 | -0.25 | 0.90 | -0.42 | 0.03 | 0.01 | -0.71 | -0.43 |
| Cu | | | | | 0.39 | 0.73 | 0.23 | -0.25 | 0.69 | -0.12 | 0.25 |
| Mn | | | | | | -0.21 | 0.95 | -0.46 | 0.88 | 0.73 | 0.96 |
| Ni | | | | | | | -0.41 | 0.01 | 0.10 | -0.71 | -0.43 |
| Pb | | | | | | | | -0.22 | 0.86 | 0.89 | 0.99 |
| Se | | | | | | | | | -0.31 | 0.03 | -0.26 |
| Mo | | | | | | | | | | 0.57 | 0.84 |
| Sr | | | | | | | | | | | 0.88 |

**Table 4.35**: Significance table for the correlation matrix at Landmark University farm

| p value | Cd | Co | Cr | Cu | Mn | Ni | Pb | Se | Mo | Sr | Zn |
|---|---|---|---|---|---|---|---|---|---|---|---|
| As | 0.562 | 0.107 | **0.012** | 0.314 | 0.130 | **0.050** | **0.046** | 0.995 | 0.508 | **0.050** | **0.038** |
| Cd | | 0.060 | 0.289 | **0.016** | 0.058 | 0.256 | 0.179 | 0.304 | **0.008** | 0.801 | 0.174 |
| Co | | | 0.530 | 0.352 | **0.000** | 0.512 | **0.000** | 0.452 | **0.002** | **0.025** | **0.000** |
| Cr | | | | 0.070 | 0.550 | **0.002** | 0.310 | 0.976 | 0.976 | **0.048** | 0.294 |
| Cu | | | | | 0.337 | **0.040** | 0.510 | 0.547 | 0.059 | 0.782 | 0.556 |
| Mn | | | | | | 0.499 | **0.000** | 0.249 | **0.004** | **0.041** | **0.000** |
| Ni | | | | | | | 0.311 | 0.984 | 0.808 | **0.048** | 0.284 |
| Pb | | | | | | | | 0.605 | **0.007** | **0.003** | **0.000** |
| Se | | | | | | | | | 0.454 | 0.950 | 0.539 |
| Mo | | | | | | | | | | 0.144 | **0.009** |
| Sr | | | | | | | | | | | **0.004** |

**Table 4.36:** Statistical comparison between the site at Landmark University farm and Covenant University farm

| Element | T | p value | U score | p value |
|---|---|---|---|---|
| As | -3.80 | **0.003** | 46 | **0.009** |
| Cd | 17.42 | **0.000** | 116 | **0.000** |
| Co | -1.32 | 0.219 | 85 | 0.450 |
| Cr | -2.62 | **0.028** | 51 | **0.030** |
| Cu | -2.26 | **0.048** | 54 | 0.056 |
| Mn | -0.61 | 0.556 | 87 | 0.351 |
| Ni | -1.19 | 0.264 | 73 | 0.824 |
| Pb | -0.86 | 0.402 | 58 | 0.120 |
| Se | -2.06 | 0.059 | 56.5 | 0.091 |
| Mo | -2.98 | **0.014** | 52 | **0.037** |
| Sr | 0.59 | 0.570 | 74 | 0.894 |
| Zn | 0.69 | 0.508 | 90 | 0.230 |

## 4.6 Other Soil Properties from Laboratory Analysis

### 4.6.1 Soil Bulk Density and Porosity

The results of the soil porosity and bulk density at Landmark University farm and Covenant University farm carried out in the Covenant University geotechnical laboratory are presented in Tables 4.37 and 4.38, respectively**.** The soil bulk density at Landmark University farm ranged from $0.13\, g/cm^3$ to $0.16\ g/cm^3$, while the soil bulk density of the site at Covenant University ranged from $0.13\ g/cm^3$ to $0.15\ g/cm^3$. The percentage void space or porosity at Landmark University farm ranged from 0.93% to 0.95%, while the soil porosity at Covenant University farm is 0.95% for all the soil samples.

### 4.6.2 Soil Moisture Content

The geotechnical laboratory analysis results of the soil moisture content (SMC) at Landmark University and Covenant University farms are presented in Tables 4.39 and 4.40. The SMC at Landmark University farm ranged from 8.08% to 15.46%, while the SMC at Covenant University farm ranged from 7.86% to 13.97%.

**Table 4.37:** Bulk density and percentage void test at Landmark University farm

| SAMPLE NO | L9 | L10 | L11 | L12 | L13 | L14 | L15 | L16 |
|---|---|---|---|---|---|---|---|---|
| Mass of Empty Can (g) | 18.3 | 18.3 | 18.3 | 18.3 | 18.3 | 18.30 | 18.3 | 18.3 |
| Diameter of the can (CM) | 6.00 | 6.00 | 6.00 | 6.00 | 6.00 | 6.00 | 6.00 | 6.00 |
| Height of the Can (cm) | 6.00 | 6.00 | 6.00 | 6.00 | 6.00 | 6.00 | 6.00 | 6.00 |
| Volume of the Can (g/cm3) (cm3) | 169.71 | 169.71 | 169.71 | 169.71 | 169.71 | 169.71 | 169.71 | 169.71 |
| Mass of Loosened Soil + Can (g) | 36.90 | 37.50 | 38.0 | 38.50 | 35.70 | 37.40 | 39.10 | 39.10 |
| Mass of Densed Soil + Can (g) | 40.70 | 40.90 | 42.0 | 45.50 | 41.30 | 40.40 | 44.80 | 41.80 |
| Mass of Loosed Soil Only (g) | 18.60 | 19.20 | 19.70 | 20.20 | 17.40 | 19.10 | 20.80 | 20.80 |
| Mass of Densed Soil Only (g) | 22.40 | 22.60 | 23.70 | 27.20 | 23.00 | 22.10 | 26.50 | 23.50 |
| Density of Loosened Soil (g/cm3) | 0.11 | 0.11 | 0.12 | 0.12 | 0.10 | 0.11 | 0.12 | 0.12 |
| Bulk Density of the Soil (g/cm3) | 0.13 | 0.13 | 0.14 | 0.16 | 0.14 | 0.13 | 0.16 | 0.14 |
| Soil Porosity (%) | 0.95 | 0.95 | 0.95 | 0.94 | 0.95 | 0.95 | 0.94 | 0.95 |

**Table 4.38:** Soil bulk density and percentage void at Covenant University

| Sample No | C11 | C12 | C13 | C14 | C15 | C16 | C17 | C18 | C19 | C20 |
|---|---|---|---|---|---|---|---|---|---|---|
| Mass of Empty Can (g) | 18.30 | 18.30 | 18.30 | 18.30 | 18.30 | 18.30 | 18.30 | 18.30 | 18.30 | 18.30 |
| Diameter of the can (CM) | 6.00 | 6.00 | 6.00 | 6.00 | 6.00 | 6.00 | 6.00 | 6.00 | 6.00 | 6.00 |
| Height of the Can (cm) | 6.00 | 6.00 | 6.00 | 6.00 | 6.00 | 6.00 | 6.00 | 6.00 | 6.00 | 6.00 |
| Volume of the Can (g/cm3) | 169.71 | 169.71 | 169.71 | 169.71 | 169.71 | 169.71 | 169.71 | 169.71 | 169.71 | 169.71 |
| Mass of Loosened Soil + Can (g) | 36.60 | 36.20 | 36.90 | 37.70 | 37.20 | 35.90 | 37.60 | 36.20 | 40.90 | 37.80 |
| Mass of Densed Soil + Can (g) | 40.40 | 41.80 | 41.90 | 42.10 | 41.50 | 42.00 | 43.40 | 42.40 | 43.90 | 41.80 |
| Mass of Loosed Soil Only (g) | 18.30 | 17.90 | 18.60 | 19.40 | 18.90 | 17.60 | 19.30 | 17.90 | 22.60 | 19.50 |
| Mass of Densed Soil Only (g) | 22.10 | 23.50 | 23.60 | 23.80 | 23.20 | 23.70 | 25.10 | 24.10 | 25.60 | 23.50 |
| Density of Loosened Soil (g/cm3) | 0.11 | 0.11 | 0.11 | 0.11 | 0.11 | 0.10 | 0.11 | 0.11 | 0.13 | 0.11 |
| Bulk Density of the Soil (g/cm3) | 0.13 | 0.14 | 0.14 | 0.14 | 0.14 | 0.14 | 0.15 | 0.14 | 0.15 | 0.14 |
| Soil Porosity (%) | 0.95 | 0.95 | 0.95 | 0.95 | 0.95 | 0.95 | 0.94 | 0.95 | 0.94 | 0.95 |

**Table 4.39**: Soil moisture content (laboratory) for the site at Landmark University farm

| **Sample No** | L9 | L10 | L11 | L12 | L13 | L14 | L15 | L16 |
|---|---|---|---|---|---|---|---|---|
| Mass of empty can -WI (g) | 35.8 | 34.5 | 32.1 | 33.2 | 35.1 | 35.3 | 36 | 35.7 |
| Mass of Can + Moist Soil W2 (g) | 44.9 | 47.2 | 47.4 | 53.2 | 45.8 | 50.1 | 52.9 | 50.8 |
| Mass of Can + Dried Soil W3 (g) | 43.8 | 45.5 | 45.6 | 51.1 | 45 | 48.5 | 51.4 | 48.9 |
| Mass of Moisture (W2- W3) (g) | 1.1 | 1.7 | 1.8 | 2.1 | 0.8 | 1.6 | 1.5 | 1.9 |
| Mass of Dried Sample (W3 – W1) (g) | 8 | 11 | 13.5 | 17.9 | 9.9 | 13.2 | 15.4 | 13.2 |
| Moisture Content % (W2-W3/W3-W1) | 13.75 | 15.46 | 13.33 | 11.73 | 8.08 | 12.12 | 9.74 | 14.39 |

L – Sample location

**Table 4.40:** Soil moisture content (laboratory) for the site at Covenant University farm

| Sample No | C11 | C12 | C13 | C14 | C15 | C16 | C17 |
|---|---|---|---|---|---|---|---|
| Mass of empty can -WI (g) | 34.2 | 33.4 | 32.9 | 35.9 | 33.4 | 33.6 | 36.2 |
| Mass of Can + Moist Soil W2 (g) | 48.8 | 49.3 | 53.1 | 50.7 | 48.7 | 48.5 | 51.7 |
| Mass of Can + Dried Soil W3 (g) | 47.3 | 47.6 | 50.7 | 51.9 | 49.1 | 47.6 | 49.8 |
| Mass of Moisture (W2-W3) (g) | 1 | 1.7 | 2.4 | 2 | 1.6 | 1.1 | 1.9 |
| Mass of Dried Sample (W3 – W1) (g) | 13.1 | 14.2 | 17.8 | 16 | 15.7 | 14 | 13.6 |
| Moisture Content % (W2-W3/W3-W1) | 11.45 | 11.97 | 13.48 | 12.5 | 10.19 | 7.86 | 13.97 |

# CHAPTER FIVE
# DISCUSSION

## 5.1 Soil Profile Delineation Using Geoelectrical Resistivity Imaging

Electrical resistivity method has been applied to aid precision agriculture in the study area. Soil properties variability has been characterised using electrical resistivity contrast in soils which reflects distinct soil properties. The application of electrical resistivity to agricultural fields can be used to characterise soil parameters including soil texture, moisture and soil salinity. The results from this study showed the potential of using electrical resistivity to measure soil water content, soil texture, and soil salinity. Soil profile is easily delineated to a depth of about 2 m depth and zones of high salinity within the field were easily delineated with electrical resistivity.

### 5.1.1 Geoelectrical Resistivity Imaging at Covenant University Farm

The resistivity models from the VES data at Covenant University farm reveals the nature of the topsoil. The topsoil is composed of sandy clay that extends to a depth of 2.0 m with model resistivity of 158 Ωm and thickness of 2.0 m. The root zone for most tropical crops lies within the topsoil except perennial crops that have depths of over 200 cm (Fan, McConkey, Wang & Jansen, 2016). Sandy clay and clayey sand are the predominant soil types of the root zone in this area. A similar work on soil electrical resistvity measurements in Ado-Ekiti, southwestern Nigeria indicated that the topsoil with resistivity values that ranged from 210 - 750 $\Omega m$ were classified as clayey sand (Eluwole, Olorunfemi & Ademilus, 2018).

The two-dimension (2D) electrical resistivity inverse models for the site at Covenant Uniiversity farm indicate that the soil profile of the topsoil is sandy clay and lateriric clay. The model resisitivty values of the lateritic clay unit ranged from a minimum of 26 Ωm to a maximum of 248 Ωm. The depth of investigation (≥ 2 m) covers the upper root zone of major crops grown in the area. The change in resistivity values observed across the traverses is attributed to variability in the degree of compaction, and amount of moisture content and organic matter content in the soil. The lateritic clay unit of the topsoil is composed of clayey-

silty and sandy soils. The lateritic clay in the upper layer in the study area has shades of rusty red to brown coloration which depicts its high iron oxide content. Lateritic clay and sandy clay seem to be prevalent in the topsoil and depth of investigation. The lateritic clay unit contributes significantly to the observed low resistivity for the topsoil of the site at Covenant University farm. The high resistivity in the topsoil typically depicts salinity but the geochemical and satellite imagery analysis have corroborated the findings that clay content in the upper soil zone was responbilble for it.

A laterally continuous high resistivity unit with resistivity ranging between 1977 and 5418 Ωm underlain the clayey sand layer. Information from drilled boreholes and hand dug wells around the area from previous study indicates that the highly resistive layer is Kaolinitic clay intercalated with phosphate (Aizebeokhai and Oyeyemi, 2014). A less resistive clayey sand unit with resistivity ranging from 400 to 592 Ωm underlain this highly resistive unit and this trend is observed at all sounding points. This relatively low resistivity unit is termed a saturated low yield aquifer (Aizebeokhai and Oyeyemi, 2014).

### 5.1.2 Geoelectrical Resistivity Imaging at Landmark University Farm

The lithologic units inferred from the geoelectric parameters at Landmark University farm are presented in Table 4.2. The results revealed the heterogeneity of the topsoil (stony zone) consisting of gravel, sand and lateritic gravelly sand with variable thickness of ≤ 2.7 m. The topsoil resistivity ranged from 614 to 1075 Ωm and delineated depth is ≤ 2 m; this depth range accommodates the root zone for most crops planted in this area. The uppermost margin of the soil profile is composed of loose, poorly sorted sandy gravel with angular to sub-angular shape and a thickness of 0.5 - 1.0 m within the soil horizon. The clay component is mainly concentrated around the upper section of the slope. Both physical and chemical weathering are prevalent in the area as indicated by the heterogeneous assemblage of transported loose sandy gravel, and the basal ferruginized lateritic units.

The two-dimension (2D) resistivity models at Landmark University farm are presented in Figures 4.8 - 4.14. The application of 2D electrical resistivity imaging provides useful information about the subsurface conditions along the profiles of interest in the study area.

High resistivity values were observed at Landmark University farm and this corresponds with the gravel and sandy constituent of the farm site. Amaya, Dahlin, Barmen and Rosberg (2016) attributed the high resistivity values observed in the site at Punata, Bolivia to gravelly and sand constituents in the area. The resistivity values of the 2D resistivity models at Landmark University farm ranged from 101 to 3149 Ωm in all the traverses. The depth of investigation covered the upper root zone of ≥ 2 m. The change in resistivity values observed is due to the differences in the degrees of compaction, moisture content and organic matter. The topsoil, as observed at Landmark University farm, is heterogeneous in nature with a mixture of clayey sand, gravelly sand and sand in varying proportion. Sandy and gravelly sands are the dominant soil delineated in the site based on the result of the geoelectrical investigation. Traverses 17 - 19 (Figures 4.18 and 4.19) are orthogonal to the other traverses (Traverses 1 - 16).

The geoelectrical resistivity images at Landmark University farm revealed that sand is the most abundant soil in the area, accounting for over half of the entire soil constituents. By virtue of the sandy nature of the soil in the study area, the crop production capacity can only be limited by the inability of the soil to retain nutrient as previously reported by Basga and Nguetnkam (2015), Tellez, Lopez, Aragon and Zayas (2016), and Basga et al. (2018). However, Basga et al. (2018) showed that soil nutrients can be restored and acidity reduced in sandy soils by the adoption of an agroforestry system known as tree planting fallowing.

The soils at Landmark University farm have weak structure with low clay content and high sand content (>70 %). The topsoil of the area, as suggested by its resistivity distribution, is composed of poorly sorted sandy gravel, sand and clay sand; the soil consistuents makes the soil of the area slightly resistive to erosion as noted by Jiang and Soga (2019). However, the farm area has a steeply/undulating topography which makes the soil of the area vulnerable to erosion but a good understanding of the soil properties and land features will allow for optimum utilisation of the soil. Due to the high percentage of pore drainage in sandy gravelly soils, dissolved substances and water are easily lost to deeper layers in the soils or transported to the groundwater (Eswaran, Vearasilp, Reich & Benroth, 2006).

Landmark University farm is a high relief area with elevation ranging from 566 - 574 m above the sea level as revealed by the topographic information in the electrical resistivity images of

the site incorporated (Figures 4.10 - 4.19). The soil of the study area is coarse in nature, a peculiar characteristic of sandy soils usually associated with the parent granitic rocks as previously noted by Zhao, Zhang, Wen-Jun and Gong (2005) and Rabitz, Hallaus, Pham, Tu and Mentler (2019). The high resistivity values observed (Table 4.2) revealed low water content in the soil of the study area even though the field work was carried out during the rainy season (July to August, 2018) and the dry period (December to January, 2019). Yetbarek and Ojha (2020) indicated that soil moisture content is a major factor controlling plant growth and soil erosion. Soil as a porous and non-conductive particle conducts electricity as a result of the electrolytes solution attached to its surface matrix as established by Aaltonen (1997), and Benderitter and Scott (1999). Therefore, continuous irrigation is required at Landmark University farm during the growing season for efficient crop production.

Other researchers have reported the importance of electrical resistivity in the monitoring of soil dynamics from surface to subsurface depths (Mostafa, Anwar & Radwan, 2017). However, soil dynamics monitoring require a combination of other geotechnical methods, and accessibility to equipment in this part of the globe is limited. The gravelly sand is a coarse soil with bigger particle size than fine sand, but has less porosity and permeability. Electrical resistivity/conductivity methods have served as an indirect method used for soil structure characterisation as reported by Kibria, Hossaini and Khan (2018). So, the exceptionally high electrical resistivity values in some part of the farm have revealed that soil salinity is at minimal and tolerant level in the site of Landmark University farm. Low resistivity indicates high soil salinity, that is the concentration of major dissolved ions such as $Ca^{2+}$, $Mg^{2+}$, $Na^{+}$, and $SO_4^{2-}$ in soil pores as noted by Visconti and De Paz (2016). Visconti and De Paz (2016) showed that fertilization practices, plant transpiration and evaporation processes build up dissolved ions in the soil and as soil salinity increases, soil pore water decreases. Soil salinity at Landmark University farm is however at minimum level as at the time of the field work. In some cases, at minimal level, salinity can improve soil structure but its negative impact on plant growth and crop yield can be devastating as noted by Warrence, Bauder and Pearson (2003). At high levels, salinity can be potentially hazardous to plants (Machado & Serrahelro, 2017).

## 5.2 Satellite Imagery and GIS Evaluation of Covenant University Farm Site

### 5.2.1 Soil Temperature Variations

Previous studies have indicated that there is a link between increase in soil temperature and nitrogen and organic carbon release rate (Jat et al., 2019; Xu, Qu, Hao, Zhu & Gutenberg, 2020), these play a vital role in agricultural production. The germination of many types of seeds depends largely on the soil's upper layer temperature (Zeynoddin, Ebtehaj and Bonakdari, 2020). However, soil temperature's spatial and temporal trends at various depths is less studied in this part of the globe. Figures 4.28 and 4.29 present the monthly soil temperature (ST) trend for 2017- 2019 at Covenant University farm. The result indicates that Covenant University farm site experienced soil temperature variations of 297 - 314 K between 2017 – 2019. Soil temperature variations at depth 0 – 10 cm for 2017 and 2018 in this farm site were higher than the ST variations at depth of 10 – 40 cm in the subsurface as shown in Figures 4.28 and 4.29. This indicates that soil temperature variation decreases with depth at the upper soil zones and ST fluctuates throughout the year in relation to the above-ground temperature. Moreso, Pepper and Brusseau (2019) have reported that soil temperature below the upper few meters of the subsurface remains constant throughout the year.

The highest ST of 314 K was observed between March and April, 2017 and 2018 while ST for 2019 peaked at 308 K between February and April. Soil temperature in this farm site was stable at 299 – 302 K between July and September for the three (3) years studied. This indicates that in the rainy months of the year (June – September) ST values can germinate seeds and most organisms still thrive in the study site. The ST trend for the years studied is from low to high from January to May (296 – 314 K) and from high to low (314 - 296 K) from October to January of the next year.

### 5.2.2 Soil Moisture Content

The wet periods as reported by Beesley, Moreno-Jimenez, Clemente, Lepp and Dicksinson (2010) and Gou et al. (2015) enhance high mobility of certain trace elements such as cadmium, zinc and arsenic. Garg, Munoth & Goyal (2016) and Zeri et al. (2018) emphasised the need for continuous soil moisture content determination in farmland to ensure effective irrigation water management and soil erosion control. As shown in Figure 4.32, at depth 0 – 10 cm, the soil

moisture content (SMC) for Covenant University farm for 2017 ranged from 23 $m^3/m^3$ to 39 $m^3/m^3$ between January and July. SMC gradually drops to 28 $m^3/m^3$ in August, 2017 and then to 26 $m^3/m^3$ in September of the same year. There was an increased SMC of 32 $m^3/m^3$ in October, 2017 and then a decline to 26 $m^3/m^3$ in December, 2017. The SMC at depth of 10 – 40 cm ranged from 75 $m^3/m^3$ to 112 $m^3/m^3$ and was obviously greater than the upper soil zone (0 – 10 cm) as water has seeped into the soil at this layer. For 2018, SMC from January to December followed same trend for both phases (depths at 0 – 10 and 10 – 40 cm) studied. However, SMC reduced significantly in 2018 from 113 $m^3/m^3$ to 109 $m^3/m^3$ at the peak level. The periods of low SMC are the dry periods of the year that is, January to March while high SMC are noticeable in the rainy months (June – September) of the year. The SMC at 0 – 10 cm depth for the three years (2017 -2019) studied are somewhat the same ranging from 22 $m^3/m^3$ to 39 $m^3/m^3$ throughout the months. At depth 10 – 40 cm underground, SMC in 2018 peaked at 109 $m^3/m^3$ as against 113 $m^3/m^3$ and 112 $m^3/m^3$ of 2017 and 2019 respectively.

This result at Covenant University farm is similar to the results of Yetbarek and Ojha (2020) on spatio-variability study of soil moisture content in a cropped agricultural plot in Ganga Basin, India. However, the soil moisture dynamics of Yetbarek and Ojha (2020) was analysed in response to an imposed evapotranspiration and irrigation/rainfall under rice and wheat crops farm.

### 5.2.3 Soil Salinity

The results have revealed that salt on the farm is sparsely distributed and not entirely on the whole farm site As shown in Figure 4.36b, the soil salinity map of the site at Covenant University farm exhibited a variation of high and low salinity across the farm site. The high salinity is pronounced towards the northern and southern parts of the farm area. The center part of the farm however, exhibited low salinity. Globally, soil salinity is a major threat to food security and therefore be monitored and controlled in agricultural soils in other to achieve sustainable agricultural production.

## 5.3 Satellite Imagery and GIS Evaluation of Landmark University Farm Site

### 5.3.1 Soil Temperature Variations

The high seasonal temperature experienced in the northern part of Nigeria can be better utilized in sustainable agricultural practices with adequate soil temperature studies. Increased soil temperature plays a significant role in the soil's physical, chemical and biological processes (Onwuka & Mang, 2018). As shown in Figures 4.30 and 4.31, the monthly soil temperature for 2017 - 2019 at depth 0 – 10 cm in the site at Landmark University farm ranged from 289 K to 317 K, while the ST for depth at 10 – 40 cm ranged from 295 K to 305 K. ST abruptly declined to 294 K from June to October of the years studied. In November and December, 2017, soil temperature increased to 309 K and further to 312 K respectively. Soil temperature in this farm site have a sinusoidal pattern with the highs (305 – 317 K) recorded from January to March and the lows (294 K to 302 K) recorded from June to October of the three (3) years studied. There was a steady ST of 294 K and 295 K between June and September of the three (3) years studied at depth 0 – 10 cm and 297 K at depth 10 – 40 cm in the subsurface as shown in Figures 4.30b and 4.31.

### 5.3.2 Soil Moisture Content

The monthly SMC for the years 2017 – 2019 at Landmark University presented in Figures 4.34 and 4.35 ranged from 10 $m^3/m^3$ to 39 $m^3/m^3$ at depth 0 – 10 cm. At the depth of 10 – 40 cm SMC for January and February 2017 – 2019 was 10 $m^3/m^3$. SMC ranged from 17 $m^3/m^3$ to 23 $m^3/m^3$ between March and May, 2017. In the early planting season of 2018 (January - April), Landmark University farm exhibited low soil moisture content of 10 – 17 $m^3/m^3$ as a result of low or no rainfall. A similar trend of monthly soil moisture content was exhibited in 2019. SMC ranged from 25 $m^3/m^3$ to 38 $m^3/m^3$ from June to November for the three (3) consecutive years studied. SMC at depth of 10 – 40 cm at Landmark University farm ranged from 60 $m^3/m^3$ to 110 $m^3/m^3$, values at the subsurface were higher than at the surface level as in Figure 4.35. Ren, Li, Liu, Cheng and Xu (2018) reported that soil moisture can be independent of evapotranspiration especially at very low soil moisture content. The same observation has been noted by Ambrosone, Matese, Gennaro, Gioli, Tudoroiu, Genesio et al. (2020). The SMC at Landmark University farm has revealed the impact of soil water scarcity

on crop yield and to enable irrigated agriculture, optimize rainfed crop yield and manage water resource for agricultural purposes in the study area.

### 5.3.3 Soil Salinity

The evaluated soil salinity result at Landmark University farm indicate high salt content in the farm site as shown in Figure 4.37. The salt covered the entire central portion of the farm area whle the extreme portions of the farm has low salinity. There were indications that the satellite imagery must have been captured after the fertilization of the farm area which may have contributed to the high salinity recorded at the centre of the farm. Soil salinity covered about 75% of the farm area. Excess chemical fertilizers on the farm site can also increase soil salinity.

## 5.4 Geochemical Evaluation at Covenant University Farm

The results of the geochemical composition of the analysed soil samples in this site indicated that the accumulation of trace/non-essential elements is in moderate to high concentration. The concentration of some toxic elements including arsenic (As), lead (Pb), chromium (Cr) and manganese (Mn) in the study area is higher than the recommended WHO/FAO (2001) and EU (2002) permissible limits. The geochemical analysis showed that the presence of rare earth elements (REEs) in the soil of this farm sites may act as pollutants in the study area. Rare elements have been tagged as the emerging soil pollutants by several researchers (Khan et al., 2017; Qin et al., 2019; Li, Zhing & Chao, 2020).

### 5.4.1 Trace Elements/Micro Nutrients

As shown in Table 4.3, trace elements including arsenic, cadmium, chromium, cobalt, copper, lead, selenium nickel and molybdenum were detected in varying concentrations at Covenant University farm. Arsenic (As) and chromium (Cr) have the highest concentrations in the soils of this site. Arsenic (As) concentration in the study site ranged from 3 - 14 mg/kg and this exceeded the FAO permissible limits of 10 mg/kg for agricultural soil.

The high level of arsenic observed in the farm can contaminate groundwater, grains, straws and other crops by impeding nutrient absorption and disrupting plant water intake (Kabir et al., 2016; Hossain, Begum & Akhta, 2017). Adewoyin, Omeje, Joel and Aborishade (2017) have

earlier reported a tolerant concentration of arsenic in the groundwater of Covenant University environs. However, Saha and Ali (2007) reported that agricultural soils of Bangladesh irrigated with arsenic contaminated groundwater significantly increased the arsenic concentration in the cultivated rice farm in the area. The geochemical evaluation method employed for this study suggests that the source of arsenic in the study site is basically anthropogenic, that is as a result of the application of pesticides, weed controller and the use of animal manures on the farmland. Animal manures such as poultry litters are potential sources of harmful trace elements such as arsenic into the agricultural soils (Ravindran, Mupambwa, Silwana & Mnkeni, 2017; Missimer et al., 2018). Other report on arsenic anthropogenic sources was noted by Jang, Somanna and Kim (2016).

Chromium (Cr) concentration at this farm ranged from 22 mg/kg to 444 mg/kg, the values exceeded the FAO/WHO permissible limits of 20 mg/kg in agricultural soils. The high concentration of chromium in this site poses threat of toxicity to plants and ecosystems in the environment. Chromium toxicity can cause decrease in germination of plants, impairment of photosynthesis, oxidative imbalances and inhibition of enzymatic activities (Ertani, Mietto, Borin & Nardi, 2017). The concentration of copper (Cu) at the farm ranged from 9.6 mg/kg to 45.1 mg/kg, with only sample C9 exceeding the WHO maximum permissible limit of 40 mg/kg in agricultural soils. Chiou and Hsu (2019) noted that copper metal toxicity is usually found in the soil and water of industrialised areas. The effects of excessive copper in soil are reduction in plant root elongation and damages to root cells as reported by Zeng, Feng and Xiang (2004) and Adrees et al. (2015).

The concentration of lead (Pb) ranged from 16.9 ppm to 81.0 ppm at the farm site. All analysed soil samples (C1 – C9) except C10 in this site are within the permissible limits (50 ppm) of WHO/FAO (2001). Lead toxicity in soils can finally be ingested by human through the intake of vegetables and crops and this poses great health challenge such as reduction in intelligence, aggressive or violent behaviour, changes in skin, cancer of the skin, liver, bladder and so on (Mattee, Kootbodien, Kapwata & Naicker, 2018).

The concentration of zinc in samples C1 - C10 (Table 4.3) ranged from 22.7 mg/kg to 85.9 mg/kg, with C9 and C10 having higher concentrations of 83.6 mg/kg and 85.4 mg/kg, respectively exceeding the WHO permissible limit. Zinc is a micronutrient in soil particles but needed in agricultural soil for protein production in plants. However, phosphorus usually interferes with zinc uptake in plants during fertilization causing zinc deficiency in soil as noted by Mousavi, Galavi and Rezaie (2012) and Darch et al. (2019). Researchers have identified the effects of zinc toxicity in soil to include deterioration in the amount of yield and quality of grain, and decrease in nitrogen content especially at a concentration of 100 mg/kg to > 1000 mg/kg (Malik et al., 2011).

Selenium (Se) concentration ranged from 0.2 ppm to 0.7 ppm at the farm as shown in Table 4.3. All the sampled soils have selenium concentration exceeding the WHO permissible limits of 0.4 mg/kg except C7 and C8. Se as a micronutrient is so beneficial to soil, plant and animal. When in excess supply, selenium can be toxic to plants causing malformed plants or inducing oxidative stress in plants both of which are harmful to plants (Gupta & Gupta, 2017). Typically, selenium occurs naturally in sedimentary rocks (White et al., 2004) but its availability still depends on the type of soil, rainfall and organic matter (Hartikainen, 2005).

The concentration of nickel (Ni) at Covenant University farm ranged from 10 ppm to 240.5 ppm as shown in Table 4.3. All samples except C9 have nickel concentrations within the WHO/FAO permissible limit of 68 mg/kg with a threshold limit of 50 mg/kg in agricultural soils (Toth, Hermann, Silva & Montanarella, 2016). Ni as a micronutrient is basically needed in small quantities for normal plant growth but its toxicity in soils inhibits plant growth, causes stunted root growth and chlorosis, that is the yellowing of leaf tissue due to lack of chlorophyll (Iyaka, 2011; Macedo, et al., 2016).

The concentration of molybdenum (Mo) at the farm ranged from 0.89 ppm to 4.77 ppm. The concemtration of Mo at Covenant University farm is within the WHO/FAO (2007) permissible limits of 5 ppm; this is contrary to the 12 ppm concentration of Mo reported in the Nile soils of Egypt (Saheen et al., 2017). Antimony (Sb) has concentration ranging from 0.13 ppm to 0.71 ppm in samples C1 - C10. European Union standard guidelines for antimony in soil is 10

mg/kg (Toth et al., 2016). All soil samples have values lower than the standard guidelines and are therefore safe from toxicity of antimony.

### 5.4.2 Major Elements/Macronutrients Concentration

The concentration of Sodium (Na) at Covenant University farm ranged from 0.01% to 0.71% as shown in Table 4.21. Exchangeable sodium percentage greater than 10 % is of serious concern in agricultural soils (Horneck, Sullivan, Owen & Hart, 2011). Sodium (Na) content in the soils of the study area are minimal and therefore beneficial for agricultural purposes. A similar report on sodium fertility was reported by Kronzucker, Coskun, Schulze, Wong and Britto (2013).

Aluminium (Al) concentration in this farm site ranged from 3.32% to 9.33%. Typically, aluminium (Al) at low concentration (< 0.0001) acts as fungicide to stimulate plant growth but its toxic effects include inhibition of root growth and reduction of uptake of several other cations such as phosphorus, magnesium and calcium (Perry & Amacher, 2010). Although Al is abundant in the earth crust and mostly in acidic soils, it has not been researched as essential for agricultural soils (Bojorquez-Quintal, Escalante & Martinez-Estevez, 2017).

The concentration of potassium (K) at the farm ranged from 0.15% - 0.79% as shown in Table 4.21. Potassium is one of the most essential macronutrients the soil needs to grow healthy crops. The iron (Fe) concentration at the farm ranged from 2.29% to 18.56%. The WHO permissible limits of the concentration of Fe in plant and soil are 20 mg/kg and 450 mg/kg, respectively (Shah et al., 2013). The concentration of iron observed in the study area is however lower than the WHO recommended limit in the samples. Researchers have noted that most iron enriched soils make less readily available iron to plants as a result of low solubility of iron oxides (Rui et al., 2016; Mendoza, Guananga, Melende & Lowy, 2020).

The concentration of calcium (Ca) at the farm ranged from 0.01% to 0.18%. The soil at Covenant University farm which consists mainly of clay has greater concentration of calcium (Ca) than the sandy gravelly soil. Usually, the concentration of calcium in sandy soils ranged from 0.04% to 0.05%, while that of clayey soils is greater than 0.25% (Espinoza, Slaton &

Mazaffari, 2006). This study showed that calcium (Ca) has greater concentrations in clay soils than in sandy or gravelly soils of the other study site. This is because of the positively charged ion tightly held by clay soil and the presence of organic matter in clayey soils (Kelling & Schulte, 2004; Horneck et al., 2011). The concentration of calcium in this study site is very low and replenishment is therefore needed to make the soil fertile. The abundance of calcium (Ca) in soils has no toxicity effects on plants but its deficiencies in crops have been termed physiological with symptoms such as chlorosis, stunted growth and fruit abnormalities as reported by Brown (2018).

As shown in Table 4.21 phosphorus concentration at Covenant University farm ranged from 0.0019% to 0.072%. Phosphorus (P) as one of the key essential elements/nutrients needed for normal plant growth is therefore usually included in the fertilization requirements for crop production (Singh et al., 2015; Renneson, Barbieux & Colinet, 2016). Magnessium concentration at Covenant University farm ranged from 0.05 – 0.10%. Magnessium generally forms association with clay minerals such as chlorite, montmorillonite and vermiculite. The study site requires magnesium replenishment as observed from the result in Table 4.21. Magnesium is absorbed by plants from the soil solution, which is slowly replenished by the soil reserves (Senbayram, Gransee, Wahle & Thiel, 2015). Hence, the application of magnesium fertilizers is crucial to sustain high crop yield and quality. Titanium concentration at Covenant University farm ranged from 0.323% to 0.993%. Chaudhary and Singh (2020) reported that low concentrations of titanium applied to the roots of crops stimulate certain enzymes that enhance crop yield increase and nutrient uptake and quality. The emerging mass production of titanium oxide ($TiO_2$) in a range of industrial products such as paintings, sunscreens and cosmetics and the uncontrolled disposal of these nanoparticles can pose risk to human and ecosystems health (Sangani et al., 2019). Titanium can be toxic though but the concentration in the study area is within considerable limits (<1.0 mg/kg). The general trend for macro elements concentrations in this study area was Fe>Al>K>Ti>Mg>Ca>P>Na as presented in Table 4.21.

### 5.4.3 Rare Earth Elements Concentrations

The concentration of Lanthanium at Covenant University ranged from 27.7 ppm to 57.7 ppm. Cerium (Ce) concentration in this site ranged from 57.49 ppm to 183.63 ppm. The concentration of praseodymium as in Table 4.4 ranged from 5.5 ppm to 12.8 ppm. Praseodymium (Pr) is one of the most abundant rare elements, about four time more abundant than Tin (Sn) (Ramos et al, 2016). Like other rare metals, praseodymium has low to moderate toxicity (Ramos et al., 2016). Since Pr is mostly found in household equipment such as glasses, fluorescent lamp, colour television which are often thrown away, Pr accumulates gradually in soil (Rim, Koo & Park, 2013).

Samarium (Sm) concentration ranged from 3.2 ppm to 8.1 ppm at Covenant University farm. This element is one of the rare earth elements (REE) and is more abundant than lanthanum (La) and praseodymium (Pr). Europium (Eu) is also a member of the rare earth elements with less abundance in nature. The concentration of europium ranged from 0.6 – 1.9 at Covenant University farm. Vanadium (V) concentration ranged from 26 ppm to 315 ppm. High concentration of vanadium was recorded at Covenant University farm (Table 4.4) thereby making the site susceptible to the adverse effect of toxicity such as microbial basal respiration and soil enzyme activity identified by Xiao et al. (2015) and Guagliardia, Cicchellab, De Rosac, Riccaa and Buttafuoco (2018).

## 5.5. Geochemical Evaluation at Landmark University

### 5.5.1 Trace Elements/Micro-nutrients Concentrations

Arsenic (As) as a trace element at Landmark University farm has concentration ranging from 1.2 ppm to 4.6 ppm as shown in Table 4.5 and are within the WHO/FAO (2001) permissible limits of 10 ppm recommended for agricultural soils. These recorded concentrations make the soil at Landmark University farm free from arsenic toxicity. This concentration at the farm site was found to be relatively lower than 2 ppm to 16 ppm and 2.0 ppm to 489 ppm in Lagos, Nigeria and Anllons River Basin, Spain as reported by Odukoya (2015) in Lagos, Nigeria and Martina-Prieto, Cancelo-Gonzalez and Barral (2018) respectively.

The concentration of copper (Cu) in the farm ranged from 16.4 ppm to 24.5 ppm and are within the WHO/FAO (2001) 40 ppm permissible limit of copper in agricultural soils. The low copper concentration reported depicts that the farm site is presently free from copper toxicity.

Lead (Pb) concentration ranged from 15.58 ppm to 49.85 ppm at this farm and are within the 50.00 ppm WHO/FAO (2001) permissible limit for lead (Pb) in agricultural soils (Fosu-Mensah, Addae, Yirenya-Tawiah & Nyame, 2017). The concentration of zinc ranged from 23.2 ppm to 156.9 ppm. The WHO permissible limit for zinc (Zn) in soil is 60 mg/kg; therefore, L7 and L8 concentration of 156.9 mg/kg and 96.0 mg/kg respectively, far exceeded the recommended limit (Table 4.5).

Selenium (Se), a naturally occurring nutrient in most soils has concentration ranging from 0.2 ppm to 0.7 ppm in samples L1 - L8. The low concentration of Se in the sandy soil of the site at Landmark University farm compared to 0.2 ppm to 1.4 ppm at Covenant University farm is consistent with the report by Lopes, Avila and Guilherme (2017) that sandy soils have lower Se than the organic or calcerous soils. The concentration of nickel (Ni) in samples L1 - L8 ranged from 12.3 ppm to 26 ppm and this is within the WHO/FAO (2001)permissible limits of 68 ppm.

The concentration of strontium (Sr) in samples L1 - L8 ranged from 17 ppm to 212 ppm, (Table 4.4). The WHO permissible limit of strontium in soil is 200 mg/kg and high toxicity as observed at L7 can enter into the food chain when incorporated by plantsin plants and causes primary threats to human health and the entire environment (Burger & Lichtscheidl, 2019). Temperature, chemical composition, soil acidity and agricultural soil cultivation are the entry channels of strontium to plant roots (Burger & Lichtscheidl, 2019). The threshold value and guideline values of vanadium in soils are 100 mg/kg and 150 mg/kg respectively (Toth et al., 2016). The concentration of vanadium (V) in samples Ll -L8 ranged from 54 ppm to 83 ppm, and 26 ppm- 315 ppm in C1 - C10. Vanadium is a naturally occurring element in the earth crust but its input in soils is as a result of phosphate fertilizers as reported by Molina, Aburto, Calderon, Cazanga and Escudey, (2009). High concentration of vanadium was observed at Landmark University farm (Table 4.4) thereby making the soil susceptible to the adverse effect

of toxicity such as microbial basal respiration and soil enzyme activity identified by Xiao et al. (2015).

The concentration of antimony (Sb) in samples L1 - L8 ranged from 0.24 ppm to 0.39 ppm. European Union standard guidelines for antimony in soil is 10 mg/kg (Toth et al., 2016). All soil samples have values lower than the standard guidelines and are therefore safe from toxicity of antimony. Antimony has no known biological functions though it can be toxic at high concentration with carcinogenic effects on humans and animals (Tschan, Robinson & Schulin, 2009). The concentration of molybdenum (Mo) in the agricultural soils at Landmark University ranged from 0.3 ppm to 4.7 ppm (Table 4.5). Basically, agricultural soils contain about 0.25 ppm to 5.0 ppm total amount of molybdenum (Mo); however, higher concentration can occur in some soils (McBride, Richards, Steenhuis and Spiers, 2000). As noted by Rutkowska, Szulc, Ewa and Natalia (2017), Mo is an essential trace element needed for normal plant growth and is required in small amounts as observed in the soil of the study area. The concentration of Mo in the soils of both farms investigated is adequate for normal plant growth; however, Rutkowska et al. (2017) reiterated that acidic sandy soil requires more amounts of Mo to balance the nutritional need of the plant. Hence, there is need to include molybdenum in fertilizers to be applied in soils where it is deficient.

### 5.5.2 Major Elements/Macro-nutrients Concentrations

The concentration of sodium (Na) at Landmark University farm ranged from 0.001% to 0.767 %. The result indicates minimal sodium content in the site as at the time of study although, the concentration varies in the farm site (Table 4.19). Sodium as a major element is not a plant nutrient but it plays a role in soil health. High concentration ($\geq 15\%$) of sodium in soils indicate toxicity and causes decline in the soil structure and reduces soil permeability resulting into compaction and soil drainage problems (Zhang, Wang, Xue & Wang, 2019). Researchers have differentiated between soil salinity and soil sodicity (Shahid, Zaman & Heng, 2018). Saline soil is described as the excessive level of soluble salt in soil solution that can affect plants negatively, decrease crop yield and may lead to the death of plants if not quickly managed. On the other hand, sodic soils have excessive level of sodium ($Na^+$) adsorbed by the soil, which breaks down the soil structure. Aluminium (Al) concentration as shown in Table 4.19 ranged

from 4.46% to 9.33% at Landmark University farm. This concentration is minimal and poses no threat to the fertility of the agricultural soil of the study area.

The concentration of potassium (K) at Landmark University farm (L1 - L8) ranged from 0.15% to 0.79% as shown in Table 4.19. Potassium concentration at the study area is not evenly distributed. The lower concentration of potassium observed in some part of the the site at Landmark University farm may be as a result of the leaching of sandy soils and low rainfall experienced (Mendes et al., 2016) as igneous rocks have higher K content than sedimentary rocks (Mouhamad, Alsaede & Igbal, 2015). Adegbite, Okafor, Adekiya, Alori and Adebiyi (2019) reported low concentration of potassium in a farm site close to the study area. Potassium is also an essential nutrient plant needed in large quantity for proper growth and reproduction. Potassium deficiency can result in slow and stunted growth, weak and unhealthy roots, uneven ripening of fruits and poor resistance to pests as previously reported by Subha and Rose, 2016. More so, higher concentration of potassium is also beneficial to human as it regulates high blood pressure (Staruschenko, 2018).

Iron (Fe) concentration at Landmark University farm ranged from 2.42% to 15.9%. Iron (Fe) is an important micronutrient in agricultural soils and its effects include the yellowing of fields with irregularly shaped areas in the subsoil (McCauley, Jones & Jacobson, 2011; Rui et al., 2016). The WHO permissible limits of the concentration of Fe in soil is 450 mg/kg (Shah et al., 2013). The concentration of iron in this study area is however lower than the WHO recommended limits.

The concentration of calcium at the farm ranged from 0.04% to 0.52% as shown in Table 4.19. A similar report of the concentrations of calcium in different soil types and importance of calcium as an essential nutrient is noted by Bonomelli, Gil and Schaffer (2019). Calcium (Ca) is one of the macronutrients required by soil to build plant cell walls (Perry & Amacher, 2010; El-Habbasha & Ibrahim, 2015). Sandy gravelly soil as in Landmark University farm usually have calcium concentration ranging from 0.04% to 0.05% as reported by Espinoza, Slaton & Mazaffari (2006). For sustainable crop production at this site, calcium should be added to the fertilization of the soil.

The concentration of phosphorus (P**)** at this farm ranged from 0.02% to 1.75%. This farm site requires phosphorus replenishment as the observed concentrations are far less than what is required for normal plant growth. Little wonder, NPK (nitrogen, phosphorus and potassium) chemical fertilizer was used in this farm site during the planting season. The significance of phosphorus as a native and finite resource has been reported by Cardoso, Silva, Colombari, Lanna and Fernandes (2019); hence, a frequent replenishment is essential in soils. Also, Singh, Goyne and Kabrick (2015) reported that the concentration of phosphorus in most soils is about 35 % to 75% and 30% to 65 % in inorganic and organic form, respectively. The concentration of magnesium as shown in Table 4.19 ranged from 0.05% to 0.39%. Magnesium (Mg) is one of the essential soil nutrients needed for crop production. A replenishment of magnesium is needed on this farm site as frequent addition of this macronutrient is essential for quality crop yield. Gransee and Fuhrs (2012) reported a similar report on the mobility of magnesium (Mg) in soils. The recorded concentration of titanium (Ti) ranged from 0.37% to 0.993% at this farm is as shown in Tables 4.19. Several researchers have reported that tropical soils and highly weathered soils of granitic origin have more titanium content (mean ≥ 3 g/kg) than the light organic soils and can also be introduced into the soil by emissions from certain titanium production based industries (Kabata-Pendias, 2000; Gomez-Merino & Trejo-Tellez, 2018; Bahnasawy, El Kad & Elwa, 2019). However, the sources of titanium (Ti) are both natural and anthropogenic, though titanium (Ti) is poorly soluble in soil and water but titanium oxides nanoparticles concentrations are more in soils than in air or water (Monteiro, Coastal, Coppola, Freitas, Vale & Pereira, 2019). Vegetables, fruits and animals metabolic activity are the target of increased titanium concentration in the soil (Zhang, Tu, Xhang & Lu, 2019).

### 5.5.3 Rare Earth Element Concentrations

The concentration of lanthanum (La) ranged from 22.8 ppm to 73.5 ppm at Landmark University farm as shown in Table 4.6. The concentration limit for lanthanum in soil is 5.0 mg/kg, this rare earth element (REE) is one of the most abundant in the soil (Sneller, Kalf, Weltje & Van-Wezel, 2000). Jinxia, Rudo and Cornelis (2017) have reported that lanthanum is been introduced into the soil in the form of lanthanides mixtures used in animal husbandry and fertilizer. Lanthanum concentration in some part of the study area exceeded the limit in soils and may have been introduced into the soil from fertilizers previously used on the farm

sites. The results of the geochemical analysis of soil samples from the farm site revealed that lanthanum (La) and cerium (Ce), with concentrations ranging from 22.8 ppm to 73.5 ppm are the most abundant REE in the study area. Similar results have been reported by Hu et al. (2006) and Ramos et al. (2016).

Praseodymium (Pr) concentration at this farm ranged from 4.2 ppm to 15.4 ppm. Pr concentration range in this site is more than that at Covenant University farm site. Samarium (Sm) at Landmark University farm ranged from 2 ppm to 8.1 ppm. Sm is toxic in soil, are highly and irreversibly absorbed into soil at low concentration but retention decreases at high concentrations (Ramirez-Guinart, Salabeirris, Vidal & Rigol, 2018). Europium (Eu) is also a member of the REE's with less abundance in nature. The concentration of europium at Landmark University farm ranged from 0.4 ppm to 1.5 ppm. This rare element has no biological role in plants and animals (Ramos et al., 2016). Gadolinium (Gd) concentration ranged from 1.3 ppm to 6.1 ppm at Landmark University farm. Gd is one of the naturally abundantly occurring REE, which serves as soil pollutant in the study area. Research has shown that gadolinium can accumulate in patients' bone, tissues and probably brain causing systemic disorder especially for patients with underlying kidney problems (Rogowska, Olkowska, Ratajczyk & Wolska, 2018; Ebrahimi & Barbieri, 2019). Terbium (Tb) recorded concentration ranged 0.2 ppm to 0.93 ppm in the study site. This element (Terbium) is a member of the REEs that has little or no biological role but can cause root cell damage at toxic level (Yang, Wang, Zhou & Huang, 2015).

## 5.6 Contamination Assessment of Toxic Elements

### 5.6.1 Contamination Assessment of Toxic Elements at Covenant University Site

The contamination assessment of toxic elements at Covenant University site (Tables 4.9, 4.11, 13 & 15) has indicated that the pollution index of the toxic elements showed the descending order of As>Cr>Pb>Cu>Cd>Co>Ni>Mn>Zn. The pollution indexes of Co, Cr, Ni, Pb, and Mn at Covenant University farm were within low to high contamination, arsenic (As) is within moderate to highly contamination; Cu and Zn are within low to medium while Cd is categorized as low contamination. The pollution load index (PLI) in the study area ranged from 0.51 - 4.05. This result indicates that the soil at Covenant University farm can be classified as

unpolluted to highly polluted. Arsenic is the major toxic element in the farm site followed by Chromium (Cr), lead (Pb) and then copper. Cadmium (Cd), cobalt (Co), nickel (Ni), manganese (Mn) and Zinc are less toxic in the soil of the farm site. The degree of contamination (Table 4.13) further indicates that arsenic(As) and chromium (Cr) exhibited high degrees of contamination, while other elements such as Copper, Cadmium, Nickel, Manganese and Zinc have low to moderate degree of contamination in the soil of this farm. The ecological risk index (Table 4.17) has indicated a very high risk of arsenic (As) in the farm soil, this may have resulted from the poultry litters used as manure in the farm site (Sanjay et al., 2018).

### 5.6.2 Contamination Assessment of Toxic Elements at Landmark University Farm

In Landmark University farm, the pollution index of the toxic elements showed the descending order of As>Pb>Cu>Mn>Zn>Cr>Ni>Co>Cd (Table 4.12). The contamination factor of toxic elements in this farm site ranged from low to moderate contamination. Pb, As, Cu, Mn, Zn, Co and Cd at Landmark University farm are within low to moderate contamination, while Cr and Ni are in low contamination. The pollution load index (PLI) ranged from 0.48 - 1.65 (Table 4.12). The pollution load index has indicated that the soil at Landmark University farm is classified as unpolluted to moderately polluted. The modified degree of contamination index (Table 4.14) has further indicated an unpolluted to moderately contaminated soil in this farm. The geoaccumulation pollution index also indicate a very low to low polluted soils in this farm site. The ecological risk index (4.16) indicated low risk of the toxic metals and a moderate risk of arsenic at this farm site.

## 5.7 Geostatistical Comparison of Macro/Micro Elements

### 5.7.1 Macro-elements/Majornutrients

The comparison of macro-elements/nutrients at Covenant University farm and that of Landmark University farm was achieved using the Mann Whitney U test at $\alpha = 0.05$. For the site at Landmark University farm the following elements are highly positively correlated at 0.05 level of significance P-Ca, Mg-Ca, P-Mg, Al-Ca, Al-Mg, Al-P, Ca-Na, P-Na, Mg-Na, Fe-P, Fe-Al, K-Ca, K-Ca, K-Mg, K-Al, K-Na (Tables 4.19 – 4.27). This result indicates that an increase in one of the nutrients automatically leads to an increase in the other and vice versa across the farmlands. The median value of titanium (Ti) is greater than the observed mean

value in Landmark University farm (Table 4.27), while the median for aluminium (Al) is greater than the observed mean value in Covenant University farm (Table 4.24). The analysis in Tables 4.25 and 4.26 revealed that these paired elements are positively correlated that is, Ca-Mg, P-Mg, Ti-Ca, Ti-P, Ti-Mg, Fe-P, Fe-Al, Ca-K, Mg-K and Na-K in Covenant University farm. This suggests that whenever there is an increase in the accumulation of one of the paired elements there will be an equal increase in the other and vice versa.

By comparing the nutrient accumulation at Landmark University farm with that of Covenant University farm, the following paired nutrients: Ca-Mg, P-Mg, Fe-Al, Ca-K, Mg-K, and Na-K are positively correlated in both farm sites (Table 4.27). The result further revealed that titanium (Ti) and iron (Fe) concentrations in the two farm sites are the same their correlation notwithstanding (Table 4.27) as previously observed by Lyu et al. (2017). Iron and titanium have been found to have antagonistic and synergistic relationship; when Fe is deficient in soil/plant, Ti will help to induce genes related to Fe acquisition thereby improving the overall quality of crop yield (Lyu et al., 2017).

### 5.7.2 Trace Elements/Micro-nutrients

The geostatistical comparison of trace elements in the study areas was achieved using the correlation matrix (P-test) and the Mann Whitney test at $\alpha = 0.05(95\%\ confidence\ level)$.

The null and alternate hypotheses are:

$H_o$: The concentration of macro-elements between both farms are not correlated.

$H_1$: The concentration of macro-nutrients between both farms are correlated.

For the P- test, p value $\prec 0.05$ indicates that there is correlation between the elements for comparison.

For Covenant University farm as in Table 4.30, the following pair of elements As-Se, As-Mo, Cd-Co, Cd-Cr, Cd-Mn, Cd-Ni, Cd-Pb, Cd-Zn, Co-Mn, Co-Ni, Co-Zn, Cr-Cu, Cr-Ni, Mn-Pb, Mn-Sr, Mn-Zn, Ni-Zn, Pb-Zn, Se-Mo and Sr-Zn are positively correlated at 0.05 significance level. This result indicates that an increase in one of the paired elements leads to an automatic increase in the other elements in Covenant University farm site. The following pair of elements

are negatively correlated As-Sr, Mo-Sr and this indicates that an increase in one of the paired elements does not necessarily mean the other element will increase. Also, there is an even distribution of Cd in Covenant University farm as indicated from the result.

At Landmark University farm, the arithmetic mean, geometric mean, harmonic means and quadratic mean are the same. This result indicates that there are no extreme values. Also, the following paired elements are positively correlated at 0.05 significance value As-Cr, As-Ni, Cu-Cd, Mo-Cd, Co-Mn, Co-Pb, Co-Mo, Co-Sr, Co-Zn, Cr-Ni, Cu-Ni, Mn-Pb, Mn-Mo, Mn-Sr, Mn-Zn, Pb-Mo, Pb-Sr and Pb-Zn. This result indicates that an increase in one of the paired elements at Landmark University farm leads to an increase in the other element and vice versa. The negatively correlated elements include As-Pb, As-Sr, As-Zn, Cr-Sr, Ni-Sr, Mo-Zn and Sr-Zn. This negatively correlated paired elements result indicates that an increase in one of the paired elements doesn't not necessary lead to an increase in the other and vice versa. The result revealed that selenium (Se) is the only element not correlated either positively or negatively with any other element at Landmark University farm. Generally, Table 4.36 has shown that the mean and median of the elements As, Cd, Cr, Cu and Mo differ significantly in both farm sites. This result indicates that when any of the elements is in large quantity in one site, it is lower in the other site and vice versa. The mean and median of the following elements Co, Mn, Ni, Se, Sr and Zn are the same in both farm sites.

## 5.8 Geospatial Maps for the Study Area

### 5.8.1 Geospatial Maps at Covenant University Farm

The geospatial distribution of phosphorus (P) at Covenant University farm is somewhat moderately uniform, moderate concentration of phosphorus was observed on the entire farmland (Figure 4.30). Magnesium (Mg) distribution in this farm site is not uniformly distributed. Higher concentration of magnessium was noticeable on the northeastern part of the field while the southwestern part has revealed low concentration as indicated by Figure 4.30b. Moderate concentration is noticeable at the centre of the field. Iron concentration is moderately high at Covenant University farm with values ranging from 9 - 15.5% across the farm (Figure 4.31). The distribution of iron concentration was generally uneven in the farmland as revealed in the geospatial map of the area. The geospatial map of sodium (Na), as presented in Figure

4.31b, showed high concentration of sodium in the northeastern part of the farm; low concentration was observed towards the southwestern part of the farm. The geospatial maps of Ca, as showed in Figure 4.32a, revealed high concentration of calcium (Ca) in the northeastern part of the farmland. The center part of the farm land revealed moderate concentration of calcium, while low concentration was noticeable at the southwestern and towards the southern part of the farm site. The geospatial distribution of aluminium (Al) at Covenant University farm as indicated in Figure 4.32b, showed high concentration in the farm area covering the entire southern to central part of the farmland. High concentration of Al was observed at the southwestern part of the farm. Low concentration of aluminium was observed at the extreme northern part and moderate concentration at the centre part of the farmland. The concentration of potassium (K) at Covenant University farm ranged from low at the southwestern part to moderately high at the northern, eastern and central part of the farm land (Figure 4.33). Titanium concentration in the farm site is relatively high at the northern and central part of the farm site as observed in Figure 4.33b. Moderately low concentration of titanium was observed at the southwestern part of the farm site.

### 5.8.2 Geospatial Maps at Landmark University Farm

The geospatial maps for Landmark University farm are presented in Figures 4.34 - 4.37. The concentration of magnesium in the farm site is generally high with moderate concentration occupying a small portion of the farmland. High concentration of magnesium (Mg) was observed in the northern, southern and eastern part of the farmsite, while a moderately low Mg was observed at the northwestern part of the farm site. Calcium (Ca) concentration in this farm site is from moderately low at the northwestern and central part to fairly at the northeastern part of the farm site as observed in Figure 4.34b. Potassium on the other hand has high concentration across the farm site, covering about 70 % of the entire farm area. Low concentration of potassium (K) was observed at the extreme southwestern part of the farm site. The geospatial map of sodium (Na) as observed in Figure 4.35b revealed higher concentration of sodium in the entire farmland with only a chunck of moderately low sodium observed towards the extreme northwestern part. Figure 4.36 revealed high concentration of phosphorus (P) at the northern, southern and eastern part of the farm. Moderately low concentration was observed towards the southeastern part of the farm site. Aluminium concentration at this farm

site is from moderate to high as observed in Figure 4.36b. Slightly high concentration of Al was noticeable in the entire part of the farmsite while pockets of higher concentration are noticeable in the northeastern and southern part of the farm site. Iron (Fe) concentration in this farm site is from moderately low to fairly high as observed in Figure 4.37. The fairly high iron concentration was noticeable at the southeastern part of the farm site with other parts of the farm exhibiting moderate concentration. Generally, titanium (Ti) concentration in this farm site is from low to medium as in Figure 4.37b. Areas of high accumulation and deficiencies have been identified by this method.

By comparing the fertility maps by Chude et al. (2011) with those obtained in the geospatial maps in the study area (Figures 4.30 - 4.37), one can easily deduce some similarities and deviations. The major similarity is that the present low phosphorus concentration recorded in Landmark University farm correlates with the previous findings of Chude et al. (2011) in that area. The deviation is that phosphorus concentration for Covenant University farm appeared lower than that observed in the study of Chude et al. (2011). Also, this study revealed that calcium (Ca) concentration (0.08% to 0.52%) in Landmark University farm exceeds the concentration in Covenant University farm (0.02% to 0.18%). Calcium concentration is generally low in the soils of both sites and this is corroborated by the findings of Chude et al. (2011).

## 5.9 Other Soil Properties from Laboratory Analysis in the Study Area

### 5.9.1 Other Soil Properties at Landmark University Farm

The soil bulk density at Landmark University farm (Table 4.37) that ranged from 0.13 $g/cm^3$ to 0.16 g/cm3 showed that compaction is evident in some part of the farm site. The lower the soil bulk density $\left(\prec 15\ \text{g/cm}^3\right)$ the more desirable the soil for agricultural production. Optimum movement of air and water through the soil was evident with low bulk density. However, soil bulk density increases with depth and numerous studies have found that compaction increases the bulk density and mechanical resistance of soil (Blanco-Canqui, Hergert & Nielsen, 2015; Zhou, Fang, Mooney & Peng, 2016; Guang-Hui, Chun-Mei, Xin-Hua, Zhang-Zhi & Li-Na, 2020), as soil bulk density increases the total pore spaces decreases.

Sandy soils as prevalent at Landmark University farm usually have higher bulk density (1.3 $g/cm^3$ to 1.7 $g/cm^3$).

Soil porosity or percentage void space is closely related to soil bulk density and this vary from soil to soil. Basically, as the soil bulk density increases there is a decrease in soil void spaces. Soil porosity is a main indicator of soil structural quality. The percentage void space range (0.93% to 0.95%) in the site at Landmark University farm indicates high porosity which is typical of sandy/gravelly soils.

Soil Moisture Content at Landmark University farm is low (8.08% to 15.46%) as revealed in Table 4.39 therefore, irrigation is highly recommended in the farm site. Coarse textured soils that is, sandy soils found in this farm site will need no irrigation if moistire content ranged from 90 % to 100% (Laurenzi, 2018).

### 5.9.2 Other Soil Properties at Covenant University Farm

The soil bulk density range (0.13 – 0.15$g/cm^3$) at Covenant University farm (Table 4.38) indicates a compacted lateritic clay soil. Clay soils usually have lower bulk density than the sandy soils ($1.1 - 1.7g/cm^3$) and the United States Department of Agriculture (USDA) has given an estimate value (< $1.10g/cm^3$) as ideal for normal plant growth. The soil of this farm site is within the permissible range of soil bulk density that emhance normal plant growth.

Soil porosity or percentage void space at this farm site is between 0.94 and 0.95 or 94% and 95%, fine textured soils such as clay have greater pore spaces. Micropores dominate fine textured soils therefore, its total porosity is greater than that in coarser soils however, air and water is somewhat restricted as a result of the smaller size of the micropores (Hao, Ball, Culley, Carter & Parkin, 2019). The compacted latertic clay unit in the subsoil of this farm site can reduce pore spaces and restrict the infusion of $O_2$ and diffusion of $CO_2$ out of the soil as a result of decreasing pore spaces.

Soil moisture content (SMC) determined in the laboratory for Covenant University farm site ranged from 7.86 – 13.98%. The moisture content at the farm site is typically low as several

researchers have reported that 80 – 100% moisture is required in a typical fine-grained soil such as clay to maintain normain plant growth (Laurenzi, 2018). Irrigation is needed in clayey soils when SMC is within 60 – 80% and SMC below 60% is tagged dangerously low in moisture to enhance normal plant growth (Laurenzi, 2018). Typically, clayey soils retain moisture and therefore little irrigation is needed as compared with the coarse soil types.

## 5.10 Implications for Precision Agriculture

### 5.10.1 Implications for Precision Agriculture at Covenant University Farm

Geoelectrical resistivity imaging has revealed the nature of the topsoil of the areas studied. The topsoil at depth of 0 - 2 m covers the normal root zone (≤ 2 m) of major crops grown in the area, thereby giving us a good representation of the root zones. The geoelectrical resistivity imaging for Covenant University farm has indicated lateritic clay unit with an alteration of clayey sand and sandy clay as the topsoil. The root zone which is paramount to farming in the area is highly conductive. As Dwevedi et al. (2017) showed, lateritic soil of this study area experience soil leaching as a result of the alternate wet and dry periods under which the soils are been formed. The lateritic clay unit of the farm's topsoil has lower content of potassium and phosphorus as observed from the geochemical analysis of trace elements conducted on the soil samples of the farm area.

The peculiarity of the lateritic soil like those found at Covenant University farm is their unique rusty red coloration. This soil type is known to have high clay content, higher ion-exchage capacity and therefore, requires good manuring (Dwevedi et al., 2017)). Lateritic clay can be agriculturally productive like sandy loamy soils when buffered with organic manure and the right application of chemical fertilizers (Lamidi, Shittu and Adeyeye, 2018). Little wonder, farmers in the area use organic manures throughout the planting season to improve soil and boost crop yield. However, crops such as tomatoes, lemon grass, tea, coffee, rubber coconut and several other crops can be grown on it when properly irrigated and with the application of appropriate fertilizers (Dwevedi et al., 2017).

Previous researchers have indicated that soil pH at Covenant University farm and environs ranged from 6.51 to 9.66 with a mean value of 7.95 (Usikalu & Achuka, 2014). Most crops

grow at a soil pH ranged from 5.5 to 7.5 as most nutrients become available at this pH range, except for ginger and cassava that are tolerant to low solution pH (Biratu, Elias & Ntawuruhunga, 2019; Zhao et al., 2019). Plant based organic manure should be used instead of the chicken litters that contain arsenic on the farm site. Also, non arsenic pesticides be introduced to reduce the amount of toxic elements in this farm site.

Soil temperature is a vital property in precision agriculture that influences soil moisture content, aeration and the availability of plant nutrients. The soil temperature observed in Covenant University farm (2017 – 2019) ranged from 294 - 315 K with the highest temperature of 315 K recorded in February, 2017. As reported in previous studies, certain fruits and vegetables such as maize, carrots, apples, spinach, lettuce, grapes, lettuce, broccoli, tomatoes and other Brassica species germinate at soil temperature range of 280 - 373 K. Such crops can be readily planted at the beginning of the year (February – April) when soil temperature is high (294 - 315 K) as shown in Figures 4.24 and 4.25 (Ayyogari, Sidhya & Pandit, 2014; Sabri, Zakaria, Mohamad, Jaafar & Hara, 2018). This farm site studied can accommodate some of the major crops as the optimum soil temperature range for successful seed germination of the major crops such as okro, lettuce, egg plants, onions, parsley, garlic, cucumber, peas, pepper, beans and watermelon have been fixed from 288.7 - 308.2 K. However, crops can germinate at lower and higher temperature under other environmental conditions as reported by O'Brien et al. (2016).

Soil moisture content (SMC) at Covenant University farm indicate lows SMC ($22 – 25\, m^3 / m^3$) between January and March for the three (3) years studied. Irrigation can be used to sustain crop production at this period of the year. Soil salinity in Covenant University farm was pronounced at the extreme portions of the farm site but the centre is sparingly affected with salt. Macro-elements and trace elements of Covenant University farm were unevenly distributed. Replenishment is needed for areas in the farm site with low macro nutrients concentrations such as potassium, phosphorus and calcium distribution as displayed by the geospatial maps of macronutrients concentrations in the farm.

### 5.10.2 Implications for Precision Agriculture at Landmark University Farm

The topography values incorporated into the inverted resistivity models at Landmark University farm investigated ranged from 563 m to 571 m. A report by Adegbite et al. (2019) on the topography of the area as it influences agricultural output has been previously established. Topography typically influences the soil physical and chemical properties, drainage, soil temperature, run-off, and soil formation as indicated by Karaca, Gulser and Selcuk (2018). However, the relationship between agricultural productivity and terrain conditions have been documented by previous researchers (Li et al., 2015; Turunen et al., 2015). A decline in agricultural output per unit area as a result of elevation have also been proved by Li et al. (2015).

With respect to precision agriculture, the subsurface section of interest is the soil horizon, marked by a high level of heterogeneity as observed from the resistivity response at Landmark University farm. The soil zone is composed of poorly sorted loose lateritic sandy gravel, sand and clayey sand; all of which has porosity and permeability consequences. This observed lithological variability within the soil zone inherently leads to variability in moisture retention capabilities and infiltration capacity as observed in Table 4.2. Porosity tendency of these lithologic units increases in the following order: clayey soil, sandy clay, sandy and gravelly sand. The more permeable sandy unit allows more moisture circulation than other lithologic units in the soil (Table 4.2). Excessive moisture accommodation and prolonged water stagnation is envisaged within the low permeable clayey zones.

Generally, gravelly sandy soils have poor water holding capacity; therefore, irrigation is the only alternative to sustainable farming practices in areas with such soil type. Adequate and uniformity of applied water on a steep landscape like Landmark University farm, sprinkler irrigation system should be adopted as practiced in China (Zhang, Xin & Chen, 2018). Moreso, the high resistivity range of 1000 Ωm to greater than 3000 Ωm measured in this farm suggests that soil conductivity is generally low in the farmland which invariably implies low sediment salinity. Therefore, it can be deduced that the topsoil is unpolluted and free from adverse fertilization effect as at the time of the field work. Also, the textural and compositional framework of delineated soil components, amongst all other factors, partly influence plant

development in the area as deficiency or excessiveness of moisture could invigorate different type of crop diseases. Crops such as grapes, melon, coconut, okra and several other vegetables; with adequate irrigation and maize grow well in gravelly sandy soils.

The results of the geochemical analysis in the study area revealed low concentration of phosphorus in the soils investigated; this is consistent with the results of Jobbagy and Jackson (2001), Salem, Al-Ethawi, Eldrazi and Nouraldien (2014) and Singh, Goyne & Kabrick (2015). Previous researchers have noted that phosphorus concentration in agricultural soils is considerably less in relation to other macronutrients especially in the deeper part of the soil horizon due to its depletion in soils for crop production (Mullins & Hajek, 1996; Jobbagy & Jackson, 2001; Singh et al., 2015). Also, the iron (Fe) content in the soil of the two farm sites are below the WHO recommended limit and therefore needs to be replenished to aid normal plant growth. Basically, sodic, saline and calcareous soils are naturally deficient in iron (Fe); this may be responsible for the observed Fe deficit in the soils of the study area (Mahender, Swamy, Anandan & Ali, 2019). Iron toxicity should be avoided as it causes tissue damage and related disease in human (Shah et al., 2013). Rice plants are however affected by iron toxicity as they tend to absorb iron in large quantities (Mitra, Sahu & Nayak, 2009').

Soil pH is slightly acidic with mean pH ranging from 5.84 – 6.90 on the non degraded soils in a similar study by several researchers in Omu-Aran and the most degraded soils ranged from slightly acidic to basic (Adegbite et al., 2019; Alikwe, 2019). Soil temperature in Landmark University farm site ranged from 289 - 317 K with the highest soil temperature of 317 K recorded in April, 2018. Soil tempeatiure regulates the transformation and absorption of nutrients by plants roots and therefore is an important property in precision agriculture (Sun et al., 2018). The results in Figures 4.26 - 4.27 indicate periods of steady ST in the farm site that is, between June and September of the years studied (2017 - 2019) when nutrient transformation and uptake was sustained regardless of the rains. Yang et al. (2019) suggested straw mulching as an effective method to maintain soil temperature especially in northern agricultural regions.

Soil moisture content in Landmark University farm (2017 - 2019) ranged from 10 to 39 $m^3 / m^3$ . Soil moisture content and soil water storage characteristics in agricultural soils varied in years with different hydrological characteristics as observed from the satellite data in the study area. A similar report by Tang et al. (2019) confirmed the variability of soil moisture content in agricultural soils. Irrigation and other water holding practices can be used to sustain crop production between December and February when the soil moisture content is low. The increased soil salinity in Landmark University farm (Figure 4.29) may be due to the application of fertilizers in the area about the time satellite imagery was captured. Soil salinity has been reported to have affected about 19 million hectares of sub-Saharan African (Tully et al., 2015). However, Sharma and Singh (2015) have suggested that salt tolerant crops such as barley, sunflower, rye and sugar beets can be grown in highly salinized salt areas.

The uneven distribution of macronutrients and trace elements have been revealed in the geospatial maps of chemical compositions of the soil in Landmark University farm sites. In achieving sustainable precision agricultural practices, all essential elements must be applied to soil at the right time and in right quantity. The geostatistical analysis of macronutrients such as phosphorus (P), magnesium (Mg), calcium (Ca), sodium (Na) and iron (Fe) in the soil of the study area revealed the nutrient status of this farm site studied. Zones with inadequate macronutrients and excess non-essential trace elements on the two farm sites have been rightly delineated using various methods in the study; when properly addressed, this will promote precision agriculture on the farms, increase yield and protect our groundwater from impending contamination.

# CHAPTER SIX
# CONCLUSIONS AND RECOMMENDATIONS

## 6.1 Summary of Findings

This study integrated different methods including electrical resistivity imaging, geochemical analysis of soil samples and satellite imagery to characterise the soil of two sites at Covenant University farm and Landmark University farm, respectively. The goal of the study was to aid the development of sustainable precision agriculture in Nigeria.

## 6.2 Conclusions

Precision agriculture entails developing site specific principles to manage crops based on soil properties variability and maximizing agricultural production while preserving soil and water resources. Geoelectrical resistivity imaging has been used to characterise the soil of the study areas and delineate management zones. Geochemical analysis of soil samples from the two sites investigated aided the determination of the soil fertility status of the farm lands. Also, satellite imagery was used to locate areas of concern requiring intervention such as high soil salinity, periods when irrigation is needed as a result of low soil moisture content and the type of crops to plants at different soil temperature range as observed in both farm sites.

The soil at Landmark University farm consists of gravelly sand as topsoil and large body of sandy soils (> 70%) as experienced in other eastern and southern African countries such as Angola, Zimbabwe and Tanzania. The texture of the soil in Landmark University farm is coarse and crops such as leafy vegetables and tomatoes may not be suitable on this soil types but crops such as root vegetables, carrot, maize, juniper, bayberry, fig trees and pomegranate grow well on the soil.

The site at Covenant University farm is mostly composed of clay and therefore has higher carbon content as soils with higher clay content are generally found to have higher carbon content and higher carbon exchange capacities (CEC). The soil at Covenant University farm, like other lateritic clay soils across the world, have low fertility as observed in the results of

the geochemical analysis for essential elements for soils fertility such as calcium, phosphorus, potassium and magnesium. The contamination assessment of toxic elements in both farm sites has showed the descending order of As>Ni>Cr>Pb>Co>Mn>Cu>Zn>Cd in the site at Covenant University farm and a descending order of As>Pb>Cu>Mn>Zn>Cr>Ni>Co>Cd at Landmark University farm. The contamination assessment result has showed that arsenic (As), nickel (Ni), chromium (Cr) and lead (Pb) are the major pollutants in the soil of Covenant University farm while the major pollutants at Landmark University farm are arsenic (As), lead (Pb), copper (Cu) and manganese (Mn). The modified degree of contamination have further indicated that arsenic (As) and chromium (Cr) have high degree of contamination while other toxic metals exhibited low to moderate degree in the soil of Covenant farm. On the other hand, Landmark University farm has exhibited low to moderate degree of contamination of toxic metals in the soil. The ecological risk index has indicated a very high risk of arsenic pollution in Covenant University farm and a moderate risk at Landmark farm. Geogenic sources may be attributed to the low concentrations of other toxic metals but the excessively high arsenic is traced to anthropogenic sources.

The geospatial maps of the chemical compositions of the two sites have revealed the uneven distributions of the essential and non-essential elements in the farmlands. Zones with accumulation and deficiency for adequate fertilization and interventions have also been delineated. The satellite imagery provided quick spatial information of the soil temperature for both sites that ranged from 0 - 285 K for three (3) consecutive years (2017 - 2019).

Geostatistical analysis revealed that for both sites studied, the following paired macronutrients: Ca-Mg, P-Mg, Fe-Al, Ca-K, Mg-K, and Na-K are positively correlated. The correlation at 0.05 level of significance suggests that an increase in the accumulation of one of the paired elements leads to an increase in the other. Titanium (Ti) and iron (Fe) have the same concentration level in the soils of the two sites, their correlation coefficient notwithstanding. Also, the following paired micro elements: As-Pb, As-Sr, As-Zn, Cr-Sr, Ni-Sr, Mo-Zn and Sr-Zn are negatively correlated at Landmark University farm. This negative correlation suggests that an increase in one of the elements does not necessarily lead to an increase in the other element in the farm site. At Covenant University farm only the following paired elements: As-Sr and Mo-Sr are

negatively correlated. The negative correlation of these pair elements also suggests that the elements are anthropogenic, that is, there presence in the soil is as a result of human activities. Integration of geophysical method and geochemical methods for soil characterisation in the study area have proved effective to aid sustainable precision agriculture. These studies can be used as basic information for the promotion and establishment of sustainable precision agriculture in the areas investigated.

## 6.3 Contributions to Knowledge

This study has contributed the following to knowledge:

i. trace, essential macro and rare earth elements associated with the agricultural soils in the study areas were generated, and this information will aid decision making for efficient and sustainable farming in the study sites by farmers and agricultural stakeholders;
ii. geospatial maps that highlights zones of high and low accumulation of essential nutrients were generated for the study areas;
iii. major soil pollutants such as arsenic (As), chromium (Cr), nickel (Ni), and lead (Pb), with carcinogenic tendencies in human were identified in the study areas; and
iv. soil nutrient-base catalogue of crops compartible with either study sites were delineated, These include; leafy vegetables, tomatoes, cucumber, grapes, lemon grass, tea, coffee, rubber and coconut for Covenant University farm, and roots and tuber crops such as potatoes, carrots, yam, cassava, ginger, turmeric, beets and cocoyam for Landmark University farm.

## 6.4 Recommendations

Based on the findings of this study, the following are recommended:

i. Soil analysis should be carried out before embarking on any agricultural activity on virgin farmlands to determine the soil fertility status;
ii. Governmental agencies and stakeholders in the zones should formulate policies and legislation that would encourage the adoption of precision agricultural technologies, thereby enhancing better management of farmlands and preservation of soil and the environment;

iii. Multidisciplinary approach and collaborations should be encouraged in agricultural researches by stakeholders to better understand the farmlands, increase crop yield and eventually attain food security which is one of the global sustainable goals; and

iv. Further research should be conducted in the study area to evaluate the extent of groundwater contamination due to the observed rare earth elements.

### 6.4.1 Limitation of the Research

The limitation of this study is the adoption of a smaller geographical area that is, Covenant University farm and Landmark University farm. However, the result of the findings may be applied to other locations of similar geographical enclave of the study.

## REFERENCES


Aaltonen, J. (1997). Seasonal changes of DC resistivity measurements. Proceedings of the 3rd Meeting of Environmental and Engineering Geophysical Society (EEGS) Conference, Aarhus, Denmark, 425-428.

Abrahim, G. M. S., Parker, R. J. (2008). Assessment of heavy metal enrichment factors and the degree of contamination in marine sediments from Tamaki Estuary, Auckland, New Zealand. *Environmental Monitoring Assessment,* 136, 227-238.

Adama, M., Esena, R., Mensah-Fosu, R., & Yirenya-Tawiah, D. (2016). Heavy metal contamination of soils around a hospital waste incinerator bottom ash dumps site. *Journal of Environmental and Public Health,* 89**,** 1- 6.

Adamchuk, V. I., Hummel, J. W., Morgan, M. T., & Upadhyaya, S. K. (2004). On-the-go soil sensors for precision agriculture. *Computer Electronic Agriculture,* 44**,** 71-91.

Adamu, S., Ayuba, M., Murtala, A., Uriah, L. A. (2014). Assessment of potentially toxic metals in soil and sediment of the Keana Brinefield in the Middle Benue Trough, Northcentral Nigeria. *American Journal of Environmental Protection, Special Issue: Integrating Earth Materials, Diet, Water and Human Health.* 3(6-2), 77-88. doi: 10.11648/j.ajep.s.2014030602.21

Adebayo, B. (2018). Nigeria overtakes India in extreme poverty ranking. Cable News Network (CNN), Lagos, Nigeria. Online Report. https://edition.cnn.com/2018/06/26.

Adegbite, K. A., Okafor, M. E., Adekiya, A. O., Alori, E. T., & Adebiyi, T. V. (2019). Characterisation and classification of soils of a toposequence in a derived Savannah agroecological zone of Nigeria. *The Open Agricultural Journal,* 14**(**13), 44-50.

Adeoti, B., & Okonkwo, C. T. (2017). Structural evolution of Iwaraja shear zone, southwestern Nigeria. *Journal of African Earth Sciences,* 131(6), 117-127.

Adewoyin, O. O., Omeje, M., Joel, E. S., & Aborishade, E. (2017). Carcinogenic risk of arsenic (As) in groundwater and bottled water samples in Covenant University and Canaanland, Ota, Ogun State, Nigeria. *Journal of Informatics and Mathematical Sciences,* 9(2), 273-281.

Adiaha, M. S. (2016). Influence of mineral fertilizer on the growth of maize (Zea mays L.) and soil fertility improvement for food security, environmental development and sustainable agriculture. *World Scientific News*, 56, 189-216.

Aditama, I. F., Widodo, Setiawan, T., Bijaksana, S., & Sanny, T. A. (2017). Use of electrical geophysical methods for supporting agricultural practices. AIP Conference Proceedings, 1861(1), 1-7.

Adrees, M., Ali, S., Rizwan, M., Ibrahim, M., Abbas F., Farid, M., Rehman, M. Z., Irshad, M. K., & Bharwana, S. A. (2015). The effect of excess copper on growth and physiology of important food crops: A review. *Environmental Science and Pollution Resource International*, 22(11), 8148-8162.

Ahmed, S. O., Abdalla, A. W. H., Inoue, T., Ping, A., & Babiker, E. E. (2014). Nutritional quality of grains of sorghum cultivar grown under different levels of micronutrients fertilization. *Food Chemistry*, 159**,** 374-380.

Aislabie, J., Deslippe, J. R., & Dymond, J. (2013). Soil microbes and their contribution to soil services. In J. Dymond (Ed.), *Ecosystem services in New Zealand: Conditions and trends* (143-161). Manaaki Whenua Press Lincoln, New Zealand.

Aizebeokhai, A. P. (2010). 2D and 3D geoelectrical resistivity imaging: theory and field design. *Scientific Research and Essays,* 5(23), 3592-3605.

Aizebeokhai, A. P., Olayinka, A. I., & Singh, V. S. (2010). Application of 2D and 3D geoelectrical resistivity imaging for engineering site investigation in a crystalline basement terrain, southwestern Nigeria. *Environmental Earth Sciences,* 61**,** 1481-1492.

Aizebeokhai, A. P., & Oyebanjo, O. A. (2013). Application of vertical electrical soundings to characterize aquifer potential in Ota, southwestern Nigeria. *International Journal of Physical Sciences,* 8(46), 2077-2085.

Aizebeokhai, A. P. & Oyeyemi, K. D. (2014). The use of the multiple-gradient array for Geoelectrical resistivity and induced polarization imaging. *Journal of Applied Geophysics*, 111, 364-376.

Akenga, P., Salim, A., Oniditi, A., Yusuf, A., & Waudo, W. (2014). Determination of selected micro and macronutrients in sugarcane growing soils at Kakamega North District, Kenya. *Journal of Applied Chemistry*, 7(7), 34-41.

Akinlalu, A. A., Adelusi, A. O., Olayanju, G. M., Adiat, K. A. N., Omosuyi, G. O., Anifowose, A. Y. B., & Akeredolu, B. E. (2018). Aeromagnetic mapping of basement structures and mineralisation characterisation of Ilesa Schist Belt, Southwestern Nigeria. *Journal of African Earth Sciences,* 138, 383-391.

Akinwumiju, A. S., & Olorunfemi, M. O. (2016). Shallow aquifer characteristics, borehole yield and groundwater resource sustainability assessment in the Osun river basin, southwestern, Nigeria. *Ife Journal of Science,* 18(2), 305-313.

Alikwe, S. (2019). Analysis of degraded and non-degraded soils in Irepodun Local Government Area of Kwara State, Nigeria. *International Journal of Research Studies in Agricultural Sciences*, 5(2), 32-39.

Allred, B., V. Adamchuk, R. Rossel, J. Doolittle, R. S. Freeland, Grote, K., & Corwin, D. (2016). Geophysical methods. In W. Chesworth (Ed.), *Encyclopedia of soil science* (3rd ed., 207 - 227). Berlin, Springer, USA.

Allred, B. J., Ehsani, M. R., & Daniels, J. J. (2008). General considerations for geophysical methods applied to agriculture. In B. J. Allred, J. J. Daniels & M. R. Ehsani (Eds.), *Hand-Book of agricultural geophysics* (3-16). CRC Press, Taylor and Francis Group, Boca Raton, Florida.

Allred, B. J., Fausey, N. R., Peters, J. L., Chen, C., Daniels, J. J., & Youn, H. (2004). Detection of buried agricultural drainage pipe with geophysical methods. *Applied Engineering in Agriculture,* 20**,** 307-318.

Allred, B. J., & Smith, B. D. (2010). Introduction to the JEEG agricultural geophysics special issue. *Journal of Environmental & Engineering Geophysics*, 15(3), V-VI.

Allred, B., Wishart, D., Martinez, L., Schomberg, H., Mirsky, S., Meyers, G., Elliot, J., & Charyton, C. (2018). Delineation of agricultural pipe patterns using ground penetration radar intehrated with a real-time kinematic global navigation satellite system. *Agriculture*, 8(167), 1-14.

Al-Shammary, A. A. G., Kouzani, A.Z., Kaynak, A., Khoo, S. Y., Norton, M., & Gates, W. (2018). Soil bulk estimation methods: a review. *Pedosphere*, 28(4), 581-596.

Amato, M., Bitella, G., Rossi, R., Gomez, J. A., Lovelli, S., & Ferreira, G. (2009). Muti-electrode 3D resistivity imaging of alfalfa root zone. *European Journal of Agronomy*, 31(4), 213-222.

Amato, J. M., Boullion, A. O. M., Serna, A. M., Sanders, A. E., Farmer, G. L., Gehrels, G. E., & Wooden, J. L. (2008). Evolution of the Mazatzal province and the timing of the Mazatzal orogeny: Insights from U-Pb geochronology and geochemistry of igneous and metasedimentary rocks in southern New Mexico. *Geological Society of America Bulletin*, 120(3-4), 328-346.

Amaya, A. G., Dahlin, T., Barmen, G., & Rosberg, J. (2016). Electrical resistivity tomography and induced polarization for mapping the subsurface of alluvial fans: A case study in Punata (Bolivia). *Geosciences*, 6(51), 1-13.

Ambrosone, M., Matese, A., Di Gennaro, S., Gioli, B., Tudoroiu, M., Genesio., … Toscano, P. (2020). Retrieving soil moisture in rainfed and irrigated fields using Sentinel-2 observations and a modified OPTRAM approach. *International Journal of Applied Earth Observation and Geoinformation*, 89(10), 1-18.

Amezketa, E. (2007). Soil salinity assessment using directed soil sampling from a geophysical survey with electromagnetic technology: a case study. *Food and Agricultural Organisation of the United Nations*, 10, 91-101.

Amor, S. (2013). An overview of geochemical methods, geological survey of newfound land and labrador apparent soil electrical conductivity, Part II, case study. *Computers and Electronics in Agriculture,* 46, 135-152.

An, N., Tang, C.S., Cheng, Q., Wang, D. Y., & Shi, B. (2020). Application of electrical resistivity method in the characterisation of 2D desiccation cracking process of clayey soil. *Engineering Geology*, 265(105416), 1-14.

Anabaraonye, B., Chukwuma, J., & Okafor, C. J. (2019). Educating farmers and fishermen in rural areas in Nigeria on climate change mitigation and adaptation for global sustainability. *International Journal of Scientific & Engineering Research,* 10(4), 1391-1398.

Aondoakaa, S. C., & Agbakwuru, P. C. (2012). An assessment of land suitability for rice cultivation in Dobi, Gwagwalada area council, FCT – Nigeria. *Ethiopian Journal of Environmental Studies and Management,* 5(4), 1-8.

Apostol, K. G., & Zwiazek, J. J. (2003). Hypoxia affects root sodium and chloride concentrations and alters water conductance in salt-treated jack pine (Pinus banksiana) seedlings. *Trees,* 17(3), 251-257.

Araghi, A., Adamouski, J., Martinez, C. J., & Olesen, J. E. (2019). Projections of future soil temperature in northern Iran. *Geoderma*, 349, 11-24.

Araghi, A., Baygi, A. A., Adamowski, J., Martinez, C., & Ploeg, M. (2017). Forecasting soil temperature based on surface air temperature using a wavelet artificial neural network. *Meteorological Applications*, 24(4), 603-611.

Artiola, J. F., Walworth, J. L., Musil, S. A., & Crimmins, M. A. (2019). Soil and land pollution. In: Brusseau, M. L., Pepper, I. L. and Gerba, C. P. (Eds.) *Environmental and Pollution Science* (3rd ed.,). Academic Press, USA, 219-235.

Aubert, B. A., Schroeder, A., & Grimaudo, J. (2012). IT as enabler of sustainable farming: An empirical analysis of farmers' adoption decision of precision agriculture technology. *Decision Support Systems*, 54, 510-520.

Ayeni, L. S., & Akinbani, A. S. (2015). Assessing of soil fertility management among the arable crop farmers in Ondo southern Nigeria. *American Journal of Research Communication,* 3(2), 25-34.

Ayyogari, K., Sidhya, P., & Pandit, M. K. (2014). Impact of climate change on vegetable cultivation – a review. *International Journal of Agriculture, Environment and Biotechnology*, **7**(1), 145-141.

Badawy, W. M., Duliu, O. G., Frontasyeva, M., El-Samman, H., & Mamikhin, S. (2019). Dataset of elemental compositions and pollution indices of soil and sediments: Nile River and Delta Egypt. *Data in Brief*, 28, 1-10.

Bado, V. B., Djaman, K., & Mei, V. (2018). Developing fertilizer recommendations for rice in Sub-Saharan Africa, achievements and opportunities. *Paddy Water Environment*, 16, 571-586.

Bahnasawy, N. M. A., El Kady, M. M., & Elwa, A. M. (2019). Mineralo-chemical study of titanium and zirconium as indicators for soil profile uniformity and development. *American-Eurasian Journal of Sustainable Agriculture*, 13(3), 10-20.

Balafoutis, A., Beck, B., Fountas, S., Vangeyte, J., Van der Wal, T., Soto, I., Gómez-Barbero, M., Barnes, A., & Eory, V. (2017). Precision agriculture technologies positively contributing to GHG emissions mitigation, farm productivity and economics Athanasios. *Sustainability*, 9(1339), 1-28.

Baldock, J. A., & Skjemstad, J, O. (1999). Soil organic carbon/ soil organic matter: In: Peverill, K. I., Sparrow, L. A, Reuter, D. J. (Eds.). Soil Analysis: An Interpretation Manual. CSIRO Publishing, 159-170.

Banerjee, D., Maji, A. K., & Mahapatra, S. (2012). A review of its traditional uses, phytochemistry, pharmacology and toxicity. *Research Journal of Phytochemistry*, 6, 31-41.

Banuelos, G. S., & Ajwa, H. A. (1999). Trace elements in soils and plants: an overview. *Journal of Environmental Science and Health*, 34(4**),** 951-974.

Banton, O., Cimon, M. A., & Seguin, M. K. (1997). Mapping field-scale physical properties of soil with electrical resistivity. *Soil Science Society of America Journal Abstracts*, 61(4), 1010-1017.

Barry, C. S., McQuinn, R. P., Chung, M. Y., Besuden, A., & Giovannoni, J. J. (2008). Amino acid substitutions in homologs of the stay-green protein are responsible for the green-flesh and chlorophyII retainer mutations of tomatoes and pepper. *Plant Physiology*, 147(1), 179-187.

Basga, S. D., Madi, O. P., Balma, J., Abib, F. C., Tsozue, D., & Njiemoun, A. (2018). Sandy soil fertility restoration and crops yields after conversion of long term Acacia Senegal planted fallows in North Cameroon. *African Journal of Agricultural Research*, 13(40), 2154-2162.

Basga, S. D., & Nguetnkam, J. P. (2015). Fertilizing effect of swelling clay materials on the growth and yield of bean "*Phaseolus vulgaris*" on the sandy ferruginous soils from Mafa Tcheboa (North Cameroun, Central Africa). *International Journal of Plant and Soil Science,* **5**(1), 10-24.

Bartsev, S. I., & Pochekutov, A. A. (2016). The vertical distribution of soil organic matter predicted by a simple continuous model of soil organic matter transformations. *Ecological Modelling*, 328**,** 95-98.

Baumgardner, M. F., Silva, L. F., Biehl, L. L., & Stoner, E. R. (1986). Reflectance properties of soils. *Advances in Agronomy*, 38**,** 1- 44.

Beesley, L., Moreno-Jiménez, E., Clemente, R., Lepp, N., & Dickinson, N. (2010). Mobility of arsenic, cadmium and zinc in a multi-element contaminated soil profile assessed by in-situ soil pore water sampling, column leaching and sequential extraction. *Environmental Pollution*, 158, 155-160.

Benderitter, Y., & Schott, J. J. (1999). Short time variation of the resistivity in an unsaturated soil: the relationship with rainfall. *European Journal of Engineering Geophysics*, 4**,** 37-49.

Benson, N. U., Essien, D. U., Essien, P. U., Anake, W. U., Adedapo, A. E., Akintokun, O. A., & Fred-Ahmadu, O. H. (2017). Geochemical fractionation and ecological risks assessment of benthic sediment- bound heavy metals from coastal ecosystems off the Equitorial Atlantic Ocean. *International Journal of Sediment Research*, 32, 1-11.

Benson, N. U., Fred-Ahmadu, O. H., Olugbuyiro, J. A. O., Anake, W. U., Adedapo, A. E., & Olajare. A. A. (2018). Concentrations, sources and risk characterisation of polycyclic aromatic hydrocarbon (PAH) in green, herbal and black tea products in Nigeria. *Journal of Food Composition and Analysis*, 66, 13-22.

Binley, A., Hubbard, S. S., Huisman, J. A., Revil, A., Robinson, D. A., Singha, K., & Slater, L. D. (2015). The emergence of hydrogeophysics for improved understanding of subsurface processes over multiple scales. *Water Resources Research*, 51(6), 3837-3866.

Biratu, G. K., Elias, E., & Ntawuruhunga, P. (2019). Soil fertility status of cassava fields treated by integrated application of manure and NPK fertilizer in Zambia. *Environmental System Research,* 8(3). https://doi.org/10.1186/s40068-019-0131-7.

Bitella, G., Rossi, R., Loperte, A., Satriani, A., Lapenna, V., Perniola, M., & Amato, M. (2015). Geophysical techniques for plant, soil, and root research related to sustainability. In A. Vastola (Ed.), *The sustainability of agro-food and natural resource systems in the Mediterranean Basin* (pp. 353-372). Springer International Press, Switzerland.

Bleam, W. F. (2016). Soil and environmental chemistry. Research and Markets Brochure. Retrieved from: http://www.researchandmarkets.com/reports/1763463/. 12/4/2020, 1-3.

Blanco-Canqui, H., Hergert, G W., & Nielsen, R. A. (2015). Cattle manure application reduces soil compactibility and increases water retention after 71 years. *Soil Science Society of America Journal*, 79, 212-223.

Bojorquez-Quintal, E., Escalante, C., & Martinez-Estevez, M. (2017). Aluminium, a friend or foe of higher plants in acid soils. *Frontier's in Plant Science*, 8, 1-18.

Bonomelli, C., Gil, P. M., & Schaffer, B. (2019). Effect of soil type on calcium absorption and partitioning in young avocado (Persea americana Mill.) trees. *Agronomy*, 9(837), 1-11.

Born, M., & Wolf, E. (1999). Basic properties of the electromagnetic field. *Principles of Optics*, (7th ed., 1-74), Cambridge University Press, Cambridge, United Kingdom.

Boulet, G., Mougenot, B., & Abdelouahab, T. B. (2009). An evaporation test based on thermal infra-red remote-sensing to select appropriate soil hydraulic properties. *Journal of Hydrology,* 376 (3-4), 589-598.

Box, S. E., Bookstrom, A. A., Ikramuddin, M., & Lindsay, J. (2001). Geochemical analysis of soils and sediments, Coeur d'Alene drainage basin, Idaho: sampling, analytical methods, and results. Open File Report, U S Geological Survey Publisher, 139. Retrieved from https://pubs.usgs.gov/of/2001/of01-139/. Accessed: 16/12/19.

Brady, N. C., & Weil, R. R. (1999). The nature and properties of soils. 12th Edition, Prentice Hall Publishers, London, 1-9(453-536), 739-740.

Brevik, E. C., Homburg, J. A., Miller, B. A., Fenton, T. E., & Doolittle, J. A. (2016). Selected highlights in American soil science history from the 1980s to the mid-2010. *Catena*, 146**,** 128-146.

Briat, J. F. (2005). Iron from soil to plant products. *Bulletin Academic National Medicine*, 189(8), 1609-1621.

Brown, O. (2018). Effects of soil temperature on some soil properties and plant growth. *Advances in Plants and Agriculture Research*, 8(1), 37-41.

Brunet, P., Clement R., & Bouvier, C. (2010). Monitoring soil water content and deficit using electrical resistivity tomography (ERT) – a case study in the Cevennes area, France. *Journal of Hydrology*, 380(1-2**),** 146-153.

Buchan, G. D. (2001). Soil temperature regime. In K. A. Smith & C. Mullins (Eds.), *Soil and environmental analysis: physical methods* (pp. 539-594*)*. New York, Marcel Dekker.

Burger, A., & Lichtscheidl, I. (2019). Strotium in the environment: Review about reactions of plants towards stable and radioactive strontium isotopes. *Science of the Total Environment*, 653, 1458-1512.

Butcher, K., Wick, A. F., DeSutter, T., Chatterjee, A., & Harmon, J. (2016). Soil salinity: a threat to global food security. *Agronomy Journal*, 108(6), 2189-2200.

Buvat, S., Thiesson, J., Michelin, J., Nicoullaud, B., Bourennane, H., Coquet, Y., & Tabbagh, A. (2014). Multi-depth electrical resistivity survey for mapping soil units within two 3ha plots. *Geoderma*, 50(10), 8356-8366.

Calamita, G., Brocca, L., Perrone, A., Piscitelli, S., Lapenna, V., Melone, F., & Moramarco, T. (2012). Electrical resistivity and TDR methods for soil moisture estimation in central Italy test-sites. *Journal of Hydrology*, 10(454 - 455), 101-112.

Calicioglu, O., Flammini, A., Braccos, S., Bellu, L., & Sims, R. (2019). The future challenges of food and agriculture: an integrated analysis of trends and solution. *Sustainability*, 11(222), 1-21.

Cardoso, A. I. I., Silva, P. N., Colombari, L. F., Lanna, N. B. L., & Fernandes, D. M. (2019). Phosphorus sources associated with organic compound in broccoli production and soil chemical attributes. *Horticultura Brasileira*, 37(92), 228-233.

Carpenter, D., Boutin, C., Allison, J. E., Parsons, J. L., & Ellis, D. M. (2015) Uptake and effects of six rare earth elements (REEs) on selected native and crop species growing in contaminated soils. *PLoS ONE*, 10(6), 1-9.

Cassman, K. G. (1999). Ecological intensification of cereal production systems: yield potential, soil quality and precision agriculture. *Proceedings of the National Academy of Sciences*, 96 (11), 5952-5959.

Cecconi, E., Incerti, G., Capozzi, F., Adamo, P., Bargagli, R., Benesperi, R., …Tretiach, M. (2019). Background element content in the lichen *Pseudevernia furfuracea*: a comparative analysis of digestion methods. *Environmental Monitoring and Assessment,* 191(260), 1-10.

Chakraborty, K., & Mistri, B. (2015). Importance of soil texture in sustenance of agriculture: a study in Burdwan-I C. D. Block, Burdwan, West Bengal. *Eastern Geographer,* XXI (1), 475-482.

Chambers, L. G., Guevara, R., Boyer, J. N., Troxler, T. G., & Davis, S. E. (2016). Effects of salinity and inundation on microbial community structure and function in a mangrove peat soil. *Wetlands,* 16, 745-752.

Champagne C., McNairna H., & Bergb A. A. (2011). Monitoring agricultural soil moisture extremes in Canada using passive microwave remote sensing. *Remote Sensing of Environment,* 115(10), 2434-2444.

Chaudhary, I., & Singh, V. (2020). Titanium dioxide nanoparticles and its impact on growth, biomass and yield of agricultural crops under environmental stress: a review. *Research Journal of Nanoscience and Nanotechnology,* 10, 1-8

Chen, B., Garre, S., Liu, H., Yan, C., Liu, C., Gong, D., & Mei, X. (2019). Two-dimensional monitoring of soil water content in fields with plastic mulching using electrical resistivity tomography. *Computers and Electronics in Agriculture,* 159, 84-91.

Cheng, X., Drozdova, J., Danek T., Huang Q., Qi, W., Yang S, Zhao, X., & Xiang, Y. (2018). Pollution assessment of trace elements in agricultural soils around copper mining area. *Sustainability,* 10(4533), 1-18.

Chiou, W., & Hsu, F. (2019). Copper toxicity and prediction models of copper content in leafy vegetables. *Sustainability*, 11(22), 1-18.

Chude, V. O., Malgwi, W. B., Amapu, I. Y., & Ano, O. A. (2011). Manual on soil fertility assessment. Federal Fertilizer Department (FFD) in collaboration with National Programme for Food Security, Abuja, Nigeria, 1-22.

Cohen, Y., Alchanatis, V., Meron, M., Saranga, Y., & Tsipris, J. (2005). Estimation of leaf water potential by thermal imagery and spatial analysis. *Journal of Experimental Botany*, 56(417), 1843-1852.

Collins, M. E., & Doolittle, J. A. (1987). Using ground-penetrating radar to study soil microvariability. *Soil Science Society of America Journal,* 51(2), 491- 493.

Condit, H. R. (1970). The spectral reflectance of American soils. *Photogrammetric Engineering*, 36**,** 955-966.

Condit, R. R. 1972. Application of characteristic vector analysis to the spectral energy distribution of daylight and the spectral reflectance of American soils. *Photogrammetric Engineering,* 40, 445-454.

Corwin, D. L., & Lesch, S. M. (2003). Application of soil electrical conductivity to precision agriculture: Theory, principles, and guidelines. *Agronomy Journal* 95(3), 455-471.

Corwin, D. L., & Lesch, S. M. (2005). Characterizing soil spatial variability with apparent soil electrical conductivity: part II. *Computers and Electronics in Agriculture,* 46(1), 136-152.

Crites, S. T., & Lucey, P. G. (2015). Revised mineral and Mg maps of the Moon from integrating results from the lunar prospector neutron and gamma-ray spectrometers with Clementine spectroscopy. *American Mineralogist*; 100(4), 973-982.

Curran, P. J. (1985). Principles of remote sensing. *International Journal of Remote Sensing*, 6(11), 1765-1777.

Davidson, E. A., & Janseen, I, A. (2006). Temperature sensitivity of soil carbon decomposition and feedbacks to climate change. *Nature*, 440(7081), 165-173.

Dahlin, T. (2001). The development of electrical imaging techniques. *Computers and Geosciences*, 27(9), 1019-1029.

Darch, T., Dunn, R. M., Guy, A., Hawkins, J. M. B., Ash, M., Frimpong, A. A., & Blackwell, M. S. A. (2019). Fertilizer produced from abattoir waste can contribute to phosphorus sustainability, and biofortify crops with minerals. *Plos One*, 14(9), 1-13.

Delgado, J. M. P., Gutierrez, E. Q., Ruvalcaba, L. P., Alcaraz, V. V., Valdes, T.D., Tafoya, F. A., & Lopez, M. V. (2015). Yield of tomato in soil treated with compost, amorphous primary minerals and microorganisms. *Open Access Library Journal*, 2(9), 1-13.

Dexter, A. R., Horn, A. R., & Kemper, W. D. (1988). Two mechanism for age-hardening of soil. *European Soil Science Journal*, **37**(2), 163-175.

Di Lonardo, D. P., Manrubia, M., DeBoer, W., Zweer, S. H, Veen, G. F., & Van der Wal, A. (2018). Relationship between home-field advantage of litter decomposition and priming of soil organic matter. *Soil Biology and Biochemistry*, 126, 49-56.

Dick, J., Tetzlaff, D., Bradford, J., & Soulsby, C. (2018). Using repeat electrical resistivity surveys to assess heterogeneity in soil moisture dynamics under contrasting vegetation types. *Journal of Hydrology*, 559, 684-697.

Diel J, Vogel, H., & Schluter S. (2019). Impact of wetting and drying cycles on soil structure dynamics. *Geoderma*, 345(1), 63-71.

Dong, J., Crow, W. T., Tobin, K. J., Cosh, M. H., Bosch, D.D., Starks, P. J., Seyfried, M., & Collins, C. H. (2020). Archaeological reconnaissance through multi-method geophysical and geochemical survey at two Iroquoian village sites, southern Ontario, Canada. *Remote Sensing of Environment*, 242(111756), 1-14.

Doolittle, J. A., & Brevik, E. C**.** (2014). The use of electromagnetic induction techniques in soil studies. *Geoderma*, 223(225), 33-45.

Doran, J. W., & Safley, M. (1997). Defining and assessing soil health and sustainable productivity. In C. Pankhurst, B. M. Doube. and V. V. S. R. Gupta (Eds.), *Biological Indicators of Soil Health*. CAB International, Wallingford, Oxon, UK, 1-28.

Dortzbach, D., Pereira, M, G., Cunhados Anjos, L. H., Fontana, A., & Silva Neto, E, D. (2016). Genesis and classification of soils from subtropical mountain regions of southern Brazil. *Revista Brara de Gencia do Solo,* 40**,** 1-15.

Dou, F., Soriano, J., Tabien, R., & Chen, K. (2016). Soil texture and cultivar effects on Rice (*Ortyza sativa, L*.) grain yield, yield components and water productivity in three water regimes. *Plos One,* 11(3), 15-23.

Douaoui, A. E. K., Nicholas, H., & Walter, C. (2006). Detecting salinity hazards within a semiarid context by means of combining soil and remote sensing data. *Geoderma,* 134 (1-2), 217-230**.**

Dwevedi, A., Kumar, P., Kumar, P., Kumar, Y., Sharma, Y. K., & Kayastha, A. M. (2017). Soil sensors: detailed insights into research updates, significance, and future prospects. *New Pesticides and Soil Sensors*, 5, 561-594.

Ebrahimi, P., & Barbieri, M (2019). Review gadolinium as an emerging microcontaminant in water resources: Threats and opportunities. *Geosciences,* 9(93), 1-44.

Eisele, A., Chabrillat, S., Heckerb, C., Hewson, R., Lau, C. I., Rogass, C., Segl, K., Cudahy, T. J., Udelhoven, T., Hostert, P., & Kaufmann, H. (2015). Advantages using the thermal infrared (TIR) to detect and quantify semi-arid soil properties. *Remote Sensing of Environment*, 163**,** 296-311.

Ekanade, O. (2007). Cultured trees, their environment and our legacies. *Obafemi Awolowo University Press Ltd.*, Inaugural Lecture Series, 198**,** 1-44.

Ekanade, O. & Egbe, N. E. (1990). An analytical assessment of agroforestry practices resulting from interplanting cocoa and kola on soil properties in southwestern, Nigeria. *Agriculture, Ecosystem and Environment,* 30(3 - 4), 337-346.

El-Habbasha, S. F., & Ibrahim, F. M. (2015). Calcium: physiological function, deficiency and absorption. *International Journal of ChemTech Research,* 8(12), 196-202.

El Nahry, A. H., Ali R. R., & El Baroudy A. A (2011). An approach for precision farming under pivot irrigation system using remote sensing and GIS techniques. *Agriculture Water Management,* 98(4), 517-531.

Eluwole, A. B., Olorunfemi, M. O., & Ademilua, O. L. (2018). Soil horizon mapping and textural classification using micro soil electrical resistivity measurements: case study from Ado-Ekiti, southwestern Nigeria. *Arabian Journal of Geosciences,* 11**(**315), 1-21. https://doi.org/10.1007/s12517-018-3652-x.

Emerald, L. (2015). Your lawn and fall fertilization. Round Rock Austin Corporate, Online Source, https://www.landscapemanagement.net/lawn-care-the-right-way/ Accessed: 9/10/2019.

Enamorado-Baez, Abril, J. M., & Gomez-Guzman, J. M. (2013). Determination of 25 trace element concentrations in biological reference materials by ICP-MS following different microwave-assisted acid digestion methods based on scaling masses of digested samples. *International Scholarly Research Notices*, 10, 1-14.

Eory, V., MacLeod, M., Topp C. F. E., Rees, R. M., Webb, J., McVittie, A., Wall, E., Borthwick, F., Watson, C., Waterhouse, A., Wiltshire, J., Bell, H., Moran, D., & Dewhurst, R. J. (2015). Review and update of the UK agriculture MACC to assess the abatement potential for the 5th carbon budget period and to 2050, the Committee on Climate Change, 1-274.

Ertani, A., Mietto, A., Borin, M., & Nardi, S. (2017). Chromium in agricultural soils and crops: a review. *Water, Air and Soil Pollution,* 228(190), 1-10.

Esmaeili, A., Moore, F., Keshavarzi, B., Jaafarzadeh, N., & Kermani, M. (2014). A geochemical survey of heavy metals in agricultural and background soils of the Isfahan industrial zone, Iran. *Catena,* 121, 88-98.

Espinoza, L., Slaton, N. & Mozaffari, M. (2006). Understanding the numbers on your soil test report. University of Arkansas Extension, *Agriculture and Natural Resources,* FSA 2118.

Eswaran, H., Vearasilp, T., Reich, P., & Benroth, F. (2006). Sandy soils of Asia: a new frontier for agricultural development? Proceedings of Management of Tropical Sandy Soils for Sustainable Agriculture: Thailand, FAO Regional Office Bangkok, 22-30.

Etesami, H., & Noori, F. (2019). Soil salinity as a challenge for sustainable agriculture and bacteria mediated alleviation of salinity stressed in crop plants. In M. Kumar, H. Etesami & V. Kumar (Eds.), Saline soil-based agriculture by halotolerant microorganisms (1-22). Springer, Singapore.

EU - European Union (2002). Heavy metals in wastes, European Commission on Environmment. Assessed: 12/11/2019. http://ec.europa.eu/environment/waste/studies/pdf/heavymetalsreport.pdf.

Ezema, O. K., Ibuot, J. C., & Obiora, D. N. (2020). Geophysical investigation of aquifer repositories in Ibagwa Aka, Enugu State, Nigeria, using electrical resistivity method. *Groundwater for Sustainble Development*, 11(100458), 1-9.

Fagbohun, B. J., Adeoti, B., & Aladejana, O. O. (2017). Litho-structural analysis of eastern part of Ilesha schist belt, Southwestern Nigeria. *Journal of African Earth Sciences*, 133, 123-137.

Fairbridge, R. W. (1998). History of geochemistry. In: Geochemistry. Encyclopedia of Earth Science. Springer, Dordrecht, 978(1), 4496-4504.

Fan, J., McConkey, B., Wang, H., & Jansen, H. (2016). Root distribution by depth for temperate agricultural crops. *Field Crops Research*, 189, 68-74.

Fang, B., Lakshmi, V., Jackson, T. J., Bindlish, R., & Colliande, A. (2019). Passive/active microwave soil moisture change disaggregation using SMAPVEX12 data, *Journal of Hydrology*, 574, 1085-1098.

FAO - Food and Agriculture Organisation (2019a). The state of food security and nutrition in the world (2019). https://www.un.org/en/sections/issues-depth/food/index.html.

FAO - Food and Agriculture Organisation (2019b). Agriculture Post, Agriculture Post Bureau, Online, 1-2.

FAO - Food and Agriculture Organisation (2017). Soils. Key to unlocking the potential of mitigating and adopting to a changing climate. Sustainable Development Goals (SDG) goal 13.

FAO - Food and Agricultural Organisation, (2005). Voluntary Guidelines to support the progressive realization of the right to adequate food in the context of national food security. Rome. Retrieved from www.fao.org/righttofood. www.gtz.de/foodsecurity 12/12/2019.

FAO - Food and Agriculture Organization of the United Nations (2001). *Bulletin of the state of food and agriculture FAO, Rome, Italy*, 1-21.

Fausey, N. R. (2005). Drainage, surface and sub surfaces. *Encyclopedia of Soils in the Environment*, 409-413.

Finch, C., Roldan, R., Walsh, L., Kelly, J., & Amor, S. (2018). Analytical methods for chemical analysis of geological materials. Government of New foundland and Labrador, Department of Natural Resources. *Geological Survey, Open File NFLD* (3316), 1-24.

Fisher, S. C., Reilly, T. J., Jones, D. K., Benzel, W. M., Griffin, D. W., Loftin, K. A., Iwanowicz, L. R., & Cohl, J. A. (2015). Standard operating procedure for collection of soil and sediment samples for the Sediment-bound Contaminant Resiliency and Response (SCoRR) strategy pilot study: U.S. Geological Survey Open-File Report 2015–1188b, 37 p., http://dx.doi.org/10.3133/ofr20151188B.

Forkuor, G., Hounkpatin, O. K. L., Welp, G., & Thiel, M. (2017). High resolution mapping of soil properties using remote sensing variables in South-Western Burkina Faso: A comparison of machine learning and multiple linear regression models. *PLoS ONE*, 12(1), 1-21.

Fosu-Mensah, B. Y., Addae, E., Yirenya-Tawiah, D., & Nyame, F. (2017). Heavy metals concentration and distribution in soils and vegetation at Korle Lagoon area in Accra, Ghana. *Cogent Environmental Science*, 3(1), 1-8.

Fukue, M., Minatoa, T., Horibe, H., & Taya, N. (1999). The micro-structure of clay given by resistivity measurements. *Engineering Geology*, 54(1-2), 43-53.

Gahoonia, T. S. & Nielsen, N. E. (2003). Phosphorus (P) uptake and growth of a root hairless barley mutant (bald root barley, brb) and wild type in low-and high-P soils. *Plant Cell and Environment*, 26(10), 1759-1766.

Ganiyu, S. A., Olurin, O. T., Oladunjoye, M. A., & Badmus, B. S. (2019). Investigation of soil moisture content over a cultivated farmland in Abeokuta Nigeria using electrical resistivity methods and soil analysis. *Journal of King Saud University of Science*, 02(016), 1-11.

Garg, A., Munoth, P., & Goyal, R. (2016). *Application of soil moisture sensors in agriculture: a review*. Proceedings of International Conference on Hydraulics, Water Resources and Coastal Engineering (pp. 1662-1672). Pune, India. Retrieved from https://www.researchgate.net/publication/311607215 (accessed April 18 2020).

Garrett, R. G., Reimann, C., Smith, D. B., & Xie, X. (2008). From geochemical prospecting to international geochemical sampling: a historical overview. *Geochemistry: Exploration, Environment, Analysis*, 8, 205-217.

Ge, Y., Thomasson, J. A. & Sui, R. (2011). Remote sensing of soil properties in precision agriculture: A review. *Frontier of Earth Science*, **5(3**), 229-238.

Gebbers, R., & Adamchuck, V. I. (2010). Precision agriculture and food security. *Science*, **327(**5967), 828-831.

Ghazali, M. F., Wikantika, K., Harto, A, B., & Kondoh, H. (2019). Generating soil salinity, soil moisture, soil pH from satellite imagery and its analysis, *Information Processing in Agriculture,* **08,** 1-13.

Giao, P., Chung, S., Kim, D., & Tanaka, H. (2003). Electric imaging and laboratory resistivity testing for geotechnical investigation of Pusan clay deposits. *Journal of Applied Geophysics*, **52,** 157-175.

Goldschmidt, V. M. (1954). Geochemistry. Clarendon Press, Oxford, 1-730.

Golovko, L., & Pozdnyakov, A. I. (2007). *Electrical geophysical methods in agriculture*. In C. Zhao (Ed.), Progress of informational technology in agriculture. Proceedings of the 4th International Symposium on Intelligent Information Technology in Agriculture (pp. 457-471). Beijing, China.

Gómez-Merino, F. C., & Trejo-Téllez, L. I. (2018). *The role of beneficial elements in triggering adaptive responses to environmental stressors and improving plant performance*. In S. Vats (Ed.), Biotic and abiotic stress tolerance in plants. Springer, Singapore. https://doi.org/10.1007/978-981-10-9029-5_6.

Gong, Q., Liu, N., Wu, X., Yan, T., Fan, T., Li, X., Liu, M., Li, R., & Albanese, S. (2020). Using regional geochemical survey data to trace anomalous samples through geochemical genes: The Tieshanlong tungsten deposit area (Southeastern China) case study. *Journal of Geochemical Exploration*, 219(106637), 1-13.

Gou, X., Tan, B., Wu, F., Yang, W., Xu, Z., Li, Z., & Zhang, X. (2015). Seasonal dynamics of soil microbial biomass c and n along an elevational gradient on the eastern Tibetan Plateau, China. *PLoS ONE*, 10(7), 1-8

Gransee, A., & Fuhrs, H. (2012). Magnesium mobility in soils as a challenge for soil and plant analysis, magnesium fertilization and root uptake under adverse growth conditions, *Plant and Soil*, 368(1-2), 5-21.

Guagliardia, I., Cicchellab, D., De Rosac, R., Riccaa, N., & Buttafuoco G. (2018). Geochemical sources of vanadium in soils: evidences in a southern Italy area. *Journal of Geochemical Exploration*, 184, 358-364.

Guang-Hui, Y., Chun-Mei, C., Xin-Hua, H., Zhiang-Zhi, Z., & Li-Na, L. (2020). Unexpected bulk density and microstructures response to long-term pig manure application in a ferralic cambisol soil: Implications for rebuilding a healthy soil. *Soil and Tillage Research*, 203, 1-8. https://doi.org/10.1016/j.still.2020.104668.

Guerinot, M. L., & Yi, Y. (1994). Iron: nutritious, noxious, and not readily available. *Plant physiology*, 104(3), 815-820.

Gupta, P., & Follette-Cook, M. (2017). Fundamentals of satellite remote sensing. Applied Remote Sensing Training: National Aeronautical and Space Administration (NASA), University of California, 1 – 31. http://arset.gsfc.nasa.gov. Accessed 09/3/2020.

Gupta, M., & Gupta, S. (2017). An overview of selenium uptake, metabolism, and toxicity in plants. *Frontiers in Plant Science*, **7,** 2074-2085.

Hakanson, L. (1980) An ecological risk index for aquatic pollution control: a sedimentological approach, *Water Resources*, 14, 975-1001.

Haldar, S. K. (Ed.). (2013). Exploration geochemistry. In: Mineral exploration, principles and applications, Australia: Elsevier, 55-71.

Halim, M. A., Majumder, R, K., & Zaman, M. N. (2015). Paddy soil heavy metal contamination and uptake in rice plants from the adjacent area of Barapukuria coal mine, northwest Bangladesh. *Arabian Journal of Geosciences*, 8, 3391-3401.

Hamman, A. A., & Mohamed, E. S. (2018). Mapping soil salinity in the East Nile Delta using several methodological approaches of salinity assessment. *The Egyptian Journal of Remote Sensing and Space Sciences*, 1, 1-7.

Hao, L. N., Su, X. L., & Singh, V. P. (2018). Cropping pattern optimization considering uncertainty of water availability and water saving potential. *International Journal of Agricultural and Biological Engineering*, 11(1), 178-186.

Hao, X., Ball, B. C., Culley, J. L. B., Carter , M. R., & Parkin, G. W. (2019). Soil density and porosity. In X. Hao (Ed.), *Soil sampling and methods of analysis* (pp. 743-759).

Hartikainen, H. (2005). Biogeochemistry of selenium and its impact on food chain quality and human health. *Journal of Trace Elements and Medical Biology*, 18(3), 309-327.

Haroun, M., Idris, A., & Syed-Omar, S. R. (2007). A study of heavy metals and their fate in the composing of tannery sludge. *Waste Management*, **27**(11), 1541-1550.

Haruna, I. V. (2017). Review of the basement geology and mineral belts of Nigeria. *Journal of Applied Geology and Geophysics*, 5(1), 37-45.

Hawkes, H. E. (1957). Principles of geochemical prospecting. United States Geological Survey Bulletin, 1000-F: 1-142.

Hazreek, Z. A. M., Raqib, A. G. A., Aziman, M., Azhar, A. T. S., Khaidie, A. T. M., Fairus, M., Rosli, S., Fakhrurrazi, I. M., & Izzaty, R. A. (2017). Preliminary groundwater assessment using electrical method at Quaternary deposits area. *IOP Conference Series*: *Materials Science and Engineering*, 226-235.

Heil, K., & Schmidhalter, U. (2017). The Application of EM38: Determination of soil parameters, selection of soil sampling points and use in agriculture and archaeology. *Sensors,* 17 (2540), 1-44.

Hengi, T., Leenaars, J. G. B., Shepherd, K. D., Walsh, M. G., Heuvelink, G. B. M., Mamo, T., Tilahum, H., Berkhout, E., Cooper, M., Fegraus, E., Wheeler, I., & Kwabena, N. A. (2017). Soil nutrient maps of Sub-Saharan Africa: assessment of soil nutrient content at 250 m spatial resolution using machine learning, *Nutrition Cycle Agroecosystem*, 109**,** 77-102.

Hicks, L. C., Meir, P., Nottingham, A, T., Reay, D. S., Stott, A. V., Salinas, N., & Whitaker, J. (2019). Carbon and nitrogen inputs differentially affect priming of soil organic matter in tropical lowland and montane soils. *Soil Biology and Biochemistry*, 129, 212-222.

Higgins, S., Schellberg, J., & Bailey, J. S. (2019). Improving productivity and increasing the efficiency of soil nutrient management on grassland farms in the UK and Ireland using precision agriculture technology, *European Journal of Agronomy, 106,* 67-74.

Hillel, D. (2003). Introduction to environmental soil physics. Academic Press, Elsevier: 1-494.

Holz. D. J., Williard, K. W. J., Edwards. P. J., & Schoonover, J. E. (2015). Soil erosion in humid regions: *A Review. Journal of Contemporary Water Research and Education,* 154: 48-59.

Horneck, D. A., Sullivan, D. M., Owen, J. S., & Hart, J. M. (2011). Soil test interpretation guide. Technical Report Number: EC1478. Oregon Cooperative Extension, 1-12.

Hooda, P. (2010). Trace elements in soils. *European Journal of Soil Science*, 61(6), 1119-1120.

Hossain, M. A., Begum, A., & Akhtar, K. (2017). Study on knowledge about arsenic contamination in drinking water among the people living in selected villages of Bangladesh. *Journal of Shaheed Suhrawardy Medical College*, 6, 57-59.

Hovhannissian, G., Podwojewski, P., Troquer, Y., Mthimkhulu, S., & Antwerpen, R, V. (2019). Geoelectrohydraulic Investigation of the surficial aquifer units and corrosivity in parts of Uyo L. G. A., AkwaIbom, Southern Nigeria. *Geoderma,* 349, 56-67.

Hu, Z., Haneklaus, S., Sparovek, G., & Schnug, E. (2006). Rare earth elements in soils. Communication in Soil Science Plant Analysis, 37(9-10), 1-16.

Hubacek, M., Almasiová, L., Dejmal, K. & Mertová, E. (2017) Combining different data types for evaluation of the soils passability. In I. Ivan, A. Singleton, J. Horák & T. Inspektor (Eds.), The rise of big spatial data. Lecture Notes in Geoinformation and Cartography, Springer, 1-7.

Husson, M. E., & Rieley, J. O. (2018). Peatland and biodiversity and conservation in southeast Asia. *Mire and Peats,* 22(1-7), 1-7.

Huuskonen, J., & Oksanen, T. (2018). Soil. sampling with drones and augmented reality in precision agriculture. *Computers and Electronics in Agriculture,* 154, 25-35.

Ibuot, J. C., Obiora, D. N., Ekpa, M. M., & Okoroh, D. O. (2017). Geoelectrohydraulic Investigation of the surficial aquifer units and corrosivity in parts of Uyo L. G. A., AkwaIbom, Southern Nigeria. *Journal of Applied Water Science,* **7**, 4705-4713.

Iloeje, N. P. (2001). A New Geography of Nigeria. New Revised Edition. Longman Nigeria, PLC. 200 p.

Imadi, S. R., Shah, S. W., Kazi, A. G., Azooz, M. M., & Ahmad, P. (2016). Phytoremediation of saline soils for sustainable agricultural productivity. In: Ahmad, P. (Ed.) Plant Metal Interaction, Elsevier, 455-468.

Irmak, S., Surucu, A. K., & Aydin, S. (2008). The effects of iron content of soils on the iron content of plants in the Cukurova region of Turkey. *International Journal of Soil Science,* **3,** 109-118.

Irons, J., Weismiller, R., & Petersen, G. (1989). Soil reflectance, In: Asrar, G, (Ed.) Theory and Application of Optical Remote Sensing. John Wiley, New York, 66-106.

Iyaka, Y. A. (2011). Nickel in soils: a review of its distribution and impacts. *Scientific Research,* 6(33), 6774-6777.

Izah, S. C., Bassey, S. E., & Ohimain, E. I. (2017). Assessment of pollution load indices of heavy metals in cassava mill effluents contaminated soil: a case study of small-scale processors in a rural community in the Niger Delta, Nigeria. *Bioscience Methods,* 8(1), 1-17.

Jadoon, K. Z., Moghadas, D., Jadoon, A., Missimer, T. M., Al-Mashharawi, S. K., & McCabe, M. F. (2015). Estimation of soil salinity in a drip irrigation system byusing joint inversion of multicoil electromagnetic induction measurements. *Water Resources Research,* 51(5), 3490-3504.

Jang, H., Somanna, Y., & Kim, H. (2016). Source, distribution, toxicity and remediation of arsenic in the environment – A review. *International Journal of Applied Environmental Sciences*, 11(2), 559-581.

Jasinski, J., Pietrek, S., Wakzykowski, P., & Orych, A. (2010). Acquisition of spectral reflectance characteristics of land cover features based on hyperspectral images. *Ostrava,* 1**,** 24-27.

Jat, S. L., Parihar, N., Dey, A., Nayak, H. S., Ghosh, A., Parihar, N., Goswam, A. K., & Singh, A. K. (2019). Dynamics and temperature sensitivity of soil organic carbon mineralization under medium-term conservation agriculture as affected by residue and nitrogen management options. *Soil and Tillage*, 190, 175-185.

Jayawickreme, D., Jobbagy, E. G., & Jackson, R. B. (2014). Geophysical subsurface imaging for ecological applications. *New Phytologist*, 201(4), 1170-1175.

Jemo, M., Souleymanou, A., Frossard, E., & Jansa, J. (2014). Cropping enhances mycorrhizal benefits to maize in a tropical soil. *Soil Biology and Biochemistry,* 79**,** 117-124.

Jiang, N., & Soga, K. (2019). Erosional behavior of gravel-sand mixtures stabilized by microbially induced calcite precipitation (MICP). *Soils and Foundations*, 59**(**3), 699-709.

Jinxia, L., Rudo, A. N., & Cornelius, A. M. G. (2017). Lanthanum toxicity to five different species of soil invertebrates in relation to availability in soil. *Chemosphere,* 193(11), 1-8.

Jinxia, L., Hong, M., Yin, X., & Liu, J. (2010). Effects of the rare earth elements on soil macrofauna community. *Journal of Rare Earths,* 28(6), 957-964

Jobbagy, E. G., & Jackson, R. B. (2001). The distribution of soil nutrients with depth: global patterns and the imprint of plants. *Biogeochemistry,* 53(1), 51-77.

Johnson, C. C., Breward, N., Ander, E L., & Ault, L. (2005). G-BASE: Baseline geochemical mapping of Great Britain and Northern Ireland. *Geochemistry: Exploration-Environment-Analysis*, **5**(4), 347-357.

Jones, C., & Olson-Rutz, K. (2016). Soil nutrient management for canola. *Bulletin of Montana State University*, 1-12.

Kabata-Pendias, A. (2000). Trace elements in soils and plants. 3rd edition, CRC Press: Boca Raton, Ann Arbor, London, 220-222.

Kabir, M. S., Salam, M. A., Paul, D. N. R., Hossain M. I., Rahman, N. M. F., Abdullah Aziz, & Latif, M. A. (2016). Spatial variation of arsenic in soil, irrigation water, and plant parts: a microlevel study. *The Scientific World Journal,* 1**,** 1-14.

Kant, S., & Kafkafi, U. (2013). Fertigation: nutrients behavior in soil. *Reference Module in Earth Systems and Environmental Sciences*, 6, 1-9.

Karaca, S., Gülser, F., & Selçuk, R. (2018). Relationships between soil properties, topography and land use in the Van Lake Basin, Turkey, Eurasian. *Journal of Soil Science*, **7**(2), 115-120.

Karlen, D. L., Andrews, S. S. & Doran, J. W. (2001). Soil quality: current concepts and applications. *Advances in Agronomy,* 74**,** 1-40.

Karlen, D. L., & Rice, C. W. (2015). Soil degradation: Will humankind ever learn? *Sustainability,* **7**(9), 12490-12501.

Katalin, S. (2011). Soil management. Book Data Base of Applied Sciences/Agriculture. *A TAMAP 4.2.5 b*, 11(1), 1-5.

Kayode, J. S., Nawawi, M., N. M., Baioumy, H. N., Khalil, A. E., & Khiruddin, B. A. (2015). Delineation of the subsurface geological structures of Omu-Aran area, south-western Nigeria, using aeromagnetic data. *AIP Conference Proceedings*, 04(12), 1657-1665.

Keary, P., Brooks, M., & Hill, I. (2002). An introduction to geophysical exploration. Blackwell Publishing, 978 (0), 1-632.

Kelling, K. A., & Schulte, E. E. (2004). Soil and Applied Calcium. Madison. *Cooperative Extension Publications,* A2523 (8), 1-2.

Khan, A. M., Behkami, S., Yusoff, I., Zain, S., AbuBakar, N. K., AbuBakar, A, F., & Alias, Y. (2017). *Chemosphere,* 184, 673-678.

Khanal, S., Fulton, J., & Shearer, S. (2017). An overview of current and potential applications of thermal remote sensing in precision agriculture. *Computer and Electronics in Agriculture*, 139**,** 22-32.

Khanal, N., Uddin, K., Matin, M. A., & Tenneson, K. (2019). Automatic Detection of Spatiotemporal Urban Expansion Patterns by Fusing OSM and Landsat Data in Kathmandu. *Remote Sensing,*11(19), 2296-3315.

Kibria, G., Hossaini, S., & Khan, M. S. (2018). Determination of consolidation properties using electrical resistivity. *Journal of Applied Geophysics*, 152, 150-160.

King, J. A., Dampney, P. M. R., Lark, R. M., Wheeler, H. C., Bradley, R. I., & Mayr, T. R. (2005). Mapping potential crop management zones within fields: use of yield-map series and patterns of soil physical properties identified by electromagnetic induction sensing. *Precision Agriculture*, 6, 167-181.

Korb, N., Jones, C., & Jacobsen, J. (2002). Macronutrients: cycling, testing, fertilizers recommendations. *Nutrient Management Module*, 6, 1-16.

Kowalczyk, S., Piotr, Z., & Mieszkowski, R. (2015). Application of electrical resistivity tomography in assessing complex soil conditions. *Geological Quarterly*, 59(2), 367-372.

Kristensen, J. A., Robert, T. B., Jones, J. A., Jones, A., Montanarella, L., Panagos, P., & Breuniung-Madsen, H. (2019). Development of a harmonized soil profile analytical database for Europe: a resource for supporting regional soil management. *Journal of European Geosciences Union*, 5(2), 289-301.

Kronzucker, H. J., Coskun, D., Schulze, L. M., Wong, J. R., & Britto, D. T. (2013). Sodium as nutrient and toxicant. *Plant Soil*, 369**,** 1-23.

Lacerda, M. P. C., Demattê, J. A. M., Sato, M. V., Fongaro, C. T., Gallo, B. C. B., & Souza, A. B. (2016). Tropical texture determination by proximal sensing using a regional spectral library and its relationship with soil classification. *Remote Sensing*, 8(9), 701- 709.

Lamidi, W. A., Shittu, K. A., & Adeyeye, A. S. (2018). Yield performances of tomatoes (*Lycopersicum esculentum*) on organic manure buffered lateritic soils. *Journal of Applied Sciences and Environmental Management*, 22(8), 1207-1212.

Lamotte, M., Bruand, A., & Pedro, G. (1997). Towards the hardening of sandy soils: A natural evolution in semi-arid tropics. *Earth and Planetary Science*, 325(8), 577-584.

Laurenzi, T. (2018). What's the ideal moisture level for soil to grow crops? Online Resource of Delmhorst Instrument Company. https://www.delmhorst.com/blog/whats-the-ideal-moisture-level-for-soil-to-grow-crops.

Lehnert, M. (2013). The soil temperature regime in the urban and sub-urban landscapes of olomoric, Czech Republic. *Morarian Geographical Reports*, 21(3), 27-36.

Leone, A. P., Wright, G. G., & Corves, C. (1995). The application of satellite remote sensing for soil studies in upland areas of southern Italy. *International Journal of Remote Sensing*, 16(6), 1087-1105.

Levitan, D. M., Zipper, C. E., Donovan, P., Screiber, M. E., Seal, R. R, Engle, … Aylor Jr., J. R. (2015). Statistical analysis of soil geochemical data to identify pathfinders associated with mineral deposits: an example from the Coles Hill uranium deposit, Virginia, USA. *Journal of Geochemical Exploration,* 154**,** 238-251.

Li, Y., Yang, X., Cai, H., Xiao, L., Xu, X., & Liu, L. (2015). Topographical Characteristics of Agricultural Potential Productivity during Cropland Transformation in China. *Sustainability*, **7,** 96-110.

Li, F., Gong, A., Qiu, L., Zhang, W., Li, J., Liu, Y., Liu, Y., & Yuang, H. (2017). Simultaneous determination of trace rare-earth elements in simulated water samples using ICP-OES with TODGA extraction/backextraction. *PLoS One,* 12 (9), 1-16.

Li, Q., Zhong, H., & Cao, Y. (2020). Effective extraction and recovery of rare earth elements (REEs) in contaminated soils using a reusable biosurfactant. *Chemosphere*, 256, 1-11.

Liang, S., Li, X., & Wang, J. (2012). A systematic view of remote sensing. In: Liang, S., Li, X., Wang, J. (Eds.), Advanced Remote Sensing, Academic Press, USA, 1-31.

Liu, Z., & Bando, Y. (2003). A novel method for preparing copper nanorods and nanowires. *Advance Materials*, 15, 303-308.

Lobell, D. B., & Asner, G. P. (2002). Moisture effects on soil reflectance. *Soil Science Society of America Journal of Abstract*, 66, 722-727.

Loke, M. H., Chambers, J. E., & Kuras, O (2011). Instrumentation, electrical resistivity, In Solid Earth Geophysics Encyclopedia (2nd Edition), Electrical and Electromagnetic, *Gupta, Harsh (ed)*, (2nd ed.) Berlin: Springer, 599-604.

Loke, M. H., & Baker, R. D. (1996) Rapid least-squares inversion of apparent resistivity pseudosections by a quasi-newton method. *Geophysical Prospecting*, 44, 131-152.

Lopes, G., Ávila, F. W., & Guilherme, L. R. G. (2017). Selenium behavior in the soil environment and its implication for human health. *Ciênciae Agrotecnologia,* 41(6), 605 - 615

Lourenco, A. M, Sequeira, E., Santovaia, H., & Gomes, C. R. (2014). Magnetic, geochemical and pedological characterisation of soil profiles from different environments and geological backgrounds near Coimbra, Portugal. *Geoderma*, 213, 408-418.

Lu, Y. & Xu, H. (2014). Distribution characteristic of soil organic carbon fraction in different types of wetland in hongze lake of China. *The Scientific World Journal*, 48, 1-5.

Lu, X., Zhang, X., Li, L. Y., & Chen, H. (2014). Assessment of metals pollution and health risk in dust from nursery schools in Xi'an, China. *Environmental Research,* 128, 27-34.

Lyu, S., Wei, X., Chen, J., Wang, C., Wang, X., & Pan, D. (2017). Titanium as a beneficial element for crop production. *Frontiers of Plant Science*, 8(597), 1-10.

Macedo, F. G., Bresolin, J. D., Santos, E. F., Furlan, F., Lopes da Silva, W. T., Polacco, J. C., & Lavres, J. (2016). Nickel availability in soil as influenced by liming and its role in soybean nitrogen metabolism. *Frontiers in Plant Science*, 8, 1-10.

Machado, R. M. A., & Serralhero, R. P. (2017). Soil salinity: effects on vegetable crop growth. Management practices to prevent and mitigate soil. *Horticulturae*, 3(2), 1-8.

Mahender, A., Swamy, B. P. M., Anandan, A., & Ali, J. (2019). Tolerance of iron-deficient and -toxic soil conditions in rice. *Plants (Basel)*, 8(2), 31-39.

Mahesh, S., Jayas, D. S., Paliwal, J., & White, N. G. (2015). Hyperspectral imaging to classify and monitor quality of agricultural materials. *Journal of Stored Products Research,* 61, 17-26.

Makkonen, H., Makinen, J. & Kontoniemi, O. (2008), Geochemical discrimination between barren and mineralized intrusions in the Svecofennian (1.9 Ga) Kotalahti Nickel Belt, Finland. *Ore Geology Reviews*, 33(1), 101-114.

Malik, N. J., Chamon, M. N., Mondol, S. F., Elahi, N. J., Chamon, A. S., Mondol, M. N., Elahi, S. F., & Faiz, S. M. A. (2011). Effects of different levels of zinc on growth and yield of red amaranth (amaranthus sp.) and rice (oryza sativa, variety-br49). *Journal of the Bangladesh Association of Young Researchers (JBAYR)*, 1(1), 79-91.

Manning, D. A. C. (2018). Innovation in resourcing geological materials as crop nutrients. *Natural Resources Research*, 27, 217-227.

Margenot, A. J., Parikh, S. J., & Calderon, F. J. (2019). Improving infrared spectroscopy characterisation of soil organic matter with spectral subtractions. *Journal of Visualized Experiments*, 143, 1-10.

Markham, B. L., Storey, J., & Morfitt, R. (2015). Landsat-8 sensor characterisation and calibration. *Remote Sensing*, 7, 2279-2282.

Marshall, T. J., & Holmes, J. W. (1988). A book review on soil physics. Cambridge university press (2nd ed., pp. 379-381). Cambridge, United Kingdom.

Martin, M. A., Reyes, M., & Taguas, F. J. (2017). Estimating soil bulk density with information metrics of soil texture. *Geoderma*, 287(1), 66-70.

Martina-Prieto, D., Cancelo-Gaonzalez, J., & Barral, M. T. (2018). Arsenic Mobility in As-containing soils from geogenic origin: fractional and leachability. *Journal of Chemistry*, 10, 1-14.

Mattee, A., Kootbodien, T., Kapwata, T. & Naicker, N. (2018). Concentration of arsenic and lead in residential garden soil from four Johannesburg neighborhoods. *Environmental Research*, 167, 524-527.

McBride, M. B., Martinez, C, E., Topp, E., & Evans, L. (2000). Trace metal solubility and speciation in a calcareous soil 18 years after no-till sludge application. *Soil Science*, 165, 646-656.

McCauley, A., Jones, C., & Jacobson, J. (2011). Plant nutrient functions and deficiency and toxicity symptoms. *Nutrient Management Module*, 9, 1-16.

McCauley, A., Jones, C., & Jacobsen, J. (2005) Soil and water management: basic soil properties. Montana State University Extension Services, Montana State University, Bozeman, 994-2721.

McRoberts, K. C., Ketterings, Q. M., Parsons, D., Hai, T. T., Quan, N. H., Ba, N. X., Nicholson, C. F., & Cherney, D. J. R. (2016). Impact of forage fertilization with Urea and composted cattle manure on soil fertility in sandy soils of south-central Vietnam. *International Journal of Agronomy*, 16, 1-14.

Meheni, Y., Guerin, R., Benderitter, Y., & Tabbagh, A. (1996). Subsurface DC resistivity mapping: approximate 1-D interpretation. *Journal of Applied Geophysics*, 34(4), 255-269.

Melo W., Delarica D., & Guedes A. (2018). Ten years of application of sewage sludge on tropical soil. *Agriculture of a Global Environment*, 643, 1493-1501.

Mendes, W. C., Alves, J. J., da Cunha, P. C. R., da Silva, A. R., Evangelista, A. W. P., & Casaroli, D. (2016). Potassium leaching in different soils as a function of irrigation depths. *Revista Brasileira de Engenharia Agrícola e Ambiental*, 20(11), 972-977.

Mendoza, B., Guananga, N., Melendez, J. R., & Lowy, D. A. (2020). Differences in total iron content at various altitudes of Amazonian Andes soil in Ecuador. *F1000Research*, 9(128), 1-9.

Meryem, B., Ji, H., Gao, Y., Ding, H., & Li, C. (2016). Distribution of rare earth elements in agricultural soil and human body (scalp hair and urine) near smelting and mining areas of Hezhang, China. *Journal of Rare Earths,* 34(11), 1156-1167.

Metternicht, G., Zinck, J. A., Bianco, P. D., & del Valle, H. F. (2010). Remote sensing of land degradation: Experiences from Latin American and the Caribbean. *Journal of Environmental Quality*, 39(1), 42-61
.

Mgbenka, R. N., & Mbah, E. N. (2016). A review of smallholder farming in Nigeria: need for transformation. *International Journal of Agricultural Extension and Rural Development Studies*, 3(2), 43-54.

Missimer, T. M., Teaf, C. M., Beeson, W. T., Maliva, R. G., Woolschlager, J., & Covert, D. J. (2018). Natural background and anthropogenic arsenic enrichment in Florida soils, surface water, and groundwater: A review with a discussion on public health risk. *International Journal of Environmental Research and Public Health,* 15(10), 2278 - 2290.

Mitra, G. N., Sahu, S. K., & Nayak, R. K. (2009). Ameliorating effects of potassium on iron toxicity in soils of Orissa. Proceedings of the Quat Bhurbaneswar International Symposium, November 5-7, Bhubaneswar, Orissa, India, 1-15.

Mohanty, B. P., Cosh, M. H., Lakshmi. V., & Montzka, C. (2017). Soil moisture remote sensing: state-of-the-science. *Vadose Zone Journal,* 16(1), 1-8.

Molina, M., Aburto, F., Calderon, R., Cazanga C. M., & Escudey, M. (2009). Trace elements composition of selected fertilizers used in Chile: Phosphorus Fertilizers as a source of long-term soil contamination. *Soil and Sediment Contamination: An International Journal, 18*(4), 497-511.

Monteiro, R., Coasta, S., Coppola, F., Freitas, R., Vale, C., & Pereira, E. (2019). Toxicity beyond accumulation of Titanium after exposure of *Mytilus galloprovincialis* to spiked seawater. *Environmental Pollution,* 244, 845-858.

Mori, Y., Mariyama, T., & Mitsuno, T. (1999). Soft X-ray radiography of drainage patterns of structured soils. *Soil Science Society of American Journal,* 63(4), 733-740.

Mostafa, M., Anwar, M. B., & Radwan, A. (2017). Application of electrical resistivity measurement as quality control test for calcareous soil. *HBRC Journal,* 14(3), 379-384.

Mouhamad, R. S., Atiyah, A. H., Mohammad, R., & Igbal, M. (2015). Decomposition of organic matter under different soil textures. *Current Science Perspectives*, **1**(1), 22-25.

Mousavi, S. R., Galavi, M., & Rezaei, M. (2012). The interaction of zinc with other elements in plants: A review. *International Journal of Agriculture and Crop Sciences*, 4 (24), 1881-1884.

Mtambanengwe, F., & Kosina, P. (2007). Organic and inorganic fertilizers. Cereal Knowledge Bank, CIMMYT and IRRI. http://www.knowledgebank.irr.org/ckb/agronomy -wheat/organic-and-inorganic-fertilizers.html. Accessed 4/3/2020.

Muchsin, M., Johnson, C. C., Crow, M. J., Djumsari, A., & Sumartono, T. (1997). Geochemical Atlas of Southern Sumatra. Regional Geochemical Atlas Series of Indonesia. *Groundwater,* 2(43), 259-269.

Mulder, V. L., de Bruina, S., Schaepmana, M. E., & Mayrc, T. R. (2011). The use of remote sensing in soil and terrain mapping - a review. *Geoderma,* 162(1-2), 1-19.

Mulder, J., Van Grinsven, J. J. M., & Van Breemen, N. (1987). Impacts of acid atmospheric deposition on woodland soils in the Netherlands: III. aluminium chemistry. *Soil Science Society of American Journal,* 51, 1640-1646.

Muller, G. (1969). Index of Geoaccumulation in Sediments of the Rhine River. *GeoJournal*, 2, 108-118.

Mullin, G. L., & Hajek, B. F. (1996). Phosphorus accumulation and loss from Alabama soils receiving poultry litters. *Alabama Agricultural Experiment Station Bulletin*, 63(2), 1-5.

Munnaf, A. M., Mouazen, A., & Nawar, S. (2019). Estimation of secondary soil properties by fusion of laboratory and on-line measured vis-nir spectra. *Remote Sensing*, 11(23), 1-21.

Murphy, B, W. (2015). Key soil functional properties affected by soil organic matter – evidence from published literature. *Soil Research,* 53(6), 605-635.

Mustafa A. R., & Hatem A. J. (2019). Calculation of salinity and soil moisture indices in south of Iraq - Using satellite image data. *Energy Procedia*, 157, 228-238.

Nawar, S., Corstanje, R., Halcro, G., Mulla, D., & Mouazen, A. M. (2017). Delineation of soil management zones for variable-rate fertilization: A review. *Advanced Agronomy, 143*, 175-245.

Ndubuisi, E. (2017). How digital technology Is changing farming in Africa. Harvard Business School Publishing. Retrieved from http://www.afrit.org. Accessed 9/10/19.

Nemerow, N. L. (1985). Stream, Lake, Estuary and Ocean Pollution (1st Ed.). Van Nostrand Reinhold Publishing Company, New York. 472 p.

Nguyen K., Liou Y., Tran H., Hoang P., & Nguyen T. (2020). Soil salinity assessment by using near-infrared channel and vegetation soil salinity index derived from Landsat 8 OLI data: a case study in the Tra Vinh Province, Mekong Delta, Vietnam. *Progress in Earth Planetary Science*, 7(1), 1-11.

Ni, J., Cheng, Y., Wang, Q., Wai Ng, C. W., & Garg, A. (2019). Effects of vegetation on soil temperature and water content: Field monitoring and numerical modelling. *Journal of Hydrology*, 571, 494-502.

Nishiyama, R., Ariga, A., Ariga, T., Lechmann, A., Mair, D., Pistillo, C., Scampoli, P., Valla, P. G., Vladymyrov, M., Ereditato, A. & Schlunegger, F. (2019). Bedrock sculpting under an active alpine glacier revealed from cosmicray muon radiography. *Scientific Reports*, 9(6970), 1-11.

Obaje, N. G. (2009). Geology and Mineral Resources of Nigeria. Springer, Dordrecht Heidelberg, London New York, 1-221.

Obiora, D. N., Alhassan, U. D., Ibuot, J. C., & Okeke, F. N. (2016). Geoelectric evaluation of aquifer potential and vulnerability of Northern Paiko, Niger State, Nigeria. *Water Environmental Research*, 88(7), 644-651.

O'Brien, J., Vega, A., Bouguyon, E., Krouk, G., Gojon, A., Coruzzi, G., & Gutiérrez, R. (2016). Nitrate transport, sensing, and responses in plants. *Molecular Plant*, 9, 837-856.

Odukoya, A. M. (2015). Contamination assessment of toxic elements in the soil within and around two dumpsites in Lagos, Nigeria. *Ife Journal of Science*, 17(2), 1-11.

Odukoya, A. M., Olobaniyi, S. B., & Oluseyi, T. O. (2018). Assessment of potentially toxic elements pollution and human health risk in soil of Ilesha gold mining site, southwest Nigeria. *Journal Geological Society of India*, 91, 743-748

Odunuga, S., & Badru, G. (2015). Landcover change, land surface temperature, surface albedo and topography in the plateau region of north-central Nigeria. *Land*, 4, 300-324.

Offordile, M. E. (2002). Groundwater Study and Development in Nigeria 2nd Edition published by Mecon Geology and Engineering Service Limited, Jos, Nigeria, 303-332.

Ogwu, I. J., Omotesho, O. A., & Muhammed-Lawal, A. (2018). Economics of soil fertility

management practices in Nigeria: Food systems sustainability and environmental policies in modern economies. In L. Amadi & F. Allen (Eds.), *Emerging research and opportunities* (pp. 236-263). IGI Global Publisher, USA.

Ojanen, P, Makiranta, P., Penttila, T., & Minkkinen, K. (2017). Do logging residue piles trigger extra decomposition of soil organic matter. *Forest Ecology Management*, 405**,** 367-380.

Ojuola. O. (2015). Status and challenges of soil management in Nigeria. Retrieved from http://www.fao.org/globalsoilpartnership: accessed: 15/11/2019.

Okezie, C. N. (1974). Geological map of Nigeria, Scale 1:2,000,000 Geological Survey of Nigeria, Abuja, 1-20.

Olabode, S. O. (2006). Siliciclastic slope deposit from the cretaceous Abeokuta Group, Dahomey (Benin) Basin, southwestern Nigeria. *Journal of African Earth Sciences*, 46**,** 187-200.

Oladele, E. O., Odeigah, P. G. C., Taiwo, I. A., & Yahaya, T. (2018). Remediative potential of Barbara nut on lead and zinc polluted soils. *Ife Journal of Science*, 18(2), 483-491.

Olatunde, P. S. (2016). Geochemical techniques for the analysis of geochemical data and its application in the Nigeria oil and gas industries, *Journal of Chemical Sciences, 7*(3), 1- 8.

Olayemi, I. K., Idris, B., Ejima, I. A. A., Adeniyi, K., Ukubuiwe, A. C. & Isah, B. (2014). The climate of North-Central Nigeria and potential influence on mosquito (Diptera: Culicidae) vectorial capacity, for disease transmission. *Global Journal of Multidisciplinary and Applied Sciences*, 2, 26-31.

Onwudike, S. U., Uzoho, B. U., Ihem, E. E., Ahukaeemere, C. M., Nkwopara, U., Irokwe, I. F., & Echeanyanwu, G. I. (2016). Evaluation of the fertility status of selected soils in Mbaise, Imo State southeastern Nigeria using nutrient index method. *Agrosearch*, 16(1), 79-90.

Onwuka, M. I., Ozurumba, U. V., & Nkwocha, O. S. (2016). Changes in soil pH and exchangeable acidity of selected parent materials as influenced by amendments in south east of Nigeria. *Journal of Geosciences and Environment Protection*, 4(05), 80-88.

Onwuka, B., & Mang, B. (2018). Effects of soil temperature on some soil properties and plant growth. *Advances in Plants and Agriculture Research*,8,1,34-37.

Osayande, P. E., Oviasogie, P. O., Orhue, E. R., Maidoh, F. U., & Osaghe, D. O. (2015).

Soil nutrient status of the Otegbo fresh water swamp in Delta State of Nigeria. *Nigerian Journal of Agriculture, Food and Environment,* 11(2), 1-8.

Ose, K., Corpetti, T., & Demagistri, L. (2016). Multispectral satellite image processing – optical remote sensing of land surface. *Techniques and Methods*, 8, 57-124.

Othman, Y. A., & Leskovar D. (2018). Organic soil amendments influence soil health, yield, and phytochemicals of globe artichoke heads. *International Journal for Sustainable Production Systems,* 34(4), 258-267.

Oyinloye, R. O., & Oloukoi, J. (2012). Spatio-temporal assessment and mapping of the landuse landcover dynamics in the central forest belt of southwestern Nigeria. *Research Journal of Environment and Earth Sciences,* 4(7), 720-730.

Pagliai, M., & Vignozzi, N. (2007). Image analysis and microscopic techniques to characterize soil pore system. In: Blahovec, J. and Kutilek, M. (Eds.), Physical Method in Agriculture. Kluwer Academic Publishers, New York. 13-38.

Pang, X., Li, D., & Peng, A. (2001). Application of rare -earth elements in the agriculture of China and its environmental behavior in soil. *Environmental Science and Pollution Research*, 9(2), 143-151.

Parent, L. E. (2017). Fractal kinetics parameters regulating carbon decomposition rate under contrasting soil management systems. *Open Journal of Soil Science,* 7(7), 111-117.

Patra, S. K., Shekher, M., Solanki, S. S, Ramachandran, R., & Krishnan, R. (2011). A technique for generating natural colour images from false colour composite images. *International Journal of Remote Sensing*, 27(14), 2977-2989.

Pepe, M., Fregonese, L., & Scaioni, M. (2018). Planning airborne photogrammetry and remote sensing missions with modern platforms and sensors. *European Journal of Modern Platforms and Sensors*, 51(1), 412-436.

Pepper, I. L., Gerba, C. P., & Brusseau, M. L. (2019). Environmental and Pollution Science (3rd ed.). Academic Press, Arizona, USA, 662.

Pereira, P., Brevik, E. C., Munoz-Rojas, M. & Miller, B. A. (Eds,). (2017). Soil mapping and process modelling for sustainable land use management. The Netherlands, Elsevier: 1-386.

Perry, C. H., & Amacher, M. C. (2010). Forest soils. In W. B. Smith, P. D. Miles, C. H. Perry & S. A. Pugh (Eds.), *Technical coordinations* (42-44). Forest resources of The United States, 2007. Department of Agriculture Forest Service. General Technical Rep. WO–78. Washington, DC: U.S.

Peters, N. A., Huntington, K. W., & Hoke, J. D. (2013). Hot or not? Impact of seasonally

variable soil carbonate formation on paleotemperature and O-isotope records from clumped isotope thermometry, *Earth and Planetary Science Letters*, 361, 208-218.

Phogat, V. K, Tomar, V. S., & Dahiya, R. (2015). Soil physical properties. In R. K. Rattan, J. M. C. Katyal, B. S. Dwivedi, A. K. Sarkar, T. Bhattachatyya, J. C. Tarafdar & S. S. Kukal (Eds.), *Soil science: An introduction* (135-171). Indian Society of Soil Science Publishers, India.

Prajapati, K. & Modi, H. A. (2012). Isolation and characterisation of potassium solubilizing bacteria from ceramic industry soils. *CIBTech Journal of Microbiology*, 1(2-3), 8-14.

Probert, R. J. (2000). The role of temperature in the regulation of seed dormancy and germination. In M. Fenner (Ed.), *Seeds: The ecology of regeneration in plant communities*, (2nd ed., pp. 261-292). CAB International, Wallingford, United Kingdom. DOI :10.1079/9780851994321.0261

Puckett, W. E., Collins, M. E., & Schellentrager, G. W. (1990). Design of soil maps units on a karst area in west central Florida. *Soil Science Society of American Journal*, 54(4), 1068-1073.

Qadir, M., Quresh, R. H., & Ahmad, N. (2002). Amelioration of calcareous saline sodic soils through phytomediation and chemical strategies. *Soil Use and Management*, 18(4), 381-385.

Qin, B., Liu, W., He, E., Li, Y., Liu, C., Ruan, J., Qin, R., & Tang, Y. (2019). Vacuumpyrolysis method for reclamation of rare earth elements from hyperaccumulator *Dicranopteris dichotoma* grown in contaminated soil. *Journal of Cleaner Production*, 229, 480-488. https://doi.org/10.1016/j.jclepro.2019.05.031.

Qingjie, G., Jun, D., Yunchan, X., Qingfei, W., & Liqiang, Y. (2008). Calculating Pollution Indices by Heavy Metals in Ecological Geochemistry Assessment and a Case Study in Parks of Beijing. Journal of China University of Geosciences, 19(3), 230-241.

Rabitz, A., Hallaus, A., Pham, D. T., Tu, M. B., & Mentler, A. (2019). Sustainability strategies and soil fertility in the dryland Binh Thuan, Vietnam. *Spanish Journal of Soil Science*, 9(2), 1-7.

Rahaman, M. A. (1976a). Review of basement geology of southwestern Nigeria. In C. A. Kogbe (Ed.), Geology of Nigeria (41-57). Elizabeth Press, Lagos.

Rahaman, M. A. (1976b). On the Olugbade large feldspar granite. *Journal of Mining and Geology*, 13, 45-53.

Raimi, A., Adeleke, R., & Roopnarain, A. (2017). Soil fertility challenges and biofertilizer

as a viable alternative for increasing smallholder farmer crop productivity in sub-Saharan Africa. *Cogent Food and Agriculture*, 3(1), 1-26.

Rajana, G. A., Dass, A., & Paramesha, V. (2019). Excess water stress: effects on crop and soil, and mitigation strategies. *Popular Kheti,* 6(3), 48-53.

Ramirez-Guinart, O., Salaberria, A., Vidal, M., & Rigol, A. (2018). Dependence of samarium-soil interactions on samarium concentration: implications for environmental risk assessment. *Environmental Pollution*, 234, 439-447.

Ramos, S. J., Dinali, G. S., Oliveira, C. Martins G. C., Cristiano G. M., Siqueira J. O., & Guilherm L. R. G. (2016). *Current Pollution Report*, 2(1), 28-50.

Rate, A. W., & Sheikh-Abdullah, S. M. (2017). The geochemistry of calcareous forest soils in Sulaimani Governorate, Kurdistan Region, Iraq. *Geoderma*, 289, 54-65.

Ravindran, B., Mupambwa, H. A., Silwana, S., & Mnkeni, P. N.S. (2017). Assessment of nutrient quality, heavy metals and phytotoxic properties of chicken manure on selected commercial vegetable crops. *Heliyon,* 3(12), e00493, 1-17.

Reimann, C., Äyräs, M., Chekushin, V., Bogatyrev, I., Boyd, R., de Cariat, P., Dutter, R., Finne, T. E., Halleraker, J. H., Jaeger, O., Kashulina, G., Lehto, O., Niskaavara, H., Pavlov, V. K., Raisanen, M. H., Strand, T., & Volden, T. (1998). Environmental geochemical atlas of the Central Barents Region. *Geological Survey of Norway*, 176(5), 1-745.

Ren, Z., Li, Z., Liu, X., Cheng, X., & Xu, G. (2018). Comparing watershed afforestation and natural revegetation impacts on soil moisture in the semiarid Loess Plateau of China. *Scientific Reports*, 8(2972), 1-8.

Renneson, M, Barbieux, S., & Colinet, G. (2016). Indicators of phosphorus status in soils: significance and relevance for crop soils in southern Belgium, a review. *Biotechnology Agronomy Social Environment,* 20(S1), 257-272.

Reynolds, J. M. (1997). An Introduction to Applied and Environmental Geophysics. Chichester. John Wiley and Sons Books and Press, 1-796.

Rhoton, F. E. & Dulker, S. (2008). Erodibility of a soil drainage sequence in the loess uplands of Mississippi. *Catena,* 75(2), 1-9.

Rim, K. T., Koo, K. H., & Park, J. S. (2013). Toxicological evaluations of rare earths and their health impacts to workers: a literature review. *Safety and Health at Work,* 4(1), 12-26.

Rimjhim, K., Sushmita, B., & Malaya, C. (2013). Application of Remote Sensing in Soil

Mapping: A Review. North East Students Geotechnical Congress on Advances in Geotechnical Engineering (NES Geo-Congress 2013) 28th September, 2013.

Robertson, M. J., Isbister, B., Maling, I., Oliver, Y., Wong, M., Adams, M., Bowden, J. W., & Tozer, P. (2007). Opportunities and constraints for managing within-field spatial variability in Western Australian grain production. *Field Crops Research*, 104, 60-67.

Rodrigues, E. S., Montanha, G. S., Marques, J. P. R., De Almeida E., Yabuki, L. N. M., Menegario, A. A., & De Carvalho, W. P. (2020). Foliar application of rare earth elements on soybean (Glycine max(L)):Effects on biometrics and characterisation of phytotoxicity. *Journal of Rare Earths*, 38, 1131-1139.

Rogowska, J., Olkowska, E., Ratajczyk, W., & Wolska, L. (2018). Gadolinium as a new emerging contaminant of aquatic environments. *Environmental Toxicology and Chemistry,* 37(6), 1523-1534.

Rossel, R. A. V., Behrens, T., Ben-Dor, E., Brown, D. J., Dematte, J. A. M., Shepherd, K. D., Stenberg, B, Stevens, A., & Ji, W. (2016). A global spectral library to characterize the world's soil. *Earth-Science Reviews*, *155,* 198-230.

Rout, G, R., & Sahoo, S. (2015). Role of iron in plant growth and metabolism. *Reviews in Agricultural Science*, 3, 1-24.

Royimani, L., Mutanga, O., Odindi, J., Dube, T., & Matongera, T. N. (2018). Advancements in satellite remote sensing for mapping and monitoring of Alien Invasive Plant species (AIPs). *Physics and Chemistry of the Earth,* 12(004), 1-8.

Rui, M., Ma, C., Hao, Y., Guo, J., Rui, Y., Tang, X., Zhao, Q., Fan, X., Zhang, Z., Hou, T., & Zhu, S. (2016). Iron oxide nanoparticles as a potential iron fertilizer for peanuts (Arachis hypogaea). *Frontier in Plant Science*, 7, 815 -822.

Rutkowska, B., Szulc, W., Ewa, S., & Natalia, P. (2017). Prediction of molybdenum availability to plants in differentiated soil conditions. *Plant, Soil and Environment,* 63(11), 491-497.

Sabri, N. S., Zakaria, Z., Mohamad, S. E., Jaafar, A. B. & Hara, H. (2018). Importance of soil temperature for the growth of temperate crops under a tropical climate and functional role of soil microbial diversity. *Microbes and Environments,* 33, 144-150.

Sadeghi, M., Billay, A., & Carranza, J. M. (2015). Analysis and mapping of soil geochemical anomalies: implications for bedrock mapping and gold exploration in Giyani area, South Africa. *Journal of Exploration Geochemistry*, 154, 180-193.

Sadeghi, S. M., Noorhosseini, S. A., & Damalas, C. A. (2018). Environmental

sustainability of corn (Zea mays L.) production on the basis of nitrogen fertilizer application: The case of Lahijan, Iran. *Renewable and Sustainable Energy Reviews*, 95, 48-55.

Saha, G. C., Ali, M. A. (2007). Dynamics of arsenic in agricultural soils irrigated with Arsenic contaminated groundwater in Bangladesh. *Science of the Total Environment*, 379(2–3),180–189.

Sahoo, R. N., Ray, S. S., & Manjunath, R. K. (2015). Hyperspectral remote sensing of agriculture. *Current Science*, 108(5), 848-859.

Salako, F. K. (2003). Soil physical conditions in Nigerian savannas and biomass production. Lecture given at the College of Soil Physics, Trieste, Italy, 3 - 21 March 2003, 365-377.

Salem, M, A., Al-Ethawi, L, H., Eldrazi, Z, S. M., & Nouraldien, A, I. (2014). A case study of the total and available phosphorus concentration in Libyan agricultural soils in different depths and seasons in long-term chemical and animal manure fertilization. *International Journal of Research Studies in Biosciences*, 2(2), 1-9.

Salminen, R. (2018). Site characterisation, data analysis and case histories: Field methods in regional geochemical survey. *Environmental Geochemistry*, 1-12.

Salminen, R., Batista, M. J., Bidovec, M., Demetriades, A., De-Vivo, B., De-Vos, W., Duris, M., & Tarvainen, T. (2005). Geochemical Atlas of Europe, Part 1: Background Information, Methodology and Maps. *Geological Survey of Finland*, 1-36.

Samouelian, A., Cousin, I., Tabbagh, A., Bruand, A., & Richard, C. (2005). Electrical resistivity survey in soil science: a review. *Soil and Tillage Research*, 83(2), 173-193.

Sangani, M. F., Owen, G., Nazari, B., Astaraei, A., Fotovat, A., & Emami, H. (2019). Different modelling approaches for predicting titanium dioxide nanoparticles mobility in intact soil media. *Science of the Total Environment*, 665, 1168-1181.

Sanjay, K., Gupta, X., Chris, Le., Kachanosky, G., Zuidhof, M. J., & Siddique, T. (2018). Transfer of arsenic from poultry feed to poultry litter: a mass balance study, *Science of The Total Environment*, 630, 302-307.

Sassenrath, G. F., Davis, K., Sassenrath-Cole, A., & Riding, N. (2018). Exploring the physical, chemical and biological components of soil: improving soil health for better productive capacity. *Kansas Agricultural Experiment Station Research Reports*, 4(3), 1-10.

Sattari, M. T., Dodangeh, E. & Abraham, J. (2017). Estimation of daily soil temperature

via data mining techniques in semi-arid climate conditions. *Earth Science and Resources Journal*, 21(2), 85-93.

Schimmelpfennig, D., & Ebel, R. (2016). Sequential adoption and cost savings from precision agriculture. *Journal of Agricultural Resource and Economics,* 41(1), 97-115.

Schlesinger, W. H. (Ed.). (1997). Biogeochemistry, an analysis of global change (2nd ed. pp. 588). Academic Press), San Diego, London, Boston, New York, Sydney, Tokyo and Toronto: Academic Press.

Schönbächler, M. (2018) Inductively Coupled Plasma Mass Spectrometry (ICP-MS). In W. White (Ed.), *Encyclopedia of geochemistry*. Encyclopedia of Earth Sciences\ Series. Springer International Publishing, 1-17.

Scudiero, E., Berti, A., Teatini, P., & Morari, F. (2012). Simultaneous monitoring of soil water content and salinity with a low-cost capacitance-resistance probe. *Sensors,* 12, 17588-17607.

Sehgal, J. L., Challo, O., Gajja, B. L., & Yadav, S. C. (1989). Suitability of swell shrink soils of India for crop growth. In V. Cleemut (Ed.), *Soil for Development*. ITC-Ghent Book and Press, 1, 29-53. http://isslup.in/wp-content/uploads/2018/09/Soil-Site-Suitability-Evaluation-for-Cotton.pdf

Senbayram, M., Gransee, A., Wahle, V. & Thiel, H. (2015). Role of magnesium fertilizers in agriculture: plant-soil continuum. *Crop and Pasture Science,* 66(912), 1219-1229.

Senesi, G. S., Baldassarre, G., Senesi, N., & Radina, B. (1999). Trace elements inputs into soils by anthropogenic activities and implications for human health. *Chemosphere,* 39(2), 343-353.

Sewell, R. J. (1999). Geochemical Atlas of Hong Kong. Geotechnical Office, Civil Engineering Department, Hong Kong, ISBN 962-02-0274-0, 1-110.

Shah, A., Naiz, A., Ullah, N., Rehman, A., Akhlaq, M., Zakir, M., & Khan, M. S. (2013). Comparative study of heavy metals in soil and selected medicinal plants. *Journal of Chemistry,* 10, 1-5.

Shah, F., & Wu, W. (2019). Soil and crop management strategies to ensure higher crop productivity within sustainable environments. *Sustainability,* 11(1485), 1-19.

Shaheen, S. M., Kwon, E. E., Biswas, J. K., Tack, F. M. G., Ok, Y. S., & Rinklebe, J.

(2017). Arsenic, chromium, molybdenum, and selenium: Geochemical fractions and potential mobilization in riverine soil profiles originating from Germany and Egypt. *Chemosphere,* 180**,** 553-563.

Shahid, S. A., Zaman, M., & Heng, L. (2018) Soil salinity: Historical perspectives and a world overview of the problem. In: *Guideline for salinity assessment, mitigation and adaptation using nuclear and related techniques* (43-53). Springer Nature, Switzerland.

Sharma, D. K., & Singh, A. (2015). Salinity research in India-achievements, challenges and future prospects. *Water and Energy International*, 58, 35- 45.

Sharma, P., Kumar, D. & Srivastava, H, S. (2018). Assessment of different methods for soil moisture: a review. *Journal of Remote Sensing and GIS*, 9(1), 65-73.

Shevnin, V., Delgado-Rodriguez, O., Mousatov, A., & Ryjov, A. (2006). Estimation of hydraulic conductivity on clay content in soil determined from resistivity data. *Geofisica Internacional*, 45(3), 195-207.

Shreatha, H. L. (2006). Using GPS and GIS in participatory mapping of community forest in Nepal. *Electronic Journal of Information Systems in Developing Countries*, 25, 1-10.

Shrivastava, P. & Kumar, R. (2015). Soil salinity: a serious environmental issue and -plant growth promoting bacteria as one of the tools for its alleviation. *Saudi Journal of Biological Science,* 22(2), 123-131.

Silva, C. B., Dias de Moraes, M. A. F., & Molin, J. P. (2011). Adoption and use of precision agriculture technologies in the sugarcane industry of São Paulo state, Brazil. *Precision Agriculture*, 12, 67-81.

Silva, R. A., Siqueira, G. M., Costa, M. K. L., Guedes-Filho, O., & Silva, E. F. F. (2018). Spatial variability of soil fauna under different land use and managements. *Revista Brasileira Cienca de Solo,* 42, 1-18.

Simansky, V., Juriga, M., Jonczak, J., Uzarowicz, L., & Stephen, W. (2019). How relationships between soil organic matter parameters and soil structure characteristics are affected by the long-term fertilization of a sandy soil. *Geoderma*, 342, 75-84.

Singh, G., Goyne, K. W., & Kabrick, J, M. (2015). Determinants of total and available phosphorus in forested Alfisols and Ultisols of the Ozark Highlands, USA. *Geoderma Regional*, 5, 117-126.

Smiley, E. T. (1990). Terravent TM: Soil fracture patterns and impact on bulk density.

*Journal of Arboriculture*, **27**(6), 326-330.

Smith, C. M., Dhuyvetter, K. C., Kastens, T. L., Kastens, D. L., & Smith, L. M. (2013). Economics of precision agricultural technologies across the Great Plains. *Journal of the ASFMRA, American Society of Farm Managers and Rural Appraisers,* 20, 185-206.

Smith, P., & Powlson, D. S. (2003). Sustainability of soil management practices - a global perspective. In D. V. Murphy & L. K. Abbott (Eds.), *Soil biological fertility - a key to sustainable land use in agriculture* (241-254). Kluwer Academic Publishers, Dordrecht, Netherlands.

Smyth, A. J., & Montgomery, R. F. (1962). Soils and land use of central western southwestern Nigeria. *Journal of African Earth Sciences*, 131, 117-127.

Sneller, F. E. C., Kalf, D. F., Weltje, L., & Van-Wezel, A. (2000). Maximum permissible concentration and negligible concentrations for rare earth elements. Research for Man and Environment, Report 601501 011. National Institute of Public Health and the Environment, Netherlands, 1-66.

Staruschenco, A. (2018). Beneficial effects of high potassium. *Hypertension,* 71(6), 1015-1022.

Subha, T. J., & Rose, G. L. (2016). Physico-chemical parameters and fertility status in selected soils of Agastheeswaram, Kalkulam and Vilavancode Taluk's of Kanyakumari District, Tamil Nadu, India: A study. *Indian Journal of Advances in Chemical Science*, 4(4), 386-393.

Sun, T., Li, G., Ning, T., Zhang, Z., Mi, Q., & Lal, R. (2018). Suitability of mulching with biodegradable film to moderate soil temperature and moisture and to increase photosynthesis and yield in peanut. *Agricultural Water Management*, 208, 214-223.

Tale, K. S., & Ingole, S. (2015). A review on role of physico-chemical properties in soil quality. *Chemical Science Review and Letters*, 4(13), 57-66.

Tang, C., Wang, D., Zhu, C., Zhou, Q., Xu, S., & Shi, B. (2018). Characterizing drying-induced clayey soil desiccation cracking process usingelectrical resistivity method. *Applied Clay Science,* 152, 101-112.

Tang, M., Zhao, X., Gao, X., Zhang, C., Wu, P., Li, H., Ling, Q., & Chau, H. (2019). Characteristics of soil moisture variation in different land uses in a small catchment on the Loess Plateau, China. *Journal of Soil Water Conservation,* 74(1), 24-32.

Tarpanelli, A., Massari, C., Ciabatta, L., Filippucci, P.; Amarnath, G., & Brocca, L. (2017)

Exploiting a constellation of satellite soil moisture sensors for accurate rainfall estimation. *Advances in Water Resources*, 108, 249-255.

Tazikeh, H., Khormali, F., Amini, A., & Motlagh, M. B. (2018). Geochemistry of soils derived from selected sedimentary parent rocks in Kopet Dagh, North East Iran. *Journal of Geochemical Exploration*, 194, 52-70.

Tejada, M. L., Geldmacher, J., Hauff, F., Heaton, D. E., Koppers, A. A. P., Schonberg, D. G., Hoernle, K., Heydolph, K., & Sager, W. W. (2016). Geochemistry and the age of shatsky, hess and ojin rise seamounts: implications for a connection between the shatsky and Hess rises. *Geochemica et Cosmochimica Acta*, 185, 302-327.

Telabpour, B., Türker, U., & Yegül, U. (2015). The role of precision agriculture in the promotion of food security. *International Journal of Agricultural Food Resources,* 4(1), 1-23.

Tellez, V., F. Lopez, J., Aragón, A., & Zayas, T. (2016) Application of nejayote as a foliar and edaphic fertiliser to native blue maize (*Zea mays* L.) crops. *American Journal of Plant Sciences*, **7,** 2221-2238.

Thornton, I., & Webb, J. S. (1980) Trace elements in soils and plants. In K. Blaxter (Ed.), Food chains and human nutrition (273-315). Springer, Dordrecht. http://doi-org-443.webvpn.fjmu.edu.cn/10.1007/978-94-011-7336-0_12.

Tokekar, P., Hook, J. V., Mulla, D., & Isler, V. (2016). Sensor planning for a symbioticUAV and UGV system for precision agriculture. *IEEE Transactions on Robotics*, 32(6), 1498-1511.

Tomlinson, D. C., Wilson, J. G., Harris, C. R., & Jeffrey, D. W. (1980). Problems in the assessment of heavy metals levels in estuaries and the formation of pollution index. *Helgoland Marine Research*, 33,566-575.

Toth, G., Hermann, T., Da Silva, M. R., & Montanarella, S. (2016). Heavy metals in soils of the European Union with implications for food safety. *Environment International*, 88, 299-309.

Toushmalani, R. (2010). Application of geophysical methods in agriculture. *Australian Journal of Basic and Applied Sciences*, 4(12), 6433-6439.

Tschan, M., Robinson, B. H., & Schulin, R. (2009). Antimony in the soil-plant system – a review. *Environmental Chemistry*, 6, 106-115.

Tully, K., Sullivan, C., Weil, R., & Sanchez, P. (2015). The state of soil degradation in Sub-Saharan Africa: baselines, trajectories, and solutions. *Sustainability*, 7, 6523-6552.

Turunen, M., Warsta, L., Paasonen-Kivekäs, M., Nurminen, J., Alakukku, L., Myllys, M., & Koivusalo, H. (2015), Effects of terrain slope on long-term and seasonal water balances in clayey, subsurface drained agricultural fields in high latitude conditions, *Agriculture and. Water Management,* 150, 139-151.

Ufoegbune, G. C., Atanley, P. A., Eruola, A. O., Makinde, A. A., & Ojekunle, Z. O. (2016). Geographical information system (GIS) application for planning and improvement of public water supply in Ota, Ogun State, Nigeria. *Journal of Applied Science and Environmental Management,* 20(2), 1105-1111.

Ugwuonah, E. N., & Obiora, C. S. (2011). Geothermometric and geobarometric signatures of metamorphism in the Precambrian basement complex rocks around Keffi, north-central Nigeria. *Ghana Journal of Science,* 51, 73-87.

Ugwuonah, E. N., Tsunogae, T., & Obiora, S. C. (2017). Metamorphic *P–T* evolution of garnet-staurolite-biotite pelitic schist and amphibolite from Keffi, north-central Nigeria: Geothermobarometry, mineral equilibrium modeling and *P-T* path. *Journal of African Earth Science,* 129, 1-16.

United States Geological Survey (USGS). https://www.usgs.gov/land-resources/nli/landsat-8. Assessed 5/6/2019.

Usikalu, M. R., & Achuka, J. A. (2014). Parameters and trace elements of soil samples collected from Ogun State, Nigeria. *Australian Journal of Basic and Applied Sciences*, 8(17), 137-141.

Van der Walt, A., Kolbe, S., Mitchell, P., Wang, Y., Butzkueven, H., Egan, Yiannikas, C., Grahams, S., & Klistorner, A. (2015). Parallel changes in structural and functional measures of optic nerve myelination after optic neuritis. *PLoS ONE*, 10(5), 1-14.

Van der Wal, A., & De Boer, W. (2017). Dinner in the dark: Illuminating drivers of soil organic matter decomposition. *Soil and Biochemistry*, 105, 45-48.

Varella, C. A. A., Gleriani, J. M., & Santos, R. M. (2015). Sugarcane: Agricultural production, Bioenergy and Ethanol. In F. Santos, A. Borem & C. Caldas (Eds.), *Precision agriculture and remote sensing* (1st ed., pp. 185-203). Academic Press, Brazil: Elsevier.

Victorian Resources (2014). Types of soil aggregates. Retrieved from http://vro.dpi.vic.gov.au/dpi/vro/vrosite.nsf/pages/soilhealth_soil_structure. Accessed 10/10/19.

Vieria, D. C. S., Fernandez, C., Vega, J. A., & Keizer, J. J. (2015). Does soil burn severity affect the post-fire runoff and interrill erosion response? A review based on meta-analysis of field rainfall simulation data. *Journal of Hydrology*, 523, 452-464.

Visconti, F., & De Paz, J. M. (2016). Electrical conductivity measurements in agriculture: the assessment of soil salinity. In L. Cocco (Ed.), *New trends and developments in metrology* (31-43). InTech Publisher United Kingdom, London, United Kingdom.

Walsh, C. O. D., Grunewaldi, E. D., Turneri, P., Hinnell, A. & Ferre, P. A. (2014). Practical limitations and applications of short dead time surface NMR. *Near Surface Geophysics,* 9(1780**),** 103-111.

Wang, J. Zhou, Y., & Xiao, F. (2020). Identification of multi-element geochemical anomalies using unsupervised machine learning algorithms: A case study from Ag–Pb–Zn deposits in north-western Zhejiang, China. *Applied Geochemistry*, 120(104679), 1-15.

Wang, L. & Qu, J. J. (2009). Satellite remote sensing applications for surface soil moisture monitoring: A review. *Frontiers of Earth Science in China*, 3(2), 237-247.

Wang, N., Zhang, N., & Wang, M. (2006). Wireless sensors in agriculture and food industry-recent development and future perspective. *Computers and Electronics in Agriculture,* 50, 1-14.

Warrence, N. J., Bauder, J. W., & Pearson, K. E. (2003). Basics of salinity and sodicity effects on soil physical properties. Department of Land Resources and Environmental Sciences: Montana State University, Bozeman, 1-29.

Watson, C. A., Oborn, I., Edwards, A. C., Dahlin, A. S., Eriksson, J., Lindstorm, B. E. M., Linse, L., Owens, K., Topp, C. F. E., & Walker, R. L. (2012). Using soil and plant properties and farm management practices to improve the micronutrient composition of food and feed. *Journal of Geochemical Exploration,* 12**,** 15-24.

Werban, U., Hagrey, S. A., & Rabbeh, W. (2008). Monitoring of root-zone water content in the laboratory by 2D geoelectrical tomography. *Journal of Plant Nutrition and Soil Science*, 171(6), 927-935.

White, P. J., Bowen, H. C., Parmaguru, P., Fritz, M., Spracklen, W. P., & Spiby, R. E. (2004). Interactions between selenium and Sulphur nutrition in Arabidopsis thaliana, I. *Journal of Experimental Botany*, 55(404), 1927-1937.

WHO/FAO. (2001). Codex alimentarius commission. Food additives and contaminants. Joint FAO/WHO Food Standards Programme, ALINORM 10/12A. Retrieved from www.transpaktrading.com/static/pdf/research/achemistry/intro to fertilizers. Accessed 14/11/2019.

WHO/FAO. (2007). Joint FAO/WHO Food standard programme codex alimentarius commission 13th session. Report of the Thirty-Eight Session of the Codex Committee on Food Hygiene. Houston, TX, ALINORM 07/30/13.

Wiegand, C. L, Rhoades, J. D., Escobar, D. E., & Everitt, J. H. (1994). Photographic and videographic observations for determining and mapping the response of cotton to soil salinity. *Remote Sensing of Environment,* 49(3), 212-223.

Wiesmeier, M., von Lützow, M., Spörlein, P., Geuß, U., Hangen, E., Reischl, A., Schilling, B., & Kogel-Kabner, I. (2015). Land use effects on organic carbon storage in soils of Bavaria: the importance of soil types. *Soil and Tillage Research,* 146, 296-302.

Wilschefski, S. C., & Baxter, M. R. (2019). Inductively coupled plasma mass spectrometry: introduction to analytical aspects. *The Clinical Biochemist Reviews,* 40(3), 115-133.

Winterburn, P. A., Noble, R. R. P., & Lawie, D. (2017). Advances in exploration geochemistry, 2007 to 2017 and beyond. In V. Tschirhart & M. D. Thoma (Eds.), Proceedings of Exploration 17: Sixth Decennial International Conference on Mineral Exploration (pp. 495-505). Toronto, Canada.

Won, J., Park, J., Choo, H., & Burns, S. (2019). Estimation of saturated hydraulic conductivity of coarse-grained soils using particle shape and electrical resistivity. *Journal of Applied Geophysics*, 167, 19-25.

Woodruff, L. G., Cannon, W. F., Eberl, D. D., Smith, D. B., Kilburn, J. E., Horton, Garrett, R. G., & Klassen, R. A. (2009). Continental-scale patterns in soil geochemistry and mineralogy: Results from two transects acro,ss the United States and Canada. *Applied Geochemistry,* 24(8), 1369-1381.

Wu, J., & Nofziger, D. L. (1999) Incorporating temperature effects on pesticide degradation into a management model. *Journal of Environmental Quality*, 28, 92-100.

Wu, W., & Chen, Y. L. (2018). Application of isolation forest to extract multivariate anomalies from geochemical exploration data. *Global Geology,* 21(1), 36-47.

Xiao, X., Yang, M., Guo, Z., Jian, Z., Liu, Y., & Cao, X. (2015). Soil vanadium pollution and microbial response characteristics from stone coal smelting district. *Transactions of Nonferrous Metals Society of China*, 25 (4), 1271-1278.

Xing, L., Li, L., Gong, J., Ren, C., Liu, J., & Chen, H. (2018). Daily soil temperatures predictions for various climates in United States using data-driven model. *Energy*, 160(C), 430-440.

Xu, C., Qu, J. J., Hao, X., Zhu, Z., & Gutenberg, L. (2020). Surface soil temperature seasonal variation estimation in a forested area using combined satellite observations and in-situ measurement. *International Journal of Earth Obs Geoinformations*, 91, 1-10.

Yang, Q., Wang, L., Zhou, Q., & Huang, X. (2015). Toxic effects of heavy metal terbium ion on the composition and functions of cell membrane in horseradish roots. *Ecotoxicology and Environmental Safety*, 111**,** 48-58.

Yang, H., Zhou, J., Feng, J., Zhai, S., Chen, W., Liu, J., & Bian, X. (2019). Ditch-buried straw return: A novel tillage practice combined with tillage rotation and deep ploughing in rice-wheat rotation systems. In D. L. Sparks (Ed.), *Advances in Agronomy* (154, pp 257-290). Berne, Switzerland, Academic Press: Elsevier.

Yemefack, M., Njomgang, R., & Rossiter, D. G. (2019). Quantified soil evolution under shifting agriculture in southern Cameroon. *Frontier in Environmental Science,* **7**(16), 1-10.

Yetbarek, E. & Ojha, R. (2020). Spatio-temporal variability of soil moisture in a cropped agricultural plot within the Ganga Basin, India. *Agricultural Water Management,* 234 (106108), 1-7.

Yeung, A. K. W., & Lo, C. P. (2002). Concepts and techniques of geographic information systems. *International Journal of Geographical Information Science,* 17, 819-820.

Yebo, B. (2015). Integrated soil fertility management for better crop production in Ethiopia. *International Journal of Soil Science,* 10, 1-16.

Yilvainio, K., & Pettovuori, T. (2012). Phosphorus acquisition by barley (Hordeum yulgar) at suboptimal soil temperature. *Agricultural and Food Science,* 21, 453-461.

Yourek, M., Brooks, E. S., Brown, D. J., Poggio, M., & Gasch, C. (2019). Development and application of the soil moisture routing (SMR) model to identify subfield-scale hydrologic classes in dryland cropping systems using Budyko framework. *Journal of Hydrology*, 573**,** 153-169.

Zanter, K. (2019). Landsat 8 (L8) Data Users Handbook, Department of the Interior, United States Geological Survey, LSDS-1574, Version 5.0, 1-114.

Zeeshan, M., Deshmulch, R. R., & Syed, S. B. (2017). An overview of different optical remote sensing techniques. *International Journal of Engineering and Advanced Technology*, 6(17), 181-183.

Zeng, Y., Feng, Z., & Xiang, N. (2004). Assessment of soil moisture using Landsat etm plus temperature and vegetation index in semi-arid environment. *Geoscience and Remote Sensing Symposium*, 6, 1-8.

Zeri, M., Alvala, R. C. S., Carneiro, R., Cunha-Zeri, G., Coasta, J. M., Spatafora, L. R., Urbano, D., Llossera, M., & Marengo, J. (2018). Tools for communicating agricultural drought over the Brazilian semiarid using the soil moisture index. *Water,* 10(1421), 1-15.

Zeynoddin, M., Ebtehaj, I., & Bonakdari, H. (2020). Development of a linear based stochastic model for daily soil temperature prediction: One step forward to sustainable agriculture. *Computers and Electronics in Agriculture*, 176, 1-24.

Zhang, L. P., Ye, X., Feng, H., Jing, Y., Quyang, T., Yu, X., Liang, R., Gao, C., & Chen, N. (2007). Heavy metal contamination in western Xiamen Bay sediments and its vicinity, China. *Marine Pollution Bulletin*, 54(5), 974-982.

Zhang, L., Xin, H., & Chen, J. (2018). Effect of terrain slope on water distribution and application uniformity for sprinkler irrigation. *International Journal of Agricultural and Biological Engineering*, 11(3), 120-125.

Zhang, R., Tu, C., Zhang, H., & Luo, Y. (2019). Stability and transport of titanium dioxide nanoparticles in three variable-charge soils. *Journal of Soils and Sediments* 20, 1395–1403. https://doi.org/10.1007/s11368-019-02509-x.

Zhang, W., Wang, C., Xue, R., & Wang, L. (2019). Effects of salinity on the soil microbial community and soil fertility. *Journal of Integrative Agriculture*, 18(6), 13.0-13.68.

Zhang, S., Xiao, K. Y., Carranza, E.J.M., Yang, F., & Zhao, Z. C. (2019). Integration of auto-encoder network with density-based spatial clustering for geochemical anomaly detection for mineral exploration. *Computers and Geoscience*, 130, 43-56.

Zhao, Y. G., Zhang, G. L., Wen-Jun, Z. T. (2005 November 27 – 2 December). Soil characteristics and crop suitability of sandy soils in Hainan, China. Conference proceedings at session 1 global extent of tropical sandy soils and their pedogenesis of the Management of Tropical Sandy Soils for Sustainable Agriculture (49-53). Khon Kaen, Thailand.

Zhao, G., Li, X., Wang, R., Li, T., & Yue, Y. (2007). Soil nutrients in intensive agricultural areas with different land use types in Qingzhou County, China. *Pedosphere*, 17(2), 165-171.

Zhao, K., Tung, C., Eizenga, G. C., Wright, M. H., Ali, M. L, Price, Reynolds, A., & McCouch, S. R. (2011). Genome-wide association mapping reveals a rich genetic architecture of complex traits in *Oryza sativa*. *Nature Communication*, 2(467), 1-10.

Zhao, Z., Liu, J., Jia, R., Bao, S., Haixia, H., & Chen, C. (2019). Physiological and TMT-based proteomics analysis of oat early seedlings in response to alkali stress. *Journal of Proteomics*, 193, 10-26.

Zhou, H., Fang, H., Mooney, S. J., & Peng, X. (2016). Effects of long-term inorganic and organic fertilizations on the soil micro and macro structures of rice paddies. *Geoderma*, 266, 66-74.

Zhu, Q. Q., & Liu, Z. (1988). REEs in soil of eastern China. *Journal of Chinese Rare Earth Society,* 8(6), 59-65.

Zribi, M., Chahbi, A., Lili Chabaane, Z., Duchemin, B., Baghdadi, N., Amri, R., & Chehbouni, A. (2011). Soil surface moisture estimation over a semi-arid region using ENVISAT ASAR radar data for soil evaporation evaluation. *Hydrological and Earth System Sciences,* 15, 345-358.

# APPENDIX A

## 2D RESISTVITY MODELS FOR COVENANT UNIVERSITY FARM

a

b

c

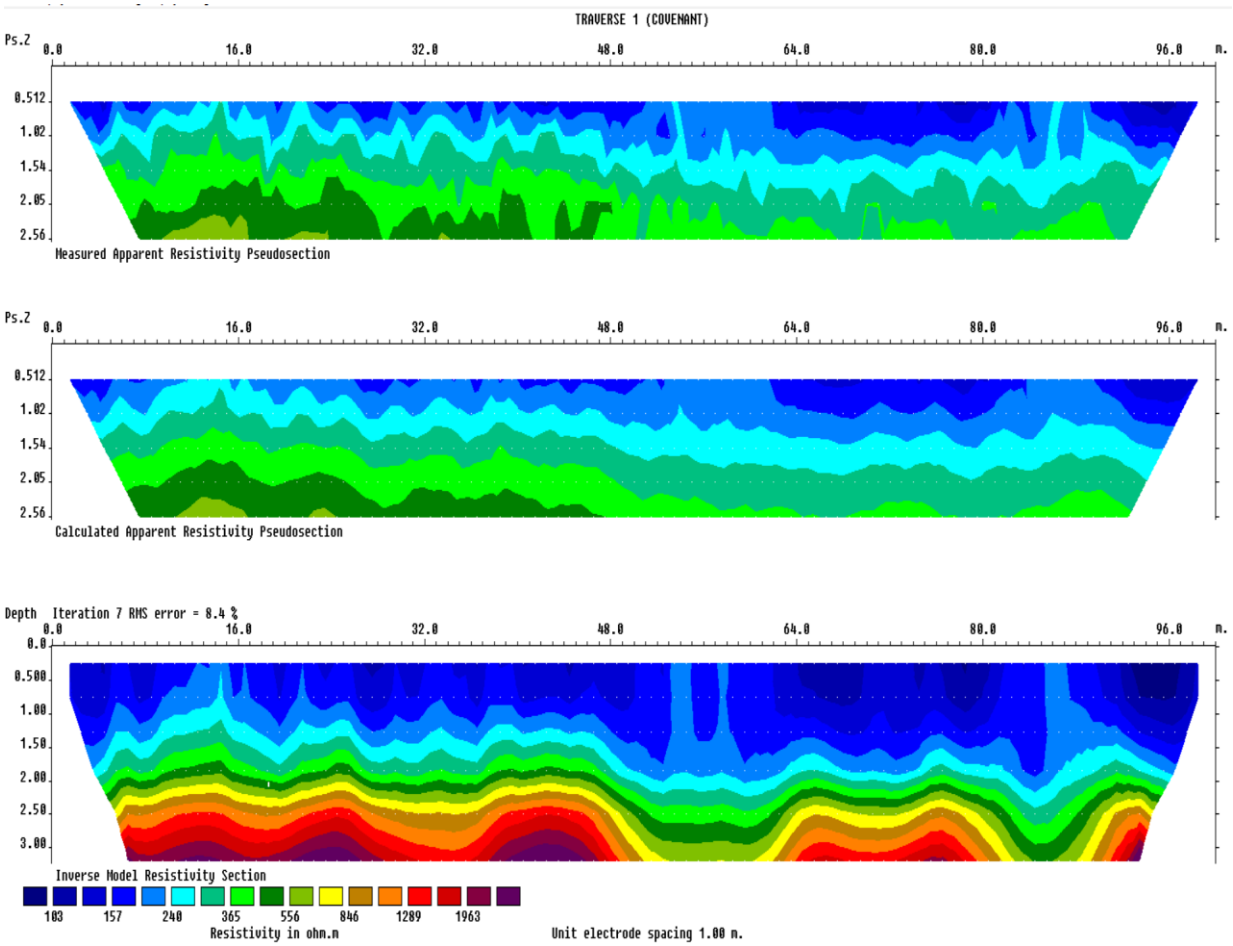


**Figure A1**: 2D resistivity inversion model for Traverse 1 at the site in Covenant University farm showing: (a) measured, (b) calculated, and (c) inversed model

.

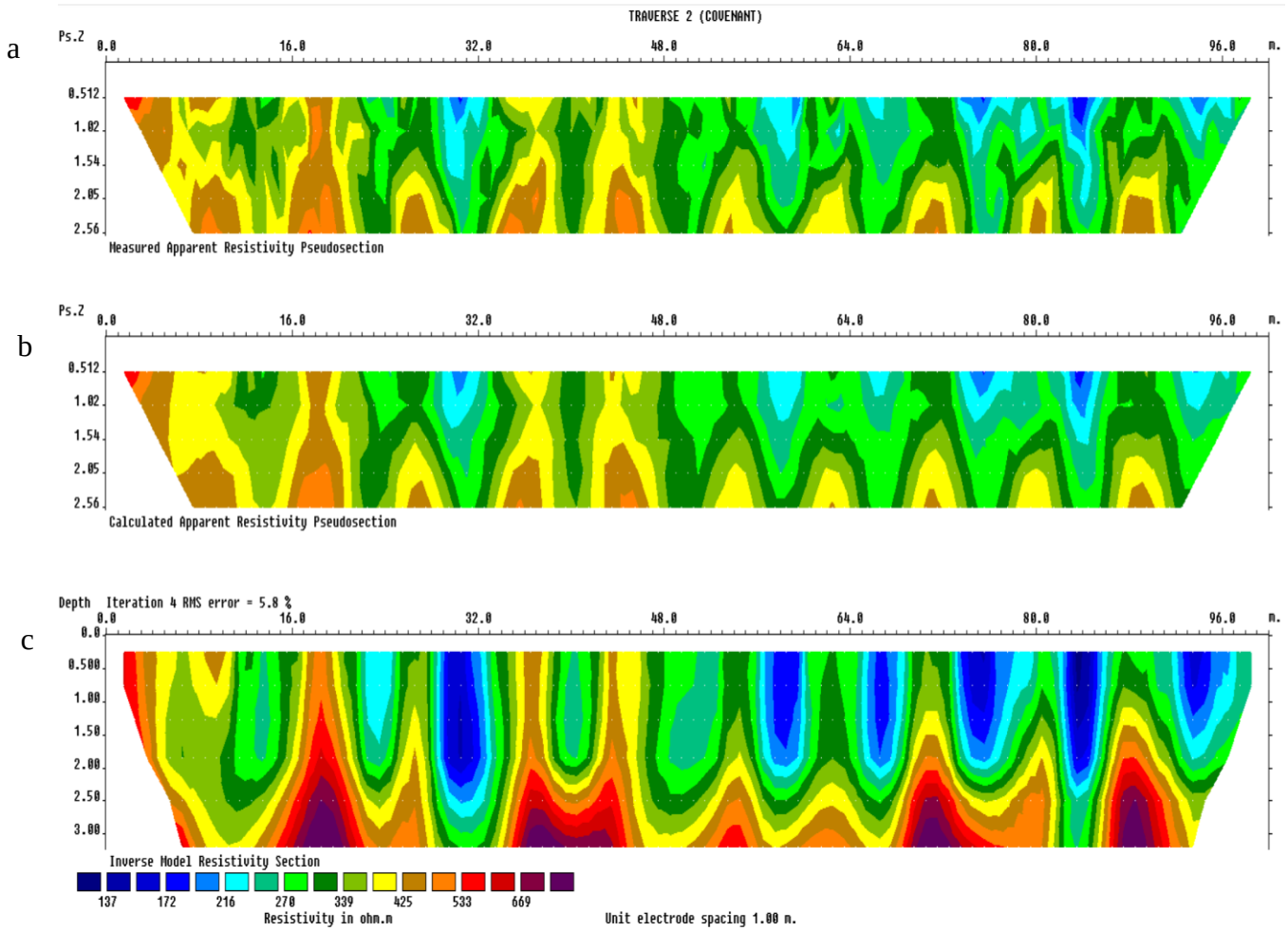


**Figure A2**: 2D resistivity inverse model for Traverse 2 for the site at Covenant University farm showing: (a) measured, (b) calculated, and (c) inversed model

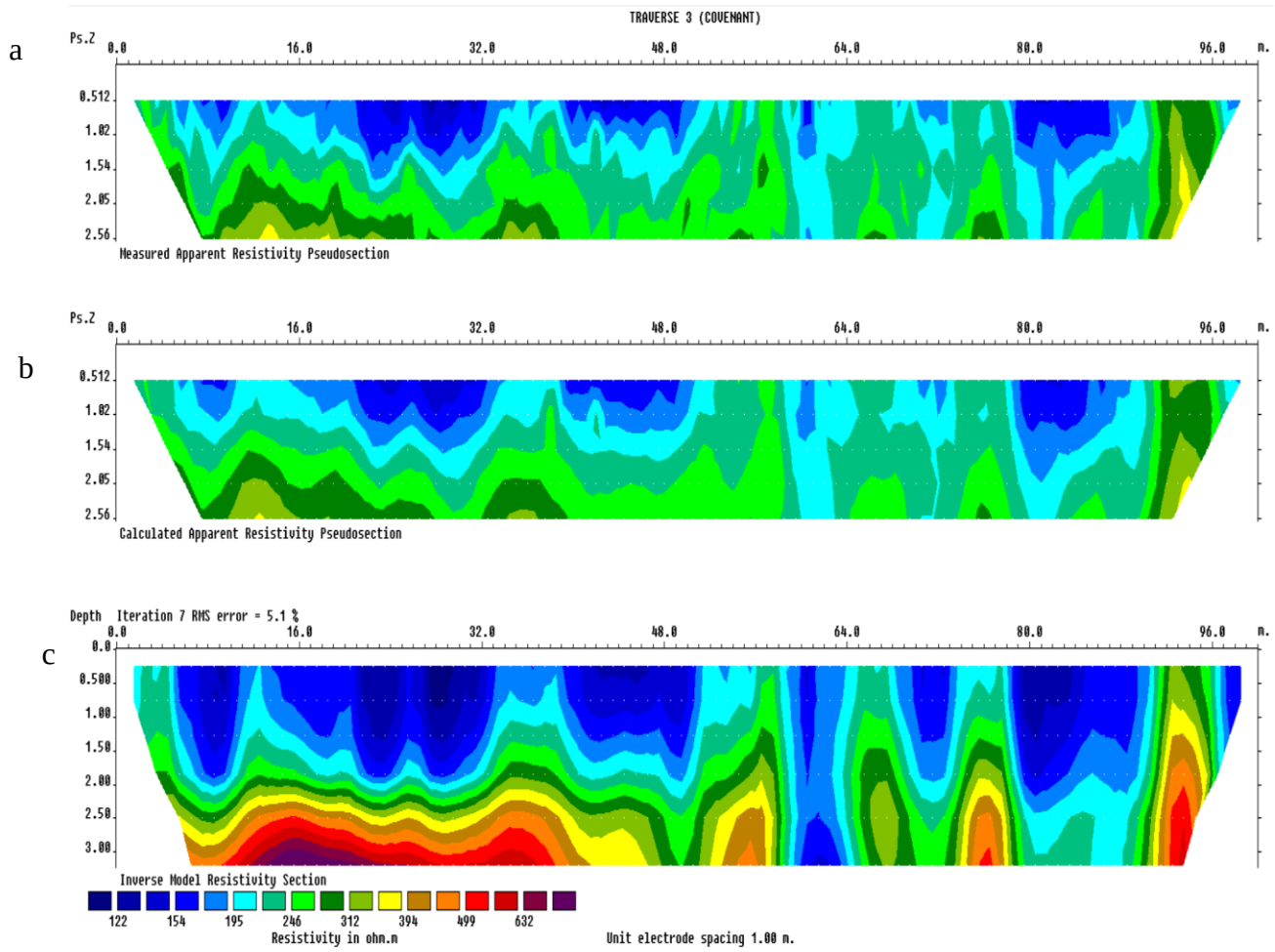


**Figure A3**: 2D resistivity inverse model for Traverse 3 at the site in Covenant University farm showing: (a) measured, (b) calculated, and (c) inversed model

a

b

c

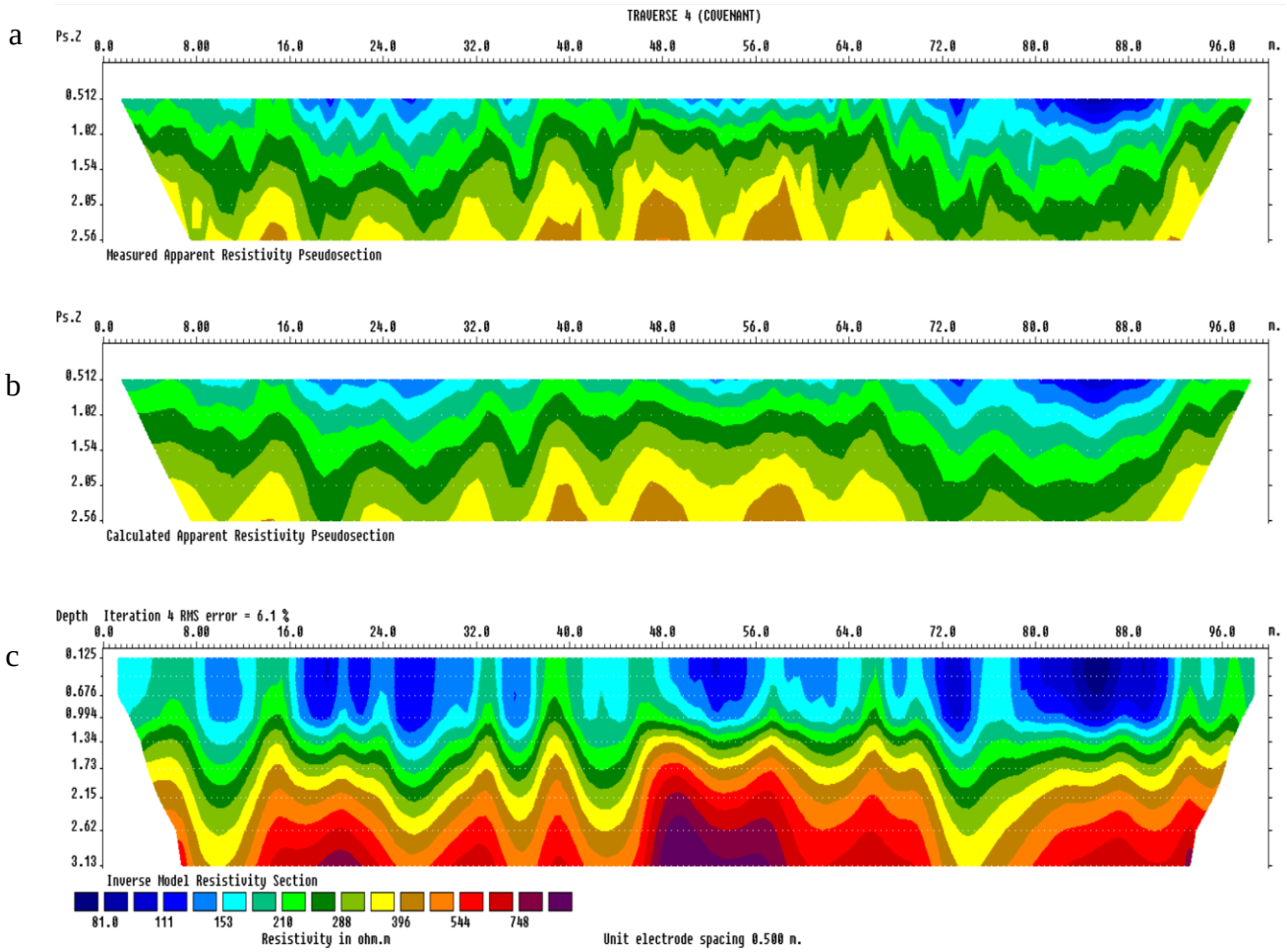


**Figure A4**: 2D resistivity inverse model for Traverse 4 at the site in Covenant University farm showing: (a) measured data, (b) calculated, and (c) inversed data

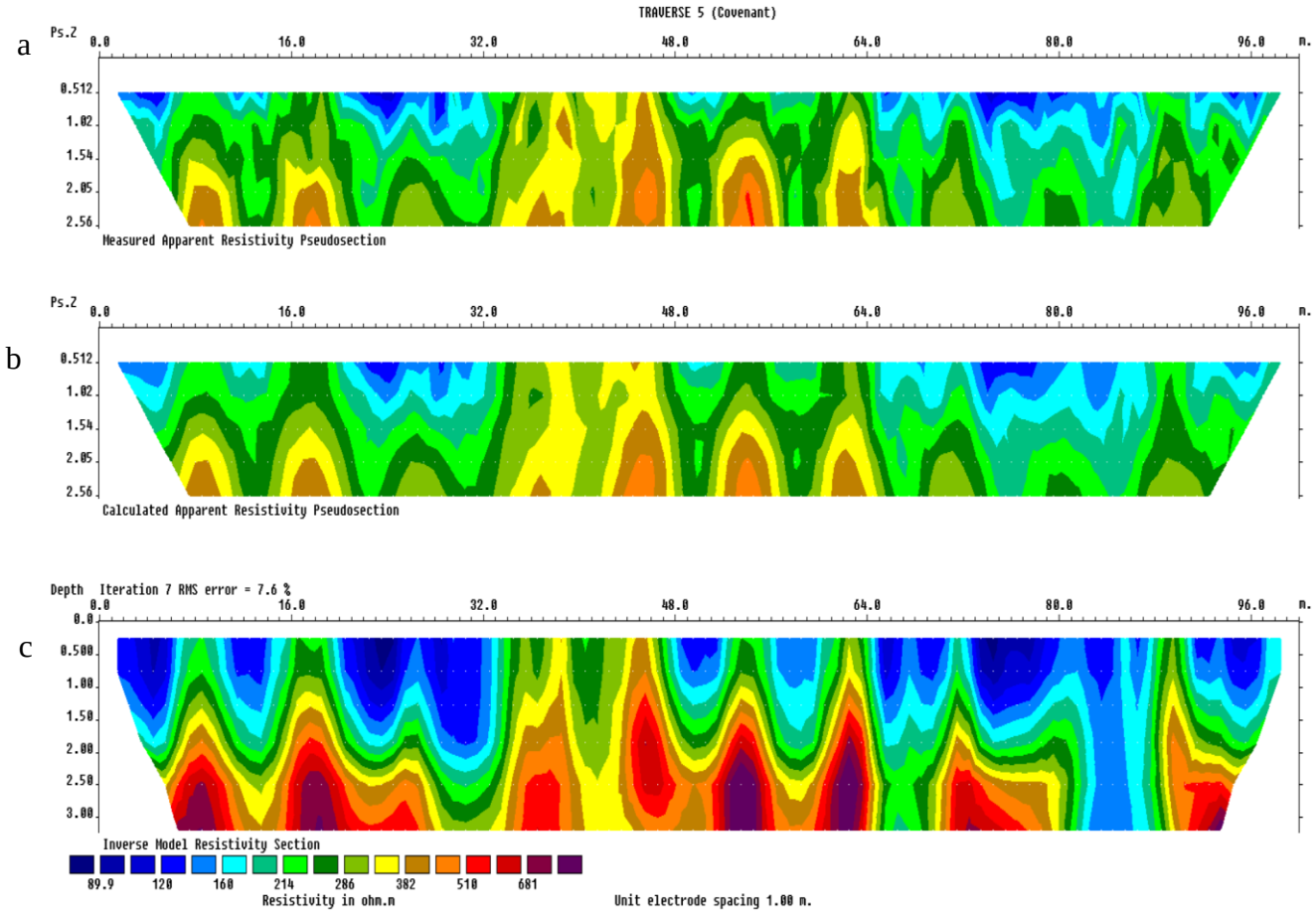


**Figure A5**: 2D resistivity inverse model for Traverse 5 at the site in Covenant University farm showing: (a) measured data, (b) calculated data, and (c) inversed model.

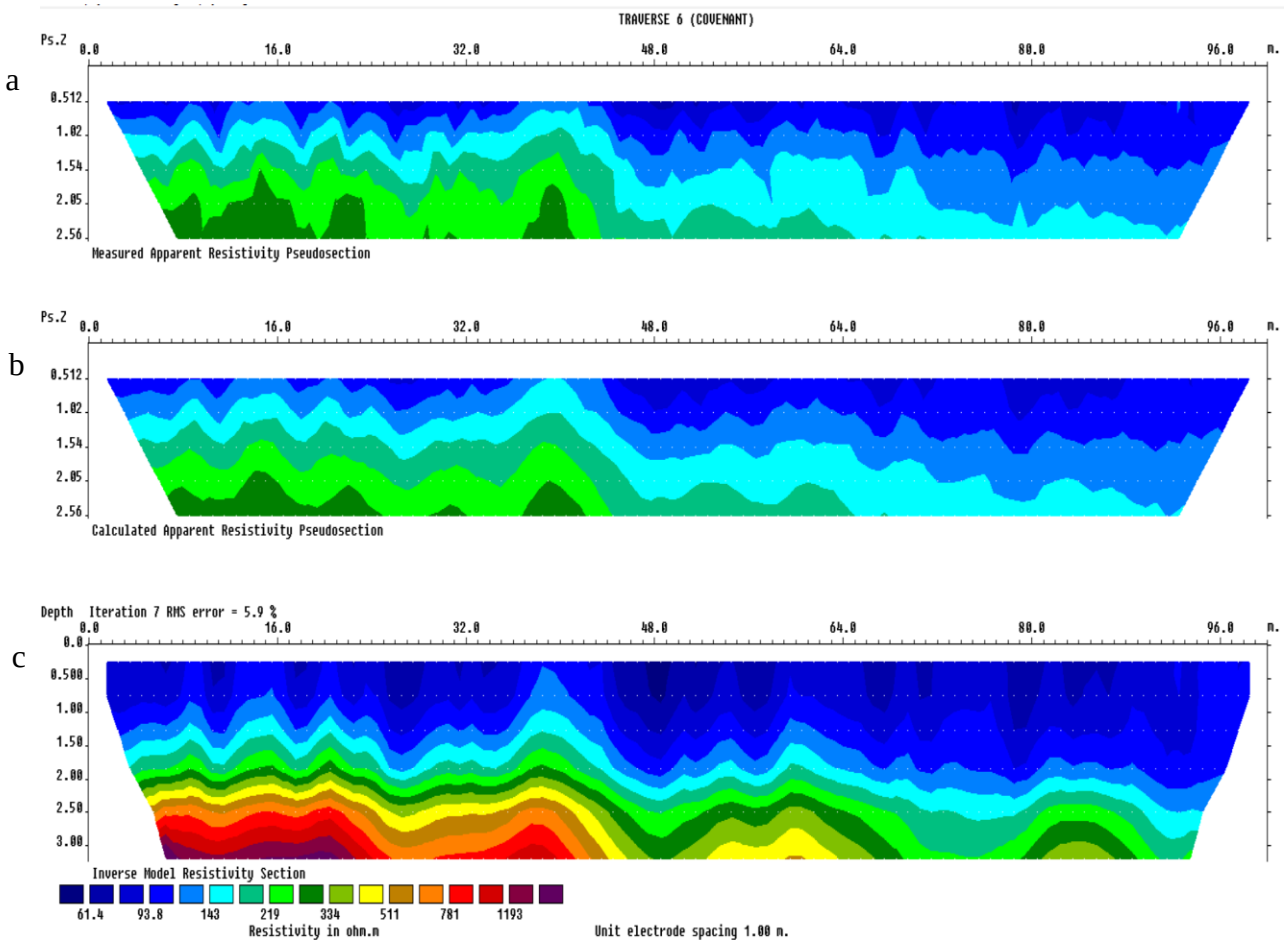


**Figure A6**: 2D resistivity inverse model for Traverse 6 at the site in Covenant University farm showing (a) measured data, (b) calculated, and (c) inversed model.

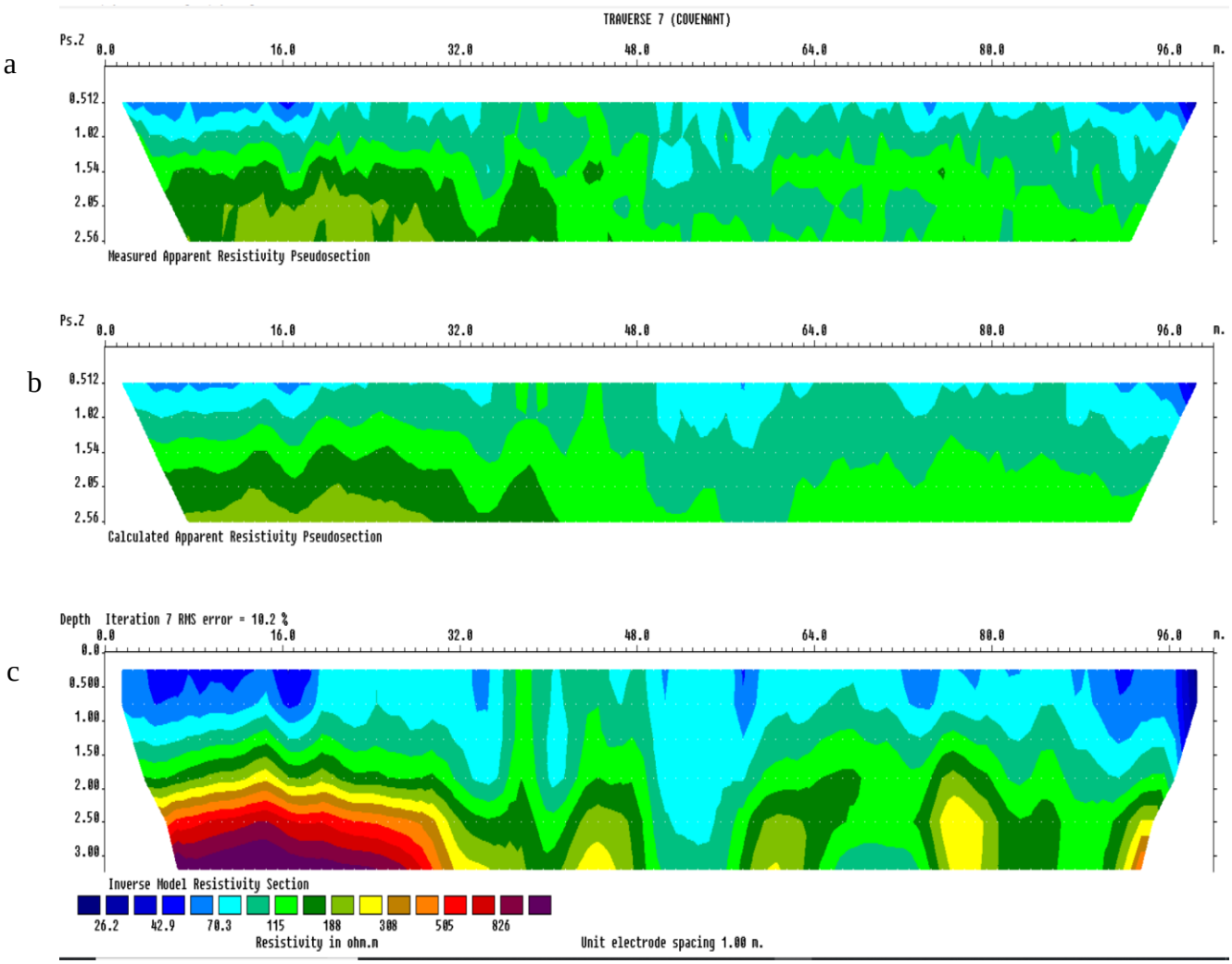


**Figure A7**: 2D resistivity inverse model for Traverse 7 at the site in Covenant University farm showing: (a) measured data, (b) calculated data, and (c) inverse model.

# APPENDIX B

## 2D RESISTVITY MODELS FOR LANDMARK UNIVERSITY FARM

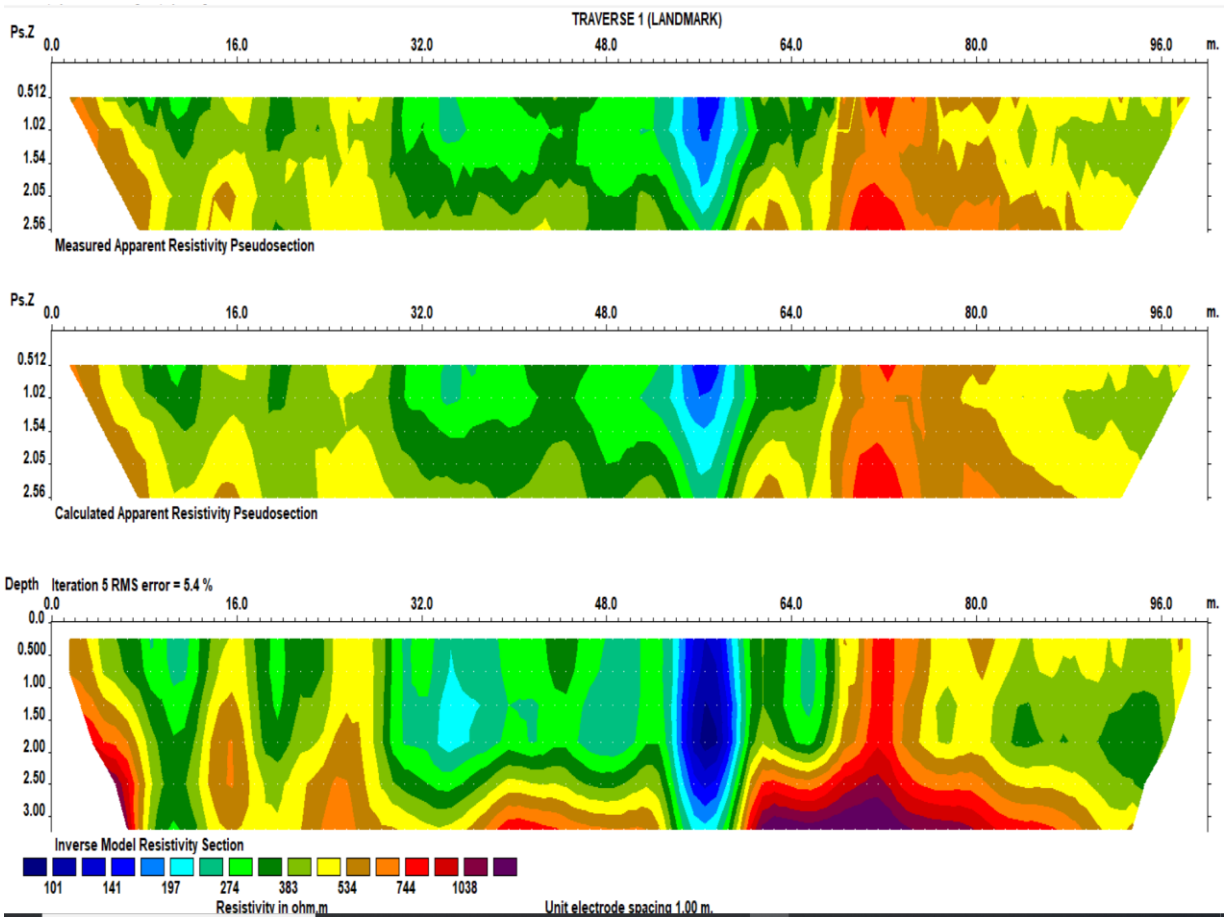


**Figure B1**: 2D resistivity inverse model for Traverse 1 at the site in Landmark University farm showing: (a) measured, (b) calculated, and (c) inversed model.

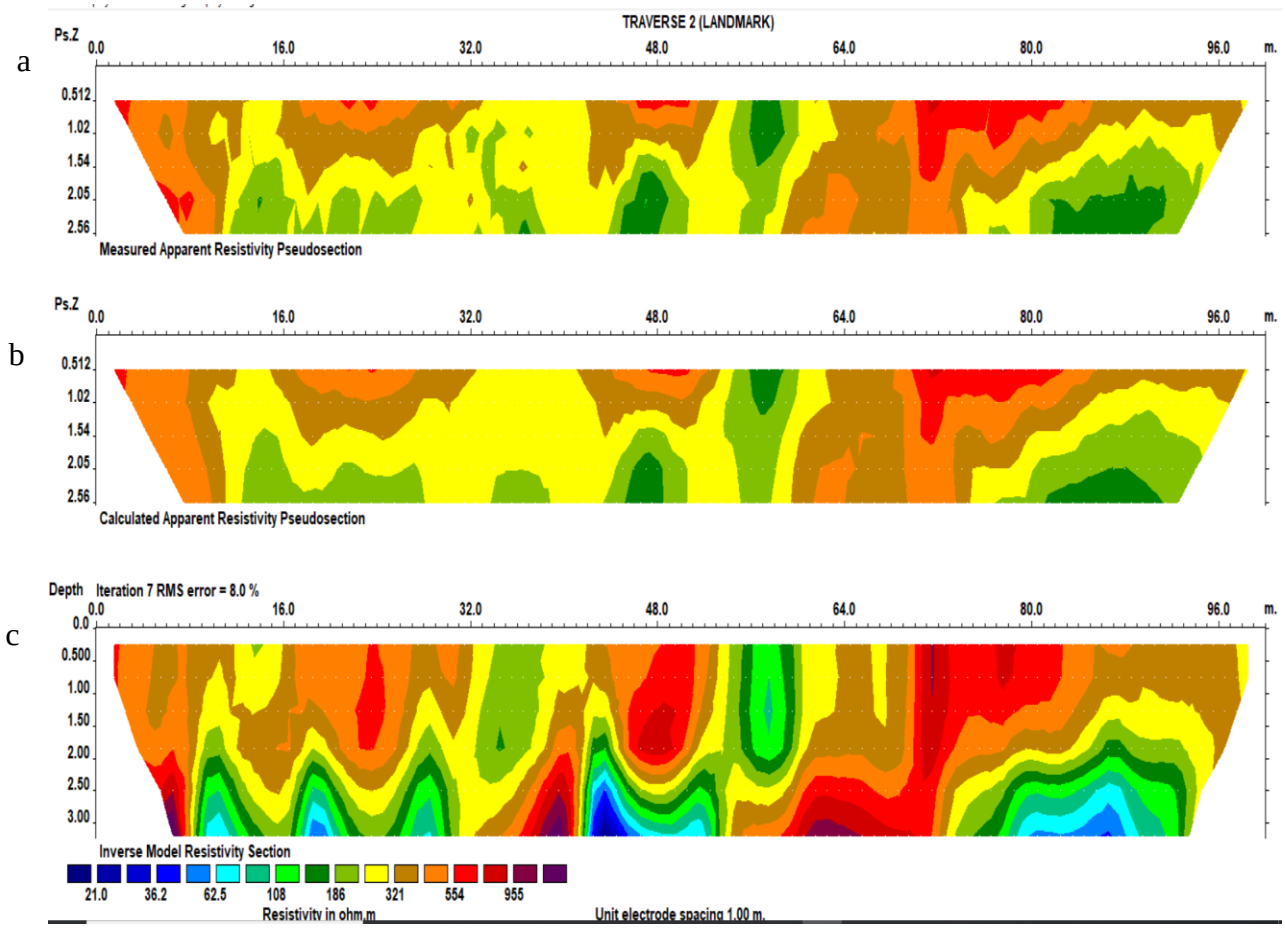


**Figure B2**: 2D resistivity inverse model for Traverse 2 at the site in Landmark University farm showing: (a) measured, (b) calculated, and (c) inversed model.

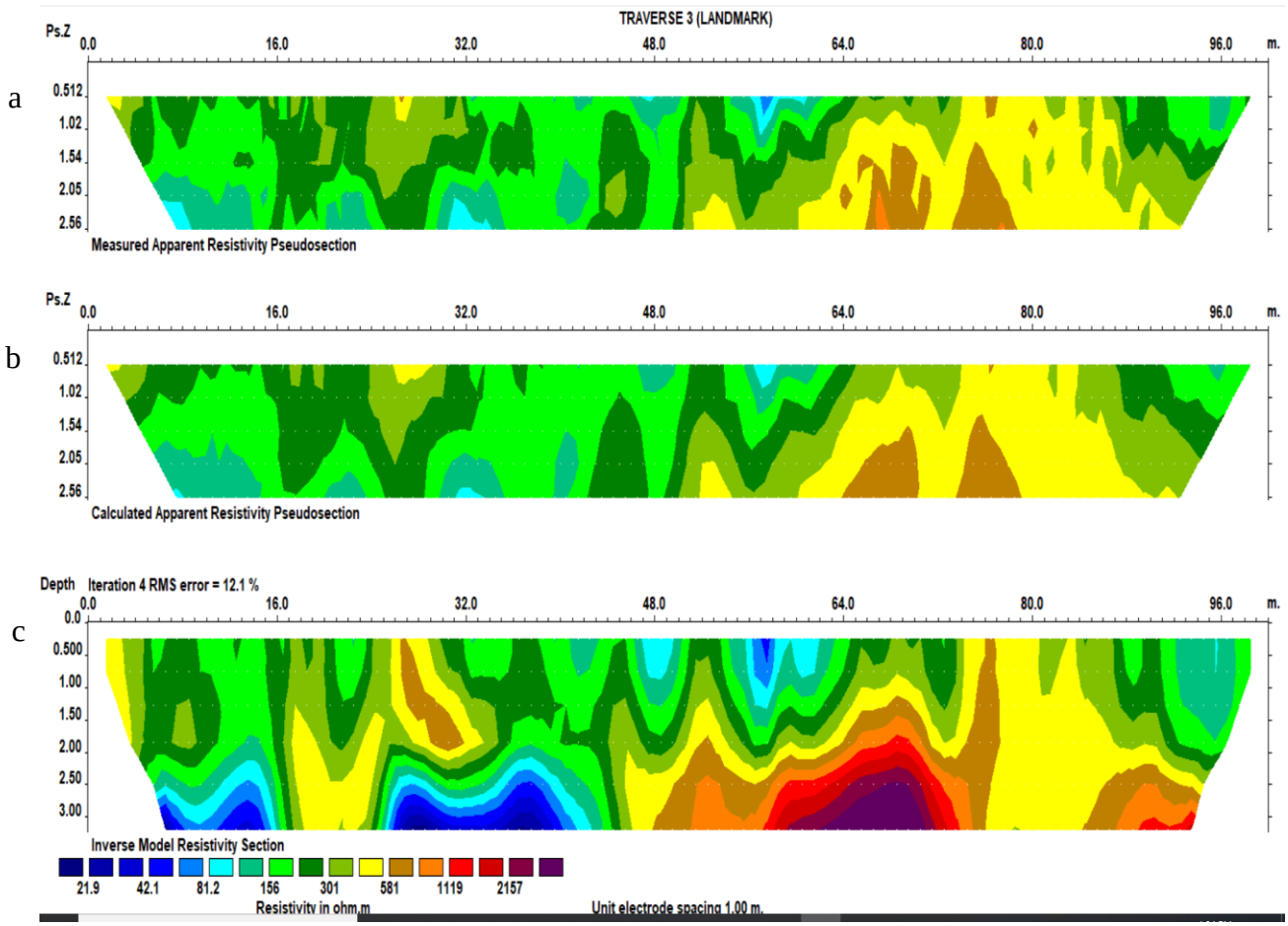


**Figure B3**: 2D resistivity inverse model for Traverse 3 at the site in Landmark University farm showing: (a) measured, (b) calculated. And (c) inversed model.

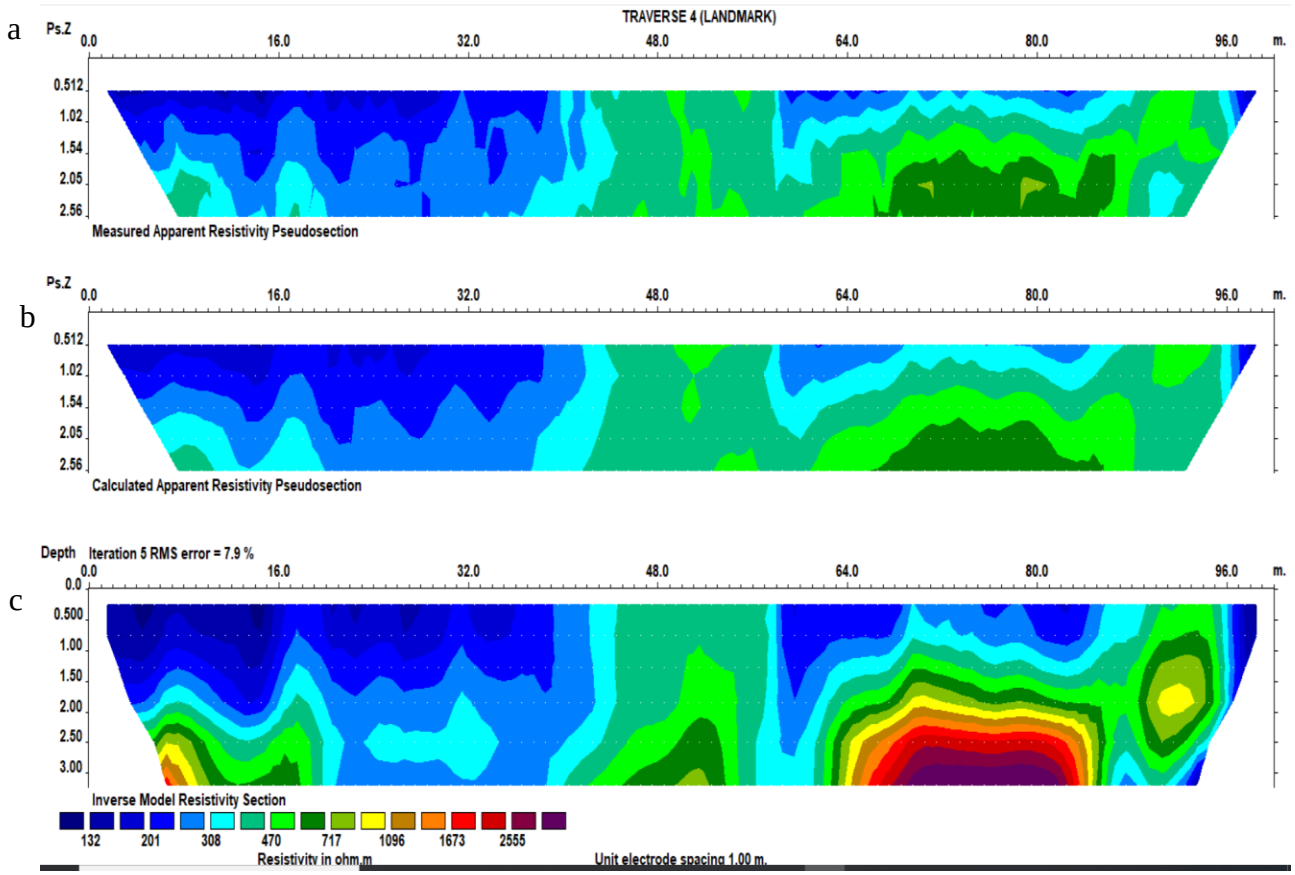


**Figure B4**: 2D resistivity inverse model for Traverse 5 at the site in Covenant University farm showing: (a) measured, (b) calculated, and (c) inverse model.

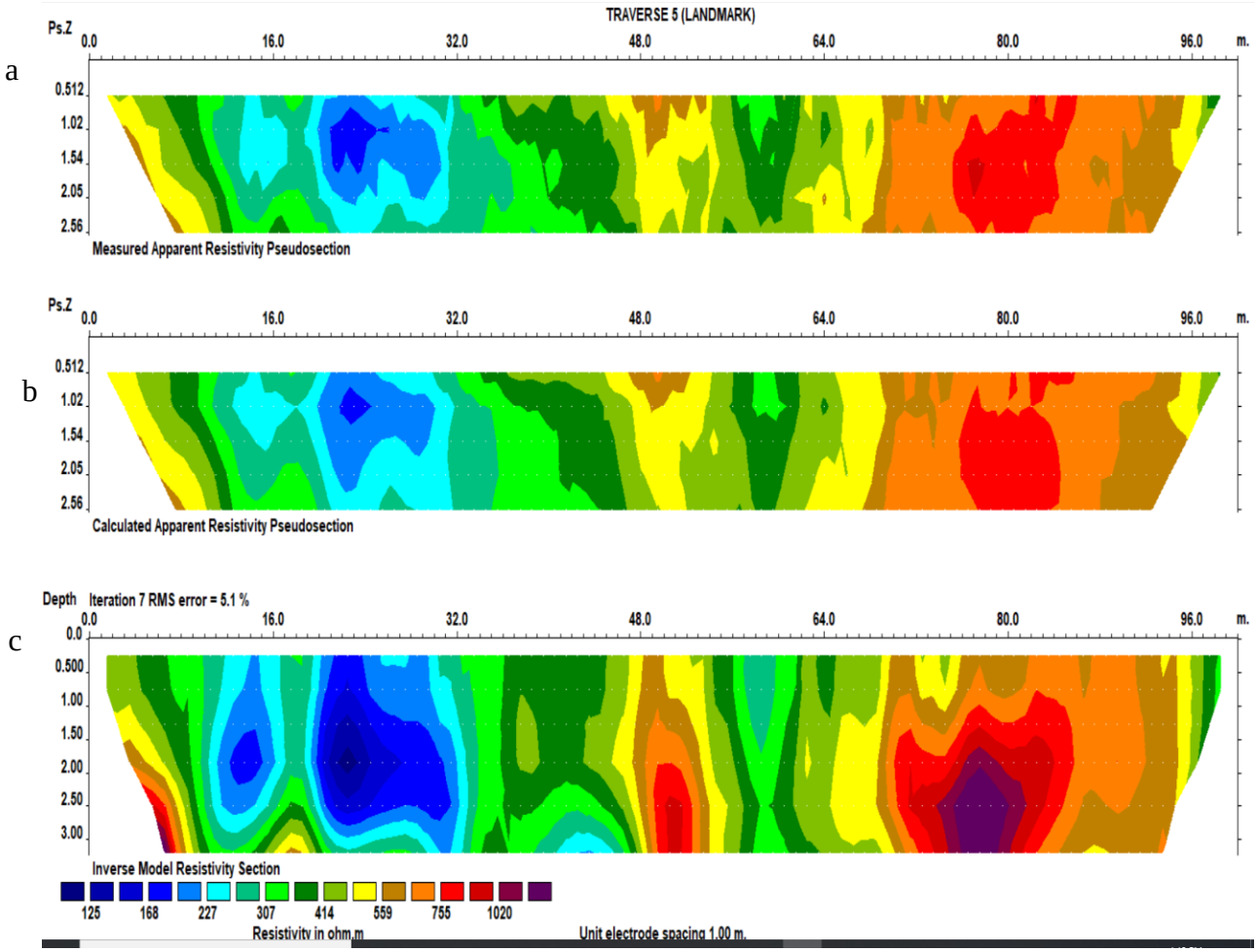


**Figure B5**: 2D inverse model for Traverse 5 at the site in Covenant University farm showing: (a) measured, (b) calculated, and (c) inverse model.

a

b

c

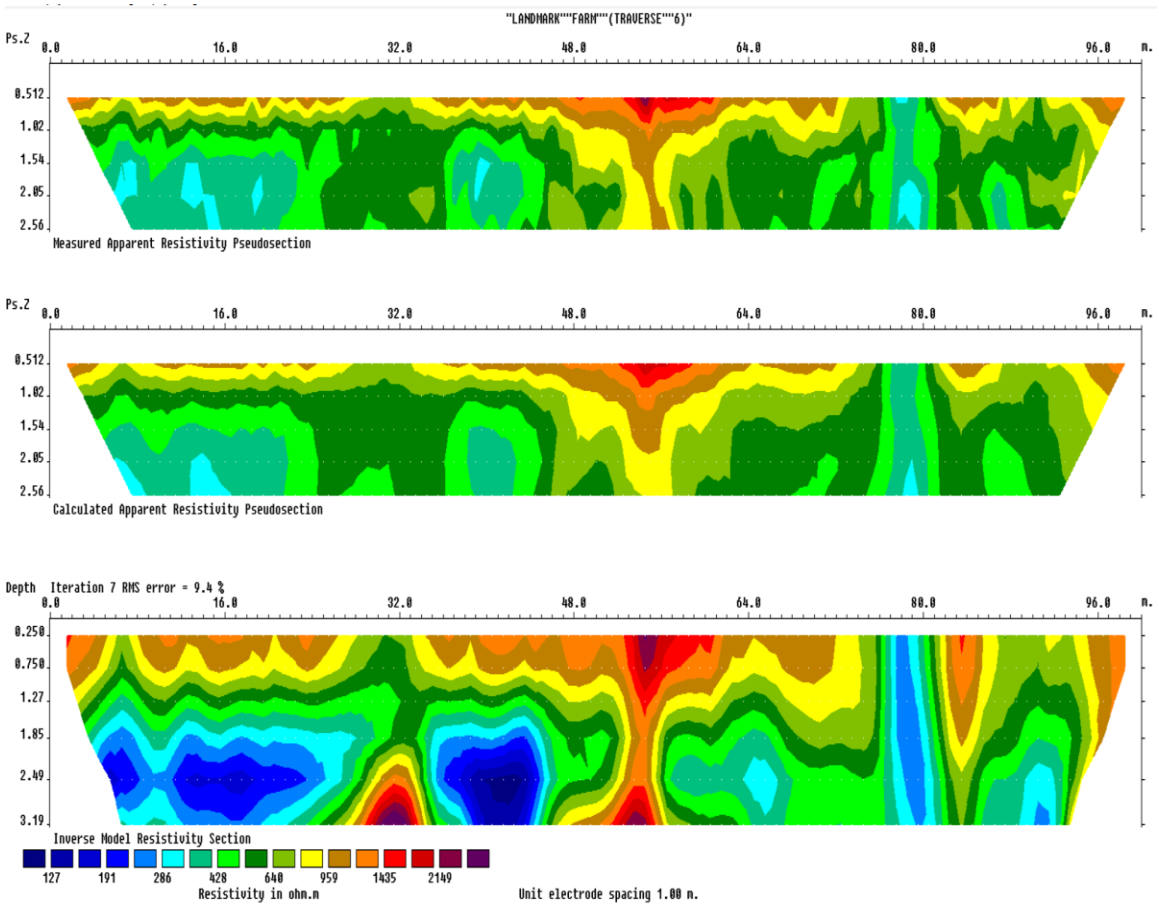


**Figure B6**: 2D resistivity inverse model for Traverse 6 at the site in Landmark University farm showing: (a) measured, (b) calculated, and (c) inverse model.

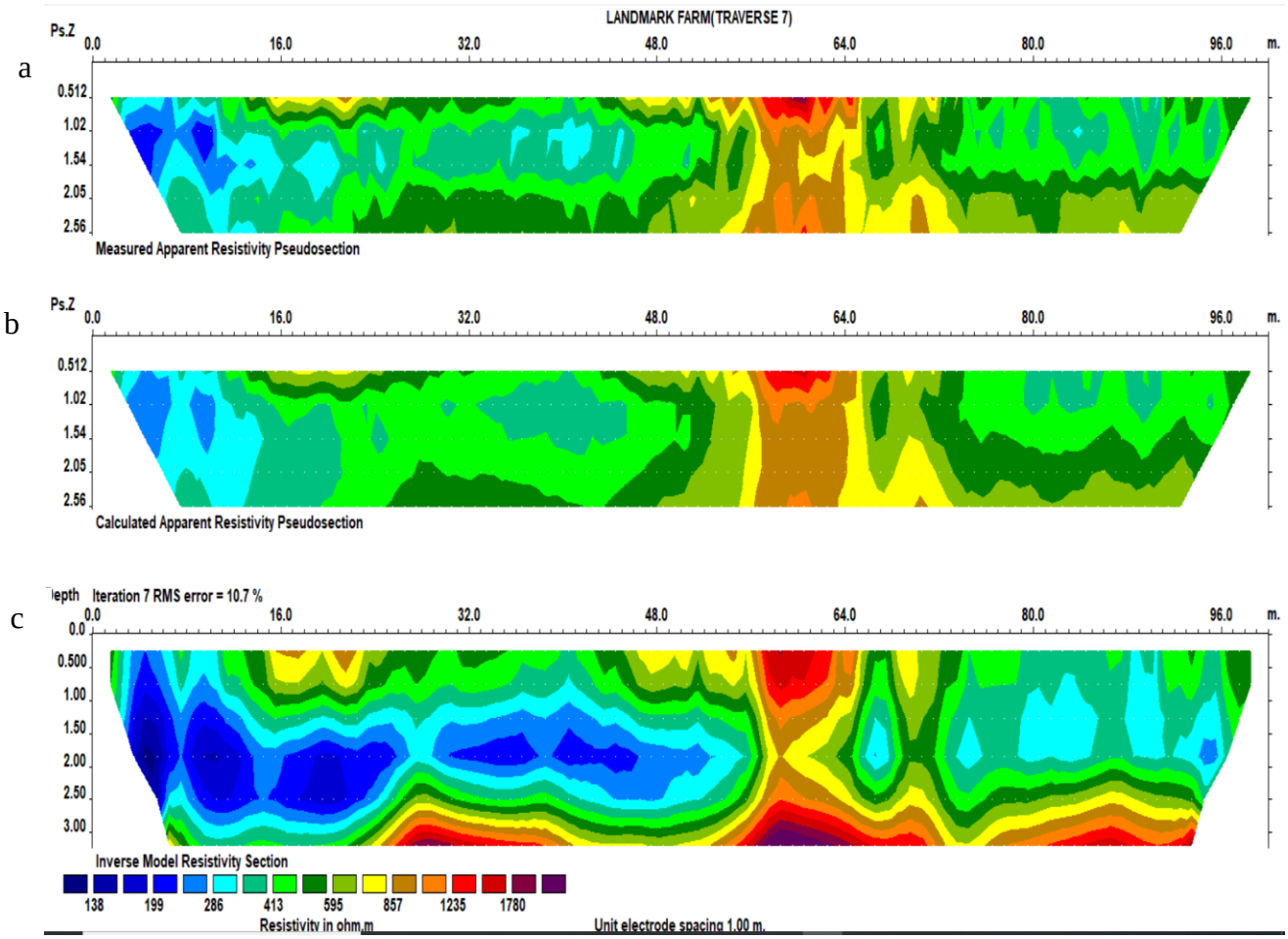


**Figure B7**: 2D resistivity inverse model for Traverse 7 at the site in Landmark University farm showing: (a) measured, (b) calculated, and inverse model.

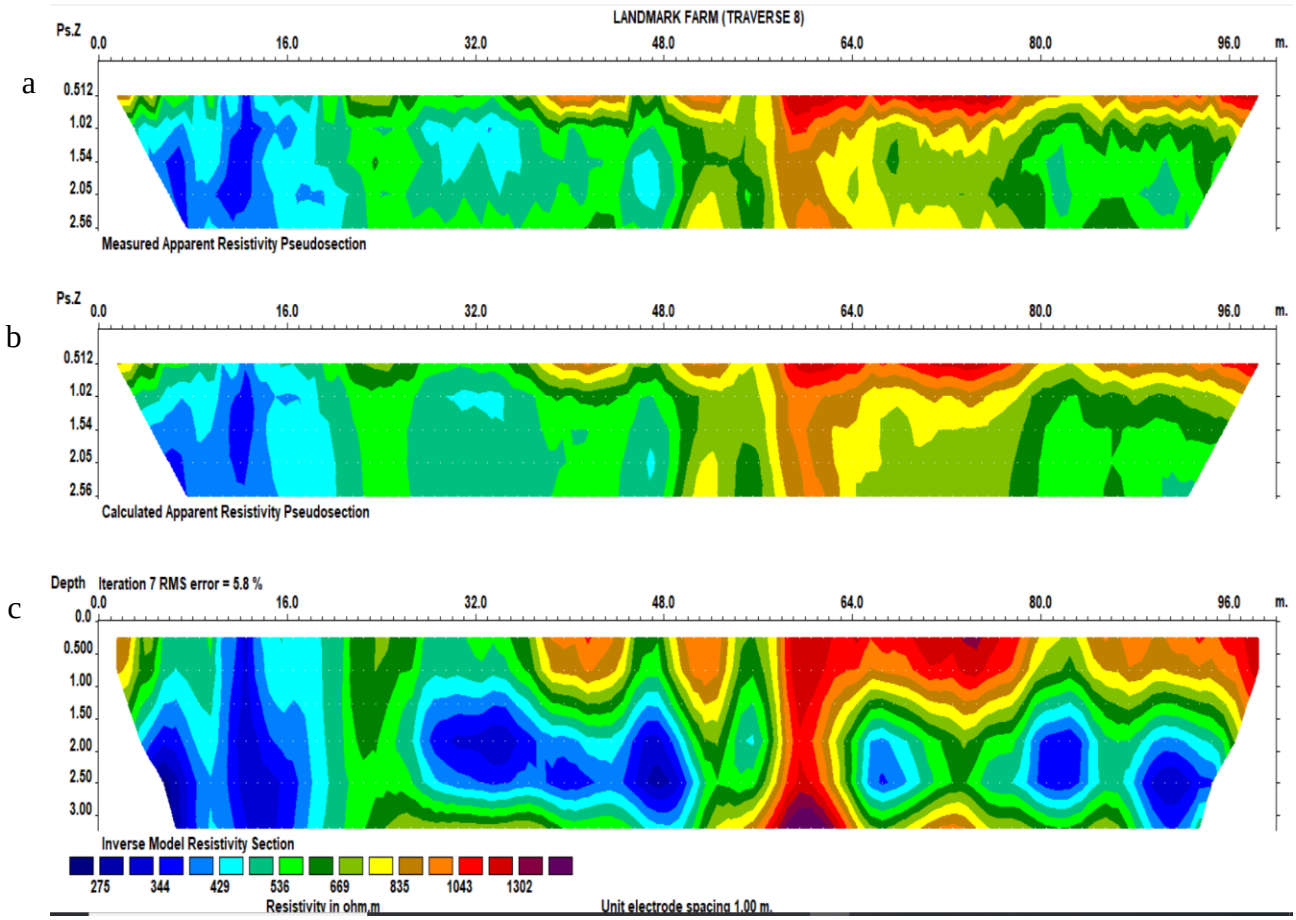


a

b

c

**Figure B8**: 2D resistivity inverse model of Traverse 8 at the site in Landmark University farm showing: (a) measured, (b) calculated, and (c) inverse model.

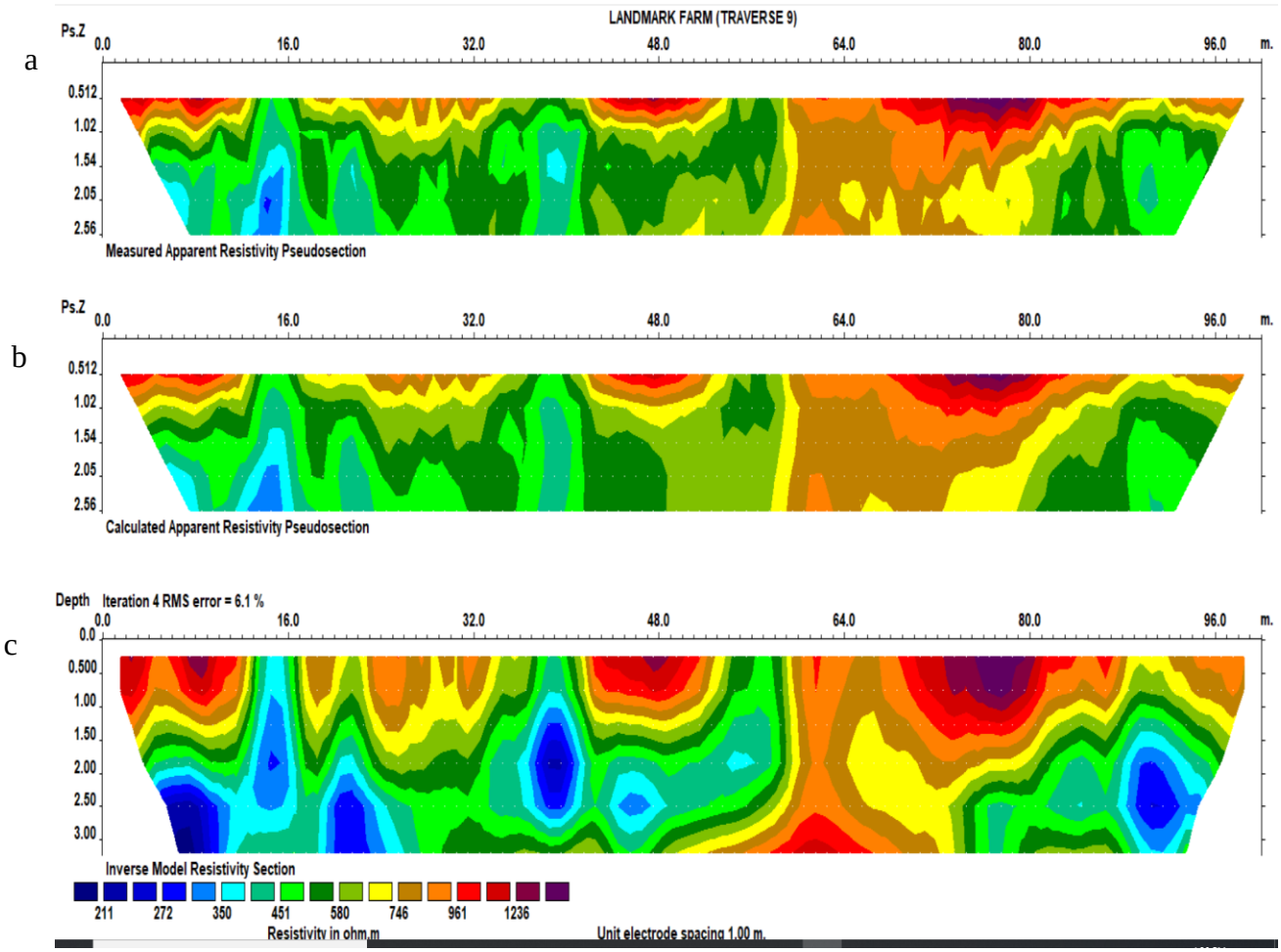


**Figure B9**: 2D resistivity inverse model of Traverse 9 at the site in Landmark University farm showing: (a) measured, (b) calculated, and (c) inverse model.

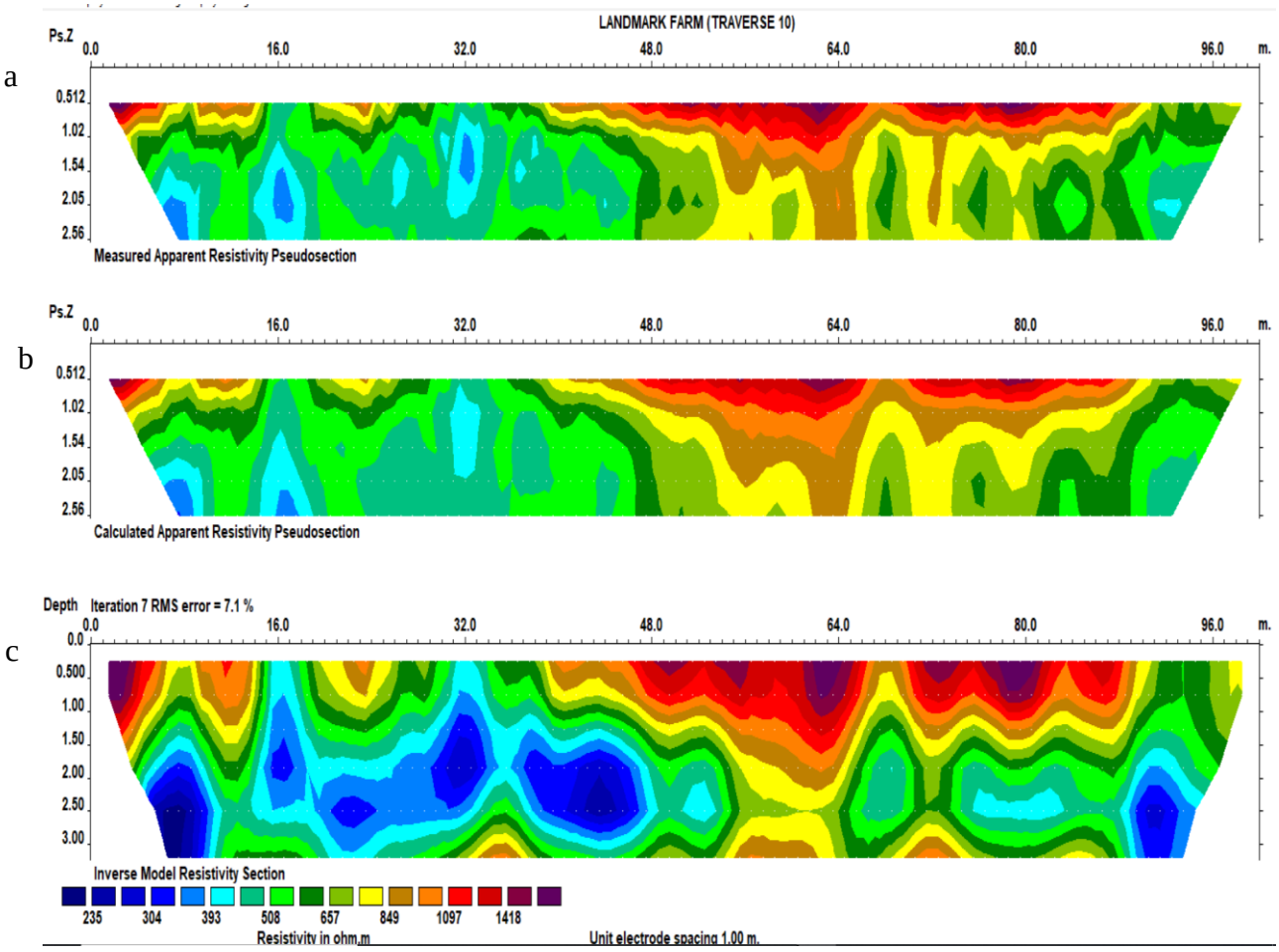


**Figure B10**: 2D resistivity inverse model of Traverse 10 at the site in Landmark University farm showing: (a) measured, (b) calculated, and (c) inverse model.

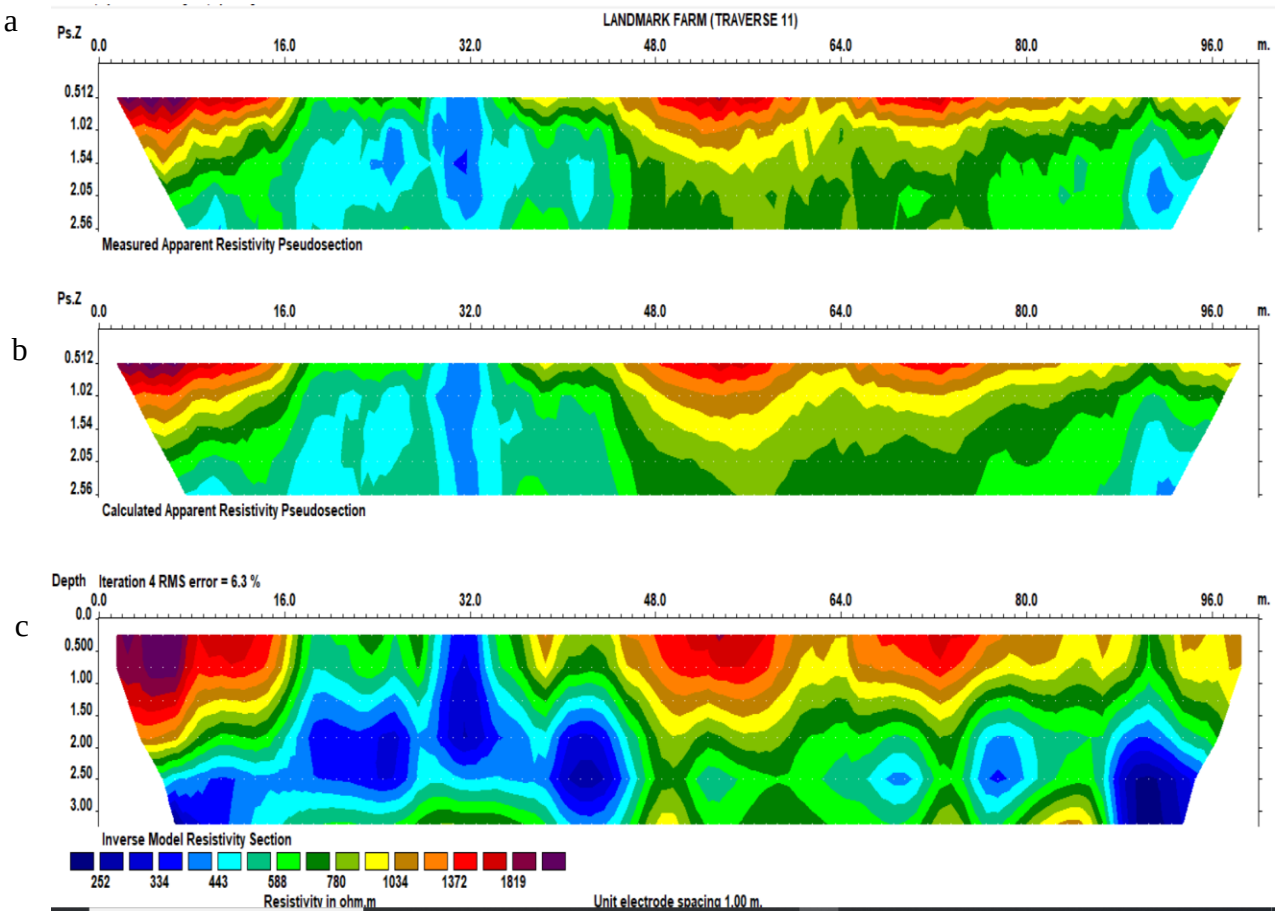


**Figure B11**: 2D resistivity inverse model of Traverse 11 at the site in Landmark University farm showing: (a) measured, (b) calculated, and (c) inverse model.

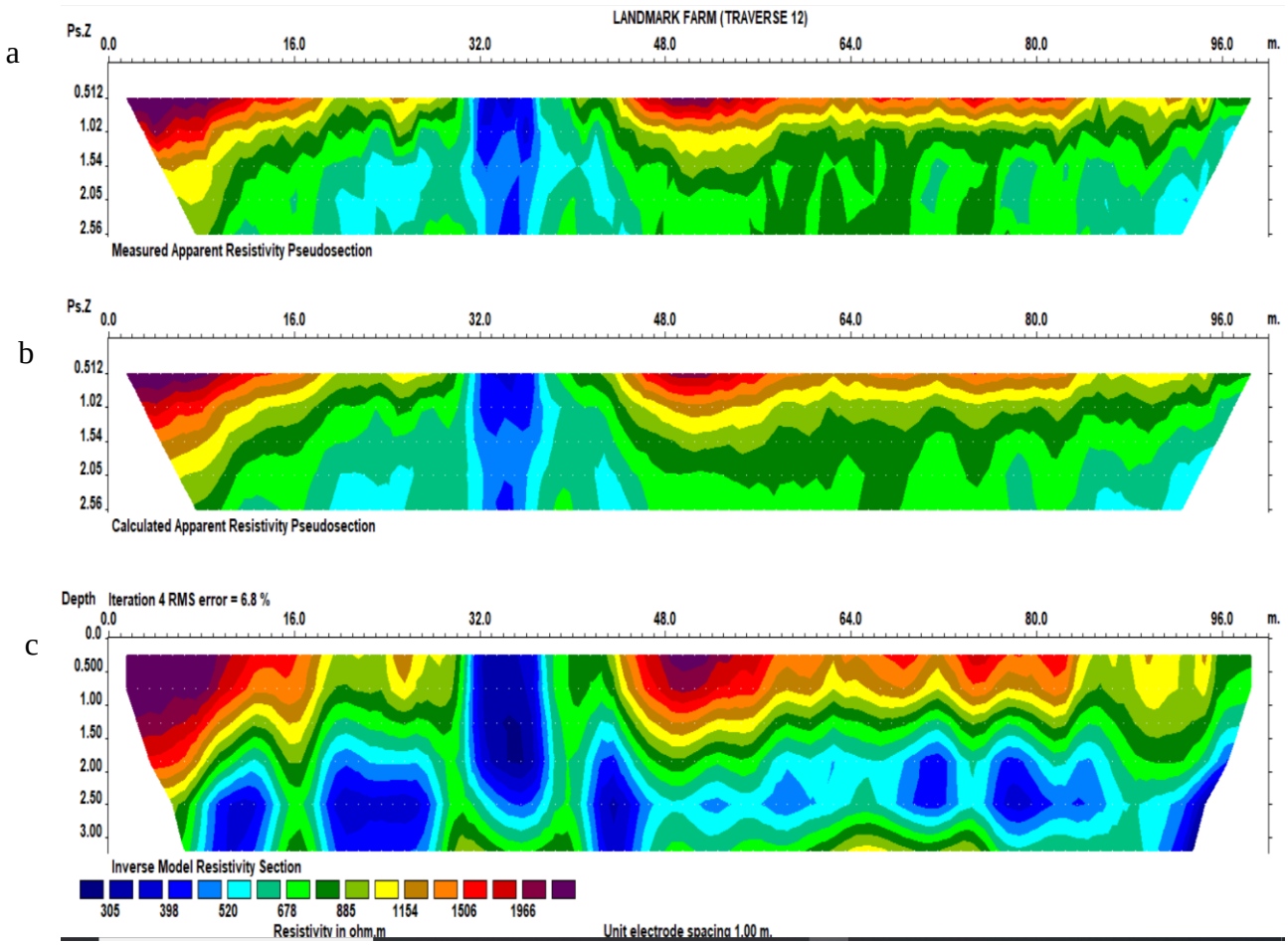


**Figure B12**: 2D resistivity inverse model of Traverse 12 at the site in Landmark University farm showing: (a) measured, (b) calculated, and (c) inverse model.

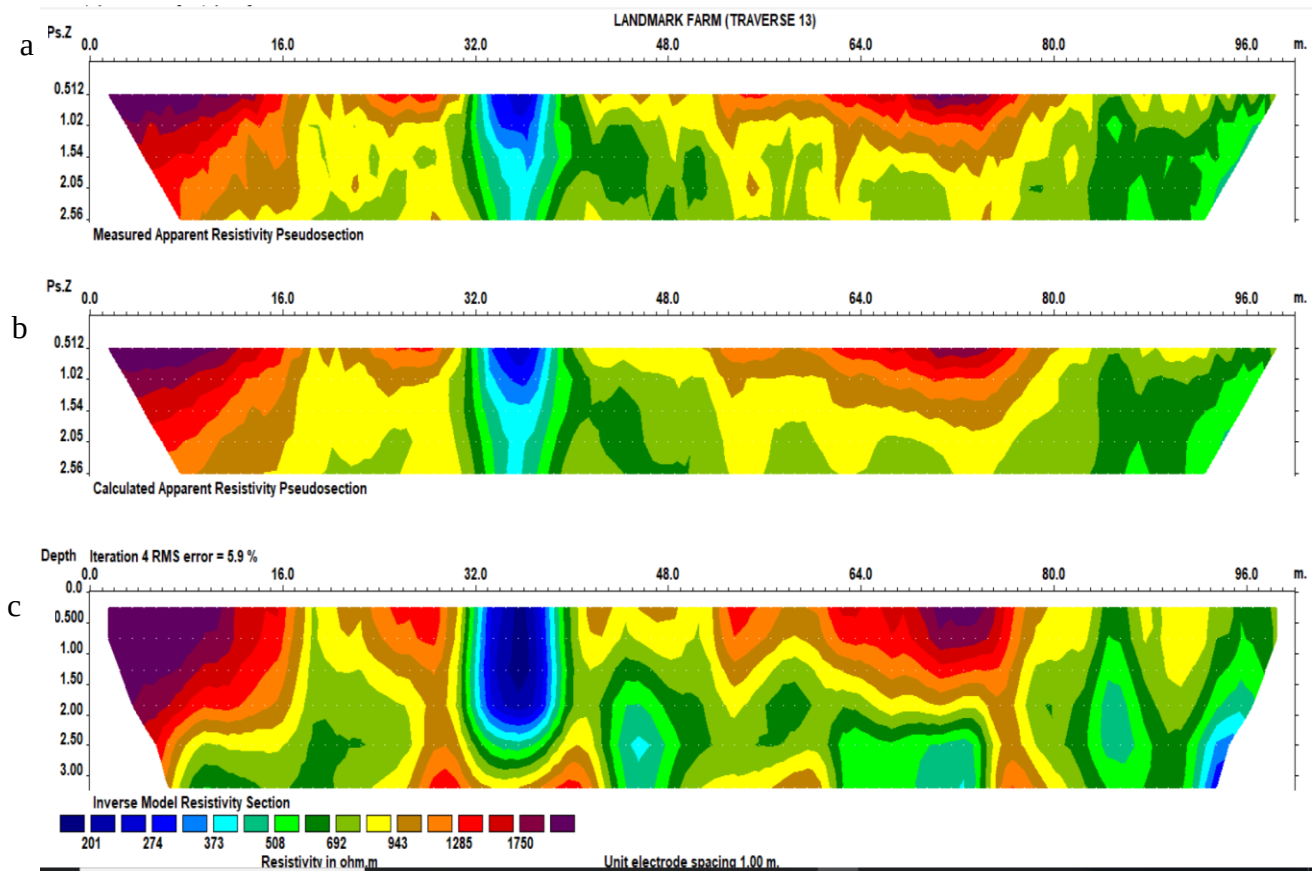


**Figure B13**: 2D resistivity inverse model of Traverse 13 at the site in Landmark University farm showing: (a) measured, (b) calculated, and (c) inverse model.

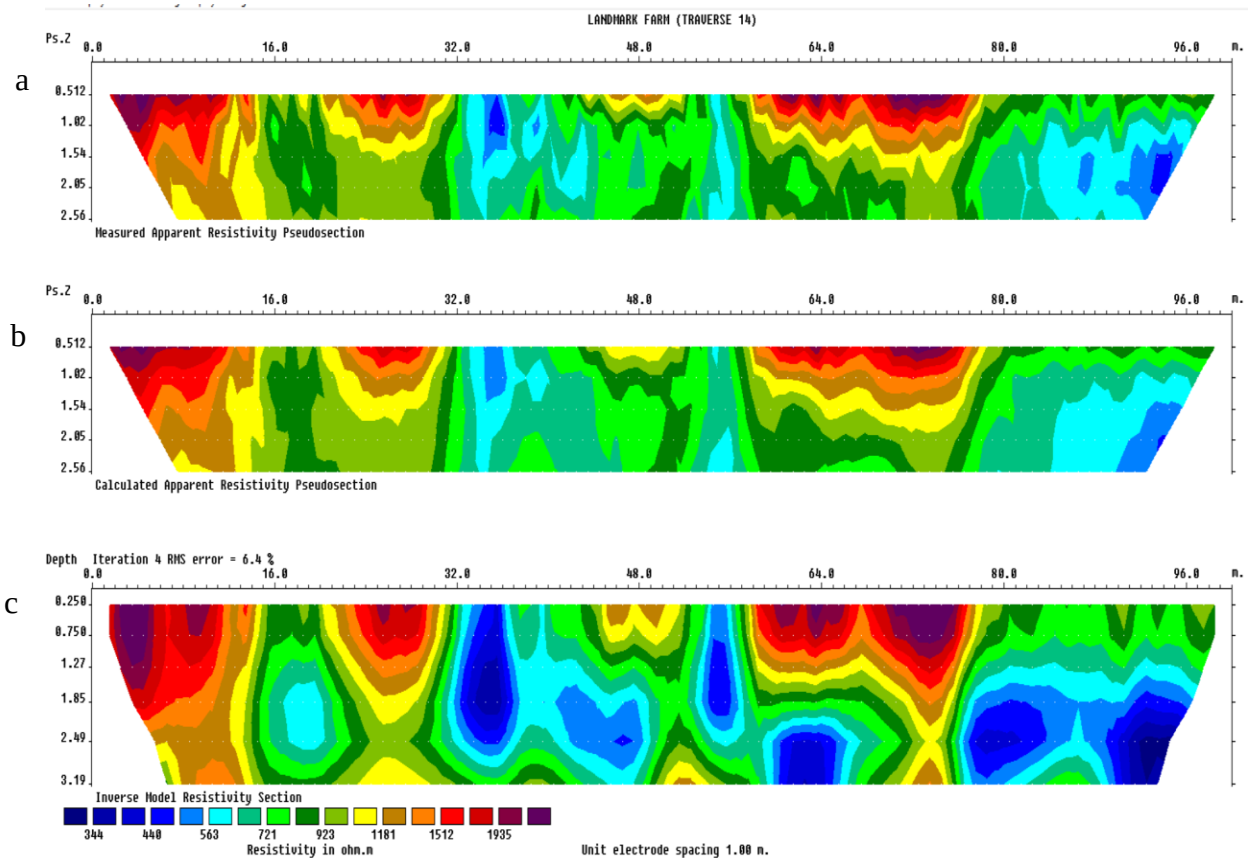


**Figure B14**: 2D resistivity inverse model of Traverse 14 at the site in Landmark University farm showing: (a) measured, (b) calculated, and (c) inverse model.

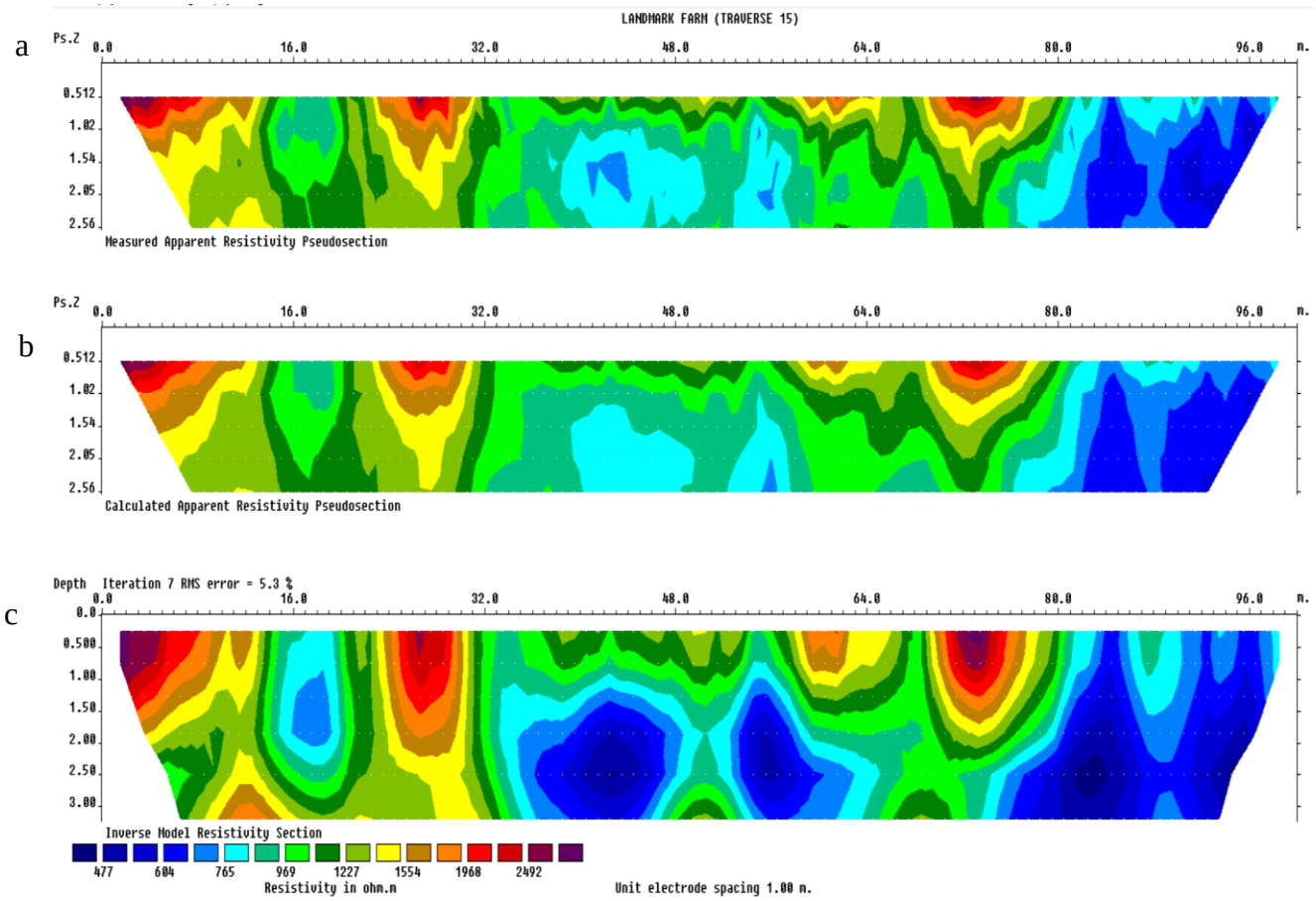


**Figure B15**: 2D resistivity inverse model of Traverse 15 at the site in Landmark University farm showing: (a) measured, (b) calculated, and (c) inverse model.

a

b

c

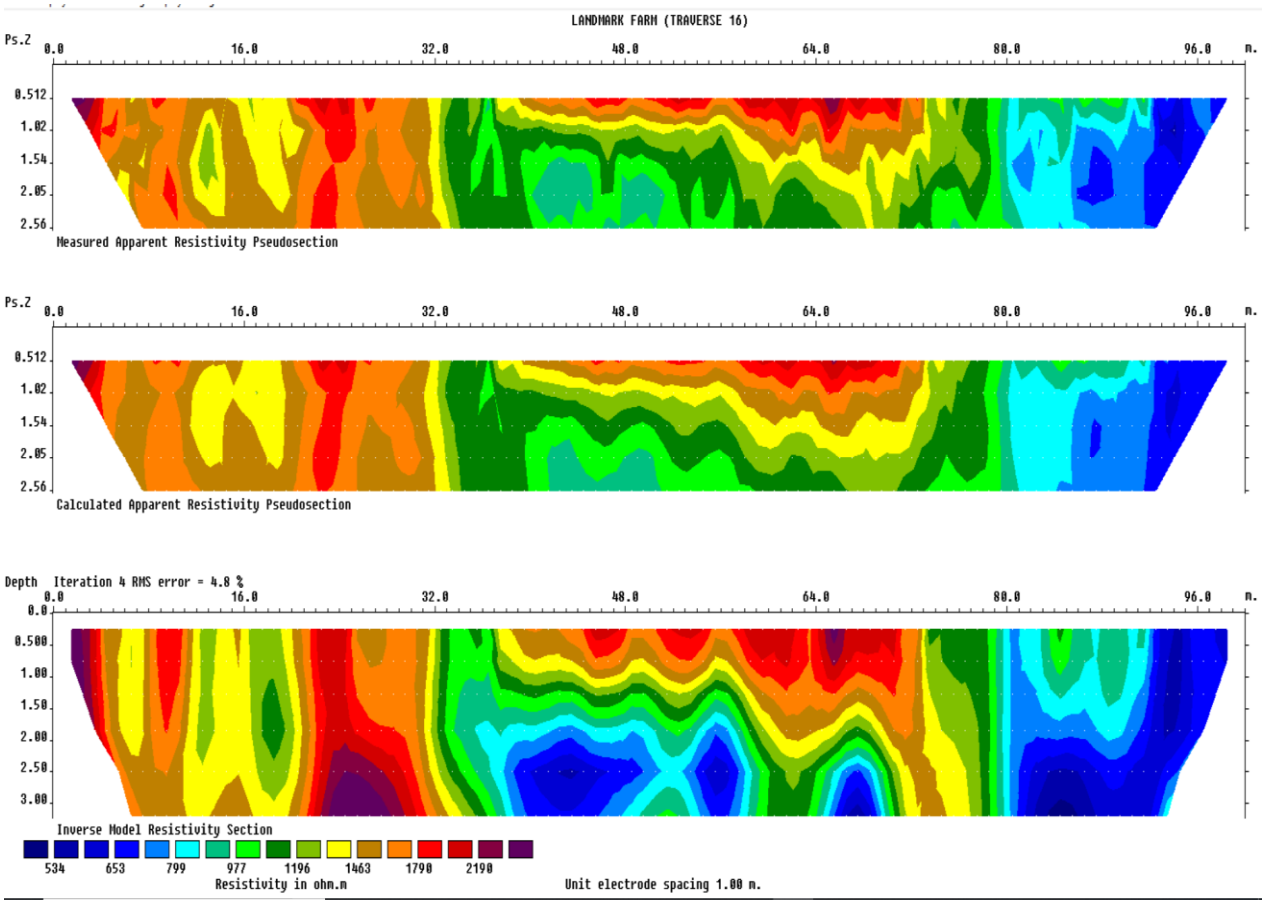


**Figure B16**: 2D resistivity inverse model of Traverse 16 at the site in Landmark University farm showing: (a) measured, (b) calculated, and (c) inverse model.

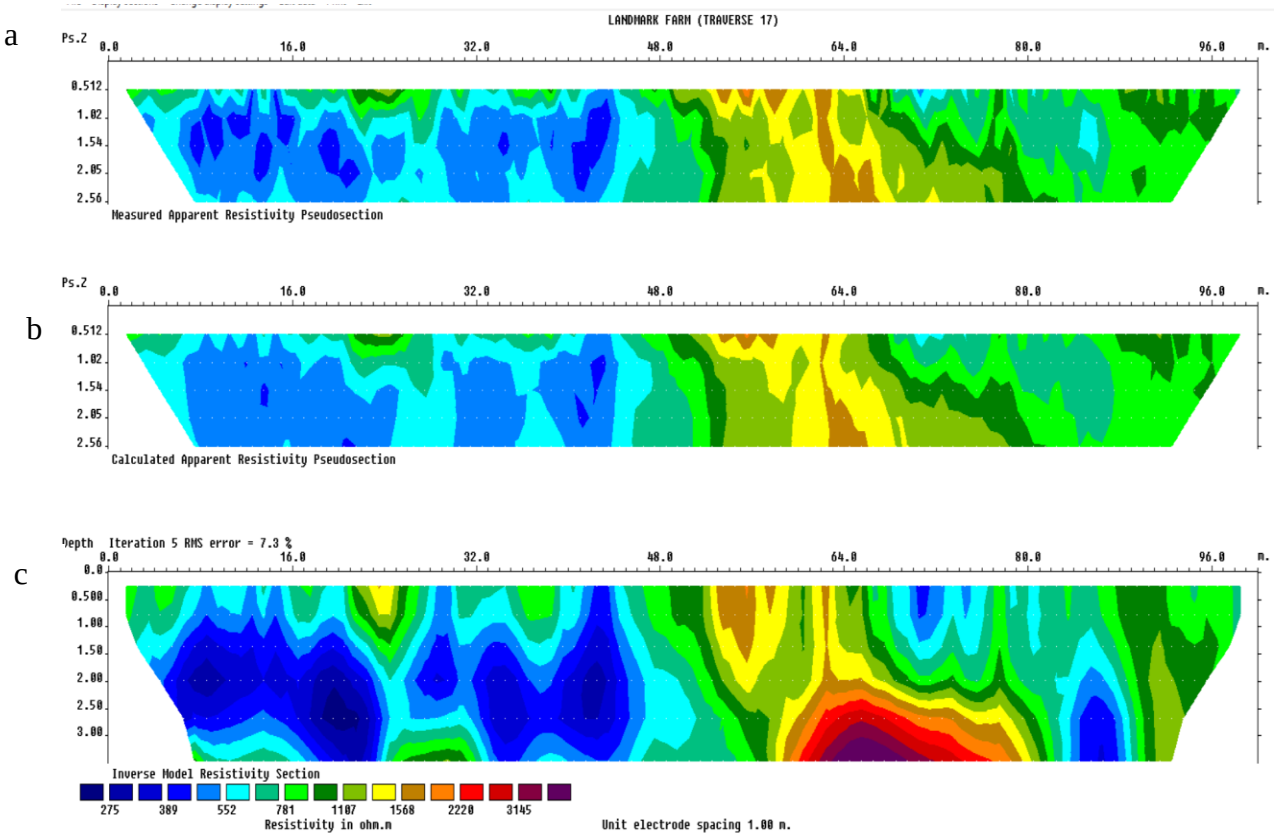


**Figure B17**: 2D resistivity inverse model of Traverse 17 at the site in Landmark University farm showing: (a) measured, (b) calculated, and (c) inverse model.

a

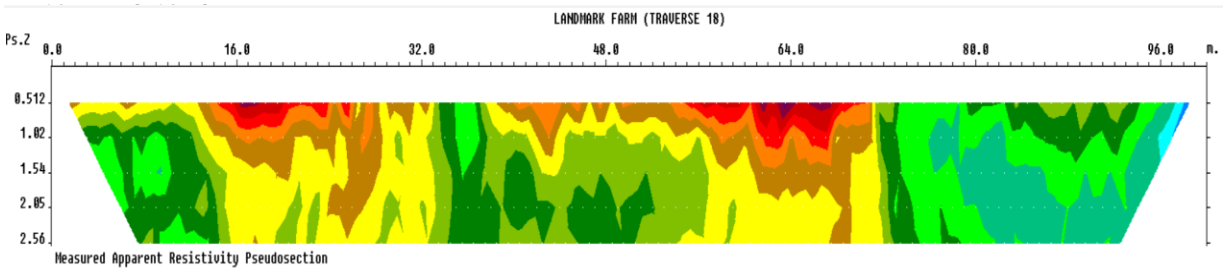


c

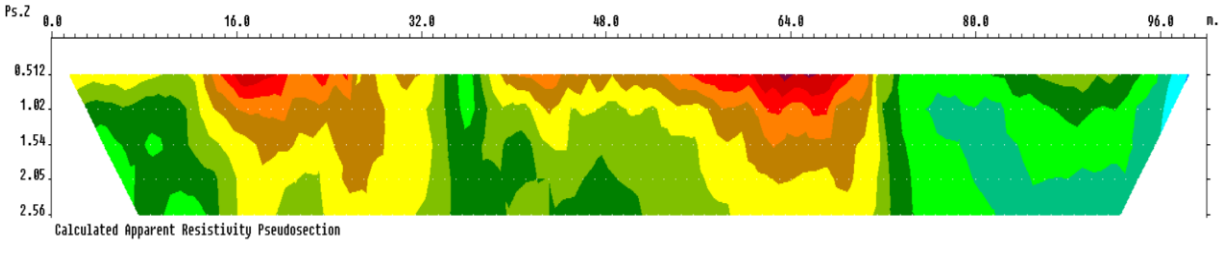


c

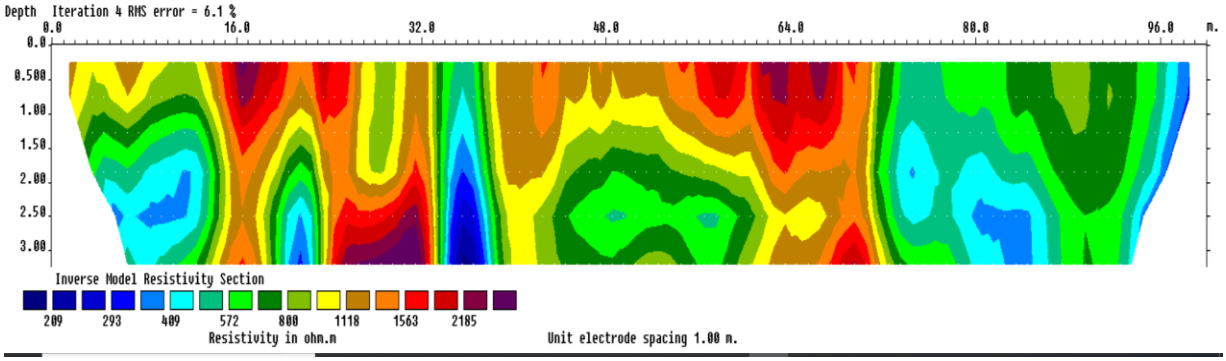


**Figure B18**: 2D resistivity inverse model of Traverse 18 at the site in Landmark University farm showing: (a) measured, (b) calculated, and (c) inverse model of the data.

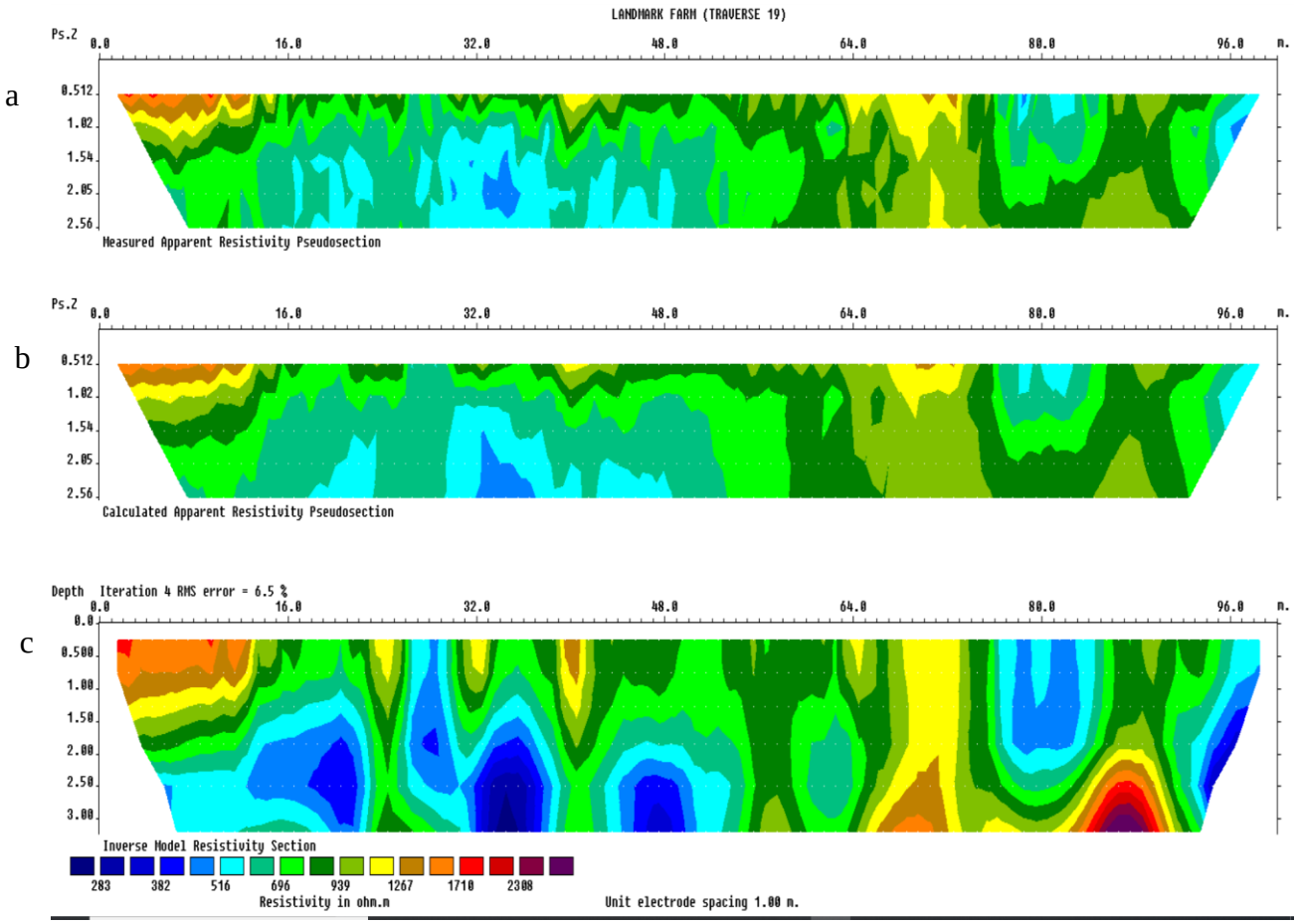


**Figure B19**: 2D resistivity inverse model of Traverse 19 at the site in Landmark University farm showing: (a) measured, (b) calculated, and (c) inverse model.

# APPENDIX C

## Pictures at the Study Sites

a.

b.

**Figure C1**: Data acquisition on the sites at: (a) Landmark University farm, and (b) Covenant University farm.